AIR-STABLE METAL CATALYSTS FOR SUZUKI–MIYAURA CROSS-COUPLING AND MIYAURA BORYLATION REACTIONS

JADSADA RATNIYOM

A THESIS SUBMITTED IN PARTIAL FULFILLMENT
OF THE REQUIREMENTS FOR
THE DEGREE OF DOCTOR OF PHILOSOPHY
(INORGANIC CHEMISTRY)
FACULTY OF GRADUATE STUDIES
MAHIDOL UNIVERSITY
2014

Thesis
entitled

AIR-STABLE METAL CATALYSTS FOR SUZUKI–MIYAURA CROSS-COUPLING AND MIYAURA BORYLATION REACTIONS

……..……..……
Mr. Jadsada Ratniyom
Candidate

……..……..……
Asst. Prof. Supavadee Kiatisevi,
Dr.rer.nat.
Major advisor

……..……..……
Asst. Prof. Preeyanuch Sangtrirutnugul,
Ph.D. (Chemistry)
Co-advisor

……..……..……
Lect. Sirilata Yotphan,
Ph.D. (Chemistry)
Co-advisor

……..……..……
Prof. Banchong Mahaisavariya,
M.D., Dip Thai Board of Orthopedics
Dean
Faculty of Graduate Studies
Mahidol University

……..……..……
Asst. Prof. Khamphee Phomphrai,
Ph.D. (Chemistry)
Program Director
Doctor of Philosophy Program in
Inorganic Chemistry
Faculty of Science
Mahidol University

Thesis
entitled

AIR-STABLE METAL CATALYSTS FOR SUZUKI–MIYAURA CROSS-COUPLING AND MIYAURA BORYLATION REACTIONS

was submitted to the Faculty of Graduate Studies, Mahidol University
for the degree of Doctor of Philosophy (Inorganic Chemistry)
on
March 27, 2014

……
Mr. Jadsada Ratniyom
Candidate

……
Lect. Charnsak Thongsornkleeb,
Ph.D. (Chemistry)
Chair

……
Asst. Prof. Supavadee Kiatisevi,
Dr.rer.nat.
Member

……
Lect. Sirilata Yotphan,
Ph.D. (Chemistry)
Member

……
Asst. Prof. Preeyanuch Sangtrirutnugul,
Ph.D. (Chemistry)
Member

……
Prof. Banchong Mahaisavariya,
M.D., Dip Thai Board of Orthopedics
Dean
Faculty of Graduate Studies
Mahidol University

……
Prof. Skorn Mongkolsuk,
Ph.D.
Dean
Faculty of Science
Mahidol University

ACKNOWLEDGEMENTS

First and foremost, I wish to express my deepest and sincere gratitude to my advisor, Asst. Prof. Supavadee Kiatisevi, for all I have learned from her since I was an undergraduate student, and for her valuable guidance, being an open person to new ideas, as well as for her assistance on the preparation of the international publications and this thesis. Her attitude toward multidisciplinary research inspired me to pursue a Ph.D. in Inorganic Chemistry program as a member of SK's Lab. I extremely appreciate it.

I am very thankful to Asst. Prof. Preeyanuch Sangtrirutnugul and Dr. Sirilata Yotphan, my co-advisors, for excellent advices, kindness, and insightful comments on crystallization and GC experiment. I would also like to thank my external committee, Dr. Charnsak Thongsornkleeb, for technical skills and his kind consideration. I also thank Assoc. Prof. Ekasith Somsook as founder of the Graduate Program in Inorganic Chemistry.

I gratefully acknowledge the Department of Chemistry, Faculty of Science, Mahidol University and the Center of Excellence for Innovation in Chemistry (PERCH-CIC) for financial support. Special thank to all staffs of Department of Chemistry, Faculty of Science, Mahidol University, particularly Mrs. Sutthiporn Chaichana and Miss Natthapat Sungchawek for recording spectral data and elemental analysis. I also thank Mr. Samran Prabpai for the help with X-ray crystallography.

Additionally, I would also like to extend my pleasure to all friends in SK group, PS group, SY group and Program in Inorganic Chemistry for any help and useful opinions. Lastly, I wish to offer my special thank to my family for the encouragement throughout my life.

Jadsada Ratniyom

AIR-STABLE METAL CATALYSTS FOR SUZUKI–MIYAURA CROSS-COUPLING AND MIYAURA BORYLATION REACTIONS

JADSADA RATNIYOM 5337130 SCIC/D

Ph.D. (INORGANIC CHEMISTRY)

THESIS ADVISORY COMMITTEE: SUPAVADEE KIATISEVI, Dr.rer.nat., PREEYANUCH SANGTRIRUTNUGUL, Ph.D., SIRILATA YOTPHAN, Ph.D.

ABSTRACT

This thesis consists of two research projects. The first one focuses on the synthesis of a series of new, air- and moisture-stable palladium complexes with imine ligands based on *N*-arylated imidazoles and their application in Suzuki–Miyaura cross-coupling reactions. Under optimized reaction conditions, coupling products from a wide range of aryl halides and aryl boronic acids were obtained in excellent yields.

The second project involves an investigation of a highly efficient and practical borylation reaction of aryl iodides with bis(pinacolato)diboron. By using $Pd(OAc)_2$, CuI and PPh_3 as ligand at room temperature under air in the presence of Cs_2CO_3, the protocol was proved to be general. Various functionalized arylboronates were obtained in moderate to excellent yields. In addition, a possible reaction mechanism was proposed.

KEY WORDS: IMIDAZOLE-IMINE LIGAND / AIR-STABLE COMPLEXES / SUZUKI–MIYAURA CROSS-COUPLING REACTION / BORON / PALLADIUM / COPPER / ATMOSPHERIC CONDITIONS

225 pages

ตัวเร่งปฏิกิริยาโลหะที่ทนต่ออากาศสำหรับปฏิกิริยาซูซูกิมิยาอูระครอสคัปปลิ้งและปฏิกิริยามิยาอูระบอริลเลชัน

AIR-STABLE METAL CATALYSTS FOR SUZUKI–MIYAURA CROSS-COUPLING AND MIYAURA BORYLATION REACTIONS

เจษฎา ราษฎร์นิยม 5337130 SCIC/D

ปร.ด. (เคมีอนินทรีย์)

คณะกรรมการที่ปรึกษาวิทยานิพนธ์: สุภาวดี เกียรติเสวี, Dr.rer.nat., ปรียานุช แสงไตรรัตน์นุกูล Ph.D., ศิริลตา ยศแผ่น, Ph.D.

บทคัดย่อ

วิทยานิพนธ์นี้ประกอบไปด้วยงานสองส่วน งานวิจัยส่วนแรกมุ่งเน้นการสังเคราะห์อนุกรมของสารประกอบเชิงซ้อนของแพลเลเดียมกับลิแกนด์ชนิดอิมีนอิมิดาโซลแบบใหม่ที่ทนต่อความชื้นและอากาศ และนำไปประยุกต์ใช้ในปฏิกิริยาซูซูกิมิยาอูระครอสคัปปลิ้งซึ่งเกิดกับสารอัลริลเฮไลด์และกรดอัลริลโบรอนิกหลากหลายชนิด และสามารถทำให้ได้สารผลิตภัณฑ์คัปปลิ้งในปริมาณมาก ภายใต้สภาวะที่เหมาะสม

งานวิจัยส่วนที่สองเกี่ยวข้องกับการศึกษาปฏิกิริยาบอริลเลชันระหว่างอัลริลไอโอไดด์กับบิสพินนาโคลาโตไดโบรอนที่ทรงประสิทธิภาพและทำได้ง่าย โดยวิธีนี้ใช้ $Pd(OAc)_2$, CuI, PPh_3 ที่ทำหน้าที่เป็นลิแกนด์ และ Cs_2CO_3 ที่อุณหภูมิห้องภายใต้อากาศ ซึ่งทำให้ปฏิกิริยานี้สะดวกต่อการนำมาใช้ได้จริงในห้องปฏิบัติการ อัลริลโบโรเนตที่มีหมู่ฟังก์ชันที่หลากหลายถูกสังเคราะห์ได้ในปริมาณตั้งแต่ปานกลางถึงสูงมาก นอกจากนี้วิทยานิพนธ์นี้ยังได้เสนอกลไกการเกิดปฏิกิริยาที่น่าจะเป็นไปได้อีกด้วย

225 หน้า

CONTENTS

CONTENTS (cont.)

CONTENTS (cont.)

CONTENTS (cont.)

CONTENTS (cont.)

CONTENTS (cont.)

LIST OF TABLES

LIST OF TABLES (cont.)

LIST OF TABLES (cont.)

LIST OF TABLES (cont.)

LIST OF FIGURES

LIST OF FIGURES (cont.)

LIST OF FIGURES (cont.)

LIST OF SCHEME

LIST OF SCHEME (cont.)

LIST OF SCHEME (cont.)

LIST OF ABBREVIATIONS

Å	angstrom
δ	chemical shift in parts per million
^{o}C	degree Celsius
μ	micro
μL	microlitre
%	percent
Ar	aryl
APCI	Atmospheric Pressure Chemical Ionization
aq	aqueous solution
BINAP	2,2'-bis (diphenylphosphino)-1,1'-binaphthyl
bipy	bipyridine
B_2pin_2	bis(pinacolato)diboron
br	board
Bu	butyl
n-BuLi	*n*-butyllithium
Calcd.	calculated
$CDCl_3$	dueterochloroform
COD	1,5-cyclooctadiene
COE	cyclooctene
COSY	correlation spectroscopy
Cp*	pentamethylcyclopentadieny
Cy	cyclohexyl
d	doublet (spectral)
dd	doublet of doublet (spectral)
DMAc	*N*,*N*-dimethylacetamide
DMF	*N*,*N*-dimethylformamide
DMSO	dimethyl sulfoxide

LIST OF ABBREVIATIONS (cont.)

dtbipy	di-*tert*-butylbipyridine
e.g.	for example
EI	electron impact
et al.	and others
etc	and so forth
Et	ethyl
equiv	equivalent
ESI	electrospray ionization
FID	flame ionization detector
g	gram
GC	gas chromatography
H	hour (s)
HMBC	heteronuclear multiple bond correlation
HMQC	heteronuclear multiple quantum correlation
HRMS	high-resolution mass spectrometry
HSAB	hard and soft acids and bases
Hz	hertz
i	iso
Ind	η^5-C_9H_7 (η^5-indenyl)
*i*Pr	isoproryl
J	coupling constant (in NMR spectrometry)
M	molar
M^+	molecular ion
m	multiplet (spectral)
MeOH	methanol
Me	methyl
mg	milligram
MHz	megahertz

LIST OF ABBREVIATIONS (cont.)

min	minute (s)
mL	millilitre
mM	millimolar (millimoles per liter)
mmol	millimole
mol	mole (s)
MS	mass spectrometry
m/*z*	mass-to-charge ratio
n	normal
NPs	nanoparticles
NOE	nuclear Overhauser effect
NMR	Nuclear Magnetic Resonance
o	ortho
OAc	acetate
OR	alkoxide
ORTEP	Oak Ridge Thermal Ellipsoid Plot (molecular modeling)
p	para
Pd_2dba_3	Tris(dibenzylideneacetone)dipalladium(0)
$Pd(dppf)Cl_2$	[1,1′-bis(diphenylphosphino)ferrocene]dichloropalladium(II)
$Pd(PPh_3)_4$	tetrakis(triphenylphosphine)palladium(0)
phen	1,10-phenanthroline
Ph	phenyl
pin	$1,2\text{-}O_2C_2Me_4$
ppm	part per million (in NMR)
Pr	propyl
q	quartet (spectral)
rt	room temperature
s	singlet (spectral)
sept	septet (spectral)

LIST OF ABBREVIATIONS (cont.)

SET	single electron transfer
t	tert
t	triplet (spectral)
TEMPO	(2,2,6,6-tetramethylpiperidin-1-yl)oxidanyl
Tf	trifluoromethylsulfonyl
THF	tetrahydrofuran
TLC	thin-layer chromatography
TMS	tetramethylsilane
TOF	turn over frequency (in catalysis)
TON	turn over number (in catalysis)

PART I
SYNTHESIS OF AIR-STABLE IMIDAZOLE-IMINE PALLADIUM COMPLEXES FOR SUZUKI–MIYAURA CROSS-COUPLING REACTION

CHAPTER I
INTRODUCTION

1.1 Suzuki–Miyaura cross-coupling reaction

Suzuki–Miyaura cross-coupling reaction is the Pd-catalyzed reaction between aryl halide and arylboronic acid in the presence of base. Many important reactions for carbon–carbon bond formation have been continuously developed over the past four decades. Among these, Suzuki–Miyaura cross-coupling reaction is one of the most effective methods for constructing biaryl structures which are wide-spread in many naturally occurring bioactive products.[1–4]

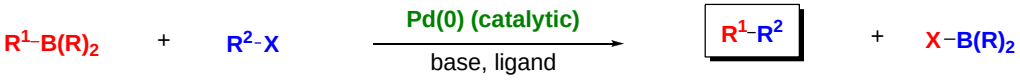

R^1= alkyl, allyl, alkenyl, alkynyl, aryl; R = alkyl, OH, O-alkyl; R^2 = alkenyl, aryl, alkyl; X = Cl, Br, I, OTf
base = Na_2CO_3, $Ba(OH)_2$, K_3PO_4, Cs_2CO_3, K_2CO_3, TlOH, KF, CsF, Bu_4F, NaOH, $M^+(^-O\text{-alkyl})$

Figure 1.1. General reaction scheme for the Suzuki–Miyaura cross-coupling reaction.[5]

1.2 General mechanism of Suzuki–Miyaura cross-coupling reaction

The mechanism of the Suzuki reaction is best viewed from the perspective of the palladium catalyst. The first step is the oxidative addition of palladium(0) **1** to the aryl halide to form the organopalladium species **2**. Reaction with base gives intermediate **3**, which via transmetalation with the complex **5** forms the organopalladium species **4**. Reductive elimination of the desired product restores the active palladium catalyst **1** which completes the catalytic cycle.

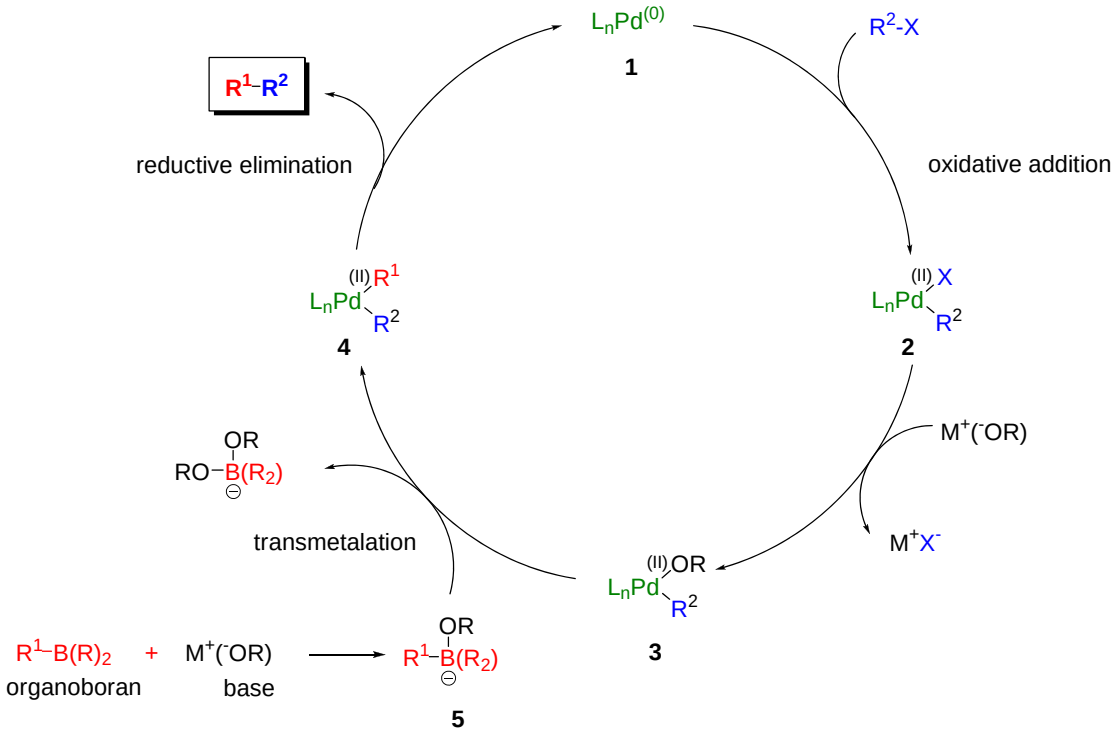

Figure 1.2. General mechanism for the Suzuki–Miyaura cross-coupling reaction.[5]

In most cases, the oxidative addition is assumed to be the rate-determining step for the cross-coupling reaction when aryl chloride and aryl bromide were used as substrate. On the other hand, the transmetalation was found to be the rate-determining step, when using iodide substrates.[6]

The role of bases on the Suzuki–Miyaura cross-coupling reaction was never fully understood. According to the mechanism, the base ($^{-}$OR) was first believed to react with R^1–$B(R^2)_2$ to form species **5**. This boron species becomes more

nucleophilic and more reactive towards the palladium complex in the transmetalation step.[7–9] The retention of configuration of the coupling product shown in Scheme 1.1 was reported by Matos and co-workers. They suggested that Boron "ate" complexes, formed via quaternization of the boron with a negatively charged base, were frequently involved in the transmetalation.[8]

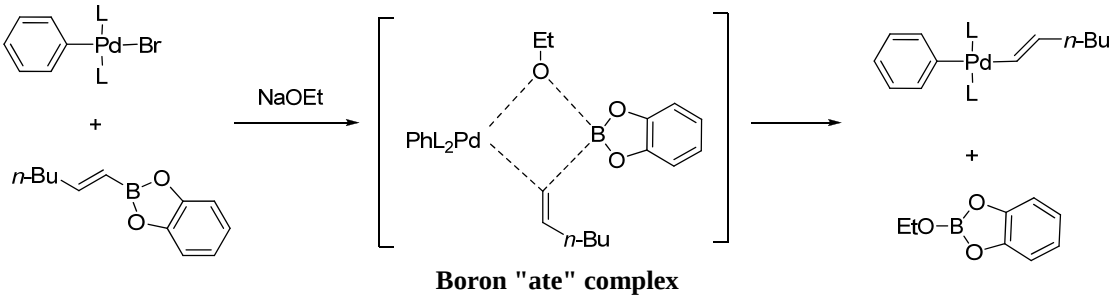

Scheme 1.1. Boron ate complex.[8]

In 2011, the kinetic study for Suzuki–Miyaura cross-coupling reaction was explored by Duc and co-workers.[9] They found an unexpected role of base in the reductive elimination that could be accelerated by base, presumably through the formation of a pentacoordinated anionic palladium intermediate **6** (Scheme 1.2).

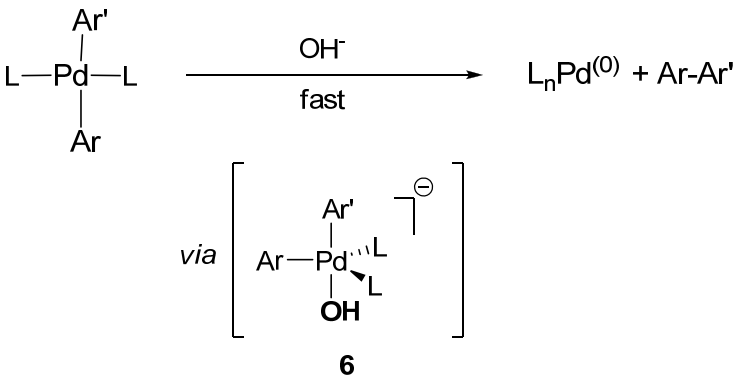

Scheme 1.2. Acceleration of reductive elimination step by the effect of base.[9]

The air-stable and readily commercial Pd(II) catalysts are commonly used in cross-coupling reactions. Notably, Pd(0) is believed to be the active catalyst in the

Pd-catalyzed cross-coupling reaction. The formation of active catalysts can be achieved by the reduction of a Pd(II) complex. For example, a phosphine ligand can convert $Pd(OAc)_2$ to a Pd(0)-phosphine complex, without the need of isolation.[10] The reduction of Pd(II) complex can also be achieved with amine, alkene, and organometallic reagents such as organoboron and organomagnesium compounds.[11] Figure 1.3 illustrates the reduction mechanism of Pd(II) to Pd(0) with various reagents.

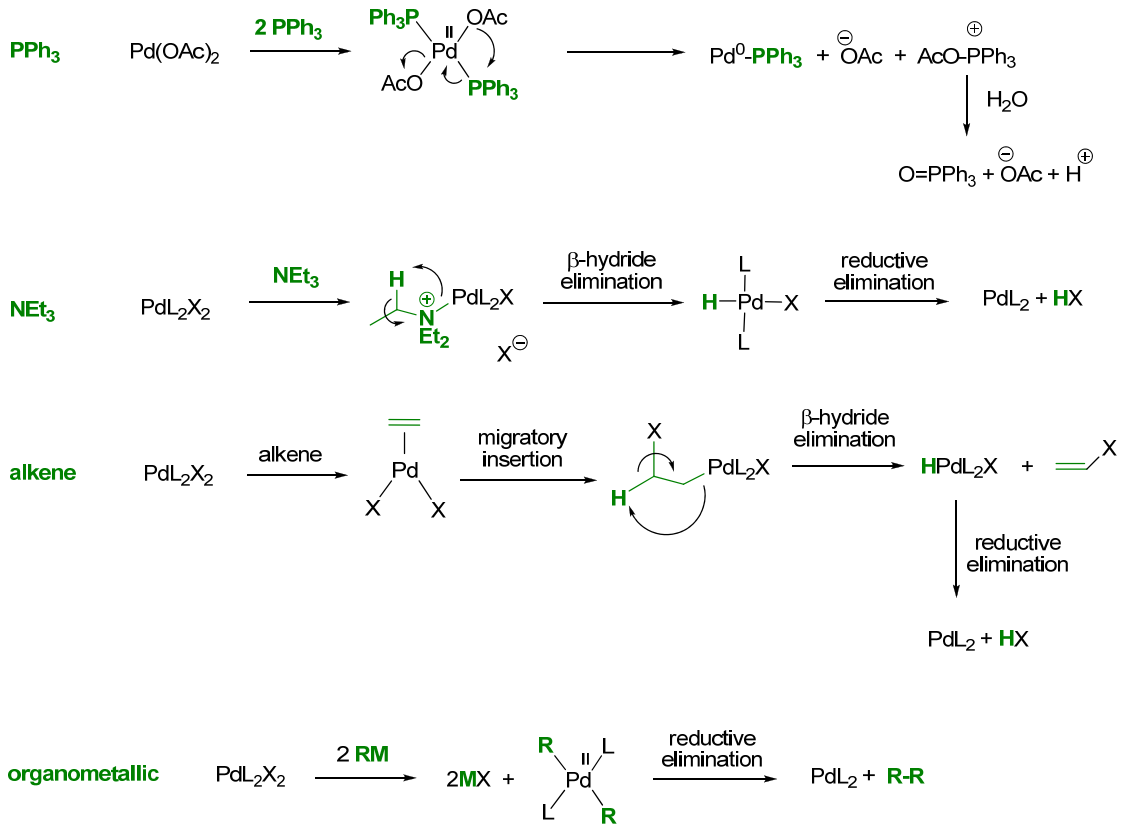

Figure 1.3. Mechanism for *in situ* reduction of Pd(II) to Pd(0).[11]

1.3 Pd(0) nanoparticles with mercury poisoning test

Hg(0) is widely used to distinguish homogeneous and heterogeneous catalyses because of its ability to deactivate metal-particle heterogeneous catalysts, by adsorption on the metal surface.[7, 12] The experiment is performed by adding Hg(0) to the reaction and is thus called "mercury poisoning test".

Palladium complexes are one of the most versatile catalysts for the Suzuki–Miyaura cross-coupling reaction. However, they are known to aggregate easily and form Pd black, causing catalyst decomposition and a decrease of catalytic activity.[13]

The mercury poisoning test was additionally applied to investigate the formation of Pd(0) nanoparticles (NPs) in the Pd-catalyzed Suzuki–Miyaura cross-coupling reaction.[14, 15] For example, Singh and co-workers reported Pd(II) complexes of pyrazolated thio/selenoethers for the Suzuki–Miyaura cross-coupling reaction, and observed no conversion of product in the presence of excess Hg. This result implied that Pd(0) NPs, which might be the active species, were deactivated under identical conditions.[16]

1.4 Advantages and disadvantages of Suzuki–Miyaura cross-coupling reaction

The Suzuki–Miyaura cross-coupling reaction has two significant advantages over other cross-coupling processes. Arylboronic acid reactants are readily available and react under mild conditions. In addition, the inorganic by-products are usually easy to remove. However, several existing Suzuki–Miyaura cross-coupling methods generally employ palladium complexes supported by phosphine ligands,[17–22] which are often sensitive to air oxidation and require careful handling.[23]

CHAPTER II
OBJECTIVES

Despite the achievements of the modest to high yields of coupling products, all catalytic systems of previous works as will be presented in Chapter III require either high reaction temperatures or inert conditions.

As an effort to develop an improved Suzuki reaction protocol, this thesis has centered on the search for a catalytic system consisting of rigid phosphine-free ligands with nitrogen-based frameworks. The new imidazole-imine backbone was selected due to its structural rigidity, strong σ-donating property and low-cost. In addition, compared to phosphine ligands, the imidazole-imine ligands are easier to prepare and more resistant to air and moisture. Substituents on the nitrogen atom of the imine moiety also play important roles in tuning steric and electronic properties of the molecule.

In order to develop a convenient synthetic protocol for the Suzuki–Miyaura cross-coupling reaction using the imidazole-imine ligands, the objectives of the first part in this thesis were:

- To synthesize a series of new, air- and moisture-stable Pd complexes with imine ligands based on *N*-arylated imidazoles;
- To investigate the catalytic activities of the Pd complexes on the Suzuki–Miyaura cross-coupling reaction;
- To study the optimization of the Suzuki–Miyaura cross-coupling reaction;
- To study the scope and functional group tolerance of substrates on the reaction.

CHAPTER III
LITERATURE REVIEW

3.1 Phosphine ligands for the Pd-catalyzed Suzuki–Miyaura cross-coupling reaction

In 2000, Fu and co-workers[17] discovered the versatile catalytic system between Pd_2dba_3 and P(*t*Bu)$_3$ for the Suzuki–Miyaura cross-coupling reaction of aryl halide and arylboronic acid in THF under inert atmosphere. Interestingly, the unreactive aryl chlorides, such as 4-chloroaniline, can undergo the cross-coupling reaction under this catalytic system. Moreover, a high selectivity for the following order of reactivity, I > Br > Cl, was observed (Scheme 3.1).

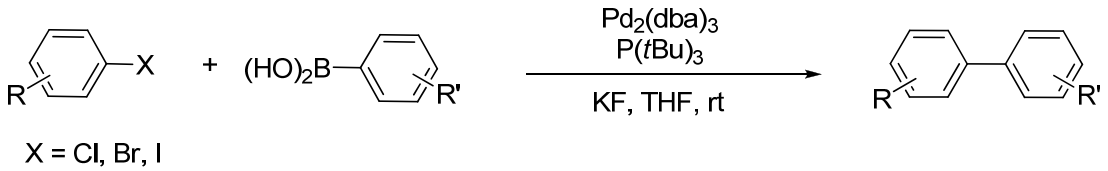

Scheme 3.1. Pd_2dba_3/P(*t*Bu)$_3$-catalyzed Suzuki–Miyaura cross-coupling reaction.[17]

After that, Buchwald and co-workers[18] developed general catalytic system for the preparation of tetra-ortho-substituted unsymmetrical biaryls using the Suzuki–Miyaura cross-coupling reaction. They stated that under the reaction conditions composed of Pd_2dba_3 and phenanthrene-substituted phosphine ligand in toluene at 110 ^oC for 24 h, unreactive substrates such as sterically hindered aryl bromide could be catalytically converted to corresponding compounds. The π-coordination phenanthrene moiety of ligand was suggested to play an important role in improving catalytic efficiency (Scheme 3.2).

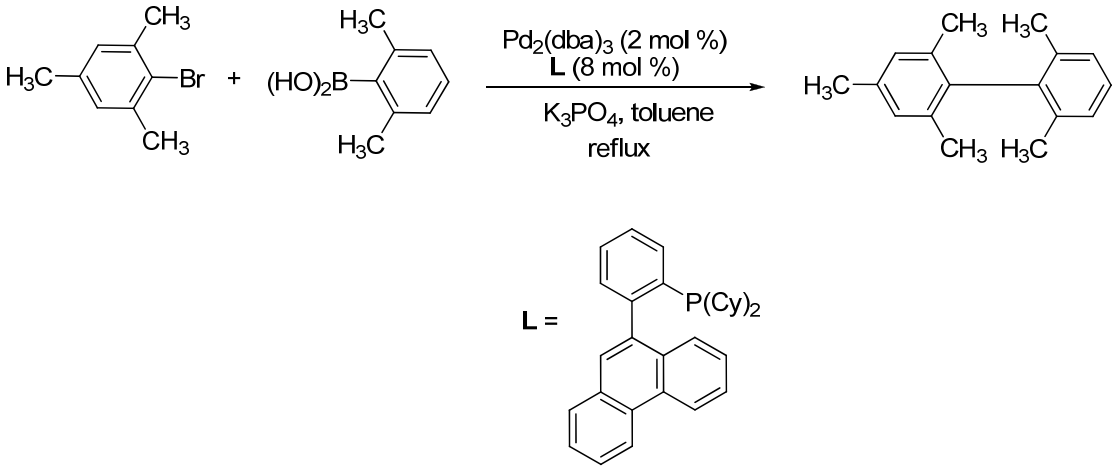

Scheme 3.2. Pd-catalyzed Suzuki–Miyaura cross-coupling reaction for the synthesis of sterically hindered biaryls.[18]

A new class of phosphine ligand based on phospha-adamantane framework for the Pd-catalyzed Suzuki–Miyaura cross-coupling reaction was later demonstrated by Capretta and co-workers (Scheme 3.3).[19] The combination of $Pd_2(dba)_3$ and phosphine ligands based on phospha-adamantane framework was shown to promote the Suzuki–Miyaura cross-coupling reaction of aryl iodide, aryl bromide and aryl chloride with arylboronic acid under mild conditions. Although the authors reported that phosphine ligands based on phospha-adamantane framework are air-stable in comparison with other reported phosphine ligand, however, the air-sensitive techniques were still required for setting up the reaction.

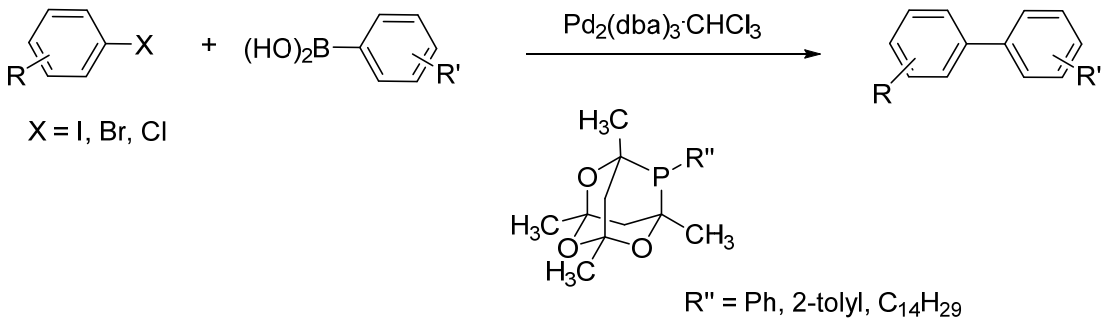

Scheme 3.3. A phosphine ligand based on phospha-adamantane framework used in the palladium-catalyzed Suzuki–Miyaura cross-coupling reaction.[19]

Eventhough, a DFT calculation of air stabilities of phosphine ligand was demonstrated,[23] air-sensitive technique has still been required practically.

This oxygen sensitivity of catalyst is one of the crucial limitations that could hamper the development of the practical biaryl synthesis. Therefore, air- and moisture-stable ligands, which are easily prepared from inexpensive, commercially available starting materials, are needed for the improvement of the Pd-catalyzed cross-coupling reactions.

3.2 Phosphine-free ligands for the Pd-catalyzed Suzuki–Miyaura cross-coupling reaction

Catalytic system consisting of rigid phosphine-free ligands with nitrogen-based frameworks such as, cyclometalated imine,[24] diazabutadiene,[25] guanidines,[26] N-heterocyclic carbenes[27-31] and nitrogen-acyclic carbenes[32] have been reported. The first cyclopalladated phosphine-free imine complex which showed high catalytic activity in Suzuki–Miyaura cross-coupling reaction of aryl bromide and arylboronic acid was reported by Milstein and Weissman in 1999.[24] This reaction was performed under inert condition in *o*-xylene at 130 ^{o}C and resulted in modest yields of coupling products (Scheme 3.4).

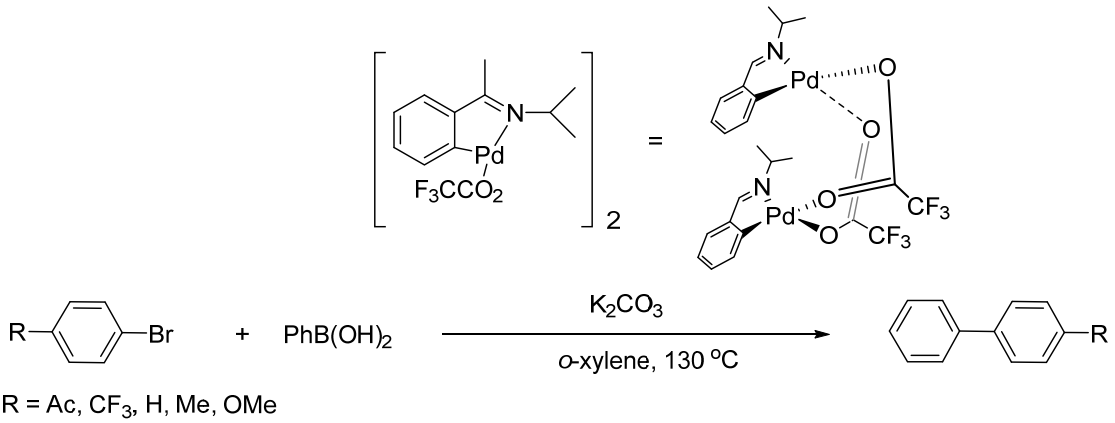

Scheme 3.4. Suzuki–Miyaura cross-coupling reaction of aryl bromide and arylboronic acid catalyzed by cyclopalladated phosphine-free imine complex.[24]

In 2001, Nolan and co-workers[25] developed the Suzuki–Miyaura cross-coupling reaction using $Pd(OAc)_2$/DAB-Cy in the presence of Cs_2CO_3 in dioxane at 80 ^oC. This catalytic system consisting of $Pd(OAc)_2$ and DAB-Cy exhibited excellent activity for coupling reaction between aryl bromide and aryl chloride with arylboronic acid (Scheme 3.5).

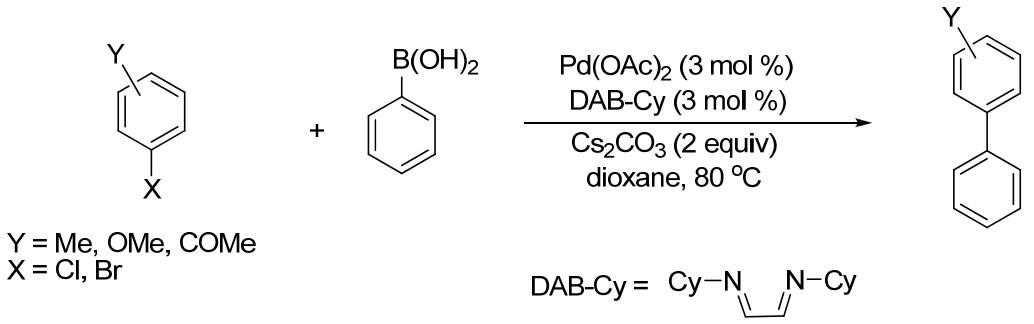

Scheme 3.5. Suzuki–Miyaura cross-coupling catalyzed by $Pd(OAc)_2$/diazabutadiene system.[25]

An interesting phosphine-free ligand based on guanidines developed for Suzuki–Miyaura cross-coupling reaction in aqueous solvent was reported by Zhang and co-workers.[26] Furthermore, the tolerance towards a broad range of functional groups in substrates was observed in this catalytic system (Scheme 3.6).

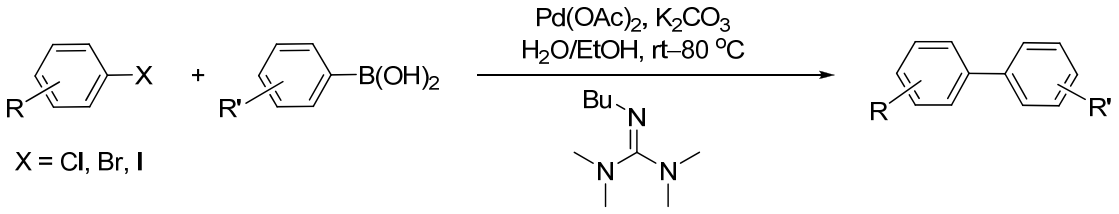

Scheme 3.6. $Pd(OAc)_2$/guanidines-catalyzed Suzuki–Miyaura cross-coupling reaction in aqueous media.[26]

Additionally, one of unique N-heterocyclic carbene (NHC) ligands which are sterically demanding, and have restricted flexibility is bioxazoline (IBiox).[29] It could act as an effective ligand for the coupling reaction of sterically hindered aryl

chlorides and arylboronic acid. The $Pd(OAc)_2$/IBiox-catalyzed Suzuki–Miyaura cross-coupling reaction was carried out under inert atmosphere in the presence of K_3PO_4 in toluene at 110 ^oC. It should be mentioned that this is the first report for the preparation of tetra-ortho-substituted biaryl compounds in the presence of a carbene ligand (Scheme 3.7).

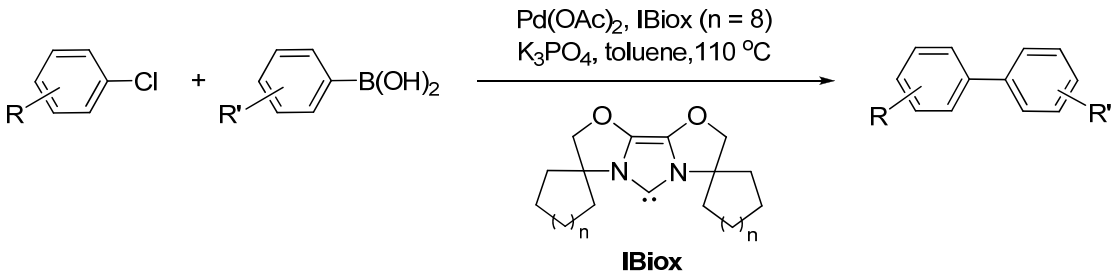

Scheme 3.7. $Pd(OAc)_2$/IBiox-catalyzed Suzuki–Miyaura cross-coupling reaction of sterically hindered substrate.[29]

Another ligand based on nitrogen framework is nitrogen acyclic carbene (NAC) investigated by Hashmi and co-workers.[32] The application of Pd(II)-NAC complexes was found on the Suzuki–Miyaura cross-coupling reaction of chlorobenzene and 2,5-dimethylphenylboronic acid. The reaction was carried out under inert condition in the presence of KO*t*Bu in EtOH at room temperature. The addition of a nitrogen nucleophile (isonitrile ligand) coordinated to Pd(II)-NAC complex indicating an increasing of nucleophilicity of Pd metal. However, Pd(II)-NAC complex showed the lower catalytic activity than Pd(II)-NHC complexes resulting in low coupling product yields This might originate from an improved stability and a longer catalyst lifetime of Pd(II)-NHC (Scheme 3.8).

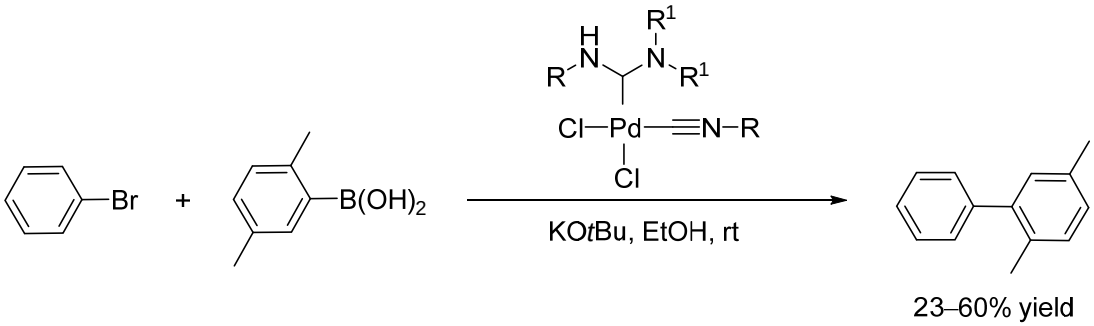

Scheme 3.8. Pd(II)-NAC-catalyzed Suzuki–Miyaura cross-coupling reaction.[32]

Recent progress in the applications of imidazole-imine ligands has shown in a study of spectroscopic and water relaxivity properties of manganese(II) complexed with tetradentate imidazole-imine ligands (Scheme 3.9),[33] as well as in the ethylene oligomerization catalyzed by nickel(II) complexes with imidazole-imine ligands (Scheme 3.10).[34]

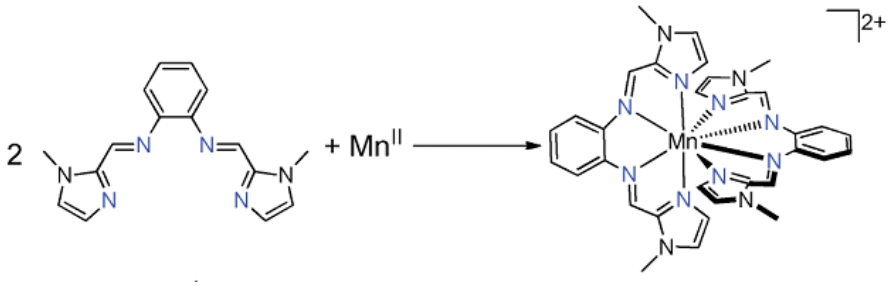

Scheme 3.9. Synthesis of manganese(II) complexed with tetradentate imidazole-imine ligands (copied from Literature[33]).

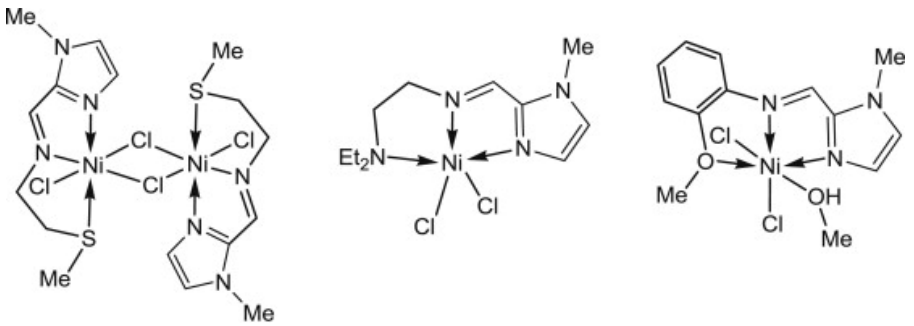

Scheme 3.10. Nickel(II) complexes with imidazole-imine ligands (copied from Literature[34]).

CHAPTER IV
RESULTS AND DISCUSSION

This chapter begins with the synthesis of imidazole-imine palladium complexes **4a**–**4h**, followed by their structural characterization based on ^{1}H, ^{13}C NMR spectroscopy, HRMS and elemental analysis. The NMR study of the complexation between the metal and free ligand was discussed. The structures of **4b** and **4h** were also confirmed by X-ray crystallography. The catalytic activity of **4a**–**4h** on the Suzuki–Miyaura cross-coupling reaction was studied. Effects of catalyst loadings, reaction time, solvents, bases and substrate scope were subsequently investigated. Moreover, mercury poisoning test was carried out to examine the actual active species in catalysis.

4.1 Synthesis of 1-(2,6-diisopropylphenyl)-1*H*-imidazole (1)

Compound **1** was prepared from a four-component condensation of a 2,6-diisopropylphenylamine with formaldehyde, ammonium chloride and glyoxal.[35] After purification, the product **1** was obtained in 35% yield (Scheme 4.1).

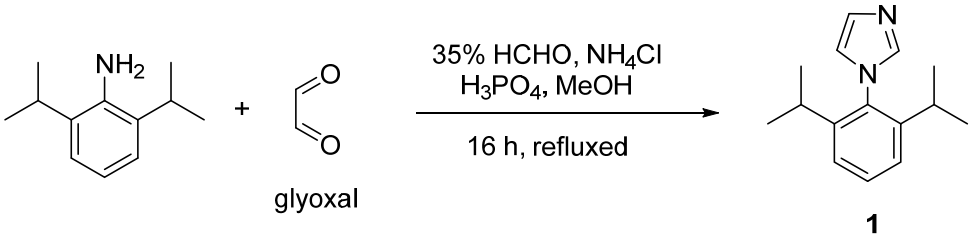

Scheme 4.1. Synthesis of 1-(2,6-diisopropylphenyl)-1*H*-imidazole **1**.

4.2 Synthesis of palladium complexes (4a–h)

As an access to a series of imidazole-imine Pd complexes **4**, the 1-(2,6-diisopropyl-phenyl)-1*H*-imidazole compound **1** was deprotonated by *n*-butyl lithium at **–**30 ^{o}C, and reacted with *N*,*N*-dimethylformamide. After purification, product **2** was obtained in almost quantitative yield (99%). Compound **3**, resulted from the condensation of **2** with corresponding primary amines was used, without further purifications, to react with $Pd(COD)Cl_2$[36] for 1 h in $CHCl_3$. The $Pd(COD)Cl_2$ is commonly used as a palladium precursor due to its good solubility in organic solvents. Crystallization of Pd complexes was carried out by slow diffusion of hexane into $CHCl_3$ solution to afford **4a**–**4h** in a range of 66–97% yields (Scheme 4.2). Notably, complex **4d** was obtained in the lowest yield (66%) compared to other Pd complexes. This might be caused by poor nucleophilicity of *p*-nitroaniline. The structural characterization of the ligands and complexes was carried out by ^{1}H, ^{13}C NMR spectroscopy, elemental analysis and HRMS.

As mentioned above, free ligands **3a**–**3h** can be complexed without purification. The change in the chemical shift of ^{1}H NMR cannot be used to evaluate the complexation between metal and ligand. However, the coordination of Pd complexes **4a**–**4h** was confirmed by HRMS and elemental analysis. Interestingly, ligand **3h** which was insoluble in CH_3CN could be isolated by using CH_3CN as solvent instead of $CHCl_3$ as described in the preparation of compound **3** (see Synthesis of **3h** in the Experimental Section). To study the coordination behavior of the imidazole-imine moiety with Pd metal, complex **4h** was chosen as the representative palladium complex because ligand **3h** can be easily isolated by washing with cool acetonitrile. Therefore, the NMR study on the complexation was investigated only for **2**, **3h** and **4h**, as shown in Section 4.3.

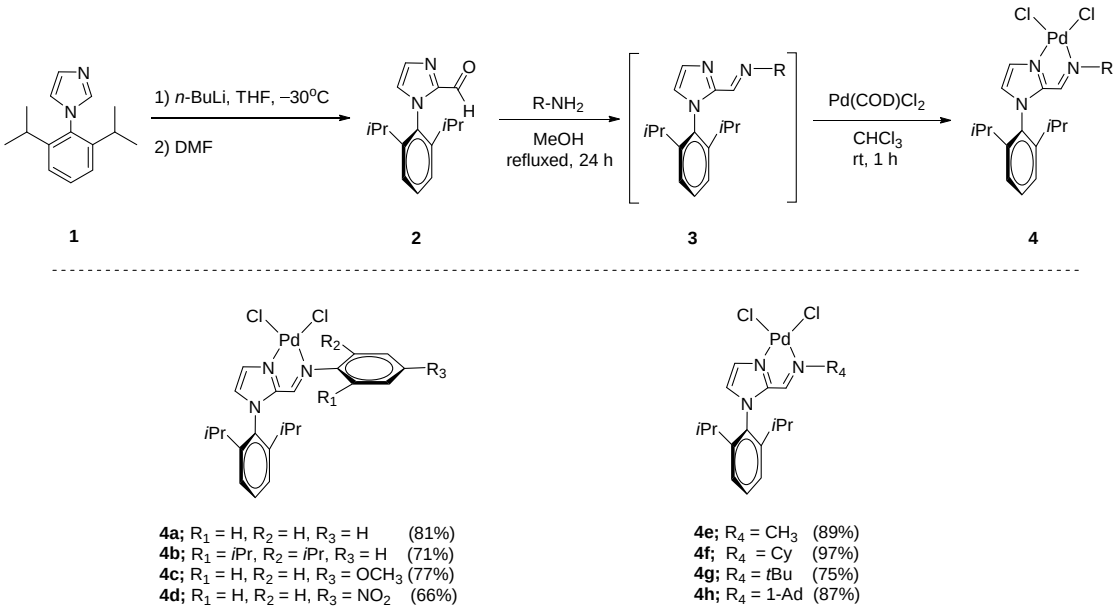

Scheme 4.2. Synthetic pathway for palladium complexes (**4a**–**h**).

4.3 NMR study of complexation between Pd metal and ligand (3h)

The ^{1}H NMR spectrum of the starting material **2** shows a signal of the aldehyde proton at 9.80 ppm and two singlet signals of imidazole protons at 7.51 ppm and 7.11 ppm which can be ascribed to H-4 and H-5, respectively (Figure 4.1 and 4.2). The NMR data are consistent with those of similar compounds described in the literature.[35, 37] These imidazole protons also gave ^{3}J cross peaks with C-2 on the basis of HMBC correlation (Table 4.3). In addition, only H-5 exhibited HMBC cross peaks with C-7, leaving the position of this proton at C-5. This result was confirmed by the signal enhancement of H-5 that was observed upon irradiation of methyl protons (H-12 and H-13) in an NOEDIFF experiment. According to the ^{1}H-COSY NMR spectral data (Table 4.2), H-4 and H-5 appeared as distinct singlet signals and no cross-peak signal was found, suggesting no correlation between these two protons. However, the NOE enhancement of H-4 was detected upon irradiation of H-5 as shown in Figure 4.1. Based on the HMBC and NOEDIFF results, H-4 and H-5 were attached on the neighboring carbon atoms and could thus be assigned as vicinal protons.

Table 4.1. Observed correlations in the HMQC spectrum of compound **2** ($CDCl_3$).

Carbon	**δ_C (ppm)**	**δ_H of correlated proton (ppm)**
C-2	144.6	-
C-4	132.0	7.51 (s, 1H, Ar*H*)
C-5	127.4	7.11 (br s, 1H, Ar*H*)
C-6	180.2	9.80 (s, 1H, C*H*O)
C-7	132.5	-
C-8	145.1	-
C-9	123.9	7.28 (d, *J* = 7.7 Hz, 2H, Ar*H*)
C-10	130.0	7.49 (t, *J* = 7.7 Hz, 1H, Ar*H*)
C-11	28.3	2.21 [sept, *J* = 6.8 Hz, 2H, (C*H*)$_2$]
C-12, C-13	24.6, 23.3	1.12 [d, *J* = 6.8 Hz, 6H, (C*H*$_3$)$_2$], 1.08 [d, *J* = 6.8 Hz, 6H, (C*H*$_3$)$_2$]

Table 4.2. Observed correlations in the COSY-45 spectrum of compound **2** ($CDCl_3$).

δ_H (ppm)	**δ_H of correlated proton (ppm)**
7.49 (H-10)	7.28 (H-9)
2.21 (H-11)	1.12 (H-12), 1.08 (H-13)

Table 4.3. Observed long-range C–H correlations in the HMBC spectrum of compound **2** ($CDCl_3$).

δ_H (ppm)	Carbon correlated with δ_H (ppm)
9.80 (H-6)	144.6 (C-2)
7.51 (H-4)	144.6 (C-2), 127.4 (C-5)
7.49 (H-10)	145.1 (C-8), 123.9 (C-9)
7.28 (H-9)	145.1 (C-8), 132.5 (C-7)
7.11 (H-5)	144.6 (C-2), 132.5 (C-7), 132.0 (C-4)
2.21 (H-11)	145.1 (C-8), 132.5 (C-7), 123.9 (C-9), 24.6 (C-12), 23.3 (C-13)
1.12 (H-12), 1.08 (H-13)	28.3 (C-11), 145.1 (C-8)

The structures of the imidazole-imine palladium complexes **4a**–**h** which were readily prepared from the reaction of ligands with $Pd(COD)Cl_2$ in chloroform also exhibited some characteristic ^{1}H NMR data and multiplicity of the two protons on the imidazole ring. Interestingly, their equivalent resonances were observed as doublet signals with low coupling constants ranging from 1.2 Hz to 1.6 Hz. For instance, the protons, H-4 and H-5, of complex **4h** appeared at 7.79 ppm and 7.07 ppm (J = 1.6 Hz), respectively, as shown in Figure 4.2. Similarly, in case of the free imine ligand **3h**, the protons also resonate as the doublet signals at 7.33 ppm and 6.94 ppm (J = 0.8 Hz) The appearance of a cross-peak signal of complex **4h** in a ^{1}H-COSY spectrum indicated the correlation between these imidazole protons (Table 4.5). The outcome of this study was also supported by the NOEDIFF results. Inspection of the NOEDIFF spectrum revealed the presence of NOE contacts which allow us to define the spatial relationship between the ligand protons, H-4 and H-5, as well as between the imine and H-16 methylene protons (Figure 4.1). Moreover, the ^{1}H NMR data was also used to confirm the coordination of complex **4h**. The upfield shift of the characteristic singlet signal of the imine proton, H-6, with respect to the free ligand ($\delta_{coord} - \delta_{free}$ = –0.8 ppm) was observed.

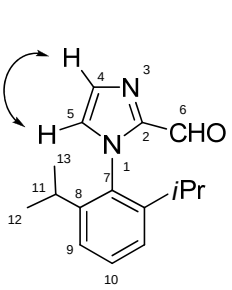

2

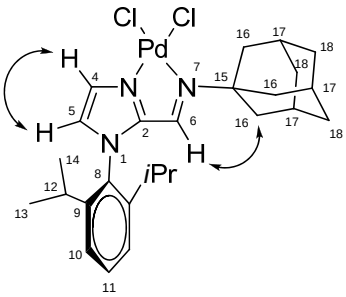

4h

Complex **4h**	δ (ppm)
H-4	7.79
H-5	7.07
H-6	7.20
H-16	2.09

Figure 4.1. Double arrows show the NOE contacts in aldehyde **2** and complex **4h**.

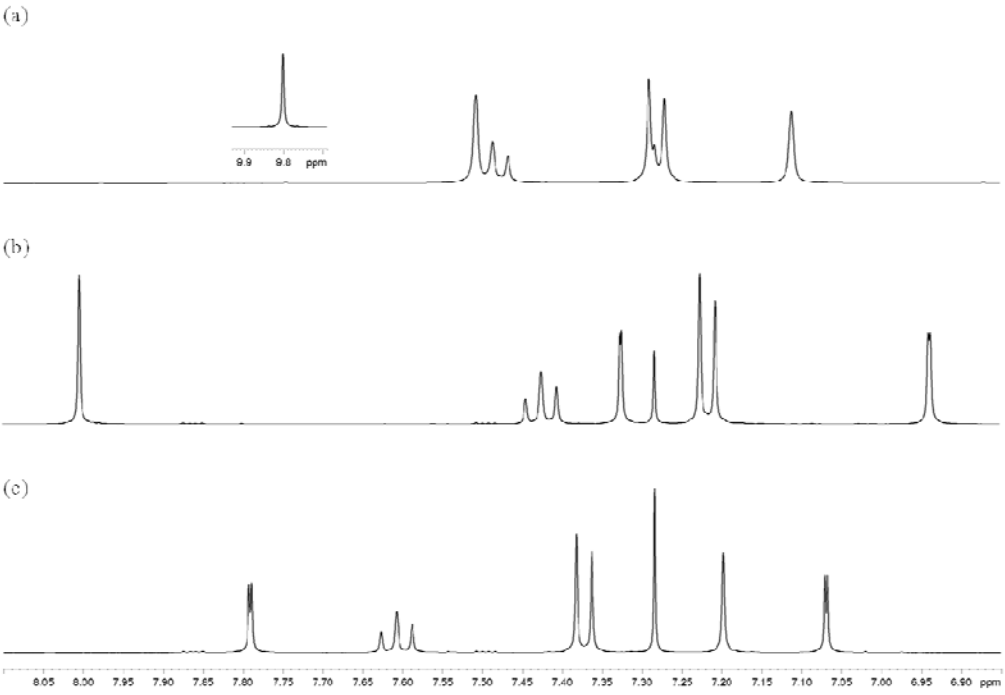

Figure 4.2. ^{1}H NMR spectra of (a) aldehyde **2**; (b) ligand **3h** and; (c) complex **4h**.

Table 4.4. Observed correlations in the HMQC spectrum of **4h** ($CDCl_3$).

Carbon	**δ_C (ppm)**	**δ_H of correlated proton (ppm)**
C-2	147.9	-
C-4	129.5	7.79 (d, *J* = 1.6 Hz, 1H, Ar*H*)
C-5	124.1	7.07 (d, *J* = 1.6 Hz, 1H, Ar*H*)
C-6	147.7	7.20 (s, 1H, N=C*H*)
C-9	145.8	-
C-8	129.7	-
C-10	124.9	7.37 (d, *J* = 7.7 Hz, 2H, Ar*H*)
C-11	132.1	7.61 (t, *J* = 7.7 Hz, 1H, Ar*H*)
C-12	28.5	2.27 [sept, *J* = 7.0 Hz, 2H, (C*H*)$_2$]
C-13, C-14	24.31, 24.30	1.20 [d, *J* = 7.0 Hz, 6H, (C*H*$_3$)$_2$], 1.14 [d, *J* = 7.0 Hz, 6H, (C*H*$_3$)$_2$].
C-15	67.0	-
C-16	42.1	2.09 [m, 6H, (C*H*$_2$)$_3$]
C-17	29.5	2.18 [m, 3H, (C*H*)$_3$]
C-18	35.5	1.70 [m, 6H, (C*H*$_2$)$_3$]

Table 4.5. Observed correlations in the COSY-45 spectrum of **4h** ($CDCl_3$).

δ_H (ppm)	**δ_H of correlated proton (ppm)**
7.79 (H-5)	7.07 (H-4)
7.61 (H-11)	7.37 (H-10)
2.27 (H-12)	1.20 (H-13), 1.14 (H-14)
2.18 (H-17)	2.09 (H-16), 1.70 (H-18)

Table 4.6. Observed long-range C–H correlations in the HMBC spectrum of **4h** ($CDCl_3$).

δ_H (ppm)	Carbon correlated with δ_H (ppm)
7.79 (H-4)	124.2 (C-5), 147.9 (C-2)
7.61 (H-11)	145.8 (C-9), 124.9 (C-10)
7.37 (H-10)	145.9 (C-9), 129.7 (C-8), 28.5 (C-12)
7.20 (H-6)	147.9 (C-2), 67.0 (C-15), 42.1 (C-16)
7.07 (H-5)	147.9 (C-2), 129.7 (C-8), 129.5 (C-4)
2.27 (H-12)	145.8 (C-9), 124.9 (C-10), 129.7 (C-8), 24.31 (C-13), 24.30 (C-14)
2.18 (H-17)	42.1 (C-16)
2.09 (H-16)	67.0 (C-15), 35.5 (C-18), 29.5 (C-17)
1.20 (H-13), 1.14 (H-14)	145.8 (C-9), 28.5 (C-12), 24.3 (C-13+C-14)

4.4 X-ray crystal structure

To further confirm the structure of the Pd complexes, crystals suitable for X-ray diffraction studies of **4b** and **4h** were obtained by slow diffusion of hexane into a chloroform solution. As shown in Figure 4.3 and 4.4, the solid state of both palladium complexes revealed a distorted square planar geometry around Pd(II) center with the angle sum of approximately 360º. The imidazole-imine ligand coordinates to Pd(II) in a bidentate binding mode through imidazole and imine nitrogen atoms as expected. The closest C---C distances between isopropyl aryl substituents on imidazole and imine substituents (2,6-*i*PrC_6H_3 and 1-adamantyl) are 3.993(13) Å (for **4b**) and 5.117(8) Å (for **4h**). The Pd–N1(imine) bond distances are slightly more than the expected range[38–40] and about 0.1 Å longer than those of Pd–N2(imidazole).[41] All Pd–Cl bond lengths are similar and in the range of 2.26–2.27 Å, indicating comparable trans influence of imidazole and imine ligands. The N1–Pd–N2 bite angles of **4b** and **4h** are 80.00(13)º and 80.04(9)º, respectively. Based on crystal data, 1-adamantyl substituent appears to be more sterically hindered than 2,6-*i*PrC_6H_3, as evidenced by

the unusually long Pd–N1 bond, larger N1–Pd–Cl2 angle of 101.33(7)° for **4h** [cf. 95.04(10)° for **4b**], and smaller Cl1–Pd–Cl2 angle of 88.45(3)° [cf. to 92.26(5)° for **4b**].

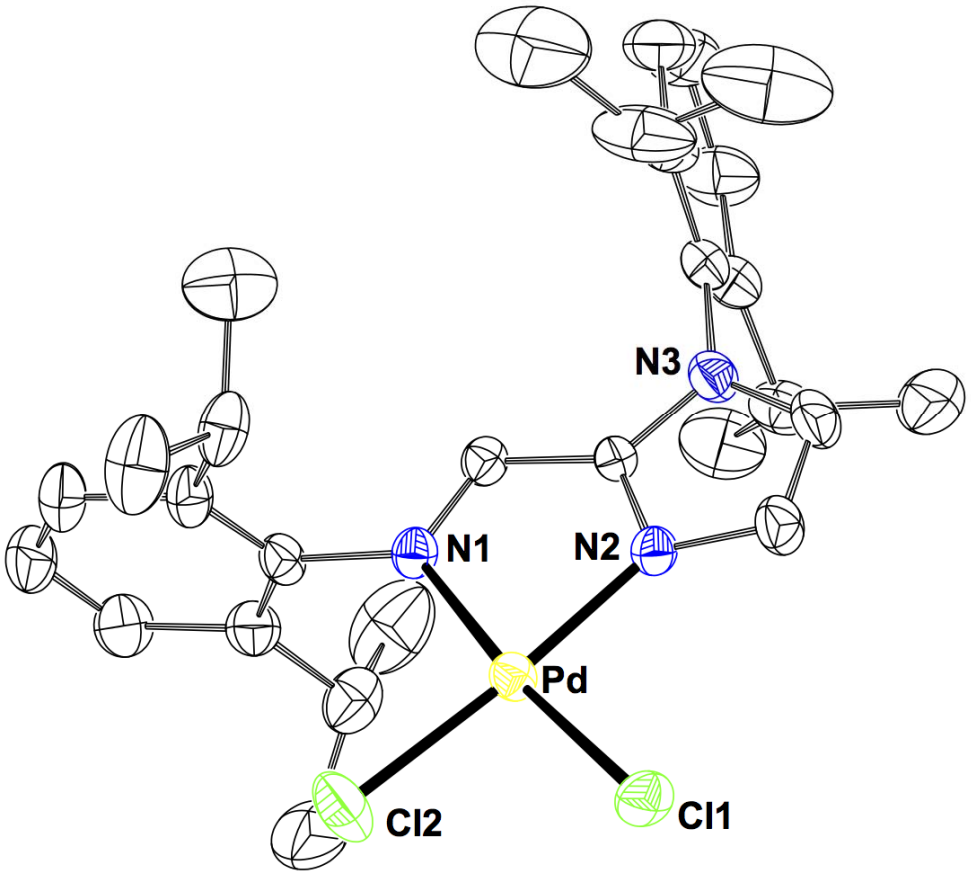

Figure 4.3. ORTEP diagram of **4b** with 30% probability ellipsoids and partial labeling scheme. Hydrogen atoms and a molecule of $CHCl_3$ are omitted for clarity.

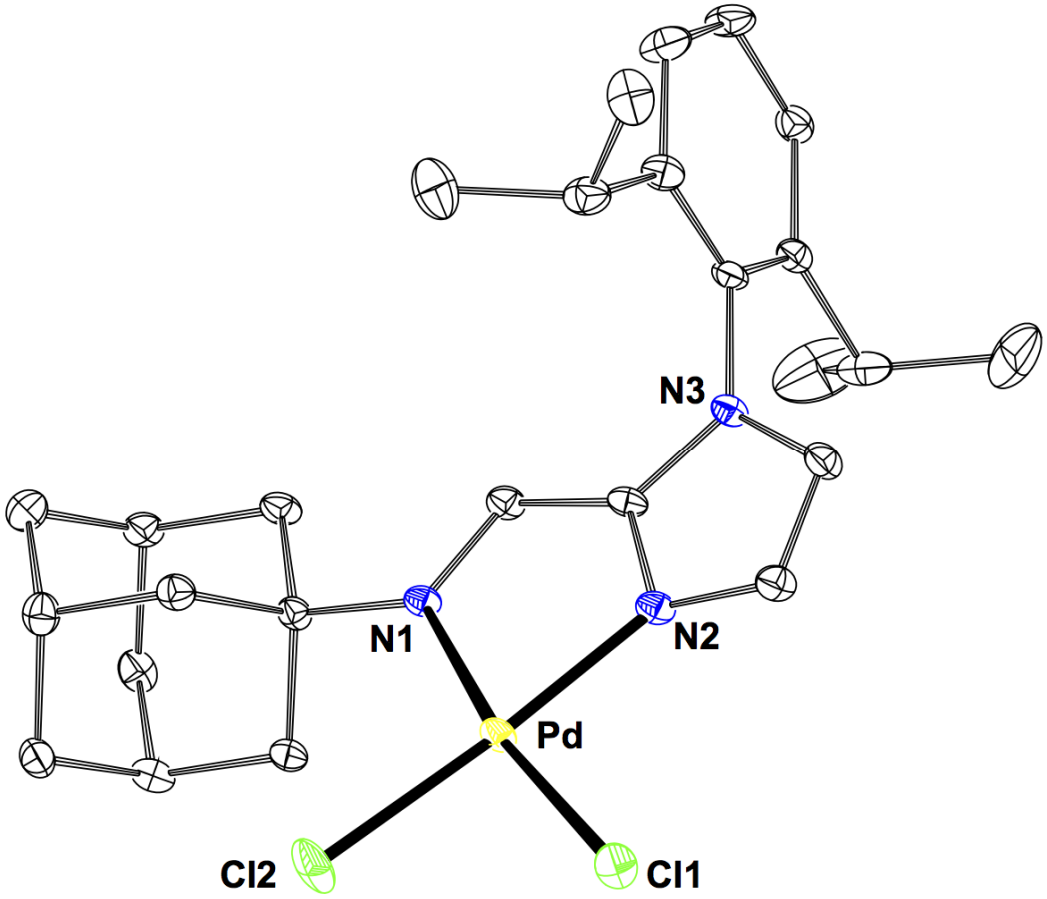

Figure 4.4. ORTEP diagram of **4h** with 30% probability ellipsoids and partial labeling scheme. Hydrogen atoms are omitted for clarity.

Table 4.7. Selected bond lengths (Å) and bond angles (°) for **4b** and **4h**.

	Bond length (Å)			Bond angle (°)	
	4b	**4h**		**4b**	**4h**
Pd–N1	2.073(3)	2.120(2)	N1–Pd–N2	80.00(13)	80.04(9)
Pd–N2	2.007(3)	2.002(2)	Cl1–Pd–Cl2	92.26(5)	88.45(3)
Pd–Cl1	2.273(1)	2.270(1)	N1–Pd–Cl2	95.04(10)	101.33(7)
Pd–Cl2	2.258(1)	2.272(1)	N2–Pd–Cl1	92.71(9)	90.60(7)

4.5 Screening of the effect of ligands on the Suzuki–Miyaura cross-coupling reaction

To evaluate the catalytic activity of **4a**–**4h** for the palladium-catalyzed Suzuki–Miyaura cross-coupling, a reaction between phenylboronic acid and *p*-bromoanisole was used as the model reaction at room temperature under aerobic conditions (Table 4.8). Interestingly, quantitative yields of the coupling product were obtained when catalysts **4b** and **4d** were used. Mercury poisoning experiment showed that Pd(0) nanoparticles (NPs) involved in catalytic cycle (see Section 4.9). On the basis of these findings, it is apparent that the π-acid property of the phenyl-substituted imine ligands enhances the reaction rates, especially with ligands **4b** and **4d** (entries 2 and 4). It is possible that the phenyl ring with *i*Pr group and nitro group may prevent the Pd(0)NPs aggregations, presumably by steric and electrostatic stabilization, respectivelty.[42] However, compared to **4b**, palladium complexes of the more sterically hindered imine ligands **4g** and **4h** afforded only moderate product yields (entries 7 and 8). Complexes **4e**–**4h** which were prepared with the alkyl substituents tend to result in lower yields than those with the aromatic ones. Moreover, appropriated steric bulks at the imine moiety are crucial to achieve good catalytic activities, as very large substituents such as *tert*-butyl and 1-adamantyl only showed low activities, presumably due to the difficult binding to Pd(0)NPs that leads to the deactivation of palladium via aggregations.

Table 4.8. Ligand screening for the Suzuki–Miyaura cross-coupling reaction between *p*-bromoanisole and phenylboronic acid.[a]

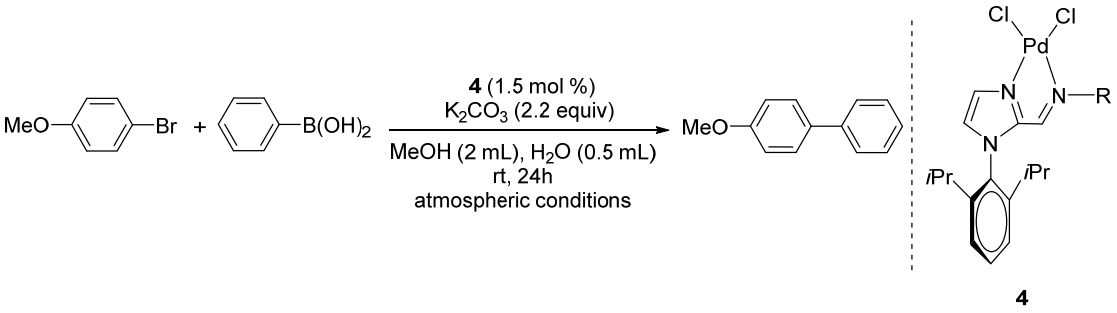

4

Entry	Complexes	R	Yield[b] (%)
1	**4a**		91
2	**4b**	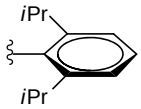	**>99**
3	**4c**		82
4	**4d**		**>99**
5	**4e**		88
6	**4f**		83
7	**4g**		73
8	**4h**	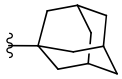	69

[a] Reaction condition: Pd catalyst (1.5 mol %), *p*-bromoanisole (0.5 mmol), phenylboronic acid (0.6 mmol), K_2CO_3 (1.1 mmol), MeOH (2 mL), H_2O (0.5 mL), rt, 24 h. All reactions were carried out in air.

[b] The yield was determined by GC analysis using hexamethylbenzene as a calibrated internal standard.

In comparison, the catalytic activity of palladium complexes containing the imidazole-imine ligands are superior to those with commercially available ligands including bipyridine (bipy), phenanthroline, BINAP, and in the absence of ligand (Table 4.9).

Table 4.9. Study the effect of commercially available ligands on the Suzuki–Miyaura cross-coupling reaction of *p*-bromoanisole with phenylboronic acid.[a]

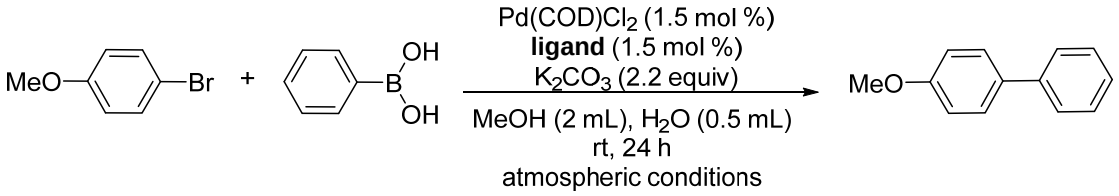

Entry	Pd source	Ligand	Premixing time (min)	Yield[b] (%)
1	-	-	-	0
2	$Pd(COD)Cl_2$	-	-	31
3	**$Pd(COD)Cl_2$**	**3b**	**15**	**49**
4	$Pd(COD)Cl_2$	bipy	15	13
5	$Pd(COD)Cl_2$	phen	15	0
6	$Pd(COD)Cl_2$	BINAP	15	23

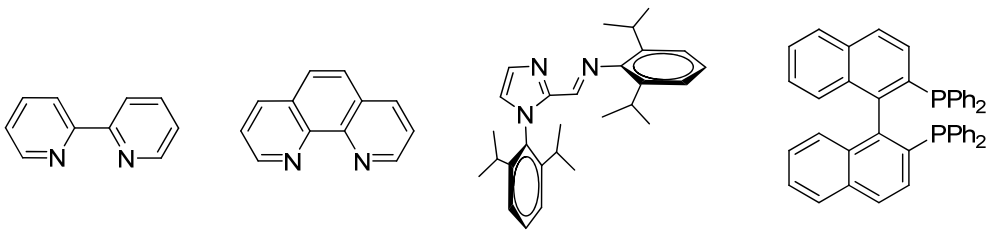

bipy phen **3b** BINAP

[a] Reaction condition: $Pd(COD)Cl_2$ (1.5 mol %), ligand (1.5 mol %), *p*-bromoanisole (0.5 mmol), phenylboronic acid (0.6 mmol), K_2CO_3 (1.1 mmol), MeOH (2 mL), H_2O (0.5 mL), rt, 24 h (catalysts were generated *in situ*). All reactions were carried out in air.

[b] The yield was determined by GC analysis using hexamethylbenzene as a calibrated internal standard.

4.6 Optimization of reaction condition on Suzuki–Miyaura cross-coupling reaction

After the catalytic activity of complex **4a**–**4h** were tested, various catalyst loadings, effect of reaction time, solvent (THF, DMF, acetonitrile, toluene, chloroform, acetone, DMSO, methanol and water), concentration and effect of base was subsequently investigated.

Despite the fact that both catalysts **4b** and **4d** exhibited similar catalytic properties, **4b** was chosen as the control catalyst for determining optimal conditions for palladium-catalyzed cross-coupling reaction of *p*-bromoanisole with phenylboronic acid due to the more complicated preparation of **4d**. The catalyst loading was initially examined. It was found that highly efficient catalysis could still be maintained even at catalyst loading as low as 0.15 mol % with a TON up to 666 (highest TON of 12,000 with 0.001 mol % catalyst loading) (Table 4.10). Complex **4b** also exhibited higher efficiencies in terms of yields/TONs than the majority of those reported for the similar *N*,*N*-bidentate palladium catalysts with 4-$MeOC_6H_4Br$ as a substrate. For example, the catalytic system consisting of $Pd(OAc)_2$/hydrazone[43] and $Pd(OAc)_2$/guadinine[26] were reported to have TONs up to 44.5 and 180, respectively. Also, the procedure using pyridyl-triazole ligands resulted in a TON up to 180.[44] Another pyridyl-triazole based catalytic system recently reported by Sangtrirutnugul and co-workers[45] exhibited a comparable activity (yields up to 85% with 0.1 mol % catalyst loading and a TON up to 850). An additional experiment under ambient conditions was carried out by varying the reaction time. The quantitative yield of 4-methoxybiphenyl could be achieved with the shortest reaction time of 4 h (Table 4.11).

Table 4.10. Catalytic activity of complex **4b** on the Suzuki–Miyaura cross-coupling reaction of *p*-bromoanisole with phenylboronic acid.[a]

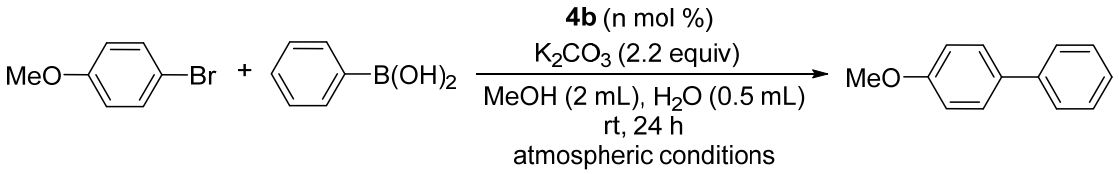

Entry	n mol %	Yield[b] (%)	TON
1	0.0001	0	0
2	0.001	12	12,000
3	0.01	85	8500
4	0.1	99	990
5	**0.15**	**>99**	**666**
6	0.2	>99	500
7	0.3	>99	333
8	0.4	>99	250
9	0.75	>99	133
10	1.5	>99	66
11	3	>99	33

[a] Reaction condition: *p*-bromoanisole (0.5 mmol), phenylboronic acid (0.6 mmol), K_2CO_3 (1.1 mmol), MeOH (2 mL), H_2O (0.5 mL), rt, 24h.

[b] The yield was determined by GC analysis using hexamethylbenzene as a calibrated internal standard.

Table 4.11. Investigation of reaction time on the Suzuki–Miyaura cross-coupling reaction of *p*-bromoanisole with phenylboronic acid.[a]

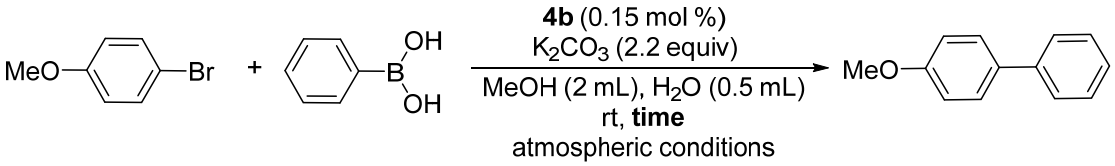

Entry	Time (h)	Yield[b] (%)
1	24	>99
2	16	>99
3	8	>99
4	**4**	**>99**
5	2	79
6	1	60

[a] Reaction condition: **4b** (0.15 mol %), *p*-bromoanisole (0.5 mmol), phenylboronic acid (0.6 mmol), K_2CO_3 (1.1 mmol), MeOH (2 mL), H_2O (0.5 mL), rt.

[b] The yield was determined by GC analysis using hexamethylbenzene as a calibrated internal standard.

The effect of solvent was also studied. The result in Table 4.12 showed that aprotic solvents such as THF, DMF, acetonitrile, toluene, chloroform, acetone, and DMSO afforded low product yields in the range of 2–27%. On contrary, higher coupling product yields were obtained in methanol. Interestingly, although the coupling reaction in H_2O resulted in a low product yield, a small percentage of water in methanol has a beneficial effect on the reaction rate as found with other catalytic systems (Table 4.12 and 4.13).[46–48] It was found that a 4:1 mixture of CH_3OH:H_2O at the *p*-bromoanisole concentration of 0.2 M provided the biaryl product in a quantitative yield. This might be a result of good stabilization and dispersion of Pd nanoparticles that could be explained by coordination bonds between the metal ions and hydroxyl group of methanol. It was reported that ionized OH group can act as a stabilizer for the size distributions in which the metal ion are dispersed in the methanol matrix.[49, 50] Additionally, the enhanced catalytic activity in the presence of water could be explained by the effect of water on the acceleration of Pd reduction which was

studied by Hii and co-workers.[51] The authors suggested that the reduction of palladium(II) acetate is accelerated by water, which can exchange with acetate anion to generate the Pd(II) hydroxide species. The Pd(II) hydroxide undergoes transmetalation with $ArB(OH)_2$ to form Ar–Pd–Ar adduct, followed by the regeneration of Pd(0) (Scheme 4.3). On the other hand, a small amount of water presumably increases the solubility of the inorganic base used in the Suzuki–Miyaura cross-coupling reaction.

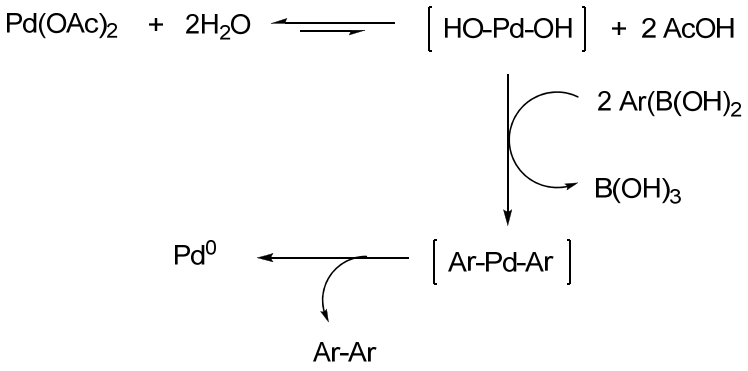

Scheme 4.3. Water effect on the reduction of palladium acetate to Pd(0).[51]

Table 4.12. Screening of solvents for the Suzuki–Miyaura cross-coupling reaction of *p*-bromoanisole with phenylboronic acid.[a]

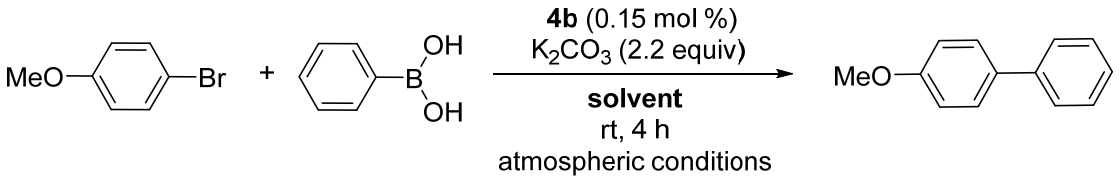

Entry	Solvent	Yield[b] (%)
1	THF	18
2	DMF	2
3	CH_3CN	4
4	toluene	27
5	$CHCl_3$	24
6	acetone	12
7	DMSO	0
8	**MeOH**	**71**
9	H_2O	6

[a] Reaction condition: **4b** (0.15 mol %), *p*-bromoanisole (0.5 mmol), phenylboronic acid (0.6 mmol), K_2CO_3 (1.1 mmol), solvent (2.5 mL), rt, 4 h.

[b] The yield was determined by GC analysis using hexamethylbenzene as a calibrated internal standard.

Table 4.13. Effect of mixed MeOH and H_2O in various ratios on the Suzuki–Miyaura cross-coupling reaction of *p*-bromoanisole with phenylboronic acid.[a]

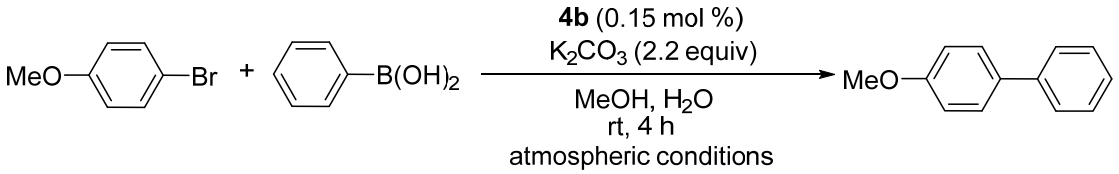

Entry	MeOH (ml)	H_2O (ml)	Concentration (M)	Yield[b] (%)
1	2.5	0	0.2	71
2	**2.0**	**0.5**	**0.2**	**>99**
3	1.5	1.0	0.2	57
4	1.0	1.5	0.2	28
5	0.5	2.0	0.2	15
6	0	2.5	0.2	6
7	0.5	0.125	0.8	67
8	1	0.25	0.4	77
9	4	1	0.1	78
10	8	2	0.05	60

[a] Reaction condition: **4b** (0.15 mol %), *p*-bromoanisole (0.5 mmol), phenylboronic acid (0.6 mmol), K_2CO_3 (1.1 mmol), rt, 4 h.

[b] The yield was determined by GC analysis using hexamethylbenzene as a calibrated internal standard.

Table 4.14. Screening of bases for the Suzuki–Miyaura cross-coupling reaction between *p*-bromoanisole and phenylboronic acid.[a]

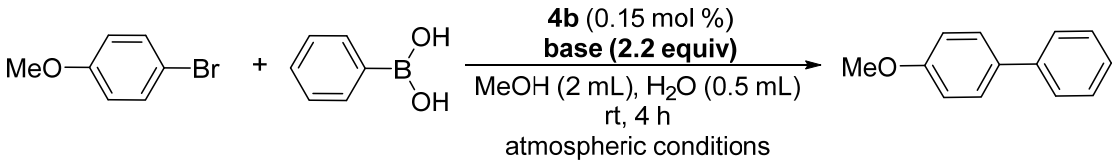

Entry	Base	Yield[b] (%)	Entry	Base	Yield[b] (%)
1	LiOH	89	8	K_3PO_4	76
2	NaOH	23	9	KF	21
3	KOH	82	10	KI	0
4	CsOH	95	11	KOMe	55
5	Na_2CO_3	82	12	KO*t*Bu	96
6	**K_2CO_3**	**>99**	13	NEt_3	48
7	Cs_2CO_3	91	14	-	0

[a] Reaction condition: **4b** (0.15 mol %), *p*-bromoanisole (0.5 mmol), phenylboronic acid (0.6 mmol), K_2CO_3 (1.1 mmol), MeOH (2 mL), H_2O (0.5 mL), rt, 4 h.

[b] The yield was determined by GC analysis using hexamethylbenzene as a calibrated internal standard.

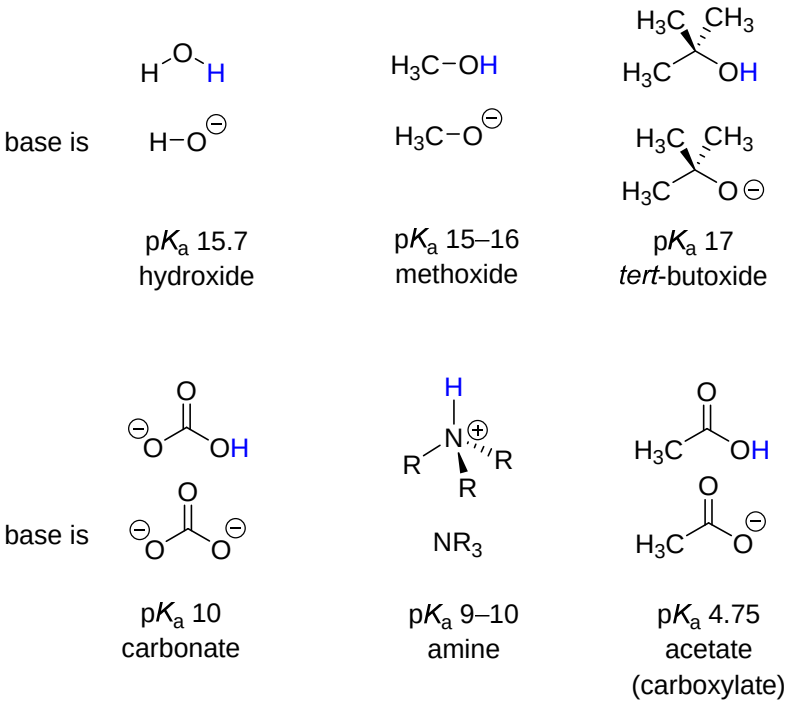

Scheme 4.4. pK_a value of common bases.[52]

Next, in order to determine which base offered the best result of the coupling reaction under the optimized conditions: 0.15 mol % of **4b** in the 4:1 CH_3OH:H_2O solvent, the various bases were screened. As a result, *p*-bromoanisole was successfully coupled with phenylboronic acid in the highest product yield when K_2CO_3 was used as a base (Table 4.14). The data showed that the product yield was not dependent on the pK_a of bases[52] (Scheme 4.4). For examples, the coupling product yield of 96% obtained by using KO*t*Bu as base is comparable to the yield afforded by using K_2CO_3 (>99%) (Table 4.14, entries 6 and 12), although the pK_a of carbonate base (pK_a = 10) is lower than that of *tert*-butoxide (pK_a = 17). When comparing the reactions in the presence of the hydroxide base (pK_a = 15.7) with that of the carbonate base (pK_a = 10), the similar trend of the experimental result was expected. In contrast, the reaction using KOH gave 82% yield whereas the other afforded the quantitative yield (Table 4.14, entries 3 and 6).

Recently, Amatore, Jutand and Le Duc studied the effects of anionic bases (OH^- and CO_3^{2-}) and their countercations (Na^+, Cs^+, K^+) on the Pd-catalyzed Suzuki–Miyaura cross-coupling reaction.[53] They revealed that the countercations kinetically

involved in the deceleration of the transmetalation step. A complexation of cation (M^+) with the OH group in [$Ar(PPh_3)_2Pd–OH$] to form **Pd-M**$^+$ species could account for the decelerating result, as shown in Scheme 4.5. This complexation would thus be competing with the transmetalation of [$Ar(PPh_3)_2Pd–OH$] by $ArB(OH)_2$. Therefore, higher the affinity of the cation for [$Ar(PPh_3)_2Pd–OH$], slower the transmetalation reaction. Base on the kinetic data, the affinity of the cations for the OH group of [$Ar(PPh_3)_2Pd–OH$] decreases in the order of $Na^+ > Cs^+ > K^+$. The authors mentioned that the experimental decelerating effect of the cation Cs^+ on the kinetic of the transmetalation ($Na^+ > Cs^+ > K^+$) was found to be inverted with respect to the expected one based on its ionic radius ($Na^+ > K^+ > Cs^+$). No simple explanation of this trend is available. Furthermore, the CO_3^{2-} anion can produce the OH^- in the presence of water traces. Hydroxide anions that are generated from carbonate anion can accelerate transmetalation due to the high concentration of [$Ar(PPh_3)_2Pd–OH$], and promote the reductive elimination in the catalytic cycle[54] (see Section 1.2 for additional details). This could be a reason why K_2CO_3 performed the best catalytic activity and gave the highest yield in the Suzuki–Miyaura cross-coupling reaction studied in this thesis.

Although the reaction required water to generated OH^- anions, the poor result was obtained when the amount of water increased (Table 4.13). The low solubility of organic substrates in water could be a possible reason. Therefore, there is a restriction on the amount of water added in the reaction in order to obtain the quantitative yield.

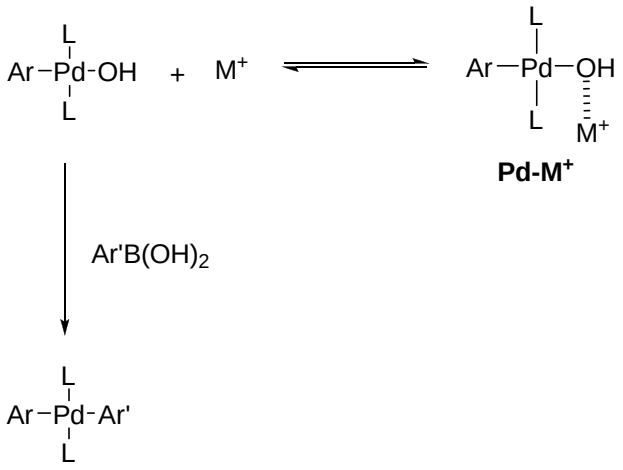

Scheme 4.5. Competitive complexation/transmetalation in the presence of cation M^+.[53]

4.7 Study of substrate scope for the Suzuki–Miyaura cross-coupling reaction between aryl halides and phenylboronic acid

Under the optimized reaction conditions, a wide variety of aryl halide substrates were highly reactive, generally giving the desired coupling products in quantitative yields (Table 4.15). The substrate scope was found to be remarkably broad, as the reaction tolerated both electron-donating and electron-withdrawing substituents affording good to excellent yields. For example, with the exception of *ortho*-methoxy substituent, the electron-donating methoxy groups at *meta* and *para* positions gave the corresponding coupling products in quantitative yields (entries 2–5). Most aryl halides with an electron-withdrawing substituent resulted in excellent product yields *i.e.*, more than 90% (entries 7–12), except for *para*-fluoro (65%), hydroxyl (84%), and phenyl (86%) groups (entries 13–15). When heterocyclic halides were used as substrates, moderate yields of the coupling products were obtained (entries 16–18), presumably due to nitrogen coordination and subsequent inactivation of the palladium catalyst. Based on the results thus far, no significant effect on product yields was observed from varying aryl bromide substrates, suggesting relatively fast oxidative addition. Moreover, no reaction was observed when *p*-chloroanisole was used as a substrate (entry 6).

Table 4.15. Study of substrate scope for the Suzuki–Miyaura cross-coupling reaction between aryl halides and phenylboronic acid.[a]

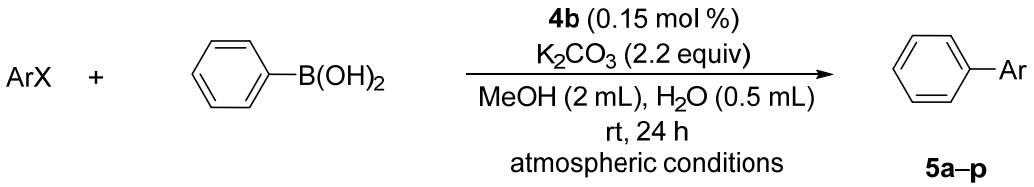

Entry	ArX	Product	Yield[b] (%)
1	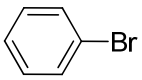	**5a**	95
2	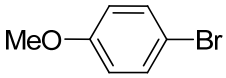	**5b**	>99[c]
3	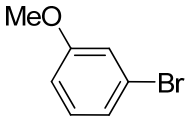	**5c**	>99
4	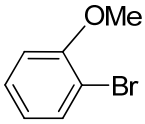	**5d**	68
5	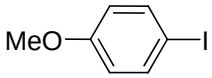	**5b**	95[c]
6	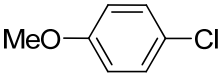	**5b**	0[d]
7	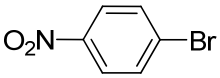	**5e**	92
8	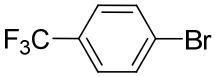	**5f**	>99
9	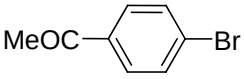	**5g**	>99

[a] Reaction condition: **4b** (0.15 mol %), aryl halide (0.5 mmol), phenylboronic acid (0.6 mmol), K_2CO_3 (1.1 mmol), MeOH (2 mL), H_2O (0.5 mL), rt, 24 h. All reactions were carried out in air.

[b] Isolated yield.

[c] GC yield.

[d] No reaction was detected by TLC/GCMS

[e] 1.5 mol % of **4b**.

Table 4.15 (cont.). Study of substrate scope for the Suzuki–Miyaura cross-coupling reaction between aryl halides and phenylboronic acid.[a]

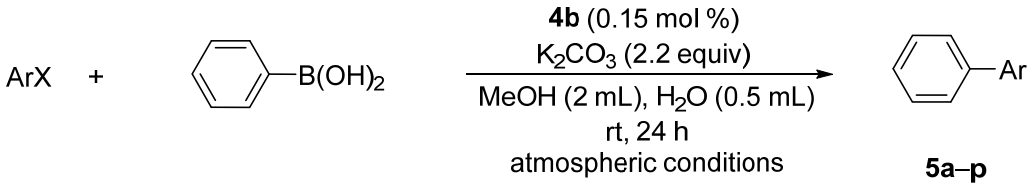

Entry	ArX	Product	Yield[b] (%)
10	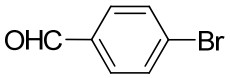	**5h**	91
11	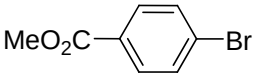	**5i**	97
12	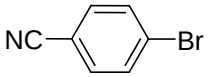	**5j**	98
13	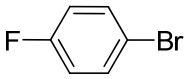	**5k**	65
14	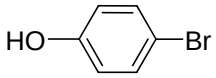	**5l**	84
15	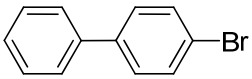	**5m**	86
16	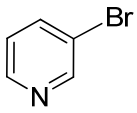	**5n**	60[e]
17	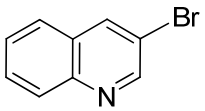	**5o**	41[e]
18	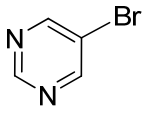	**5p**	45[e]

[a] Reaction condition: **4b** (0.15 mol %), aryl halide (0.5 mmol), phenylboronic acid (0.6 mmol), K_2CO_3 (1.1 mmol), MeOH (2 mL), H_2O (0.5 mL), rt, 24 h. All reactions were carried out in air.

[b] Isolated yield.

[c] GC yield.

[d] No reaction was detected by TLC/GCMS

[e] 1.5 mol % of **4b**.

4.8 Study of substrate scope for the Suzuki–Miyaura cross-coupling reaction between aryl halides and arylboronic acids

In Table 4.16, C–C coupling between the electron-rich 4-methoxyphenylboronic acid and bromobenzene gave products in high yields (entries 1–3). However, the yields decreased with the electron-withdrawing 4-acetylphenylboronic acid substrate (entries 4 and 5). Furthermore, an electron-deficient acetyl substituent on aryl bromide afforded an increase in product yields, from 80% to 90% (entries 1 and 6). It seems that although electronic properties of aryl halides do not significantly affect the reaction rates, the presence of electron-withdrawing substituent on phenylboronic acid apparently decreases product yields. One possible reason is that electron-deficient arylboronic acids are less nucleophilic and, as a consequence, transmetalate slower than electron-neutral/rich analogues.[55] A drop of the coupling product yield observed when the poorly nucleophilic arylboronic acids were used indicated that the transmetalation might be the rate determining step in this Suzuki–Miyaura cross-coupling reaction.

Table 4.16. Study of substrate scope for the Suzuki–Miyaura cross-coupling reaction between aryl halides and arylboronic acids.[a]

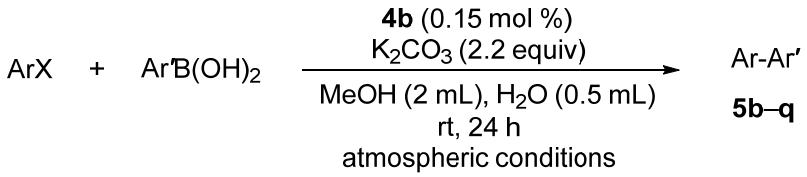

Entry	ArX	Ar′B(OH)$_2$	Product	Yield[b] (%)
1	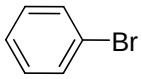	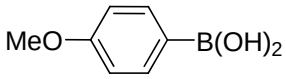	**5b**	80
2	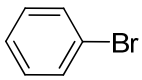	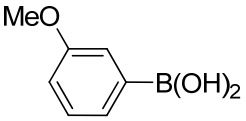	**5c**	75
3	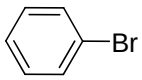	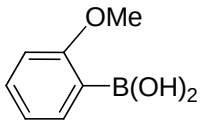	**5d**	85[c]
4	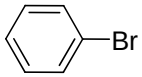	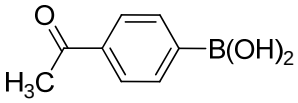	**5g**	64[c]
5	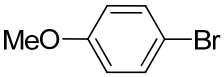	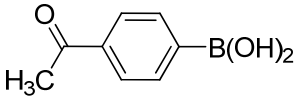	**5q**	68[c]
6	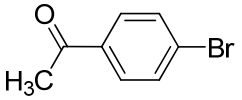	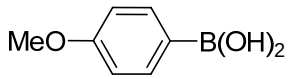	**5q**	90[c]

[a] Reaction condition: **4b** (0.15 mol %), aryl halide (0.5 mmol), arylboronic acid (0.6 mmol), K_2CO_3 (1.1 mmol), MeOH (2 mL), H_2O (0.5 mL), rt, 24 h. All reactions were carried out in air.

[b] Isolated yield.

[c] 1.5 mol % of **4b**.

4.9 Mercury poisoning test

It should be noted that, formation of palladium black was not observed with catalyst **4b** during the course of the reactions. However, to elucidate whether Pd(0) nanoparticles are involved in the reaction, mercury poisoning test with **4b** was also carried out. A coupling reaction between *p*-bromoanisole and $PhB(OH)_2$ in the presence of excess Hg (Hg:Pd = 400:1) under the reaction conditions described for entry 2 (Table 4.15) showed a decrease of product yield (down to 33%). The drop in the coupling product yield implies that the cross-coupling reactions were catalyzed, to some extent, by heterogeneous Pd(0) nanoparticles.[14, 15] Pd(0) that is obtained from Pd(II) reduction might first dissociate from the ligand followed by the Pd aggregration to form the Pd(0) nanoparticles. The ligands consequently coordinate to stabilize the Pd(0) nanoparticles and prevent the catalyst aggregation (see Section 4.5 for additional details). Furthermore, a previous study on the catalytic active of Pd(0) species in the Suzuku–Miyaura cross-coupling reaction has shown that O_2 can prevent Pd(0) nanoparticle aggregation (Figure 4.5),[51] probably by inhibiting the formation of Pd–Pd bond through the reoxidation of some palladium species.[56] This could be a reason why this catalytic system can be operated in air.

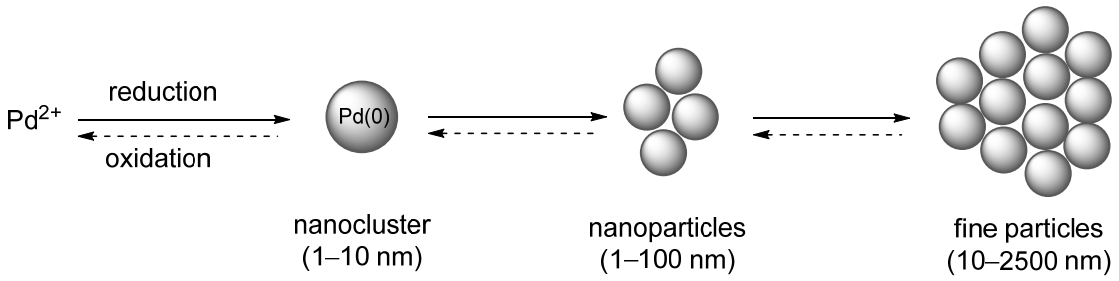

Figure 4.5. Process of catalyst activation and deactivation by aggregation.[51]

CHAPTER V
CONCLUSION

In summary, a new class of palladium complexes (**4a**–**4h**) was prepared by the reaction between Pd(COD)Cl_2 and corresponding imidazole-imine ligands. Complexes (**4a**–**4h**) were characterized by ^{1}H, ^{13}C NMR spectroscopy, HRMS and elemental analysis. According to X-ray crystallographic studies, **4b** and **4h** revealed the similar square planar structure using the N donor of the imidazole ring and imine moieties to coordinate to the Pd metal.

The palladium complexes **4b** and **4d** were found to be effective catalysts for the Suzuki–Miyaura cross-coupling reaction. Complex **4b** was chosen as the controlled catalyst for the cross-coupling reaction of aryl halides and arylboronic acid because of the complicated preparation of **4d**. An efficient protocol for the aerobic Pd-catalyzed Suzuki–Miyaura cross-coupling reaction was successfully developed by using K_2CO_3 (2.2 equiv) as a base in the presence of MeOH (2 mL) and H_2O (0.5 mL) as a solvent at room temperature under air atmosphere for 4 h (for 0.5 mmol scale of aryl halide substrates). It was found that the coupling product yield was not affected by the pK_a of bases. The use of imidazole-imine supporting ligands offers substantial improvements including air-stability and catalytic efficiency. Given that high product yields could be achieved for a wide range of substrates with the catalyst loading as low as 0.15 mol % under mild reaction conditions in air. Under optimized reaction conditions, coupling products from a wide range of aryl halides and arylboronic acids were obtained in excellent yields.

Mercury poisoning test suggested that the Suzuki–Miyaura cross-coupling reaction was catalyzed, to some extent, by Pd(0) NPs. Furthermore, the role of O_2 for preventing Pd(0) NPs aggregation through the reoxidation of some palladium species was proposed to support a reason why this reaction can be performed in air.

CHAPTER VI
EXPERIMENTAL SECTION

6.1 General methods

All reagents were purchased from commercial sources (Aldrich, Merck and Fluka) and used without further purification. *n*-BuLi was titrated with diphenylacetic acid to confirm the correct concentration. DMF was distilled from CaH_2, stored over 4 Å molecular sieves, and handled under argon atmosphere. Thin layer chromatography (TLC) was purchased on Merck siliga gel 60 F254 aluminium sheets. Column chromatography was performed using Merck silica gel 60 (70–230 mesh.). NMR spectra were recorded on a Bruker DPX-300 (300 MHz) and Bruker Ascend^{TM} 400 (400 MHz) spectrometer. The chemical shifts (δ) for ^{1}H are given in ppm and referenced to the residual proton signal of the deuterated solvent. The chemical shifts (δ) for ^{13}C are referenced relative to the signal from the carbon of the deuterated solvent. The high resolution mass spectra were recorded on HR-TOF-MS Micromass model VQ-TOF2 spectrometer. The elemental analyses were performed by Perkin Elmer Elemental Analyzer 2400 CHN. Gas chromatography analysis was performed on Agilent Technologies 6890N with FID detector and HP-1 capillary column (polymethylsiloxane, 25 m, 0.32 mm, 0.17 μm film thickness). Gas chromatography-mass analysis was performed on Agilent Technologies 7890A with 5975C inert XL MSD with Triple-Axis detector and HP-5 capillary column (polydimethylsiloxane with 5% phenyl group, 20 m, 0.25 mm, 0.25 μm film thickness) using helium as a carrier gas.

6.2 Synthesis of 1-(2,6-diisopropylphenyl)-1*H*-imidazole-2-carboxaldehyde

6.2.1 Synthesis of 1-(2,6-diisopropylphenyl)-1*H*-imidazole (1)

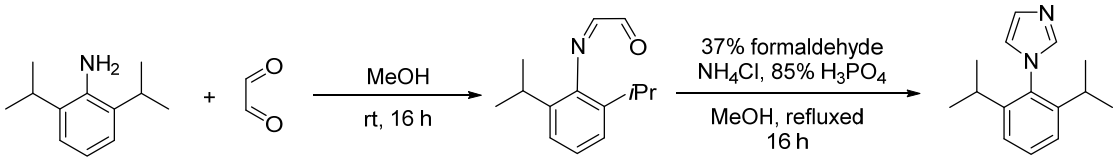

1

In a 100 mL round-bottomed flask equipped with a magnetic stir bar was charged with 2,6-diisopropylaniline (3.5 g, 20 mmol, 1.0 equiv) in MeOH (20 mL). The solution of glyoxal dihydrat (1.16 g, 20 mmol, 1.0 equiv) in water (3.3 mL) was added to the reaction flask. After stirring at room temperature for 16 h, a yellowish mixture was formed. NH_4Cl (2.14 g, 40 mmol, 2.0 equiv) and 37% aq formaldehyde (3.2 mL, 40 mmol, 2.0 equiv) was subsequently added. The mixture was diluted with MeOH (80 mL) and the resulting mixture was refluxed for 1 h. The reaction was allowed to cool to room temperature. 85% aq H_3PO_4 (2.8 mL) was carefully added to reaction flask. The resulting mixture was stirred at refluxing temperature for 16 h. After removal of the solvent, the brown residue was poured onto ice (30 g) and neutralized with 40% aq KOH solution until the pH 9. The mixture was extracted with ether (3 × 20 mL). The combined organic phase was washed with water (2 × 20 mL), brine (1 × 20 mL) and dried over Na_2SO_4. The solvent was removed under reduced pressure. The crude product was purified by column chromatography (SiO_2,ethyl acetate) and recrystallized by using MeOH and water to afford product **1** (1.59 g, 35%) as a white solid. The NMR spectra of **1** agree with the literature data.[35]

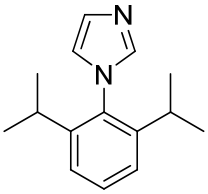

1

^{1}H NMR (300 MHz, $CDCl_3$): δ 7.48 (s, 1H, Ar*H*), 7.46 (t, *J* = 7.9 Hz, 1H, Ar*H*), 7.28 (s, 1H, Ar*H*), 7.27 (d, *J* = 7.4 Hz, 2H, Ar*H*), 6.96 (s, 1H, Ar*H*), 2.41 (sept, *J* = 6.9 Hz, 2H, C*H*), 1.15 [d, *J* = 6.9 Hz, 12H, $(CH_3)_4$].

^{13}C NMR (75 MHz, $CDCl_3$): δ 146.5 (2 × C), 138.5 (CH), 132.8 (C), 129.8 (CH), 129.3 (CH), 123.7 (2 × CH), 121.5 (CH), 28.1 (2 × CH), 24.4 (2 × CH_3), 24.3 (2 × CH_3).

HRMS (ESI): calcd. for $C_{15}H_{21}N_2$ [M^+ + H] 229.1705; found: 229.1727.

Anal. Calcd. for $C_{15}H_{20}N_2$: C, 78.90; H, 8.83; N, 12.27. Found: C, 79.91; H, 9.38; N, 12.30.

6.2.2 Synthesis of 1-(2,6-diisopropylphenyl)-1*H*-imidazole-2-carboxaldehyde (2)

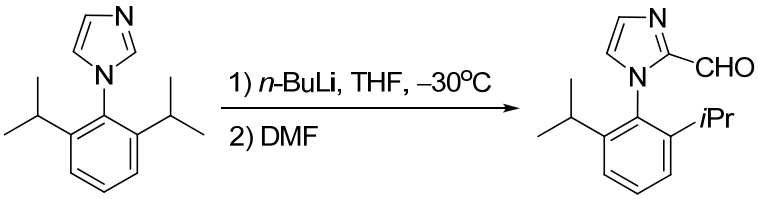

1 **2**

In a 100 mL round-bottomed flask equipped with a magnetic stir bar was charged with 1-(2,6-diisopropylphenyl)-1*H*-imidazole (855 mg, 3.74 mmol, 1.0 equiv), closed with three-way, evacuated and backfilled with argon (this procedure was repeated three times). Dry THF (20 mL) was added via syringe. Then *n*-BuLi (1.17 M in hexane, 3.9 mL, 4.48 mmol, 1.2 equiv) was slowly added at –30 °C. The reaction mixture was allowed to warm to room temperature and stirred for 3 h. The color of solution changed from yellow to brown. Dry DMF (0.45 mL, 5.61 mmol, 1.5

equiv) was added under argon atmosphere and continually stirred for 16 h. The saturated NH_4Cl solution was added to reaction flask and poured into the separatory funnel. The aqueous phase was extracted with CH_2Cl_2 (3 × 10 mL), washed with brine (1 × 10 mL) and dried over Na_2SO_4. The combined organic phase was concentrated under vacuum. The crude product was purified by column chromatography (SiO_2, CH_2Cl_2) to afford the pure product **2** (955 mg, 99%) as a white solid.

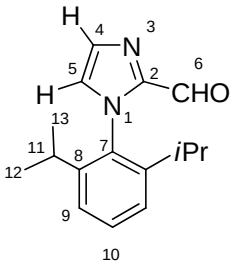

2

^{1}H NMR (400 MHz, $CDCl_3$): δ 9.80 (s, 1H, C*H*O), 7.51 (s, 1H, Ar*H*), 7.49 (t, *J* = 7.7 Hz, 1H, Ar*H*), 7.28 (d, *J* = 7.7 Hz, 2H, Ar*H*), 7.11 (br s, 1H, Ar*H*), 2.21 [sept, *J* = 6.8 Hz, 2H, (C*H*)$_2$], 1.12 [d, *J* = 6.8 Hz, 6H, (C*H*$_3$)$_2$], 1.08 [d, *J* = 6.8 Hz, 6H, (C*H*$_3$)$_2$].

^{13}C NMR (75 MHz, $CDCl_3$): δ 180.2 (CH), 145.1 (2 × C), 144.6 (C), 132.5 (C), 132.0 (CH), 130.0 (CH), 127.4 (CH), 123.9 (2 × CH), 28.3 (2 × CH), 24.6 (2 × CH_3), 23.3 (2 × CH_3).

HRMS (ESI): calcd. for $C_{16}H_{21}N_2O$ [M^+ + H] 257.1654; found: 257.1631.

Anal. Calcd. for $C_{16}H_{20}N_2O$: C, 74.97; H, 7.86; N, 10.93. Found: C, 75.88; H, 8.20; N, 11.04.

Table 6.1. Observed correlations in the HMQC spectrum of **2** ($CDCl_3$).

Carbon	**δ_C (ppm)**	**δ_H of correlated proton (ppm)**
C-2	144.6	-
C-4	132.0	7.51 (s, 1H, Ar*H*)
C-5	127.4	7.11 (br s, 1H, Ar*H*)
C-6	180.2	9.80 (s, 1H, C*H*O)
C-7	132.5	-
C-8	145.1	-
C-9	123.9	7.28 (d, *J* = 7.7 Hz, 2H, Ar*H*)
C-10	130.0	7.49 (t, *J* = 7.7 Hz, 1H, Ar*H*)
C-11	28.3	2.21 [sept, *J* = 6.8 Hz, 2H, (C*H*)$_2$]
C-12, C-13	24.6, 23.3	1.12 [d, *J* = 6.8 Hz, 6H, (C*H*$_3$)$_2$], 1.08 [d, *J* = 6.8 Hz, 6H, (C*H*$_3$)$_2$]

Table 6.2. Observed correlations in the COSY-45 spectrum of **2** ($CDCl_3$).

δ_H (ppm)	**δ_H of correlated proton (ppm)**
7.49 (H-10)	7.28 (H-9)
2.21 (H-11)	1.12 (H-12), 1.08 (H-13)

Table 6.3. Observed long-range C–H correlations in the HMBC spectrum of **2** ($CDCl_3$).

δ_H (ppm)	**Carbon correlated with δ_H (ppm)**
9.80 (H-6)	144.6 (C-2)
7.51 (H-4)	144.6 (C-2), 127.4 (C-5)
7.49 (H-10)	145.1 (C-8), 123.9 (C-9)
7.28 (H-9)	145.1 (C-8), 132.5 (C-7)
7.11 (H-5)	144.6 (C-2), 132.5 (C-7), 132.0 (C-4)
2.21 (H-11)	145.1 (C-8), 132.5 (C-7), 123.9 (C-9), 24.6 (C-12), 23.3 (C-13)
1.12 (H-12), 1.08 (H-13)	28.3 (C-11), 145.1 (C-8)

NOE data of compound 2

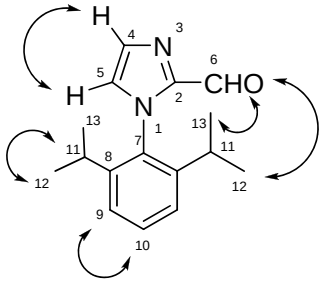

2

6.3 Synthesis of $Pd(COD)Cl_2$

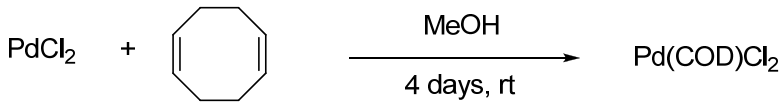

In a 100 mL round-bottomed flask equipped with a magnetic stir bar was charged with $PdCl_2$ (1.0 g, 5.64 mmol, 1.0 equiv) in MeOH (30 mL). Cyclooctadiene (2.1 mL, 16.92 mmol, 3.0 equiv) was added with a syringe, capped with a stopper, and stirred for 4 days at room temperature. The color of the suspension changed from red to yellow. The yellow solid was collected on a glass-frit, washed with methanol, and dried under vacuum to afford the $Pd(COD)Cl_2$ (140.7 mg, 87%) as yellow powder. The NMR spectra of $Pd(COD)Cl_2$ agree with the literature data.[36]

^{1}H NMR (400 MHz, $CDCl_3$): δ 6.34 [s, 4H, (C*H*)$_4$], 2.99–2.90 [m, 4H, (C*H*$_2$)$_2$], 2.60–2.56 [m, 4H, (C*H*$_2$)$_2$].

^{13}C NMR (100 MHz, $CDCl_3$): δ 116.7 (4 × CH), 31.0 (4 × CH_2).

Anal. Calcd. for $C_8H_{12}Cl_2Pd$: C, 33.65; H, 4.24. Found: C, 33.58; H, 4.17.

6.4 General procedure for the preparation of palladium complexes (4a–h)

In a 50 mL round-bottomed flask equipped with a magnetic stir bar and a reflux condenser was charged with 1-(2,6-diisopropylphenyl)-1*H*-imidazole-2-carboxaldehyde (1.0 equiv) and the corresponding primary amine (1.0 equiv). Then, MeOH (6 mL) was added into the reaction vial. The reaction mixture was refluxed for 16 h and concentrated under reduced pressure to afford the target imine ligand (the imine ligand was used in the next step without further purification). (Note: If the starting material is *p*-nitroaniline, a Dean-Stark trap will be used and the reaction mixture will be refluxed for 48 h) In a 10 mL vial equipped with magnetic stir bar was charged with $Pd(COD)Cl_2$ (1.0 equiv) and the corresponding imine ligand (1.0 equiv) under air condition. Chloroform (0.05 M) was added as solvent into the reaction vial. The resulting red-orange solution was stirred at room temperature for 1 h. The solvent

was evaporated. The crude product was recrystallized three times by using chloroform and hexanes to give pure palladium complexes.

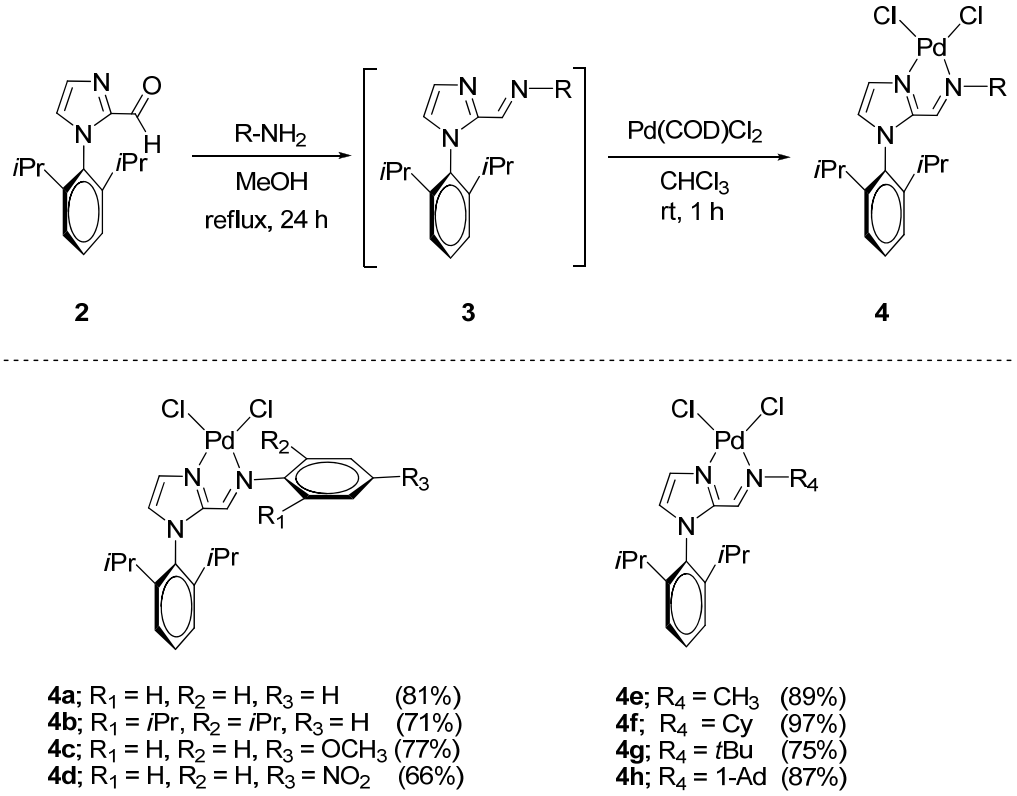

Scheme 6.1. Synthesis of palladium complexes (**4a**–**4h**).

6.4.1 Synthesis of palladium complex (4a)

(1-(2,6-Diisopropylphenyl)-1*H*-imidazol-2-yl)methylene)aniline ligand was prepared from **2** (76.9 mg, 0.3 mmol, 1.0 equiv) and aniline (27.4 μL, 0.3 mmol, 1.0 equiv) in MeOH (6 mL, 0.05 M). The crude imine ligand was reacted with $Pd(COD)Cl_2$ (86.2 mg, 0.3 mmol, 1.0 equiv) in chloroform (6 mL, 0.05 M) following the General procedure for the preparation of palladium complexes to afford complex **4a** as a red crystalline (124 mg, 81%).

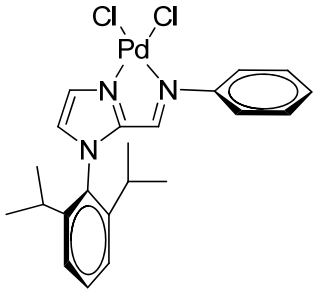

4a

^{1}H NMR (400 MHz, $CDCl_3$): δ 7.84 (d, *J* = 1.4 Hz, 1H, Ar*H*), 7.59 (t, *J* = 8.0 Hz, 1H, Ar*H*), 7.49 (s, 1H, N=C*H*), 7.40–7.36 (m, 5H, Ar*H*), 7.30–7.27 (m, 2H, Ar*H*), 7.25 (d, *J* = 1.4 Hz, 1H, Ar*H*), 2.35 [sept, *J* = 6.9 Hz, 2H, (C*H*)$_2$], 1.21 [d, *J* = 6.9 Hz, 6H, (CH_3)$_2$], 1.19 [d, *J* = 6.9 Hz, 6H, (CH_3)$_2$].

^{13}C NMR (75 MHz, $CDCl_3$): δ 151.5 (CH), 147.5 (C), 146.7 (C), 145.8 (2 × C), 132.2 (CH), 130.3 (CH), 129.6 (C), 129.5 (CH), 128.7 (2 × CH), 126.0 (CH), 124.9 (2 × CH), 123.7 (2 × CH), 28.6 (2 × CH), 24.6 (2 × CH_3), 24.2 (2 × CH_3).

HRMS (ESI): calcd. for $C_{22}H_{25}Cl_2N_3PdNa$ [M^+ + Na] 532.0351; found: 532.0352.

Anal. Calcd. for $C_{22}H_{25}Cl_2N_3Pd$: C, 51.94; H, 4.95; N, 8.26. Found: C, 49.95; H, 5.02; N, 7.72.

6.4.2 Synthesis of palladium complex (4b)

(1-(2,6-Diisopropylphenyl)-1*H*-imidazol-2-yl)methylene)-2,6-diisopropylaniline ligand was prepared from **2** (76.9 mg, 0.3 mmol, 1.0 equiv) and 2,6-diisopropylamine (56.6 μL, 0.3 mmol, 1.0 equiv) in MeOH (6 mL, 0.05 M). The crude imine ligand was reacted with $Pd(COD)Cl_2$ (86.2 mg, 0.3 mmol, 1.0 equiv) in chloroform (6 mL, 0.05 M) following the General procedure for the preparation of palladium complexes to afford complex **4b** as a red crystalline (127 mg, 71%).

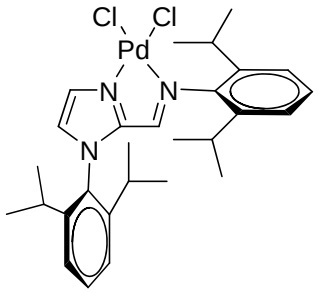

4b

^{1}H NMR (300 MHz, $CDCl_3$): δ 7.88 (d, *J* = 1.2 Hz, 1H, Ar*H*), 7.57 (t, *J* = 7.9 Hz, 1H, Ar*H*), 7.47 (s, 1H, N=C*H*), 7.35–7.26 (m, 3H, Ar*H*), 7.14 (d, *J* = 7.9 Hz, 2H, Ar*H*), 3.27 [sept, *J* = 6.9 Hz, 2H, (C*H*)$_2$], 2.34 [sept, *J* = 6.7 Hz, 2H, (C*H*)$_2$], 1.42 [d, *J* = 6.9 Hz, 6H, (C*H*$_3$)$_2$], 1.21 [d, *J* = 6.7 Hz, 6H, (C*H*$_3$)$_2$], 1.18 [d, *J* = 6.7 Hz, 6H, (C*H*$_3$)$_2$], 1.06 [d, *J* = 6.9 Hz, 6H, (C*H*$_3$)$_2$].

^{13}C NMR (75 MHz, $CDCl_3$): δ 207.0 (C), 153.8 (CH), 146.8 (C), 145.7 (2 × C), 142.6 (C), 140.6 (2 × C), 132.3 (CH), 130.3 (CH), 129.6 (C), 128.9 (CH), 126.3 (CH), 124.8 (3 × CH), 123.3 (3 × CH), 28.7 (CH), 24.7 (2 × CH_3), 24.2 (2 × CH_3), 23.8 (2 × CH_3), 23.2 (2 × CH_3).

HRMS (ESI): calcd. for $C_{28}H_{37}Cl_2N_3PdNa$ [M^+ + Na] 616.1291; found: 616.1291.

Anal. Calcd. for $C_{28}H_{37}Cl_2N_3Pd$: C, 56.72; H, 6.29; N, 7.09. Found: C, 56.85; H, 6.74; N, 7.15.

6.4.3 Synthesis of palladium complex (4c)

(1-(2,6-Diisopropylphenyl)-1*H*-imidazol-2-yl)methylene)-4-methoxyaniline ligand was prepared from **2** (76.9 mg, 0.3 mmol, 1.0 equiv) and *p*-anisidine (36.9 mg, 0.3 mmol, 1.0 equiv) in MeOH (6 mL, 0.05 M). The crude imine ligand was reacted with $Pd(COD)Cl_2$ (86.2 mg, 0.3 mmol, 1.0 equiv) in chloroform (6 mL, 0.05 M) following the General procedure for the preparation of palladium complexes to afford complex **4c** as a red crystalline (124 mg, 77%).

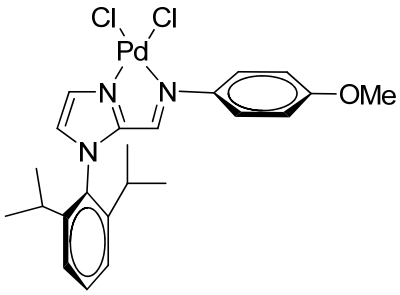

4c

^{1}H NMR (300 MHz, $CDCl_3$): δ 7.82 (d, *J* = 1.3 Hz, 1H, Ar*H*), 7.60 (t, *J* = 7.8 Hz, 1H, Ar*H*), 7.41 (s, 1H, N=C*H*), 7.37 (d, *J* = 7.8 Hz, 2H, Ar*H*), 7.29–7.26 (m, 2H, Ar*H*), 7.22 (d, *J* = 1.3 Hz, 1H, Ar*H*), 6.87 (d, *J* = 9.0 Hz, 2H, Ar*H*), 3.81 (s, 3H, OCH_3), 2.35 [sept, *J* = 6.9 Hz, 2H, (C*H*)$_2$], 1.21 [d, *J* = 6.9 Hz, 6H, (CH_3)$_2$], 1.18 [d, *J* = 6.9 Hz, 6H, (CH_3)$_2$].

^{13}C NMR (75 MHz, $CDCl_3$): δ 160.7 (C), 149.7 (CH), 147.7 (C), 145.8 (2 × C), 140.0 (C), 132.1 (CH), 130.0 (CH), 129.7 (C), 125.5 (CH), 125.3 (2 × CH), 124.9 (2 × CH), 113.8 (2 × CH), 55.6 (CH_3), 28.6 (2 × CH), 24.5 (2 × CH_3), 24.2 (2 × CH_3).

HRMS (ESI): calcd. for $C_{23}H_{27}Cl_2N_3OPdNa$ [M^+ + Na] 562.0457; found: 562.0457.

Anal. Calcd. for $C_{23}H_{27}Cl_2N_3OPd$: C, 51.27; H, 5.05; N, 7.80. Found: C, 50.62; H, 5.12; N, 7.45.

6.4.4 Synthesis of palladium complex (4d)

(1-(2,6-Diisopropylphenyl)-1*H*-imidazol-2-yl)methylene)-4-nitroaniline ligand was prepared from **2** (76.9 mg, 0.3 mmol, 1.0 equiv) and *p*-nitroaniline (41.4 mg, 0.3 mmol, 1.0 equiv) in MeOH (6 mL, 0.05 M). The crude imine ligand was reacted with $Pd(COD)Cl_2$ (86.2 mg, 0.3 mmol, 1.0 equiv) in chloroform (6 mL, 0.05 M) following the General procedure for the preparation of palladium complexes to afford complex **4d** as a orange solid (110 mg, 66%).

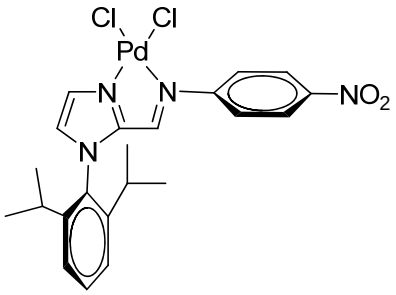

4d

^{1}H NMR (300 MHz, $CDCl_3$): δ 8.21 (d, *J* = 9.0 Hz, 2H, Ar*H*), 7.85 (d, *J* = 1.2 Hz, 1H, N=C*H*), 7.62-7.57 (m, 2H, Ar*H*), 7.49 (d, *J* = 9.0 Hz, 2H, Ar*H*), 7.37 (d, *J* = 7.8 Hz, 2H, Ar*H*), 2.41 [sept, *J* = 6.8 Hz, 2H (C*H*)$_2$], 1.22–1.18 [m, 12H, CH_3)$_4$].

^{13}C NMR (75 MHz, $CDCl_3$): δ 153.1 (CH), 150.9 (C), 147.6 (C), 147.3 (C), 146.0 (C), 132.3 (CH), 130.9 (CH), 129.9 (C), 129.6 (C), 126.9 (CH), 125.1 (2 × CH), 125.0 (2 × CH), 124.1 (2 × CH), 28.6 (2 × CH), 24.8 (2 × CH_3), 24.3 (2 × CH_3).

HRMS (ESI): calcd. for $C_{22}H_{24}Cl_2N_4O_2PdNa$ [M^+ + Na] 577.0202; found: 577.0202.

Anal. Calcd. for $C_{22}H_{24}Cl_2N_4O_2Pd$: C, 47.72; H, 4.37; N, 10.12. Found: C, 46.83; H, 4.40; N, 9.46.

6.4.5 Synthesis of palladium complex (4e)

(1-(2,6-Diisopropylphenyl)-1*H*-imidazol-2-yl)methylene)methylamine ligand was prepared from **2** (64 mg, 0.25 mmol, 1.0 equiv) and 40% w/w methylamine solution(22 μL, 0.25 mmol, 1.0 equiv) in MeOH (4 mL, 0.05 M). The crude imine ligand was reacted with $Pd(COD)Cl_2$ (71.8 mg, 0.25 mmol, 1.0 equiv) in chloroform (5 mL, 0.05 M) following the General procedure for the preparation of palladium complexes to afford complex **4e** as a yellow solid (99.3 mg, 89%).

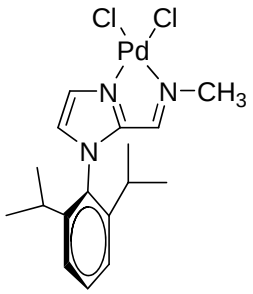

4e

^{1}H NMR (300 MHz, $CDCl_3$): δ 7.68 (d, *J* = 1.4 Hz, 1H, Ar*H*), 7.59 (t, *J* = 7.8 Hz, 1H, Ar*H*), 7.45 (m, 1H, N=C*H*), 7.37 (d, *J* = 7.8 Hz, 2H, Ar*H*), 7.14 (d, *J* = 1.4 Hz, 1H, Ar*H*), 3.70 (s, 3H, CH_3), 2.31 [sept, *J* = 6.8 Hz, 2H, (C*H*)$_2$], 1.20–1.16 [m, 12H, CH_3)$_4$].

^{13}C NMR (75 MHz, $CDCl_3$): δ 152.8 (CH), 147.2 (C), 145.8 (2 × C), 132.1 (CH), 129.7 (C), 129.6 (CH), 124.8 (3 × CH), 49.1 (CH_3), 28.5 (2 × CH), 24.7 (2 × CH_3), 24.1 (2 × CH_3).

Anal. Calcd. for $C_{17}H_{23}Cl_2N_3Pd$: C, 45.71; H, 5.19; N, 9.41. Found: C, 45.77; H, 5.21; N, 9.22.

6.4.6 Synthesis of palladium complex (4f)

(1-(2,6-Diisopropylphenyl)-1*H*-imidazol-2-yl)methylene)cyclohexylamine ligand was prepared from **2** (128 mg, 0.3 mmol, 1.0 equiv) and cyclohexylamine (34.4 μL, 0.3 mmol, 1.0 equiv) in MeOH (6 mL, 0.05 M). The crude imine ligand was reacted with $Pd(COD)Cl_2$ (86.2 mg, 0.3 mmol, 1.0 equiv) in chloroform (5 mL, 0.05 M) following the General procedure for the preparation of palladium complexes to afford complex **4f** as a red crystalline (149.9 mg, 97%).

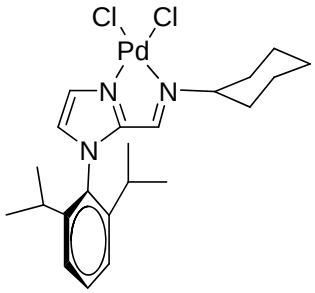

4f

^{1}H NMR (300 MHz, $CDCl_3$): δ 7.69 (d, *J* = 1.4 Hz, 1H, Ar*H*), 7.60 (t, *J* = 7.8 Hz, 1H, Ar*H*), 7.36 (d, *J* = 7.8 Hz, 2H, Ar*H*), 7.28 (m, 1H, N=C*H*), 7.14 (d, *J* = 1.4 Hz, 1H, Ar*H*), 4.29 (m, 1H, C*H*), 2.30–2.20 [m, 4H, (CH)$_2$, CH_2], 1.81–1.65 [m, 4H, (CH_2)$_2$], 1.41 (m, 2H, CH_2), 1.19–1.10 [m, 12H, (CH_3)$_4$], 1.04–0.99 (m, 2H, CH_2).

^{13}C NMR (75 MHz, $CDCl_3$): δ 148.7 (CH), 147.9 (C), 145.6 (2 × C), 132.1 (CH), 129.6 (C), 129.4 (CH), 124.9 (2 × CH), 124.6 (CH), 65.5 (CH), 33.8 (2 × CH_2), 28.4 (2 × CH), 25.1 (CH_2), 25.0 (2 × CH_2), 24.2 (4 × CH_3).

HRMS (ESI): calcd. for $C_{22}H_{31}Cl_2N_3PdNa$ [M^+ + Na] 538.0820; found: 538.0820.

Anal. Calcd. for $C_{22}H_{31}Cl_2N_3Pd$: C, 51.33; H, 6.07; N, 8.16. Found: C, 47.16; H, 6.05; N, 7.20.

6.4.7 Synthesis of palladium complex (4g)

(1-(2,6-Diisopropylphenyl)-1*H*-imidazol-2-yl)methylene)-*tert*-butylamine ligand was prepared from **2** (64 mg, 0.25 mmol, 1.0 equiv) and *tert*-butylamine (26.4 μL, 0.25 mmol, 1.0 equiv) in MeOH (4 mL, 0.05 M). The crude imine ligand was reacted with $Pd(COD)Cl_2$ (71.8 mg, 0.25 mmol, 1.0 equiv) in chloroform (5 mL, 0.05 M) following the General procedure for the preparation of palladium complexes to afford complex **4g** as a red crystalline (93.9 mg, 75%).

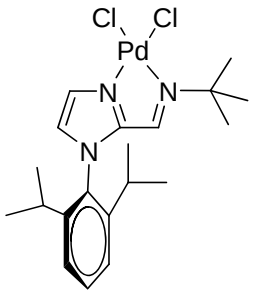

4g

^{1}H NMR (300 MHz, $CDCl_3$): δ 7.78 (d, *J* = 1.4 Hz, 1H, Ar*H*), 7.61 (t, *J* = 7.8 Hz, 1H, Ar*H*), 7.37 (d, *J* = 7.8 Hz, 2H, Ar*H*), 7.26 (m, 1H, N=C*H*), 7.11 (d, *J* = 1.4 Hz, 1H, Ar*H*), 2.26 [sept, *J* = 6.7 Hz, 2H, (C*H*)$_2$], 1.54 [s, 9H, (CH_3)$_3$], 1.19 [d, *J* = 6.7 Hz, 6H, (CH_3)$_2$], 1.12 [d, *J* = 6.7 Hz, 6H, (CH_3)$_2$].

^{13}C NMR (75 MHz, $CDCl_3$): δ 147.7 (CH), 147.6 (C), 145.6 (2 × C), 132.2 (CH), 129.6 (CH), 129.5 (C), 124.9 (2 × CH), 124.4 (CH), 66.7 (C), 29.6 (3 × CH_3), 28.4 (2 × CH), 24.3 (2 × CH_3), 24.2 (2 × CH_3).

Anal. Calcd. for $C_{20}H_{29}Cl_2N_3Pd$: C, 49.14; H, 5.98; N, 8.60. Found: C, 49.28; H, 6.03; N, 8.48.

6.4.8 Synthesis of ligand (3h)

(1-(2,6-Diisopropylphenyl)-1*H*-imidazol-2-yl)methylene) adamantylamine ligand **3h** was prepared from 1-(2,6-diisopropylphenyl)-1*H*-imidazole-2-carbox-aldehyde (744 mg, 2.9 mmol, 1.2 equiv) and 1-adamantylamine (366 mg, 2.416 mmol, 1.0 equiv) in CH_3CN (1mL). The product began to precipitate out of solution. After 16 h, the white solid was collected and washed with cold acetronitrile to afford the corresponding ligand **3h** as a white powder in 68% yield (643.7 mg).

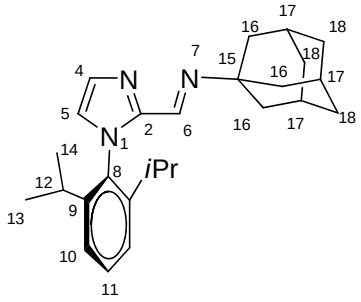

3h

^{1}H NMR (400 MHz, $CDCl_3$): δ 8.00 (s, 1H, N=C*H*), 7.43 (t, *J* = 7.6 Hz, 1H, Ar*H*), 7.33 (d, *J* = 0.8 Hz, 1H, Ar*H*), 7.22 (d, *J* = 7.6 Hz, 2H, Ar*H*), 6.94 (d, *J* = 0.8 Hz, 1H, Ar*H*), 2.33 [sept, *J* = 6.8 Hz, 2H, (C*H*)$_2$], 1.94 [m, 3H, (C*H*)$_3$], 1.67–1.54 [m, 6H, (C*H*$_2$)$_3$], 1.48–1.47 [m, 6H, (C*H*$_2$)$_3$], 1.10 [d, *J* = 6.8 Hz, 6H, (C*H*$_3$)$_2$], 1.07 [d, *J* = 6.8 Hz, 6H, (C*H*$_3$)$_2$].

^{13}C NMR (100 MHz, $CDCl_3$): δ 145.6 (2 × C), 145.1 (C), 144.3 (CH), 133.9 (C), 129.8 (CH), 129.2 (CH), 124.0 (CH), 123.4 (2 × CH), 57.9 (C), 42.7 (3 × CH_2), 36.4 (3 × CH_2), 29.3 (3 × CH), 28.1 (2 × CH), 24.7 (2 × CH_3), 23.2 (2 × CH_3).

HRMS (APCI): calcd. for $C_{26}H_{36}N_3$ [M^+ + H] 390.2909; found: 390.2920.

Table 6.4. Observed correlations in the HMQC spectrum of **3h** ($CDCl_3$).

Carbon	**δ_C (ppm)**	**δ_H of correlated proton (ppm)**
C-2	145.1	-
C-4	129.8	7.33 (d, *J* = 0.8 Hz, 1H, Ar*H*)
C-5	124.0	6.94 (d, *J* = 0.8 Hz, 1H, Ar*H*)
C-6	144.3	8.00 (s, 1H, N=C*H*)
C-8	133.9	-
C-9	145.6	-
C-10	123.4	7.22 (d, *J* = 7.6 Hz, 2H, Ar*H*)
C-11	129.2	7.43 (t, *J* = 7.6 Hz, 1H, Ar*H*)
C-12	28.1	2.33 [sept, *J* = 6.8 Hz, 2H, (C*H*)$_2$]
C-13, C-14	24.7, 23.2	1.10 [d, *J* = 6.8 Hz, 6H, (CH_3)$_2$],
		1.07 [d, *J* = 6.8 Hz, 6H, (CH_3)$_2$]
C-15	57.9	-
C-16	42.7	1.48–1.47 [m, 6H, (CH_2)$_3$]
C-17	29.3	1.94 [m, 3H, (C*H*)$_3$]
C-18	36.4	1.67–1.54 [m, 6H, (CH_2)$_3$]

Table 6.5. Observed correlations in the COSY-45 spectrum of **3h** ($CDCl_3$).

δ_H (ppm)	**δ_H of correlated proton (ppm)**
7.43 (H-11)	7.22 (H-10)
2.33 (H-12)	1.10 (H-13), 1.07 (H-14)
1.94 (H-17)	1.48–1.47 (H-16), 1.67–1.54 (C-18)

Table 6.6. Observed long-range C–H correlations in the HMBC spectrum of **3h** ($CDCl_3$).

δ_H (ppm)	Carbon correlated with δ_H (ppm)
8.00 (H-6)	145.1 (C-2), 57.9 (C-15), 42.7 (C-16)
7.43 (H-11)	145.6 (C-9), 123.4 (C-10)
7.33 (H-4)	145.1 (C-2), 124.0 (C-5)
7.22 (H-10)	145.6 (C-9), 133.9 (C-8), 129.2 (C-11), 28.1 (C-12)
6.94 (H-5)	145.1 (C-2), 133.9 (C-8), 129.8 (C-4)
2.33 (H-12)	145.6 (C-9), 133.9 (C-8), 123.4 (C-10), 24.7 (C-13), 23.2 (C-14)
1.94 (H-17)	57.9 (C-15), 36.4 (C-18)
1.48-1.47 (H-16)	57.9 (C-15), 36.4 (C-18), 29.3 (C-17)
1.67-1.54 (H-18)	42.7 (C-16), 29.3 (C-17)

6.4.9 Synthesis of palladium complex (4h)

(1-(2,6-Diisopropylphenyl)-1*H*-imidazol-2-yl)methylene)adamantylamine ligand was prepared from **2** (89.7 mg, 0.35 mmol, 1.0 equiv) and 1-adamantylamine (52.9 mg, 0.35 mmol, 1.0 equiv) in MeOH (7 mL, 0.05 M). The crude imine ligand was reacted with $Pd(COD)Cl_2$ (100 mg, 0.35 mmol, 1.0 equiv) in chloroform (7 mL, 0.05 M) following the General procedure for the preparation of palladium complexes to afford complex **4h** as a red microcrystalline (86.7 mg, 87%).

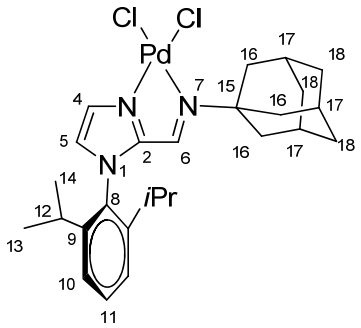

4h

^{1}H NMR (400 MHz, $CDCl_3$): δ 7.79, (d, *J* = 1.6 Hz, 1H, Ar*H*), 7.61 (t, *J* = 7.7 Hz, 1H, Ar*H*), 7.37 (d, *J* = 7.7 Hz, 2H, Ar*H*), 7.20 (s, 1H, N=C*H*), 7.07 (d, *J* = 1.6 Hz, 1H, Ar*H*), 2.27 [sept, *J* = 7.0 Hz, 2H, (C*H*)$_2$], 2.18 [m, 3H, (C*H*)$_3$], 2.09 [m, 6H, (CH_2)$_3$], 1.70 [m, 6H, (CH_2)$_3$], 1.20 [d, *J* = 7.0 Hz, 6H, (CH_3)$_2$], 1.14 [d, *J* = 7.0 Hz, 6H, (CH_3)$_2$].

^{13}C NMR (75 MHz, $CDCl_3$): δ 147.9 (C), 147.7 (CH), 145.8 (2 × C), 132.1 (CH), 129.7 (C), 129.5 (CH), 124.9 (2 × CH), 124.1 (CH), 67.0 (C), 42.1 (3 × CH_2), 35.5 (3 × CH_2), 29.5 (3 × CH), 28.5 (2 × CH), 24.31 (2 × CH_3), 24.30 (2 × CH_3).

Anal. Calcd. for $C_{26}H_{35}Cl_2N_3Pd$; C, 55.09; H, 6.22; N, 7.41. Found: C, 55.16; H, 6.59; N, 7.31.

Table 6.7. Observed correlations in the HMQC spectrum of **4h** ($CDCl_3$).

Carbon	**δ_C (ppm)**	**δ_H of correlated proton (ppm)**
C-2	147.9	-
C-4	129.5	7.79 (d, *J* = 1.6 Hz, 1H, Ar*H*)
C-5	124.1	7.07 (d, *J* = 1.6 Hz, 1H, Ar*H*)
C-6	147.7	7.20 (s, 1H, N=C*H*)
C-9	145.8	-
C-8	129.7	-
C-10	124.9	7.37 (d, *J* = 7.7 Hz, 2H, Ar*H*)
C-11	132.1	7.61 (t, *J* = 7.7 Hz, 1H, Ar*H*)
C-12	28.5	2.27 [sept, *J* = 7.0 Hz, 2H, (C*H*)$_2$]
C-13, C-14	24.31, 24.30	1.20 [d, *J* = 7.0 Hz, 6H, (CH_3)$_2$], 1.14 [d, *J* = 7.0 Hz, 6H, (CH_3)$_2$]
C-15	67.0	-
C-16	42.1	2.09 [m, 6H, (CH_2)$_3$]
C-17	29.5	2.18 [m, 3H, (C*H*)$_3$]
C-18	35.5	1.70 [m, 6H, (CH_2)$_3$]

Table 6.8. Observed correlations in the COSY-45 spectrum of **4h** ($CDCl_3$).

δ_H (ppm)	δ_H of correlated proton (ppm)
7.79 (H-5)	7.07 (H-4)
7.61 (H-11)	7.37 (H-10)
2.27 (H-12)	1.20 (H-13), 1.14 (H-14)
2.18 (H-17)	2.09 (H-16), 1.70 (H-18)

Table 6.9. Observed long-range C–H correlations in the HMBC spectrum of **4h** ($CDCl_3$).

δ_H (ppm)	Carbon correlated with δ_H (ppm)
7.79 (H-4)	124.2 (C-5), 147.9 (C-2)
7.61 (H-11)	145.8 (C-9), 124.9 (C-10)
7.37 (H-10)	145.9 (C-9), 129.7 (C-8), 28.5 (C-12)
7.20 (H-6)	147.9 (C-2), 67.0 (C-15), 42.1 (C-16)
7.07 (H-5)	147.9 (C-2), 129.7 (C-8), 129.5 (C-4)
2.27 (H-12)	145.8 (C-9), 124.9 (C-10), 129.7 (C-8), 24.31 (C-13), 24.30 (C-14)
2.18 (H-17)	42.1 (C-16)
2.09 (H-16)	67.0 (C-15), 35.5 (C-18), 29.5 (C-17)
1.20 (H-13), 1.14 (H-14)	145.8 (C-9), 28.5 (C-12), 24.3 (C-13 + C-14)

NOE data of complex (4h)

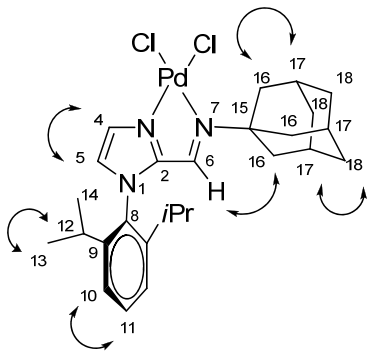

4h

6.5 X-ray crystallography

Crystallographic analyses of complexes **4b** and **4h** were carried out at the Mahidol crystallographic facility. Diffraction measurements were made on a 4 K Bruker SMART[57] CCD area detector diffractometer using graphite-monochromated Mo *Kα* radiation (λ = 0.71073 Å). Crystals were mounted in paratone oil and held at room temperature during data collection. Cell constants and an orientation matrix for data collection were obtained from a least-square refinement using the measured positions of reflections in the range $0.998^o < \theta < 28.4^o$ (for **4b**) and $0.998^o < \theta < 29.1^o$ (for **4h**). The frame data were integrated by the program SAINT[58] and corrected for Lorentz and polarization effects. The structure was solved by the maXus crystallographic software package,[59] using direct methods (SIR97)[60] and refined by full-matrix least-squares method on (F_{obs})[58] using the SHELXTL-PC V 6.12 software package.[61]

X-ray quality crystals of **4b** and **4h** were grown by layer diffusion of hexanes onto the $CHCl_3$ solution of the palladium complexes at room temperature.

Complex **4b** crystallizes in the orthorhombic P*bca* space group with each asymmetric unit cell containing one molecules of **4b** and one distorted $CHCl_3$ molecule. The $CHCl_3$ molecule was modeled with Cl5 and Cl6 atoms each occupying a half-occupancy with no hydrogen. Large thermal ellipsoids were observed for isopropyl groups. All non-hydrogen atoms were refined anisotropically while the hydrogen atoms were placed in calculated positions and not refined.

Complex **4h** crystallized in the monoclinic P$2_1/c$ space group with each asymmetric unit containing one molecule of **4h**. Large thermal ellipsoids were observed for isopropyl groups. All non-hydrogen atoms were refined anisotropically while the hydrogen atoms were placed in calculated positions and not refined.

Table 6.10. Crystal data for **4b** and **4h**.

	4b•CHCl$_3$	**4h**
empirical formula	$C_{29}H_{37}Cl_5N_3Pd$	$C_{26}H_{35}Cl_2N_3Pd$
FW	711.27	566.87
cryst color, habit	orange, cube	orange, cube
cryst size (mm)	0.35×0.25×0.20	0.30×0.25×0.20
cryst system	Orthorhombic	Monoclinic
space group	P*bca* (#61)	P2$_1$/*c* (#14)
a (Å)	13.6508(2)	14.2165(6)
b (Å)	21.1682(4)	11.9991(3)
c (Å)	23.4645(4)	18.7543(7)
α (deg)	90.00	90.00
β (deg)	90.00	125.0801(14)
γ (deg)	90.00	90.00
volume (Å^3)	6780.50(2)	2618.09(16)
θ range (deg)	0.998–26.4	0.998–29.1
Z	8	4
T/K	298	298
D_{calc} (g/cm^3)	1.392	1.438
μ (mm^{-1})	0.963	0.931
no. of reflns	6914	7035
no. of params refined	353	289
refln/param ratio	19.6	24.3
final residuals R_1[a]; wR_2[b]	0.0557; 0.1852	0.0478; 0.1126
goodness of fit indicator[c]	1.331	0.987
max.shift/error in final LS cycle	0.001	0.001

[a] $R = \Sigma||F_o| - |F_c||/\Sigma|F_o|$.

[b] $wR_2 = [\Sigma[w(F_o^2 - F_c^2)^2]/\Sigma[w(F_o^2)^2)]^{1/2}$, where $w = [\sigma^2(F_o^2) + (aP)^2 + bP]^{-1}$.

[c] GOF = $[\Sigma w(\ |F_o| - |F_c|\ )^2 / (N_{obs} - N_{param})]^{1/2}$.

6.6 General procedure for screening of palladium complexes on the Suzuki–Miyaura cross-coupling reaction (Table 4.8)

In the air condition, a 10 mL vial equipped with a magnetic stir bar was charged with Pd complexes (1.5 mol %), hexamethylbenzene (0.05 mmol, 0.0081 g, 0.1 equiv) phenylboronic acid (0.6 mmol, 0.073 g, 1.2 equiv), K_2CO_3 (1.1 mmol, 0.153 g, 2.2 equiv) and *p*-bromoanisole (0.5 mmol, 0.062 mL, 1.0 equiv). MeOH (2 mL) and water (0.5 mL) were mixed and added to the reaction mixture. The reaction vial was capped and vigorously stirred at room temperature for 24 h. The resulting milky solution was extracted with CH_2Cl_2 (3 × 10 mL), washed with water (2 × 10 mL), brine (1 × 10 mL) and dried over Na_2SO_4. Solvent was then evaporated. The reaction was monitored by GC-FID to determine the yield of the product based on integration relative to hexamethylbenzene as an internal standard.

The GC conditions are as follows: initial temperature: 150 ºC (1min), ramp 1 at 5 ºC/min to 200 ºC, ramp 2 at 35 ºC/min to 325 ºC, hold at 325 ºC (1min). Retention times: hexamethylbenzene internal standard (2.9 min), product **5b** (4.5 min), *p*-bromoanisole substrate (1.8 min), phenylboronic acid substrate (13.3 min).

6.7 General procedure for the investigation of the effect of catalyst loading, base, solvent, time and substrate scopes on the Suzuki–Miyaura cross-coupling reaction (Table 4.9–4.16)

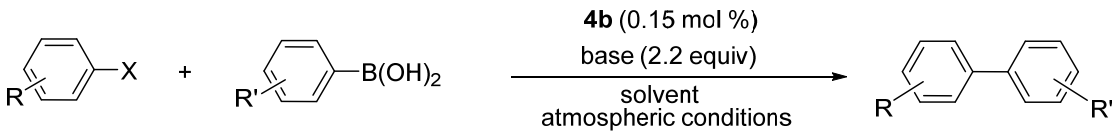

(1.0 equiv) (1.2 equiv) **5a–p**

In the air condition, hexamethylbenzene (0.05 mmol, 0.0081 g, 0.1 equiv), aryl halide (0.5 mmol, 1.0 equiv), arylboronic acid (0.6 mmol, 1.2 equiv), base (1.1 mmol, 2.2 equiv) and solvent was subsequently added into a 10 mL vial equipped with a magnetic stir bar. The 5 mM Pd catalyst solution in MeOH was added as indicated in the tables. The reaction vial was capped and vigorously stirred at room temperature for

desired time as indicated. The resulting milky solution was extracted with CH_2Cl_2 (3 × 10 mL), washed with water (2 × 10 mL), brine (1 × 10 mL) and dried over Na_2SO_4. The combined organic phase was then concentrated to afford the crude coupling product. The reaction was monitored by GC-FID based on integration relative to hexamethylbenzene as an internal standard. The crude product was finally isolated by column chromatography (0–10%: ethyl acetate/hexanes) to afford the desired product.

6.8 Analytical data of biphenyl compounds (5a–p)

6.8.1 Synthesis of biphenyl (5a)

5a was prepared from bromobenzene (53 μL, 0.5 mmol, 1.0 equiv) and phenylboronic acid (73 mg, 0.6 mmol, 1.2 equiv) following the General procedure for the investigation of substrate scope on Suzuki–Miyaura cross-coupling reaction. The crude product was purified by column chromatography (SiO_2, hexanes) to afford **5a** as a white solid (73.4 mg, 95% yield).

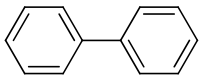

5a

^{1}H NMR (300 MHz, $CDCl_3$): δ 7.65 (d, *J* = 7.6 Hz, 4H, Ar*H*), 7.49 (t, *J* = 7.7 Hz, 4H, Ar*H*), 7.37 (m, 2H, Ar*H*).

^{13}C NMR (75 MHz, $CDCl_3$): δ 141.2 (2 × C), 128.7 (4 × CH), 127.2 (4 × CH), 127.1 (2 × CH).

EI-MS (*m*/*z*, relative intensity): 155 (14), 154 (M^+, 100), 153 (42), 152 (29).

CAS Number: 92-52-4.

6.8.2 Synthesis of 4-methoxybiphenyl (5b)

5b (Table 4.15, entry 2) was prepared from 4-bromoanisole (62 μL, 0.5 mmol, 1.0 equiv) and phenylboronic acid (73 mg, 0.6 mmol, 1.2 equiv) following the

General procedure for the investigation of substrate scope on Suzuki–Miyaura cross-coupling reaction. The yield of product **5b** was determined by GC method (>99%). The crude product was purified by column chromatography (SiO_2, 0–10% ethyl acetate/hexanes) to afford **5b** as a white solid (89.3 mg, 97% yield).

5b (Table 4.15, entry 5) was prepared from 4-iodoanisole (117 mg, 0.5 mmol, 1.0 equiv) and phenylboronic acid (73 mg, 0.6 mmol, 1.2 equiv) following the General procedure for the investigation of substrate scope on Suzuki–Miyaura cross-coupling reaction. The yield of product **5b** was determined by GC method (95%).

5b (Table 4.16, entry 1) was prepared from bromobenzene (52.5 μL, 0.5 mmol, 1.0 equiv) and 4-methoxyphenylboronic acid (91.2 mg, 0.6 mmol, 1.2 equiv) following the General procedure for the investigation of substrate scope on Suzuki–Miyaura cross-coupling reaction. The crude product was purified by column chromatography (SiO_2, 10% CH_2Cl_2/hexanes) to afford **5b** as a white solid (74.0 mg, 80% yield).

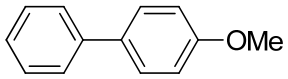

5b

^{1}H NMR (300 MHz, $CDCl_3$): δ 7.57–7.52 (m, 4H, Ar*H*), 7.44 (t, *J* = 7.5 Hz, 2H, Ar*H*), 7.35–7.28 (m, 1H, Ar*H*), 7.00 (d, *J* = 8.8 Hz, 2H, Ar*H*), 3.88 (s, 3H, OC*H*$_3$).
^{13}C NMR (75 MHz, $CDCl_3$): δ 159.1 (C), 140.8 (C), 133.7 (C), 128.7 (2 × CH), 128.1 (2 × CH), 126.7 (2 × CH), 126.6 (CH), 114.2 (2 × CH), 55.3 (CH_3).
EI-MS (*m*/*z*, relative intensity): 185 (14), 184 (M^+, 100), 169 (46), 141 (45), 115 (33).
CAS Number: 613-37-6.

6.8.3 Synthesis of 3-methoxybiphenyl (5c)

5c (Table 4.15, entry 3) was prepared from 3-bromoanisole (63.3 μL, 0.5 mmol, 1.0 equiv) and phenylboronic acid (73 mg, 0.6 mmol, 1.2 equiv) following the General procedure for the investigation of substrate scope on Suzuki–Miyaura cross-coupling reaction. The crude product was purified by column chromatography (SiO_2, 0–10% ethyl acetate/hexanes) to afford **5c** as a colorless oil (100.8 mg, 99% yield).

5c (Table 4.16, entry 2) was prepared from bromobenzene (52.5 μL, 0.5 mmol, 1.0 equiv) and 3-methoxyphenylboronic acid (91.2 mg, 0.6 mmol, 1.2 equiv) following the General procedure for the investigation of substrate scope on Suzuki–Miyaura cross-coupling reaction. The crude product was purified by column chromatography (SiO_2, 10% ethyl acetate/hexanes) to afford **5c** as a colorless oil (68.8 mg, 75% yield).

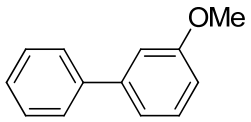

5c

^{1}H NMR (300 MHz, $CDCl_3$): δ 7.62 (d, *J* = 7.6 Hz, 2H, Ar*H*), 7.47 (t, *J* = 7.4 Hz, 2H, Ar*H*), 7.42–7.36 (m, 2H, Ar*H*), 7.22 (d, *J* = 8.1 Hz, 1H, Ar*H*), 7.16 (m, 1H, Ar*H*), 6.94 (d, *J* = 8.1 Hz, 1H, Ar*H*) 3.90 (s, 3H, OCH_3).

^{13}C NMR (75 MHz, $CDCl_3$): δ 159.9 (C), 142.7 (C), 141.0 (C), 129.7 (CH), 128.7 (2 × CH), 127.3 (CH), 127.1 (2 × CH), 119.6 (CH), 112.8 (CH), 112.6 (CH), 55.2 (CH_3).

EI-MS (*m*/*z*, relative intensity): 185 (15), 184 (M^+, 100), 154 (23), 153 (20), 141 (32), 115 (30).

CAS Number: 2113-56-6.

6.8.4 Synthesis of 2-methoxybiphenyl (5d)

5d (Table 4.15, entry 4) was prepared from 2-bromoanisole (62 μL, 0.5 mmol, 1.0 equiv) and phenylboronic acid (73 mg, 0.6 mmol, 1.2 equiv) following the General procedure for the investigation of substrate scope on Suzuki–Miyaura cross-coupling reaction. The crude product was purified by column chromatography (SiO_2, hexanes) to afford **5d** as a colorless oil (62.3 mg, 68% yield).

5d (Table 4.16, entry 3) was prepared from bromobenzene (52.5 μL, 0.5 mmol, 1.0 equiv) and 2-methoxyphenylboronic acid (91.2 mg, 0.6 mmol, 1.2 equiv) following the General procedure for the investigation of substrate scope on Suzuki–Miyaura cross-coupling reaction. The crude product was purified by column chromatography (SiO_2, hexanes) to afford **5d** as a colorless oil (78.6 mg, 85% yield).

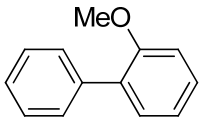

5d

^{1}H NMR (300 MHz, $CDCl_3$): δ 7.64 (d, *J* = 7.2 Hz, 2H, Ar*H*), 7.51 (t, *J* = 7.4 Hz, 2H, Ar*H*), 7.42 (t, *J* = 7.3 Hz, 3H, Ar*H*), 7.15–7.06 (m, 2H, Ar*H*), 3.89 (s, 3H, OCH_3).
^{13}C NMR (75 MHz, $CDCl_3$): δ 156.4 (C), 138.5 (C), 130.8 (CH), 130.7 (C), 129.5 (2 × CH), 128.5 (CH), 127.9 (2 × CH), 126.9 (CH), 120.8 (CH), 111.2 (CH), 55.5 (CH_3).
EI-MS (*m*/*z*, relative intensity): 185 (14), 184 (M^+, 100), 183 (21), 169 (54), 168 (15), 141 (37), 139 (17), 115 (37).
CAS Number: 86-26-0.

6.8.5 Synthesis of 4-nitrobiphenyl (5e)

5e was prepared from 4-bromonitrobenzene (101 mg, 0.5 mmol, 1.0 equiv) and phenylboronic acid (73 mg, 0.6 mmol, 1.2 equiv) following the General procedure for the investigation of substrate scope on Suzuki–Miyaura cross-coupling reaction. The crude product was purified by column chromatography (SiO_2, 10% ethyl acetate/hexanes) to afford **5e** as a light yellow solid (91.6 mg, 92% yield).

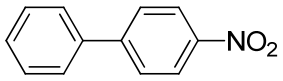

5e

^{1}H NMR (300 MHz, $CDCl_3$): δ 8.33 (d, *J* = 9.0 Hz, 2H, Ar*H*), 7.76 (d, *J* = 9.0 Hz, 2H, Ar*H*), 7.67–7.64 (m, 2H, Ar*H*), 7.56–7.47 (m, 3H, Ar*H*).
^{13}C NMR (75 MHz, $CDCl_3$): δ 147.5 (C), 147.0 (C), 138.6 (C), 129.0 (2 × CH), 128.8 (CH), 127.6 (2 × CH), 127.3 (2 × CH), 124.0 (2 × CH).
EI-MS (*m*/*z*, relative intensity): 200 (13), 199 (M^+, 97), 169 (35), 153 (28), 152 (100), 151 (30), 141 (28).
CAS Number: 92-93-3.

6.8.6 Synthesis of 4-(trifluoromethyl)biphenyl (5f)

5f was prepared from 4-bromobenzotrifluoride (80 μL, 0.5 mmol, 1.0 equiv) and phenylboronic acid (73 mg, 0.6 mmol, 1.2 equiv) following the General procedure for the investigation of substrate scope on Suzuki–Miyaura cross-coupling reaction. The crude product was purified by flash column chromatography (SiO_2, 10% ethyl acetate/hexanes) to afford **5f** as a white solid (118.2 mg, 99% yield).

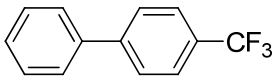

5f

^{1}H NMR (300 MHz, $CDCl_3$): δ 7.61–7.55 (m, 4H, Ar*H*), 7.49 (m, 2H, Ar*H*), 7.39–7.27 (m, 3H, Ar*H*).

^{13}C NMR (75 MHz, $CDCl_3$): δ 144.7 (C), 139.8 (C), 129.3 (d, J = 32.2 Hz, C), 129.0 (2 × CH), 128.2 (CH), 127.4 (2 × CH), 127.3 (2 × CH), 125.7 (q, J = 3.7 Hz, 2 × CH), 124.3 (d, J = 270.4 Hz, CF_3).

^{19}F NMR (282 MHz, $CDCl_3$): δ −62.3 (s, 3F).

EI-MS (*m*/*z*, relative intensity): 223 (13), 222 (M^+, 100), 201 (10), 151 (20).

CAS Number: 398-36-7.

6.8.7 Synthesis of 1-(biphenyl-4-yl)ethanone (5g)

5g (Table 4.15, entry 9) was prepared from 4′-bromoacetophenone (99.5 mg, 0.5 mmol, 1.0 equiv) and phenylboronic acid (73 mg, 0.6 mmol, 1.2 equiv) following the General procedure for the investigation of substrate scope on Suzuki–Miyaura cross-coupling reaction. The crude product was purified by column chromatography (SiO_2, 10% ethyl acetate/hexanes) to afford **5g** as a white solid (102.5 mg, 99% yield).

5g (Table 4.16, entry 4) was prepared from bromobenzene (52.5 μL, 0.5 mmol, 1.0 equiv) and 4-acetylphenylboronic acid (98.4 mg, 0.6 mmol, 1.2 equiv) following the General procedure for the investigation of substrate scope on Suzuki–Miyaura cross-coupling reaction. The crude product was purified by column chromatography (SiO_2, CH_2Cl_2) to afford **5g** as a white solid (62.4 mg, 64% yield).

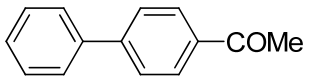

5g

^{1}H NMR (300 MHz, $CDCl_3$): δ 8.06 (d, *J* = 8.6 Hz, 2H, Ar*H*), 7.71 (d, *J* = 8.6 Hz, 2H, Ar*H*), 7.66 (d, *J* = 8.1 Hz, 2H, Ar*H*), 7.50 (t, *J* = 7.2 Hz, 2H, Ar*H*), 7.43 (t, *J* = 7.2 Hz, 1H, Ar*H*), 2.66 (s, 3H, COC*H*$_3$).

^{13}C NMR (75 MHz, $CDCl_3$): δ 197.7 (C), 145.7 (C), 139.8 (C), 135.8 (C), 128.9 (2 × CH), 128.8 (2 × CH), 128.2 (CH), 127.2 (2 × CH), 127.1 (2 × CH), 26.6 (CH_3).

EI-MS (*m*/*z*, relative intensity): 196 (M^+, 50), 181 (100), 153 (35), 152 (58), 151 (16).

CAS Number: 92-91-1.

6.8.8 Synthesis of biphenyl-4-carbaldehyde (5h)

5h was prepared from 4-bromobenzaldehyde (92.5 mg, 0.5 mmol, 1.0 equiv) and phenylboronic acid (73 mg, 0.6 mmol, 1.2 equiv) following the General procedure for the investigation of substrate scope on Suzuki–Miyaura cross-coupling reaction. The crude product was purified by column chromatography (SiO_2, 10% ethyl acetate/hexanes) to afford **5h** as a light yellow solid (82.9 mg, 91% yield).

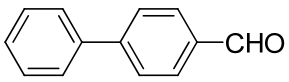

5h

^{1}H NMR (300 MHz, $CDCl_3$): δ 10.09 (s, 1H, C*H*O), 7.98 (d, *J* = 8.2 Hz, 2H, Ar*H*), 7.77 (d, *J* = 8.2 Hz, 2H, Ar*H*), 7.66 (d, *J* = 6.8 Hz, 2H, Ar*H*), 7.54–7.44 (m, 3H, Ar*H*).

^{13}C NMR (75 MHz, $CDCl_3$): δ 191.8 (CH), 147.0 (C), 139.5 (C), 135.1 (C), 130.1 (2 × CH), 128.9 (2 × CH), 128.4 (CH), 127.5 (2 × CH), 127.2 (2 × CH).

EI-MS (*m*/*z*, relative intensity): 183 (13), 182 (M^+, 96), 181 (100), 153 (38), 152 (63), 151 (18).

CAS Number: 3218-36-8.

6.8.9 Synthesis of methyl biphenyl-4-carboxylate (5i)

5i was prepared from methyl 4-bromobenzoate (107.5 mg, 0.5 mmol, 1.0 equiv) and phenylboronic acid (73 mg, 0.6 mmol, 1.2 equiv) following the General procedure for the investigation of substrate scope on Suzuki–Miyaura cross-coupling reaction. The crude product was purified by column chromatography (SiO_2, hexanes) to afford **5i** as a white solid (103.1 mg, 97% yield).

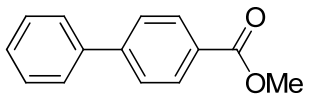

5i

^{1}H NMR (300 MHz, $CDCl_3$): δ 8.14 (d, *J* = 8.2 Hz, 2H, Ar*H*), 7.69 (d, *J* = 8.4 Hz, 2H, Ar*H*), 7.65 (d, *J* = 7.5 Hz, 2H, Ar*H*), 7.50 (t, *J* = 7.3 Hz, 2H, Ar*H*), 7.42 (t, *J* = 7.1 Hz, 1H, Ar*H*), 3.97 (s, 3H, CO_2CH_3).

^{13}C NMR (75 MHz, $CDCl_3$): δ 166.8 (C), 145.4 (C), 139.8 (C), 130.0 (2 × CH), 128.8 (2 × CH), 128.8 (C), 128.0 (CH), 127.1 (2 × CH), 126.9 (2 × CH), 52.0 (CH_3).

EI-MS (*m*/*z*, relative intensity): 212 (M^+, 65), 182 (13), 181 (100), 153 (28), 152 (60), 151 (17).

CAS Number: 720-75-2.

6.8.10 Synthesis of biphenyl-4-carbonitrile (5j)

5j was prepared from 4-bromobenzonitrile (91 mg, 0.5 mmol, 1.0 equiv) and phenylboronic acid (73 mg, 0.6 mmol, 1.2 equiv) following the General procedure for the investigation of substrate scope on Suzuki–Miyaura cross-coupling reaction. The crude product was purified by column chromatography (SiO_2, 10% ethyl acetate/hexanes) to afford **5j** as a white solid (88.3 mg, 98% yield).

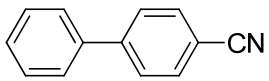

5j

^{1}H NMR (300 MHz, $CDCl_3$): δ 7.76 (d, *J* = 8.6 Hz, 2H, Ar*H*), 7.71 (d, *J* = 8.6 Hz, 2H, Ar*H*), 7.62 (d, *J* = 6.9 Hz, 2H, Ar*H*), 7.54–7.45 (m, 3H, Ar*H*).
^{13}C NMR (75 MHz, $CDCl_3$): δ 145.5 (C), 139.0 (C), 132.4 (2 × CH), 129.0 (2 × CH), 128.5 (CH), 127.5 (2 × CH), 127.1 (2 × CH), 118.8 (C), 110.7 (C).
EI-MS (*m*/*z*, relative intensity): 179 (M^+, 100), 178 (24), 151 (12).
CAS Number: 2920-38-9.

6.8.11 Synthesis of 4-fluorobiphenyl (5k)

5k was prepared from 1-bromo-4-fluorobenzene (55 mg, 0.5 mmol, 1.0 equiv) and phenylboronic acid (73 mg, 0.6 mmol, 1.2 equiv) following the General procedure for the investigation of substrate scope on Suzuki–Miyaura cross-coupling reaction. The crude product was purified by column chromatography (SiO_2, hexanes) to afford **5k** as a white solid (56.1 mg, 65% yield).

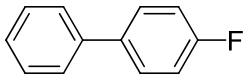

5k

^{1}H NMR (300 MHz, $CDCl_3$): δ 7.62–7.58 (m, 4H, Ar*H*), 7.50 (t, *J* = 7.5 Hz, 2H, Ar*H*), 7.40 (t, *J* = 7.2 Hz, 1H, Ar*H*), 7.18 (t, *J* = 8.7 Hz, 2H, Ar*H*).
^{13}C NMR (75 MHz, $CDCl_3$): δ 162.5 (d, *J* = 244.9 Hz, CF), 140.2 (C), 137.3 (d, *J* = 3.2 Hz, C), 128.8 (2 × CH), 128.7 (d, *J* = 8.0 Hz, 2 × CH), 127.2 (CH), 127.0 (2 × CH), 115.6 (d, *J* = 21.3 Hz, 2 × CH).
^{19}F NMR (282 MHz, $CDCl_3$): δ –115.8 (s, F).
EI-MS (*m*/*z*, relative intensity): 173 (13), 172 (M^+, 100), 171 (36), 170 (25).
CAS Number: 324-74-3.

6.8.12 Synthesis of biphenyl-4-ol (5l)

5l was prepared from 4-bromophenol (86.5 mg, 0.5 mmol, 1.0 equiv) and phenylboronic acid (73 mg, 0.6 mmol, 1.2 equiv) following the General procedure for the investigation of substrate scope on Suzuki–Miyaura cross-coupling reaction. The

crude product was purified by column chromatography (SiO_2, 10% ethyl acetate/hexanes) to afford **5l** as a white solid (71.5 mg, 84% yield).

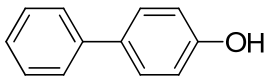

5l

^{1}H NMR (300 MHz, $CDCl_3$): δ 7.58 (d, *J* = 8.6 Hz, 2H, Ar*H*), 7.52 (d, *J* = 8.5 Hz, 2H, Ar*H*), 7.45 (t, *J* = 7.7 Hz, 2H, Ar*H*), 7.34 (t, *J* = 7.3 Hz, 1H, Ar*H*), 6.94 (d, *J* = 8.4 Hz, 2H, Ar*H*), 5.08 (br s, 1H, O*H*).

^{13}C NMR (100 MHz, $CDCl_3$): δ 155.1 (C), 140.8 (C), 134.0 (C), 128.7 (3 × CH), 128.4 (3 × CH), 115.7 (3 × CH).

EI-MS (*m*/*z*, relative intensity): 171 (13), 170 (M^+, 100), 141 (22), 115 (28).

CAS Number: 92-69-3.

6.8.13 Synthesis of *p*-terphenyl (5m)

5m was prepared from 4-bromobiphenyl (86.5 mg, 0.5 mmol, 1.0 equiv) and phenylboronic acid (73 mg, 0.6 mmol, 1.2 equiv) following the General procedure for the investigation of substrate scope on Suzuki–Miyaura cross-coupling reaction. The crude product was purified by column chromatography (SiO_2, hexanes) to afford **5m** as a white solid (98.8 mg, 86% yield).

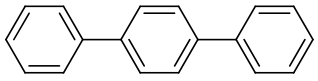

5m

^{1}H NMR (300 MHz, $CDCl_3$): δ 7.73–7.71 (m, 4H, Ar*H*), 7.69 (d, *J* = 7.4 Hz, 4H, Ar*H*), 7.51 (t, *J* = 7.4 Hz, 4H, Ar*H*), 7.41 (t, *J* = 7.34 Hz, 2H, Ar*H*).

^{13}C NMR (75 MHz, $CDCl_3$): δ 140.7 (2 × C), 140.1 (2 × C), 128.8 (4 × CH), 127.5 (4 × CH), 127.3 (2 × CH), 127.0 (4 × CH).

EI-MS (*m*/*z*, relative intensity): 231 (19), 230 (M^+, 100), 228 (13).

CAS Number: 92-94-4.

6.8.14 Synthesis of 3-phenylpyridine (5n)

5n was prepared from 3-bromopyridine (48.2 μL, 0.5 mmol, 1.0 equiv) and phenylboronic acid (73 mg, 0.6 mmol, 1.2 equiv) following the General procedure for the investigation of substrate scope on Suzuki–Miyaura cross-coupling reaction. The crude product was purified by column chromatography (SiO_2, 10% ethyl acetate/hexanes) to afford **5n** a colorless liquid (46.2 mg, 60% yield).

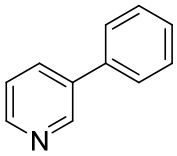

5n

^{1}H NMR (300 MHz, $CDCl_3$): δ 8.88 (s, 1H, Ar*H*), 8.62 (d, *J* = 4.4 Hz, 1H, Ar*H*), 7.91 (d, *J* = 8.0 Hz, 1H, Ar*H*), 7.61 (d, *J* = 7.3 Hz, 2H, Ar*H*), 7.51 (t, *J* = 7.4 Hz, 2H, Ar*H*), 7.46-7.37 (m, 2H, Ar*H*).

^{13}C NMR (75 MHz, $CDCl_3$): δ 148.3 (CH), 148.2 (CH), 137.7 (C), 136.6 (C), 134.3 (CH), 129.0 (2 × CH), 128.0 (CH), 127.1 (2 × CH), 123.5 (CH).

EI-MS (*m*/*z*, relative intensity): 155 (M^+, 100), 154 (50), 127 (14), 102 (11).

CAS Number: 1008-88-4.

6.8.15 Synthesis of 3-phenylquinoline (5o)

5o was prepared from 3-bromoquinoline (68 μL, 0.5 mmol, 1.0 equiv) and phenylboronic acid (73 mg, 0.6 mmol, 1.2 equiv) following the General procedure for the investigation of substrate scope on Suzuki–Miyaura cross-coupling reaction. The crude product was purified by column chromatography (SiO_2, 0–10% ethyl acetate/hexanes) to afford **5o** as a white solid (41.8 mg, 41% yield).

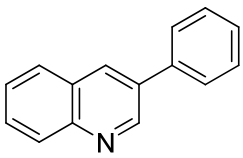

5o

^{1}H NMR (300 MHz, $CDCl_3$): δ 9.21 (s, 1H, Ar*H*), 8.32 (s, 1H, Ar*H*), 8.18 (d, *J* = 8.5 Hz, 1H, Ar*H*), 7.90 (d, *J* = 8.1 Hz, 1H, Ar*H*), 7.77–7.22 (m, 3H, Ar*H*), 7.62–7.52 (m, 3H, Ar*H*), 7.46 (t, *J* = 7.2 Hz, 1H, Ar*H*).

^{13}C NMR (75 MHz, $CDCl_3$): δ 149.9 (CH, C), 147.3 (C), 137.8 (C), 133.8 (C), 133.2 (CH), 129.3 (CH), 129.2 (CH), 129.1 (2 × CH), 128.1 (CH), 128.0 (CH), 127.4 (2 × CH), 127.0 (CH).

EI-MS (*m*/*z*, relative intensity): 206 (16), 205 (M^+, 100), 204 (53), 176 (14).

CAS Number: 1666-96-2.

6.8.16 Synthesis of 5-phenylpyrimidine (5p)

5p was prepared from 5-bromopyrimidine (79.5 mg, 0.5 mmol, 1.0 equiv) and phenylboronic acid (73 mg, 0.6 mmol, 1.2 equiv) following the General procedure for the investigation of substrate scope on Suzuki–Miyaura cross-coupling reaction. The crude product was purified by column chromatography (SiO_2, 20% ethyl acetate/hexanes) to afford **5p** as a white solid (34.7 mg, 45% yield).

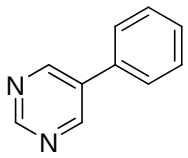

5p

^{1}H NMR (300 MHz, $CDCl_3$): δ 9.23 (s, 1H, Ar*H*), 8.98 (s, 2H, Ar*H*), 7.62–7.49 (m, 5H, Ar*H*).

^{13}C NMR (75 MHz, $CDCl_3$): δ 157.4 (CH), 154.8 (2 × CH), 134.3 (C), 134.2 (C), 129.4 (2 × CH), 129.0 (CH), 126.9 (2 × CH).

EI-MS (*m*/*z*, relative intensity): 157 (12), 156 (M^+, 100), 155 (17), 102 (64).

CAS Number: 34771-45-4.

6.8.17 Synthesis of 1-(4'-methoxybiphenyl-4-yl)ethanone (5q)

5q (Table 4.16, entry 5) was prepared from 4-bromoanisole (62 μL, 0.5 mmol, 1.0 equiv) and 4-acetylphenylboronic acid (94 mg, 0.6 mmol, 1.2 equiv)

following the General procedure for the investigation of substrate scope on Suzuki–Miyaura cross-coupling reaction. The crude product was purified by column chromatography (SiO_2, 10% ethyl acetate/hexanes) to afford **5q** as a white solid (77.2 mg, 68% yield).

5q (Table 4.16, entry 6) was prepared from 4′-bromoacetophenone (99.5 mg, 0.5 mmol, 1.0 equiv) and 4-methoxyphenylboronic acid (91.2 mg, 0.6 mmol, 1.2 equiv) following the General procedure for the investigation of substrate scope on Suzuki–Miyaura cross-coupling reaction. The crude product was purified by column chromatography (SiO_2, CH_2Cl_2) to afford **5q** as a white solid (101.2 mg, 90% yield).

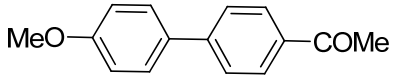

5q

^{1}H NMR (300 MHz, $CDCl_3$): δ 8.02 (d, *J* = 8.2 Hz, 2H, Ar*H*), 7.66 (d, *J* = 8.2 Hz, 2H, Ar*H*), 7.60 (d, *J* = 8.9 Hz, 2H, Ar*H*), 7.02 (d, *J* = 8.4 Hz, 2H, Ar*H*), 3.87 (s, 3H, OC*H*$_3$), 2.64 (s, 3H, COC*H*$_3$).

^{13}C NMR (75 MHz, $CDCl_3$): δ 197.6 (C), 159.8 (C), 145.2 (C), 135.1 (C), 132.1 (C), 128.8 (2 × CH), 128.2 (2 × CH), 126.5 (2 × CH), 114.3 (2 × CH), 55.2 (CH_3), 26.5 (CH_3).

EI-MS (*m*/*z*, relative intensity): 226 (M^+, 66), 212 (18), 211 (100), 183 (11), 168 (19), 139 (25).

CAS Number: 13021-18-6.

6.9 Mercury poisoning test for the Suzuki–Miyaura cross-coupling reaction

The reaction vial charged with an excess of Hg (Hg:Pd = 400:1) was added hexamethylbenzene (0.05 mmol, 8.1 mg, 0.1 equiv), phenylboronic acid (0.6 mmol, 73 mg, 1.2 equiv), K_2CO_3 (1.1 mmol, 0.153 g, 2.2 equiv), *p*-bromoanisole (0.5 mmol, 0.062 μL, 1.0 equiv), MeOH (2 mL) and water (0.5 mL), followed by 0.00075 mmol

of Pd catalyst **4b** (0.15 mol %). After 24 h, the mixture was extracted by CH_2Cl_2 (3 × 10 mL), washed with water (2 × 10 mL), brine (1 × 10 mL), dried over Na_2SO_4, and solvent was concentrated to afford the crude 4-methoxybiphenyl product. The yield was determined by GC method. A 33% yield was obtained in the presence of excess Hg.

PART II
SYNTHESIS OF ARYLBORONATES THROUGH THE SYNERGISTIC Pd/Cu-CATALYZED MIYAURA BORYLATION REACTION

CHAPTER VII
INTRODUCTION

Arylboronic acids and their esters are important and useful reagents that are widely used in organic synthesis for functional group transformations.[3, 62–65] They play a key role as a coupling partner in the Suzuki–Miyaura cross-coupling reaction. The most commonly used organoboron nucleophiles for Suzuki–Miyaura cross-coupling reactions are arylboronic acids, arylboronate esters and aryltrifluoroborates (Table 7.1). The advantages of these organoboron compounds in cross-coupling reactions include their high stability and low toxicity. Arylboronic acids and esters are typically produced by the reaction of trialkyl borates with either organolithium or Grignard reagents. However, these methods are incompatible with sensitive functional groups (*e.g.* aldehyde, ketone, nitrile and *etc*) and require rigorous anhydrous reaction conditions (Scheme 7.1).

Table 7.1. Organoboron compounds typically used in Suzuki–Miyaura cross-coupling reaction.[66]

Transmetalation reagent	Abbreviated notation	General comments
organoboronic acid	$RB(OH)_2$	most common commercial organoboron compounds
organoboronate esters	$RB(OR')_2$	usually more stable to protodeboronation and more soluble in organic solvent than organoboronic acid
organotrifluoroborates	RBF_3^-	usually more stable to protodeboronation than organoboronic acid, but B–F bond can be hydrolyzed

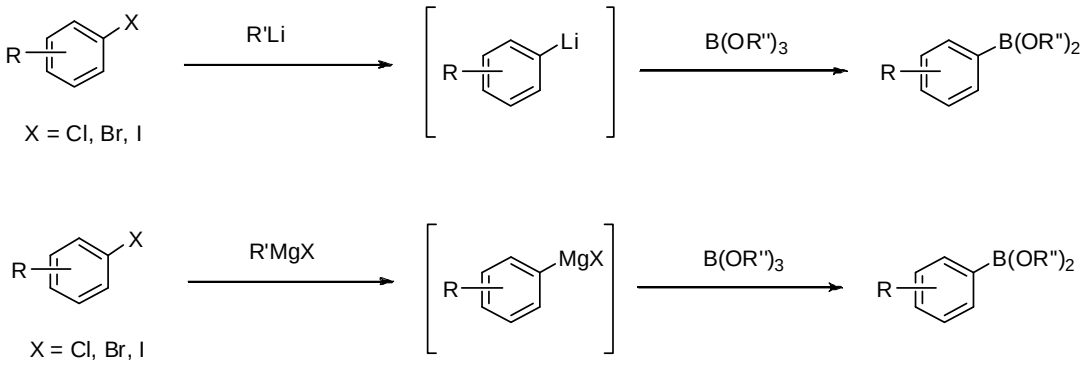

Scheme 7.1. Classical methods for C–B bond formation.

Due to these disadvantages, several alternative routes to synthesize borylation products have been developed as will be presented in Chapter IX. Many of them used transition-metal-catalyzed borylation reactions. For example, synthetic chemist found the use of Pd- and Ni-catalyzed borylation reactions of aryl halides have been used in the preparation of arylboronates.[62, 66–72] The C–H borylations of aromatic substrates catalyzed by iridium have been reported.[73–85] The Cu-catalyzed

borylation for the synthesis of arylboronates was found to be efficient and economical.[86, 87] Also, transition-metal-free borylations have been studied.[88–90]

CHAPTER VIII
OBJECTIVES

Due to the significant roles of the arylboronates in organic synthesis, various borylation protocols were developed as can be seen in the next Chapter. However, they require an inert atmosphere and have either prolong reaction times or high reaction temperatures. Therefore, the second part in this thesis aims:

- To develop a new transition-metal catalytic system for the Miyaura borylation reaction for which an air-sensitive technique is not required;
- To screen reaction conditions for the Miyaura borylation reaction under atmospheric condition;
- To expand the substrate scope of the optimized Miyaura borylation reaction.

CHAPTER IX
LITERATURE REVIEW

9.1 Palladium and nickel-catalyzed Miyaura borylation of aryl halides

Pd-catalyzed borylation reactions have been developed as alternative routes to construct borylation products. One of the earliest transition metal-catalyzed borylations was discovered by Miyaura in 1995.[62] Pd-catalyzed Miyaura borylation was performed with an aryl halide and bis(pinacolato)diborane (B_2Pin_2) in the presence of $Pd(dppf)Cl_2$ in DMSO at 80 °C (Scheme 9.1).

X = I, Br
Ar = 4-$Me_2NC_6H_4$, 4-$MeOC_6H_4$, 4-$MeO_2CC_6H_4$, 4-$MeCOC_6H_4$, 4-NCC_6H_4, mesityl, 3-benzothienyl

Scheme 9.1. Pd-catalyzed Miyaura borylation reaction.[62]

The mechanism for Pd-catalyzed borylation reaction proposed by Miyaura is shown in Figure 9.1. It starts with the oxidative addition of Pd(0) complex with aryl halide to obtain the Ar–Pd(II)–X species **8**. The displacement of the halide group with base affords the reactive acetoxopalladium(II) complexe **9**, Ar–Pd(II)–OAc. The high reactivity of acetoxopalladium(II) complex **9** attributes to the weak Pd–O bond, which consists of a soft acid and a hard base on the basic of HSAB concept. Then B_2pin_2 undergoes transmetalation with **9** to generate the Ar–Pd(II)–Bpin species **10**. The reductive elimination finally takes place to produce the borylation product and regenerate the catalyst.

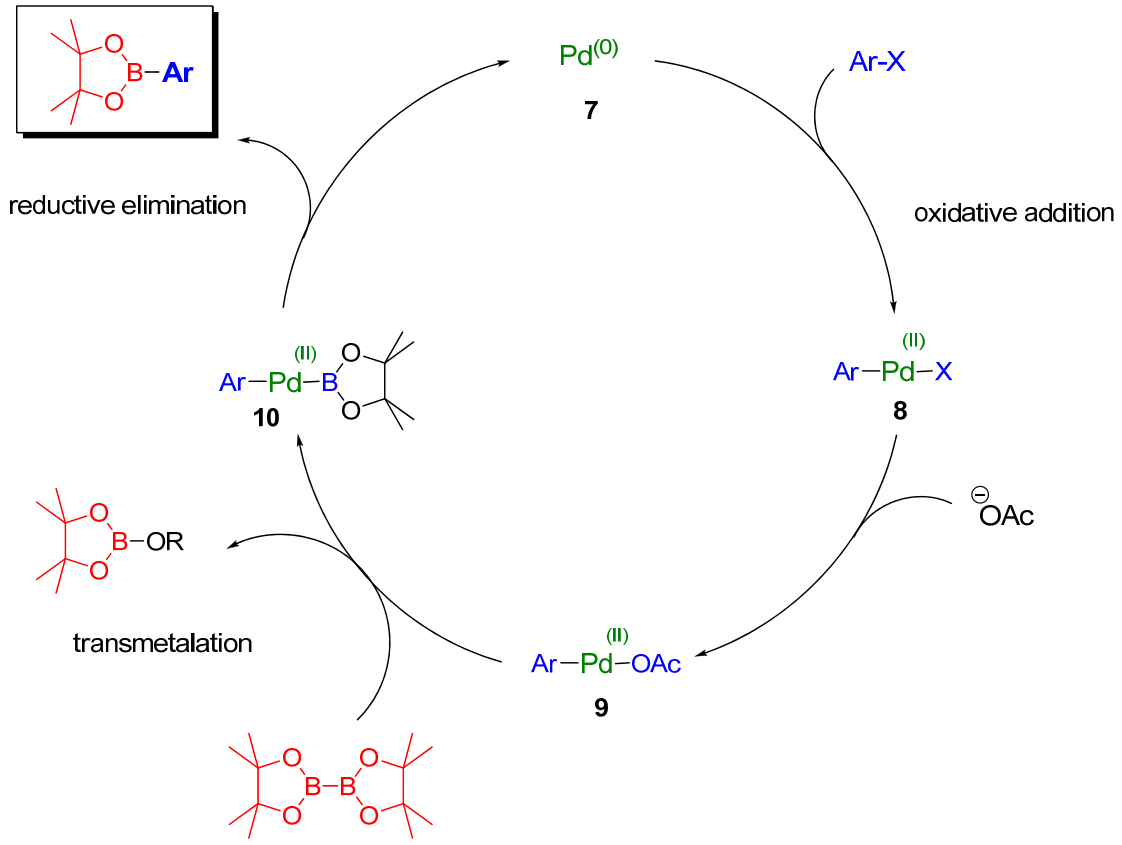

Figure 9.1. Proposed mechanism for Pd-catalyzed Miyaura borylation reaction.[62]

A modified borylation reaction, which was reported by the same group[67] can be operated in less toxic solvent such as dioxane instead of DMSO. The aryl triflates were good substrates for optimized Pd-catalyzed borylation. Furthermore, the addition of 1 equivalent of dppf ligand could suppress formation of the palladium black formation (Scheme 9.2).

In 2001, Miyaura highlighted that the cross-coupling reaction of aryl chlorides with bis(pinacolato)diboron could be achieved with the use of the electron-rich PCy_3 ligand[68] (Scheme 9.3). Bis(pinacolato)diboron is one of the most popular borylation reagents predominantly due to excellent aqueous and chromatographic stabilities of the resulting arylboronates, as well as its high solubility in organic solvents.[66]

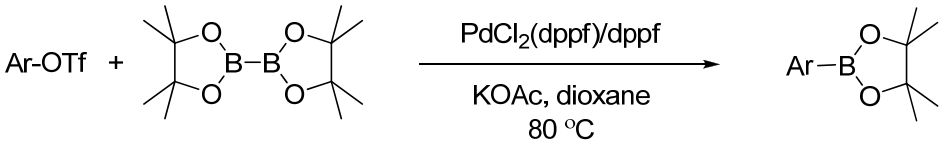

Scheme 9.2. Palladium-catalyzed borylation of aryl triflates with bis(pinacolato)-diborane.[67]

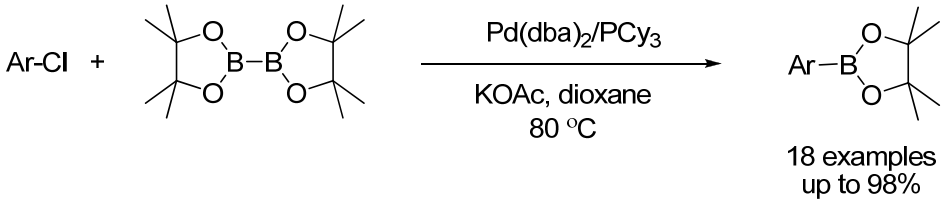

Scheme 9.3. Borylation of aryl chlorides with bis(pinacolato)diboron catalyzed by palladium-tricyclohexylphosphine complex.[68]

After the Palladium-catalyzed Miyaura borylation was reported, the improvements of borylation conditions were intensively investigated. Until 2007, the first general catalytic system for the borylation of aryl chlorides was introduced by Buchwald and co-workers.[69] In this work, a highly active catalytic system consisting of $Pd(OAc)_2$/SPhos for borylation of aryl chlorides was employed at room temperature (Scheme 9.4).

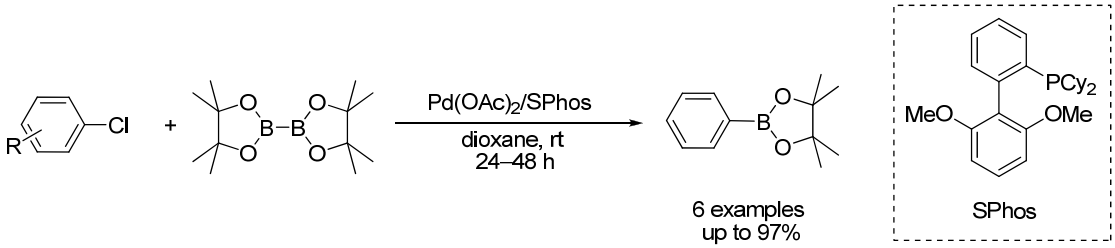

Scheme 9.4. Preparation of arylboronate esters using $Pd(OAc)_2$/SPhos catalytic system.[69]

One of major challenges in borylation reactions is the low product yield of highly sterically demanding aryl halides. Classical methods often suffer from difficult purification, and are usually incompatible with a variety of functional groups. Tang investigated the borylation of sterically hindered aryl bromides in the combination with Bedford Pd precursor (Scheme 9.5),[70] and found that borylation method can be carried out under low catalytic loading with aryl bromide substrates. On contrary, this combination failed to catalyze sterically demanding aryl chlorides. The authors suggested that the oxidative addition of aryl chlorides might be more difficult than that of aryl bromides, presumably due to the π-acidity of the phosphine ligand.

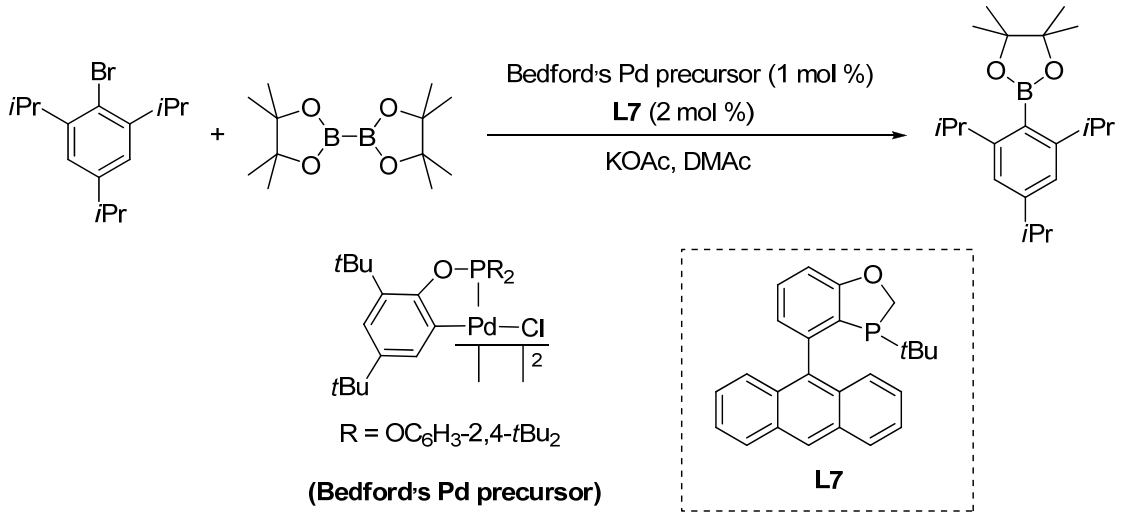

Scheme 9.5. Palladium-catalyzed borylation of highly sterically hindered aryl bromides using the Bedford Pd precursor.[70]

In 2011, Sawamura and co-workers demonstrated an efficient borylation of aryl chlorides and bromides using silica-supported phosphine Silica-SMAP (silicon-contained monodentate trialkyphosphane) as a ligand (Scheme 9.6).[71] The sterically demanding aryl halides were able to undergo this catalytic reaction. This immobilization allowed only one phosphine ligand associating to the metal center, generating the possible activated catalyst as presented in the dotted rectangle shown in Scheme 9.6.

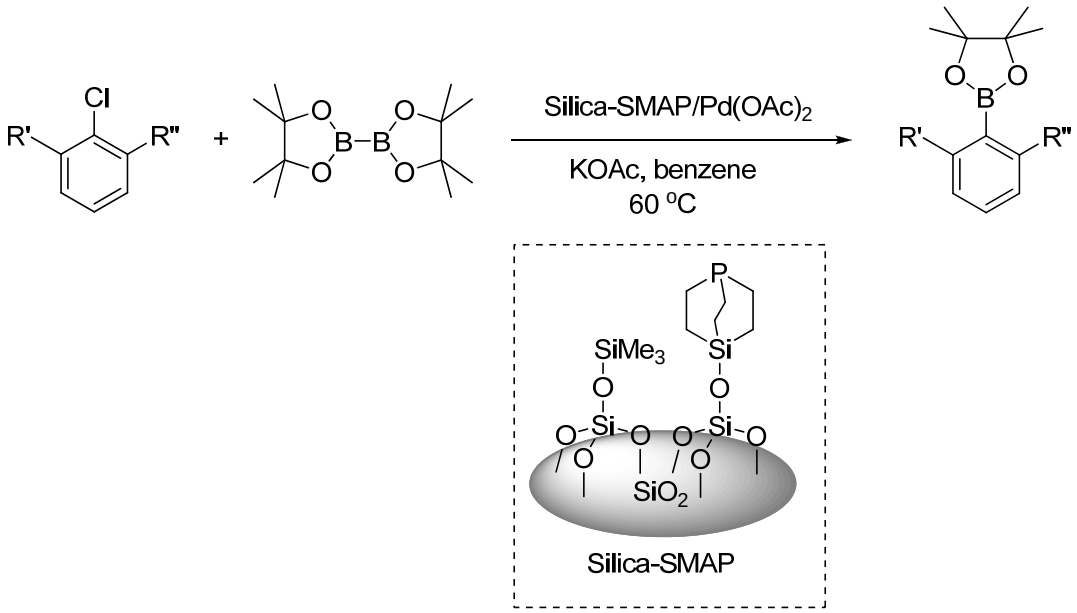

Scheme 9.6. A silica-supported compact phosphine ligand used in the palladium-catalyzed borylation of 2,6-disubstituted aryl chlorides.[71]

Owing to the relatively high cost of palladium, less expensive metals, such as nickel, become an attractive alternative to palladium catalysts. Therefore, a new generation of borylation methodologies based on Ni catalysts has attracted intense research interest.

The first example of Ni-catalyzed borylation of a 2,6-disubstituted aryl chloride was published in 2011 by Yamakawa and co-workers.[72] The author employed $NiCl_2(PMe_3)_2$ to catalyze the reaction. The substrate scope was further expanded to functionalized aryl chlorides, including sterically challenging substrates, which could perform the coupling reaction in THF at 100 °C in the presence of CsF, and $TMSOCH_2CF_3$ as additive (Scheme 9.7).[72] Remarkably, cesium 2,2,2-trifluoro-ethoxide that was generated *in situ* from the combination of CsF and $TMSOCH_2CF_3$ significantly improved the product yields of this $NiCl_2(PMe_3)_2$-catalyzed borylation reaction.

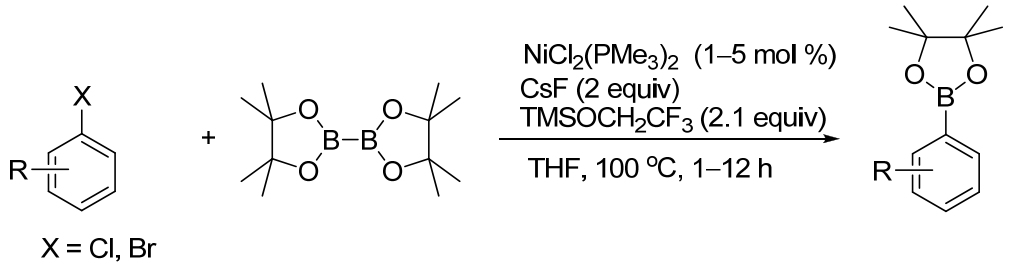

Scheme 9.7. $NiCl_2(PMe_3)_2$-catalyzed borylation of aryl chlorides in the combination with CsF and $TMSOCH_2CF_3$.[72]

9.2 Iridium-catalyzed borylation of arenes

Another important borylation method is the Ir-catalyzed C–H borylation for aromatic substrates. $Cp^*Ir(PMe_3)(H)(Bpin)$ complexes prepared by Smith and co-workers in 1999 were the first catalysts for direct borylation of arenes.[73, 74] (Scheme 9.8).

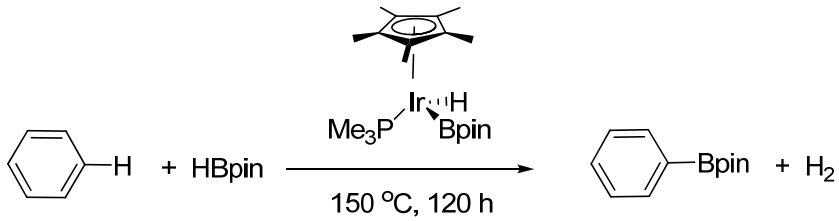

Scheme 9.8. $Cp^*Ir(PMe_3)(H)(Bpin)$-catalyzed borylation of arene with HBpin.[73]

Three years later, the same research group discovered a selective borylation of arene with HBpin catalyzed by (Ind)Ir(COD) and 1,2-bis(diphenyl-phosphino)ethane (dppe) ligand at 150 °C. PhBpin was obtained in 95% yield after 2 h (Scheme 9.9).[75]

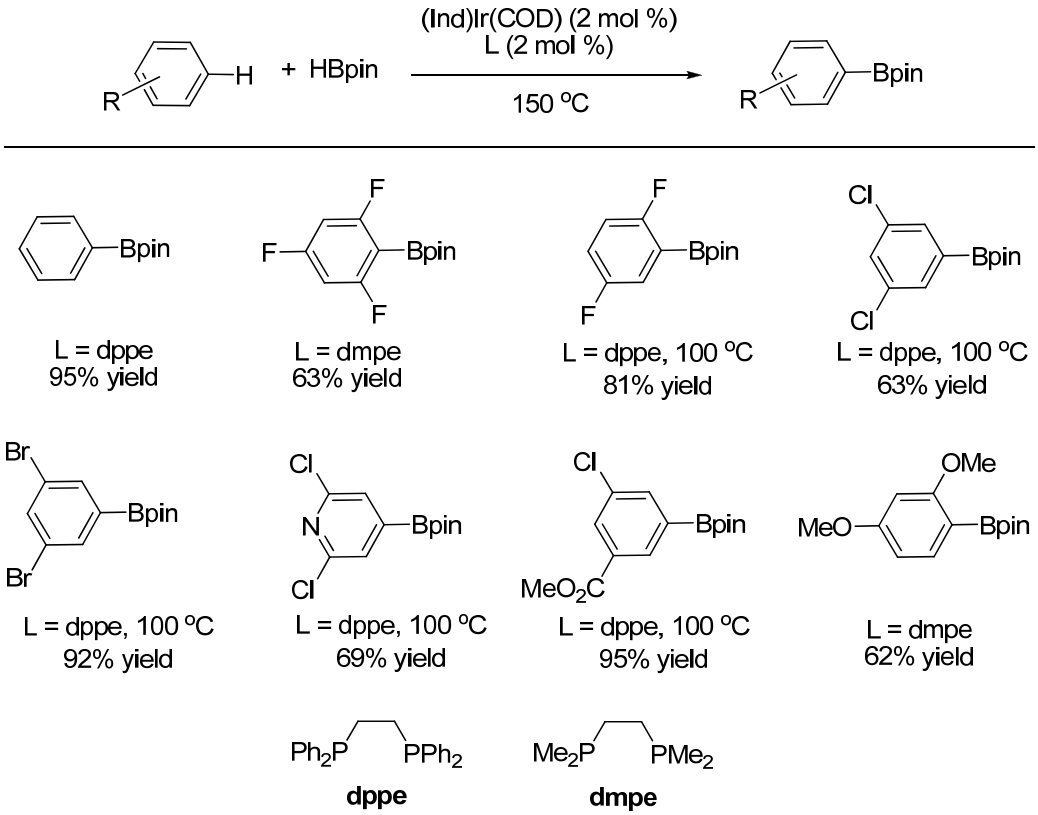

Scheme 9.9. Borylation of arenes with HBpin catalyzed by the combination of (Ind)Ir(COD) and phosphine ligands.[75]

Moreover, Miyaura and Ishiyama introduced the catalytic borylation using a combination of $[Ir(COD)Cl]_2$ and the air-stable bipyridine (bipy) ligand. B_2pin_2 was used as boron source in this catalytic borylation. The reaction was carried out using the catalytic amount of Ir catalyst and bipyridine ligand at 80 °C.[76] Furthermore, Miyaura, Ishiyama, Hartwig and co-workers reported Ir-catalyzed borylation reactions conducted at room temperature.[77] $[Ir(COD)(OMe)]_2$ and various bipyridine ligands as catalysts were examined for the reactions of arenes with B_2pin_2. Under the optimization in the presence of 1.5 mol % of $[Ir(COD)(OMe)]_2$ and 3 mol % of 4,4′-di-*tert*-butylbipyridine (dtbipy) at room temperature in hexane, the borylation product was obtained in excellent yield (Scheme 9.10). The substrate scope of $[Ir(COD)(OMe)]_2$-catalyzed borylation, including heterocyclic substrates,[78–82] substituted ferrocenes[83] and polycyclic aromatic compounds[84] was further studied.[85]

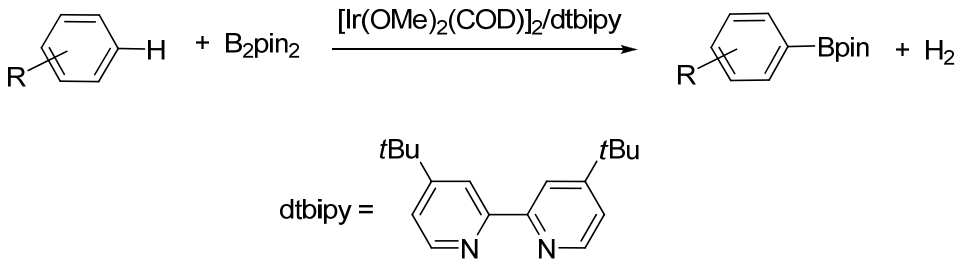

Scheme 9.10. [Ir(COD)(OMe)]$_2$/dtbipy-catalyzed borylation reaction of arene and B_2pin_2.[77]

9.3 Copper-catalyzed borylation of aryl halides

In addition to Pd, Ni and Ir catalysts, inexpensive copper catalyst can also enable borylation of aryl halides.

The first methodology using inexpensive Cu catalyst in borylation of aryl halides and pinacolborane at room temperature was reported by Ma and co-workers.[86] They carried out the cross coupling reaction of aryl iodides and pinacolborane (HBpin) under the condition of CuI (10 mol %) and sodium hydride in THF at room temperature (Scheme 9.11).[86] The result showed that aryl bromide afforded the poor conversion. For example, 4-bromoanisole coupled with pinacolborane at room temperature after running the reaction for 48 h gave only 20% yield. Increasing the reaction temperature to 70 °C did not fully promote the coupling reaction. However, both electron-rich and electron-deficient aryl iodides were achieved under this borylation conditions. Not surprisingly, highly reductive ability of pinacolborane and sodium hydride was found to be problematic for functionalized aryl iodides. For examples, when 4-acetylphenyl iodide is used as a substrate, α-hydroxy-4-iodophenylethane (reduction product) will be obtained instead of the borylation product. In addition, the authors also proposed a possible mechanism of this Cu-catalyzed borylation in the presence of NaH as shown in Figure 9.2.

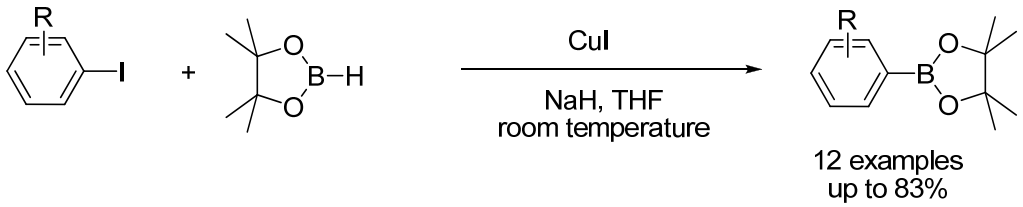

Scheme 9.11. Copper-catalyzed borylation of aryl iodides with pinacolborane in the presence of NaH.[86]

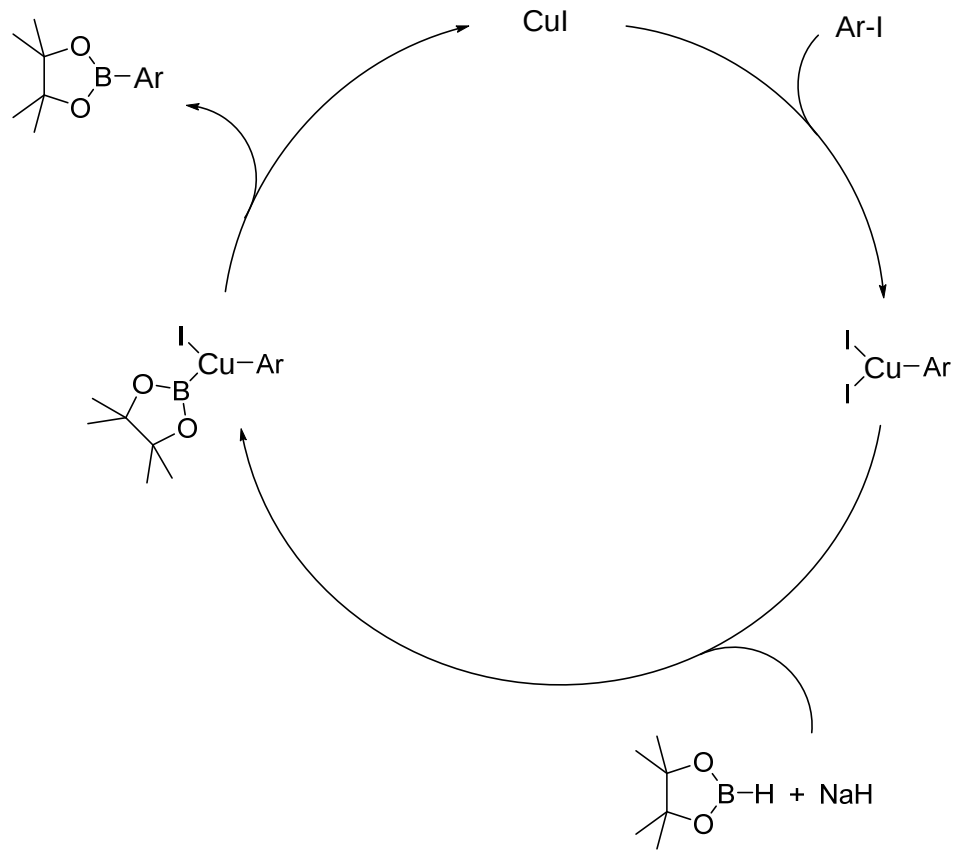

Figure 9.2. A proposed mechanism for copper-catalyzed borylation of aryl iodides with pinacolborane.[86]

In 2009, Marder, Lin and co-workers investigated a catalytic system for the borylation of aryl halides with alkoxy diboron reagents under mild conditions.[87] Electron-rich aryl iodides and sterically hindered aryl bromides were successfully catalyzed to the corresponding arylboronates at room temperature (Scheme 9.12). Not only B_2pin_2 gave excellent results, but also B_2neop_2 provided the corresponding Ar-Bneop compounds in good yields. According to DFT calculations and spectroscopic data, a catalytic cycle for copper-catalyzed borylation of aryl halides was presented in Figure 9.3.

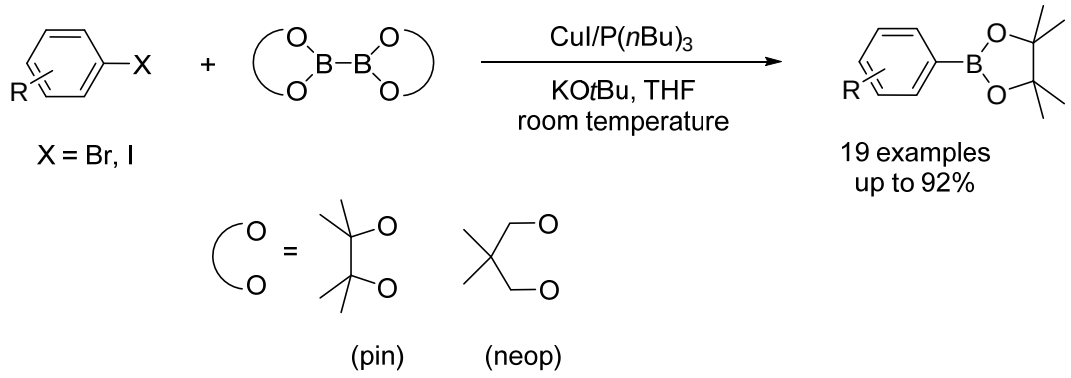

Scheme 9.12. Copper-catalyzed borylation of aryl halides with alkoxy diboron reagents.[87]

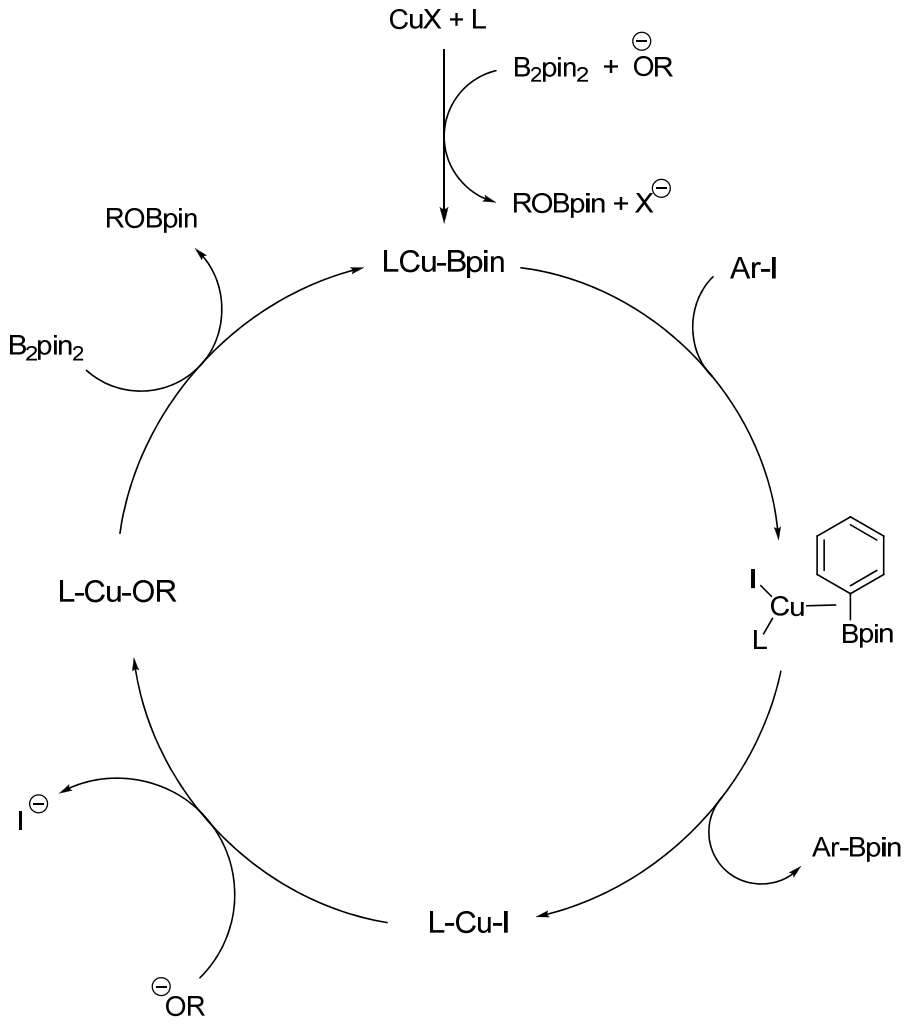

Figure 9.3. A possible catalytic cycle for the copper-catalyzed borylation of aryl halides.[87]

9.4 Transition-metal free for borylation reaction of aromatic compounds

In 2010, the novel metal-free conversion of arylamines to arylboronates was demonstrated by Wang and co-workers.[88] They prepared arylboronates by the reaction of B_2pin_2 and arylamines in the presence of *tert*-butyl nitrile (Scheme 9.13). In 2012, the substrate scope for the transformation of arylamine to arylboronates was further investigated by the same group.[89] Additionally, a possible mechanism

involving SET between aryldiazonium ion and tetra-coordinated boron complex has been proposed (Figure 9.4).

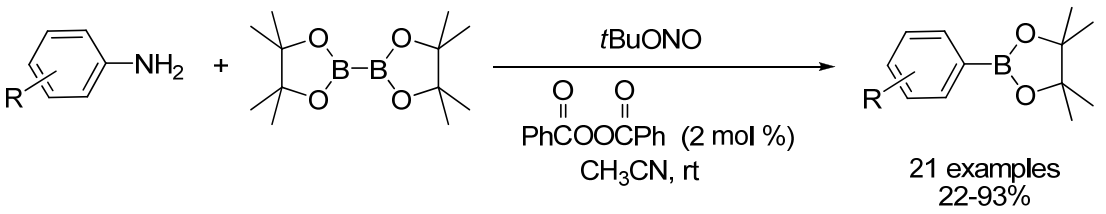

Scheme 9.13. Conversion of arylamine to arylboronates.[88]

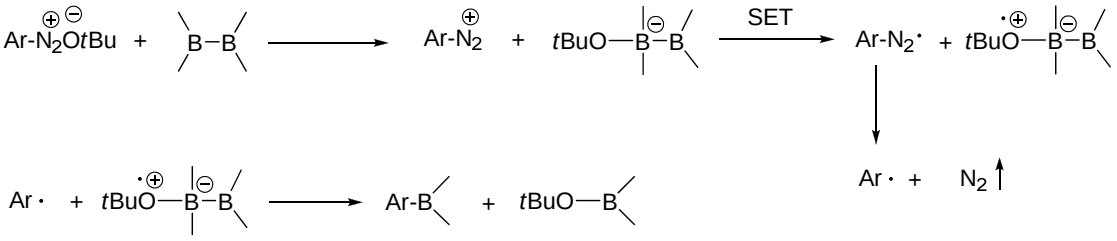

Figure 9.4. A possible mechanism for conversion of arylamine to arylboronates.[89]

Recently, Zhang and Wu reported an unexpected borylation of aryl iodides promoted by Cs_2CO_3 and MeOH system.[90] The protocol is one of the rare cases for transition-metal-free borylations in the presence of B_2pin_2 as the boron source. This method could be exploited to synthesize the corresponding arylboronic esters in moderate to high yields (Scheme 9.14). In order to investigate the mechanism of this protocol, TEMPO [(2,2,6,6-tetramethylpiperidin-1-yl)oxidanyl], the well-known radical scavenger, was added into the reaction mixture. However, efficient borylation was regained in the presence of 4 equivalents of TEMPO. They claimed that the radical-mediated mechanism could be ruled out and cesium cation was able to promote the cleavage of the C–I bond.[91]

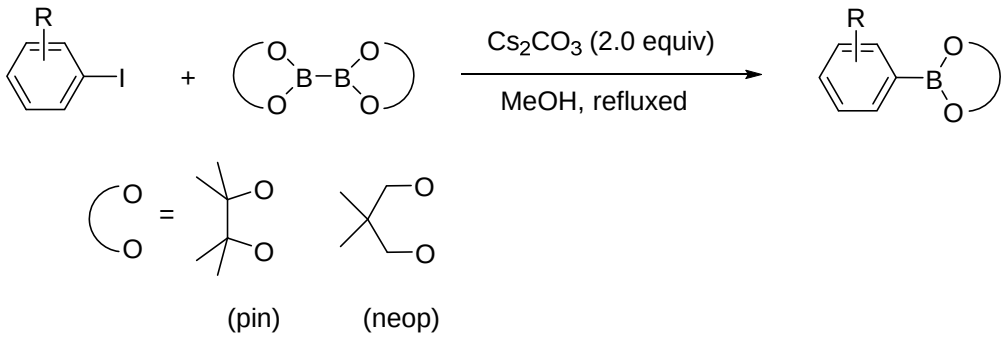

Scheme 9.14. Cs_2CO_3/MeOH-catalyzed borylation reaction.[90]

CHAPTER X
RESULTS AND DISCUSSION

In this Chapter, a development of a new transition-metal catalytic system for Miyaura borylation that can be conveniently performed without the need of air-sensitive techniques is described. Various palladium and copper catalysts were screened to optimize the reaction condition under air atmosphere. Effects of co-catalysts, bases, solvents, reaction time and solvent concentration on Pd/Cu-catalyzed Miyaura borylation reaction were examined. Furthermore, the substrate scope was investigated with aryl iodide including aryl bromide and aryl chloride. Various functionalized arylboronates were obtained in moderate to excellent yields. The possible reaction mechanism of Pd/Cu-catalyzed Miyaura borylation reaction was also discussed.

10.1. Screening of reaction conditions for the Pd/Cu-catalyzed Miyaura borylation reaction

To achieve the goal of this project, phenyl iodide and bis(pinacolato)diboron was initially used as substrate in a catalytic combination between $Pd(OAc)_2$ and CuI. For the present borylation under ambient conditions, a moderate yield was obtained (Table 10.1, entry 1). The yields of the product **8a** declined to 13% in the absence of PPh_3 and 30% with only $Pd(OAc)_2$ (Table 10.1, entries 2 and 3). A catalytic systems consisting of only CuI/PPh_3 or CuI was found ineffective for this borylation (Table 10.1, entries 4 and 5). Moreover, no reactions were observed in the absence of both $Pd(OAc)_2$ and CuI (Table 10.1, entries 6 and 7). The effect of the amount of air-stable PPh_3 ligand on the reaction was subsequently investigated. Interesting result showed that decreasing the amount of PPh_3 positively affected the yield of **8a** (Table 10.1, entries 8–13). A 60% yield of borylation product was afforded even with the use of 2 mol % of PPh_3 in the presence of 0.5 mL of water

(Table 10.1, entry 13). The amount of CuI was next examined (Table 10.1, entries 13–18). An improved product yield (65%) upon using 20 mol % of CuI was observed (Table 10.1, entry 16). In order to increase the yield, various Pd sources were screened to examine their effects on the reaction (Table 10.1, entries 19–22). Notably, $Pd(PPh_3)_4$ delivered a higher product yield (79%). However, this reagent requires an inert gas for storing and handling, whereas $Pd(OAc)_2$ is air- and moisture-stable and hence does not require any air-sensitive technique, which is the main interest of this research. Thus, the conditions constituted of $Pd(OAc)_2$ (2 mol %), CuI (20 mol %), and PPh_3 (2 mol %) was chosen for further evaluation of the other effects.

Table 10.1. Screening of reaction conditions for the Pd/Cu-catalyzed Miyaura borylation of iodobenzene and bis(pinacolato)diboron.[a]

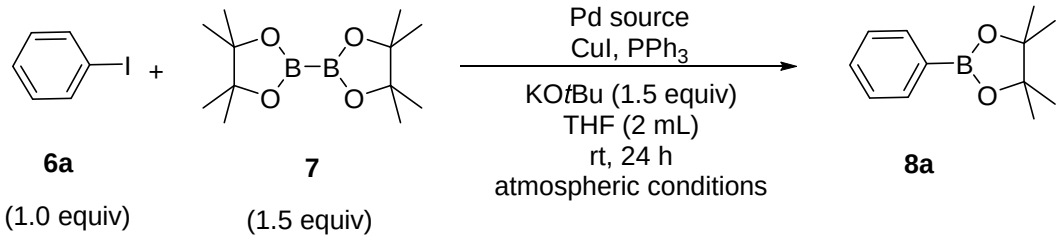

6a (1.0 equiv) **7** (1.5 equiv) **8a**

Entry	Pd source	CuI (mol %)	PPh_3 (mol %)	Yield[b] (%)
1	$Pd(OAc)_2$	10	13	51
2	$Pd(OAc)_2$	10	-	13
3	$Pd(OAc)_2$	-	-	30
4	-	10	13	28
5	-	10	-	4
6	-	-	-	0[d]
7	-	-	13	0[d]
8[c]	$Pd(OAc)_2$	10	30	57
9[c]	$Pd(OAc)_2$	10	18	58
10[c]	$Pd(OAc)_2$	10	13	62
11[c]	$Pd(OAc)_2$	10	10	60
12[c]	$Pd(OAc)_2$	10	5	60
13[c]	$Pd(OAc)_2$	10	2	60
14[c]	$Pd(OAc)_2$	2.5	2	47
15[c]	$Pd(OAc)_2$	5	2	56
16[c]	**$Pd(OAc)_2$**	**20**	**2**	**65**
17[c]	$Pd(OAc)_2$	30	2	65
18[c]	$Pd(OAc)_2$	50	2	63
19[c]	$PdCl_2$	20	2	53
20[c]	$Pd(PPh_3)_2Cl_2$	20	2	55
21[c]	Pd_2dba_3	20	2	56
22[c]	$Pd(PPh_3)_4$	20	2	79

[a] Reaction conditions, unless otherwise stated: Pd source (0.012 mmol), CuI, PPh_3, aryl iodide (0.6 mmol), bis(pinacolato)diboron (0.9 mmol), KO*t*Bu (0.9 mmol), THF (2 mL), air, room temperature, 24 h.

[b] Yield was determined by GC integration relative to hexamethylbenzene as an internal standard.

[c] 0.5 mL of water was added.

[d] No reaction was detected by TLC/GCMS.

10.2 Study of co-catalyst for the Miyaura borylation reaction

A variety of co-catalysts were screened. Various copper salts and other metal sources were investigated. The results are summarized in Table 10.2. CuCl and $Cu(OTf)_2$ gave a product yield similar to that obtained with CuI (65%). In contrast, other metal co-catalysts, such as $NiCl_2$, $Ni(OAc)_2$, $ZnCl_2$, AgOAc, and Ag_2CO_3 and

Table 10.2. Screening of co-catalysts for the Miyaura borylation reaction.[a]

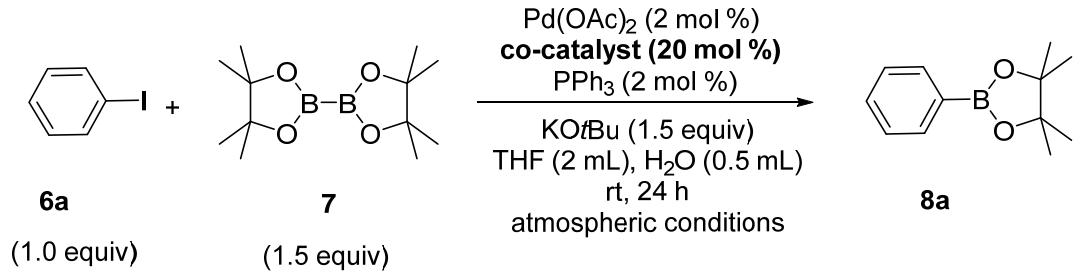

Entry	Co-catalyst	Yield[b] (%)
1	**CuCl**	**65**
2	CuBr	58
3	**CuI**	**65**
4	CuCN	3
5	$CuBr_2$	62
6	$Cu(OAc)_2$	51
7	CuO	47
8	**$Cu(OTf)_2$**	**65**
9	$Ni(OAc)_2 \cdot 4H_2O$	14
10	$NiCl_2 \cdot 6H_2O$	19
11	$ZnCl_2$	15
12	AgOAc	13
13	Ag_2CO_3	15
14	-	27

[a] Reaction conditions: $Pd(OAc)_2$ (0.012 mmol), co-catalyst (0.12 mmol), PPh_3 (0.012 mmol), aryl iodide (0.6 mmol), bis(pinacolato)diboron (0.9 mmol), KO*t*Bu (0.9 mmol), THF (2 mL), H_2O (0.5 mL), air, room temperature, 24 h.

[b] Yield was determined by GC integration relative to hexamethylbenzene as an internal standard.

the absence of co-catalyst gave poor results. CuI was chosen as a co-catalyst to avoid the interference of other anionic species in the reaction. Moreover, it was stated in the previous reports that copper played a key role as a promoter in the transmetalation step[92, 93] (see Section 10.6 for additional details).

10.3 Investigation of effects of base, solvent, reaction time and concentration for the Pd/Cu-catalyzed Miyaura borylation reaction

Then, the effects of inorganic bases and equivalency were studied (Table 10.3, entries 1–13). The highest product yield was obtained with the use of 1.5 equivalent of Cs_2CO_3. In contrast, the absence of base resulted in a drastically lower yield of **8a** (Table 10.3, entry 14). In addition, the product yields tend to be independent of the pK_a values of bases used in this Pd/Cu-catalyzed borylation (Scheme 4.4). For examples, the borylation product obtained by using K_2CO_3 was afforded in the higher yield than the reaction that was performed by using KO*t*Bu (Table 10.3, entries 3 and 5), although *tert*-butoxide has a higher pK_a (pK_a = 17) than the carbonate (pK_a = 10). Similarly, the acetate anion which possesses the lowest pK_a in this Table 10.3 led to the higher yield of **8a** than stronger bases, such as hydroxide bases (pK_a = 15.7) (Table 10.3, entries 9 and 11).

Table 10.3. Screening of bases for the Pd/Cu-catalyzed Miyaura borylation reaction.[a]

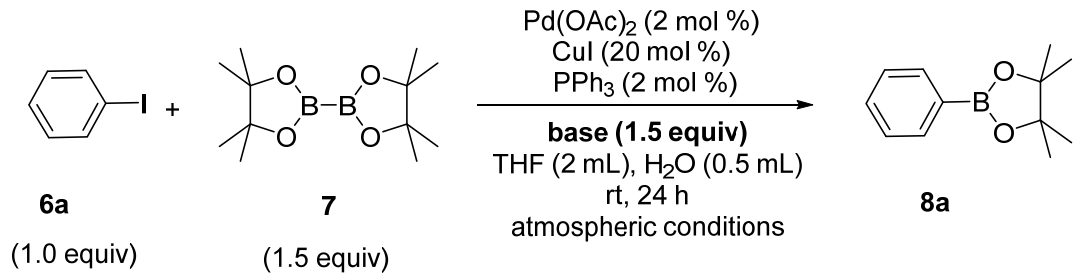

Entry	Base	Yield[b] (%)	Entry	Base	Yield[b] (%)
1	LiO*t*Bu	57	8	NaOH	58
2	NaO*t*Bu	59	9	KOH	57
3	KO*t*Bu	65	10	$CsOH \cdot H_2O$	53
4	K_3PO_4	74	11	KOAc	69
5	K_2CO_3	75	12	KOMe	67
6	**Cs_2CO_3**	**82**	13	NEt_3	65
7	Ag_2CO_3	26	14	-	5

[a] Reaction conditions: $Pd(OAc)_2$ (0.012 mmol), CuI (0.12 mmol), PPh_3 (0.012 mmol), aryl iodide (0.6 mmol), bis(pinacolato)diboron (0.9 mmol), base (0.9 mmol), THF (2 mL), H_2O (0.5 mL), air, room temperature, 24 h.

[b] Yield was determined by GC integration relative to hexamethylbenzene as an internal standard.

The optimized reaction conditions furnished **8a** with various types of solvents (Table 10.4). A quantitative yield can be obtained when using acetonitrile as solvent (Table 10.4, entry 8). This result suggests that lone-pair electrons of the nitrogen atom in CH_3CN would help stabilize the palladium active species.[94] In addition, the reaction was performed by using a mixture of water (0.5 mL) and acetonitrile (2 mL). As a result, the yield slightly declined to 91% (Table 10.4, entry 10). By varying the reaction time, a quantitative yield was also obtained after 2 h (Table 10.5, entry 6).

Table 10.4. Screening of solvents for the Pd/Cu-catalyzed Moyaura borylation reaction.[a]

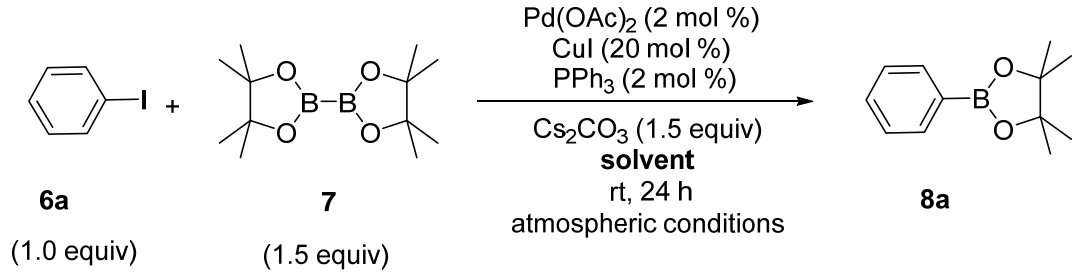

Entry	Solvent (mL)	Yield[b] (%)
1	dioxane (2 mL)	68
2	DMF (2 mL)	73
3	MeOH (2 mL)	72
4	THF (2 mL)	67
5	THF: H_2O (2: 0.5 mL)	82
6	EtOH (2 mL)	70
7	DMSO (2 mL)	75
8	**CH_3CN (2 mL)**	**97**
9	H_2O (2 mL)	16
10	CH_3CN: H_2O (2: 0.5 mL)	91

[a] Reaction conditions: $Pd(OAc)_2$ (0.012 mmol), CuI (0.12 mmol), PPh_3 (0.012 mmol), aryl iodide (0.6 mmol), bis(pinacolato)diboron (0.9 mmol), Cs_2CO_3 (0.9 mmol), solvent (2 mL), air, room temperature, 24 h.

[b] Yield was determined by GC integration relative to hexamethylbenzene as an internal standard.

This borylation reaction was also applied to various ratios of acetonitrile/water so that this protocol could meet the character of green chemistry (Table 10.6). Poor yields were obtained if the volume of water increased, and the use of only water afforded a very low yield. Moreover, the product yield was found to be independent of the amount of solvent (Table 10.7).

Table 10.5. Effect of reaction time on the Pd/Cu-catalyzed Miyaura borylation reaction.[a]

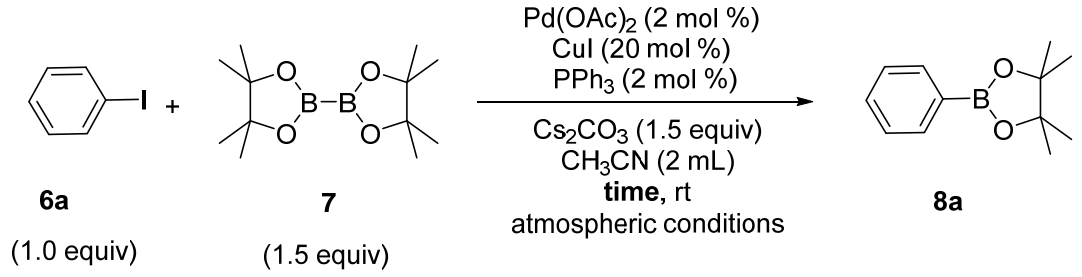

Entry	Time (h)	Yield[b] (%)
1	48	93
2	24	97
3	16	96
4	8	96
5	4	95
6	**2**	**97**
7	1	67
8	0.5	65

[a] Reactions were carried out under air condition at room temperature for the time indicated with $Pd(OAc)_2$ (0.012 mmol), CuI (0.12 mmol), PPh_3 (0.012 mmol), aryl iodide (0.6 mmol), bis(pinacolato)-diboron (0.9 mmol), Cs_2CO_3 (0.9 mmol), CH_3CN (2 mL).

[b] Yield was determined by GC integration relative to hexamethylbenzene as an internal standard.

Table 10.6. Effect of water concentrations in CH_3CN on the Pd/Cu-catalyzed Miyaura borylation reaction.[a]

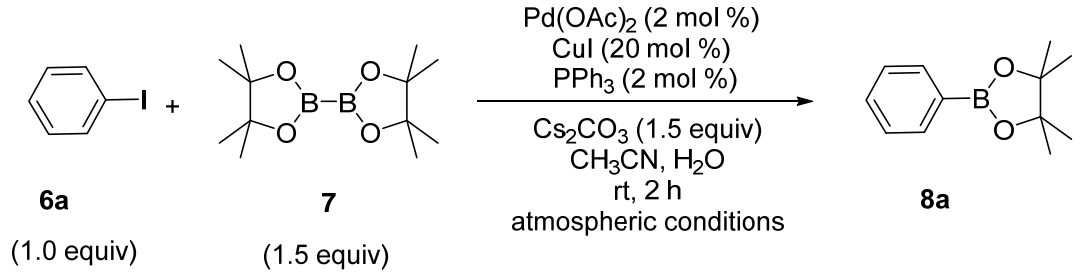

Entry	CH_3CN (mL)	H_2O (mL)	Yield[b] (%)
1	2.5	0	72
2	2.0	0.5	91
3	1.5	1	81
4	1.0	1.5	47
5	0.5	2	17
6	0	2.5	18

[a] Reaction conditions: $Pd(OAc)_2$ (0.012 mmol), CuI (0.12 mmol), PPh_3 (0.012 mmol), aryl iodide (0.6 mmol), bis(pinacolato)diboron (0.9 mmol), Cs_2CO_3 (0.9 mmol), air, room temperature, 2 h.

[b] Yield was determined by GC integration relative to hexamethylbenzene as an internal standard.

Table 10.7. Effect of solvent concentrations on the Pd/Cu-catalyzed Miyaura borylation reaction.[a]

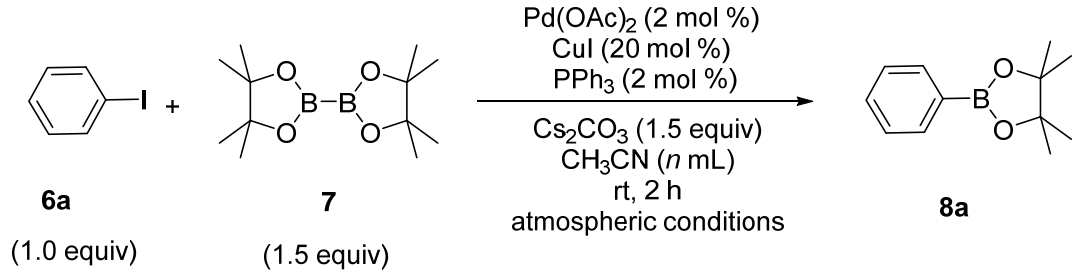

Entry	*n* (mL)	Yield[b] (%)
1	8	97
2	6	96
3	4	97
4	2	97
5	1	94

[a] Reaction conditions: $Pd(OAc)_2$ (0.012 mmol), CuI (0.12 mmol), PPh_3 (0.012 mmol), aryl iodide (0.6 mmol), bis(pinacolato)diboron (0.9 mmol), Cs_2CO_3 (0.9 mmol), CH_3CN (*n* mL), air, room temperature, 2 h.

[b] Yield was determined by GC integration relative to hexamethylbenzene as an internal standard.

10.4 Investigation of substrate scope on the Pd/Cu-catalyzed Miyaura borylation reaction

On the basis of the above optimization results, the following reaction conditions: a mixture of $Pd(OAc)_2$ (2 mol %), CuI (20 mol %), PPh_3 (2 mol %), and Cs_2CO_3 (1.5 equiv) in acetonitrile (2 mL) stirred at room temperature for 2 h which provide **8a** in 97% yield, was chosen for further studies.

Under the optimal reaction conditions, the scope of the substrates was next examined. Only aryl iodides were effective substrates, whereas aryl chlorides and bromides gave the corresponding product in the very low yields (Table 10.8, entries 1 and 2). This result suggests that this protocol can be useful for chemoselective borylation at C–I bond if other halogen substituents are present.

Table 10.8. Investigation of substrate scope on the Pd/Cu-catalyzed Miyaura borylation reaction.[a]

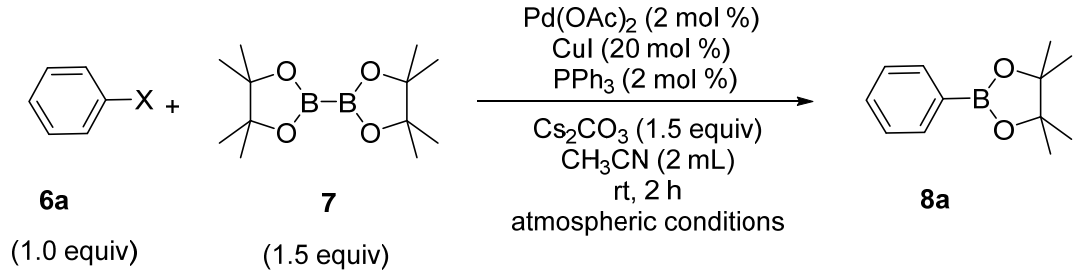

Entry	X	Yield[b] (%)
1	Cl	2
2	Br	5
3	I	97 (90)[c] (91)[d]

[a] Reaction conditions: $Pd(OAc)_2$ (0.012 mmol), CuI (0.12 mmol), PPh_3 (0.012 mmol), aryl iodide (0.6 mmol), bis(pinacolato)diboron (0.9 mmol), Cs_2CO_3 (0.9 mmol), CH_3CN (2 mL), air, room temperature, 2 h.

[b] Yield was determined by GC integration relative to hexamethylbenzene as an internal standard.

[c] The reaction was operated under inert atmosphere.

[d] The reaction was carried out in the presence of excess Hg.

10.5 Study of substituent groups on aryl iodide substrates

The present method could be applied successfully to a variety of aryl iodides bearing various types of functionalities. The results are summarized in Table 10.9. The scope of aryl iodide derivatives was found to be remarkably broad. Excellent yields were obtained for substrates with both electron-donating and electron-withdrawing substituents (Table 10.9, entries 2 and 3). The borylation reaction performed in air showed good tolerance for various functional groups, including hydroxide (**8d**), trifluoromethyl (**8e**), ketone (**8f**), amide (**8g**), and ester (**8h**) groups (Table 10.9, entries 4–8).

Interestingly, excellent chemoselectivity was observed upon using 1-chloro-4-iodobenzene (**6i**) and 1-bromo-4-iodobenzene (**6j**), as only mono-borylated

products **8i** and **8j** were obtained (Table 10.9, entries 9 and 10). The remaining halogen and substituent groups are ready for further transformations. This advantage could find general usage in organic synthesis and polymerization. Introducing alkyl or dialkyl groups at *ortho* positions of aryl iodides (**6k** and **6l**) resulted in moderate yields (Table 10.9, entries 11 and 12), presumably because of the steric hindrance of the *ortho*-substituents can hamper the oxidative addition step of the catalytic cycle. Additionally, the heteroaromatic iodide (**6m**) also gave the corresponding product (**8m**) in high yield (Table 10.9, entry 13).

Table 10.9. Screening of aryl iodides for the Pd/Cu-catalyzed Miyaura borylation reaction.[a]

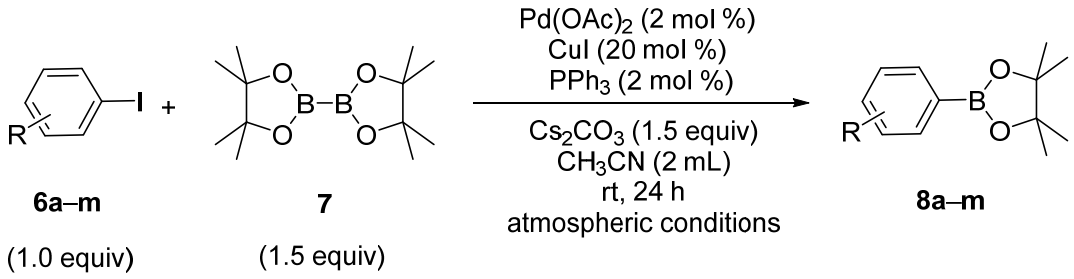

Entry	Aryl iodide	Product	Yield[b] (%)
1	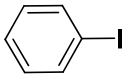 **6a**	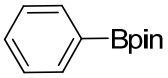 **8a**	76 (97)[c]
2	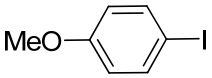 **6b**	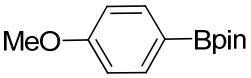 **8b**	92
3	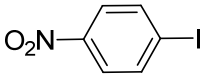 **6c**	 **8c**	93
4	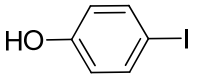 **6d**	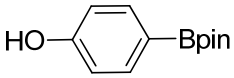 **8d**	76
5	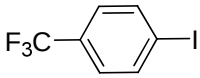 **6e**	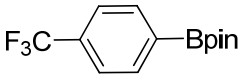 **8e**	66
6	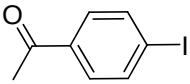 **6f**	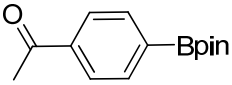 **8f**	91
7	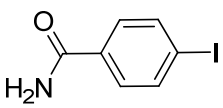 **6g**	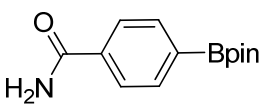 **8g**	89

[a] Reaction conditions, unless otherwise stated: $Pd(OAc)_2$ (0.012 mmol), CuI (0.12 mmol), PPh_3 (0.012 mmol), aryl iodide (0.6 mmol), bis(pinacolato)diboron (0.9 mmol), Cs_2CO_3 (0.9 mmol), CH_3CN (2 mL), air, room temperature, 24 h.

[b] Isolated yield.

[c] GC yield.

Table 10.9 (cont.). Screening of aryl iodides for the Pd/Cu-catalyzed Miyaura borylation reaction.[a]

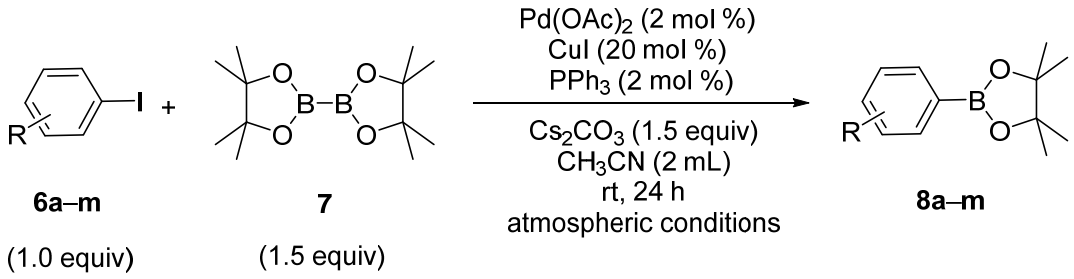

Entry	Aryl iodide	Product	Yield[b] (%)
8	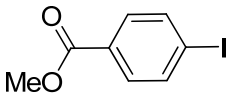 **6h**	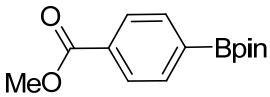 **8h**	81
9	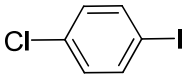 **6i**	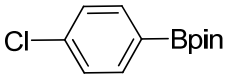 **8i**	96
10	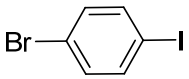 **6j**	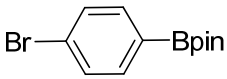 **8j**	70
11	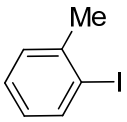 **6k**	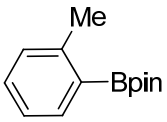 **8k**	50
12	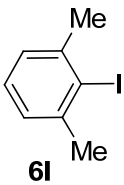 **6l**	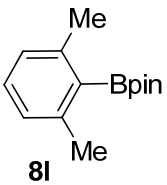 **8l**	31
13	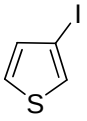 **6m**	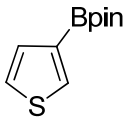 **8m**	63

[a] Reaction conditions, unless otherwise stated: $Pd(OAc)_2$ (0.012 mmol), CuI (0.12 mmol), PPh_3 (0.012 mmol), aryl iodide (0.6 mmol), bis(pinacolato)diboron (0.9 mmol), Cs_2CO_3 (0.9 mmol), CH_3CN (2 mL), air, room temperature, 24 h.

[b] Isolated yield.

[c] GC yield.

10.6 Proposed plausible mechanism of the Pd/Cu-catalyzed Miyaura borylation reaction

The mechanism of this transformation is assumed to involve oxidative addition of the aryl iodide and Pd(0) to form the Pd(II) complex **10**, as presented in Figure 10.1. Complex **10** reacts with an alkoxide base to form ArPd(II)–OR species **11**, which is more reactive than the ArPd(II)–X adduct.[62] Copper iodide acting as a transmetalating agent reacts with the base and ligand to form the L–Cu–OR intermediate **12**.[87] Ligand exchange has been reported to occur between **12** and bis(pinacolato)diboron to afford intermediate **13**.[87] Subsequently, **11** and **13** undergo the transmetalation to form complex **14**, which induces regeneration of the copper intermediate **12**. Finally, reductive elimination of **14** produces a new C–B bond of the corresponding borylation product.

Effects of copper on the Miyaura borylation remain unclear. However, according to the proposed mechanism, the role of copper in borylation reaction is assumed to be a Bpin-tranfer agent in the transmetalation step.[92, 93]

To test whether oxygen in the air participates in the catalytic Pd/Cu-catalyzed borylation reaction, the optimized Miyaura borylation under inert atmosphere was operated under the same condition described in Table 10.8 (entry 3). A borylated product between iodobenzene and B_2pin_2 in the absence of air was obtained in 90% yield, whereas the same reaction in air could reach 97% yield. This result indicated that the borylation protocol developed in this thesis is resistant to the air atmosphere and the copper may prevent catalyst deactivation, probably by adsorption of O_2 on the Cu(I) species. The $Cu(I)O_2$ species may represent in another resonance structures, *i.e.*, $Cu(II)O_2^-$, [$Cu(I)O_2 \leftrightarrow Cu(II)O_2^-$].[95, 96]

Notably, the palladium black was observed in the reaction. To prove whether Pd(0) nanoparticles (Pd(0)NPs) are the actual active catalyst in the borylation system developed in this thesis, the mercury poisoning test was carried out under the same reaction condition described in Table 10.8 (entry 3). A decrease in the coupling product yield (down to 91%) was observed in the excess of Hg. This result suggested that the borylation products were catalyzed, to some extent, by molecular palladium catalyst and the appearance of black particles might occur from the residual Pd catalyst.

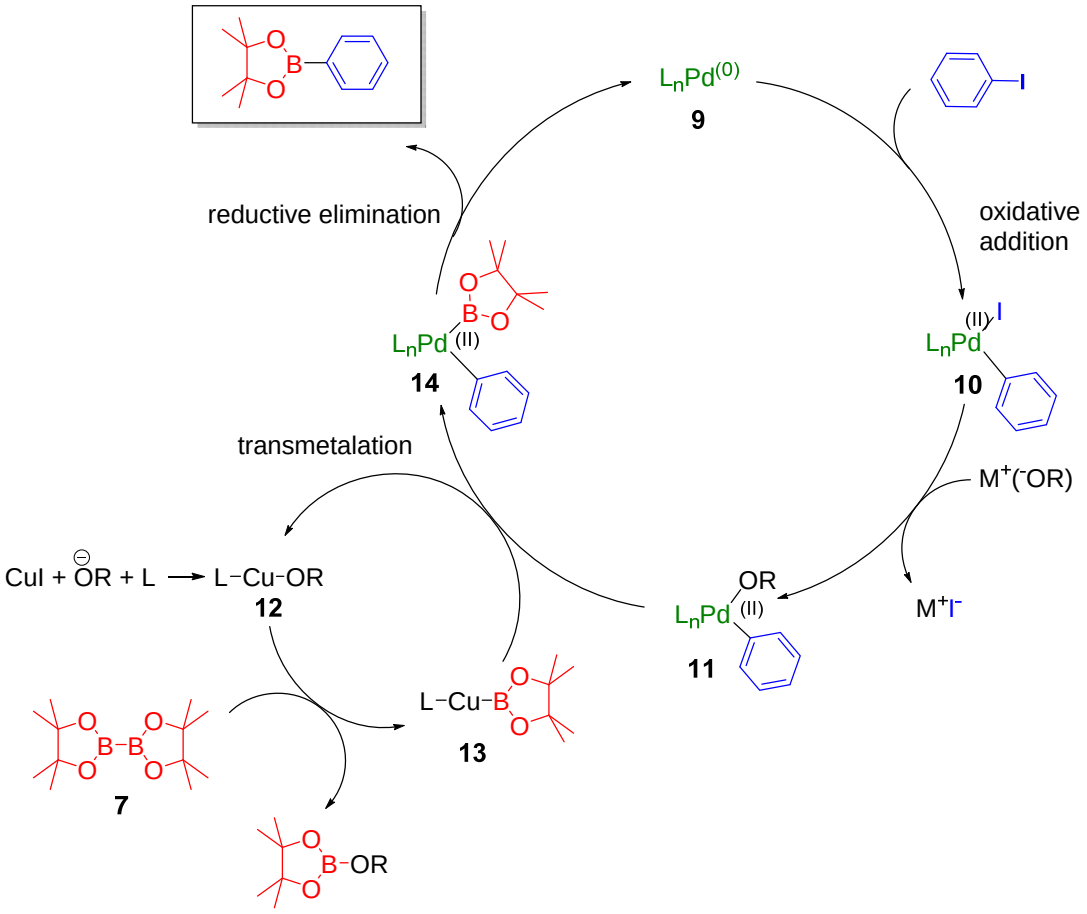

Figure 10.1. Proposed plausible mechanism of the Pd/Cu-catalyzed Miyaura borylation reaction.

CHAPTER XI
CONCLUSION

An efficient Pd/Cu-catalyzed protocol for Miyaura borylation of aryl and heteroaryl iodides has been successfully developed. Under the optimized reaction conditions, a mixture of $Pd(OAc)_2$ (2 mol %), CuI (20 mol %), PPh_3 (2 mol %) and Cs_2CO_3 (1.5 equiv) in acetonitrile (2 mL) allowed the facile synthesis of arylboronate **8a** in almost quantitative yield (97%) (for 0.6 mmol scale of phenyl iodide). The product yield of this borylation reaction was independent of the pK_a of bases and solvent concentrations. The synergistic catalysis could be performed in air at room temperature. Therefore, this method serves as an inexpensive and convenient synthetic route to afford arylboronates. The chemoselectivity of C–I bond was observed in this catalytic combination. The reaction conditions are also compatible with various sensitive functional groups including electron-withdrawing and electron-donating groups and gave high product yields.

Moreover, the mercury poisoning test revealed that this borylation occur through the molecular palladium catalyst. The roles of copper in this Pd/Cu-catalyzed Miyaura borylation reaction were proposed as the Bpin-tranfer agent and the catalyst deactivator.

CHAPTER XII
EXPERIMENTAL SECTION

12.1 General methods

All reagents were purchased from commercial sources (Aldrich, Merck and Fluka) and used without further purification. Thin layer chromatography (TLC) was purchased on Merck siliga gel 60 F254 aluminium sheets. Column chromatography was performed using Merck silica gel 60 (70–230 mesh.). NMR spectra were recorded on a Bruker Ascend^{TM} 400 (400 MHz) spectrometer. The chemical shifts (δ) for ^{1}H are given in ppm and referenced to the residual proton signal of the deuterated solvent. The chemical shifts (δ) for ^{13}C are referenced relative to the signal from the carbon of the deuterated solvent. The chemical shifts (δ) for ^{11}B are reported relative to external $BF_3 \cdot OEt_2$ (δ = 0 ppm). Gas chromatography analysis was performed on Agilent Technologies 6890N with FID detector and HP-1 capillary column (polymethylsiloxane, 25 m, 0.32 mm, 0.17 μm film thickness). Gas chromatography-mass analysis was performed on Agilent Technologies 7890A with 5975C inert XL MSD with Triple-Axis detector and HP-5 capillary column (polydimethylsiloxane with 5% phenyl group, 20 m, 0.25 mm, 0.25 μm film thickness) using helium as a carrier gas.

12.2 General procedure for reaction condition optimization of the Pd/Cu-catalyzed Miyaura borylation reaction

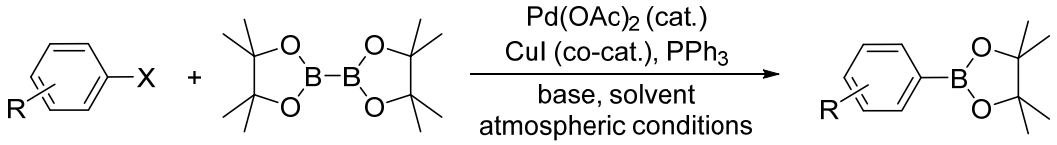

6(a–m) **7** **8(a–m)**

Under atmospheric condition, a 10 mL screw cap vial equipped with a magnetic stir bar was charged with hexamethylbenzene (0.06 mmol, 9.7 mg, 0.1 equiv) and the Pd source (0.012 mmol, 2 mol %). Triphenylphosphine and the copper source were added in the specific amount as indicated in the tables. Bis(pinacolato)-diboron (0.9 mmol, 228 mg, 1.5 equiv), base (0.9 mmol, 1.5 equiv), aryl halide (0.6 mmol, 1.0 equiv), and solvent (2 mL) was subsequently added into the reaction vial. The reaction vial was capped and stirred at room temperature for the desired time as indicated to generally give a dark mixture. The reaction mixture was diluted with 5 mL of dichloromethane, washed with water (2 × 15 mL), brine (1 × 15 mL), and dried over Na_2SO_4. The organic layer was concentrated *in vacuo* to afford the crude product. The yield of the product was determined by GC analysis based on integration relative to hexamethylbenzene as an internal standard. The crude product was finally isolated by column chromatography.

The GC conditions are as follows: initial temperature: 110 ºC (1 min), ramp 1 at 5 ºC/min to 140 ºC, ramp 2 at 35 ºC/min to 325 ºC, hold at 325 ºC (1 min). Retention times: hexamethylbenzene internal standard (6.4 min), product **8a** (4.9 min).

12.3 Analytical data for borylation compounds (8a–m)

12.3.1 4,4,5,5-Tetramethyl-2-phenyl-1,3,2-dioxaborolane (8a)

Following the General procedure for reaction condition optimization of Pd/Cu-catalyzed Miyaura borylation reaction, a mixture of $Pd(OAc)_2$ (2.7 mg, 0.012

mmol, 0.02 equiv), CuI (22.8 mg, 0.12 mmol, 0.2 equiv), PPh_3 (3.1 mg, 0.012 mmol, 0.02 equiv), Cs_2CO_3 (293.2 mg, 0.9 mmol, 1.5 equiv), bis(pinacolato)diboron (228 mg, 0.9 mmol, 1.5 equiv), iodobenzene (67 μL, 0.6 mmol, 1.0 equiv) and CH_3CN (2 mL) was stirred at room temperature for 24 h. The crude product was purified by column chromatography on silica gel (hexanes to 10% ethyl acetate/hexanes) to afford the title compound as a colorless liquid (90.2 mg, 74% yield). The NMR spectra of **8a** agree with the literature data.[62, 97, 98]

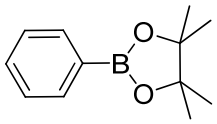

8a

^{1}H NMR (400 MHz, $CDCl_3$): δ 7.88 (d, *J* = 6.9 Hz, 2H, Ar*H*), 7.50 (m, 1H, Ar*H*), 7.42 (m, 2H, Ar*H*), 1.35 [s, 12H, (C*H*$_3$)$_4$].

^{13}C NMR (100 MHz, $CDCl_3$): δ 134.7 (2 × CH, C), 131.2 (CH), 127.6 (2 × CH), 83.7 (2 × C), 24.8 (4 × CH_3).

^{11}B NMR (128 MHz, $CDCl_3$): δ 31.2 (s).

EI-MS (*m*/*z*, relative intensity): 204 (M^+, 30), 189 (74), 188 (21), 118 (68), 105 (100), 104 (42).

12.3.2 2-(4-Methoxyphenyl)-4,4,5,5-tetramethyl-1,3,2-dioxaborolan (8b)

Following the General procedure for reaction condition optimization of Pd/Cu-catalyzed Miyaura borylation reaction, a mixture of $Pd(OAc)_2$ (2.7 mg, 0.012 mmol, 0.02 equiv), CuI (22.8 mg, 0.12 mmol, 0.2 equiv), PPh_3 (3.1 mg, 0.012 mmol, 0.02 equiv), Cs_2CO_3 (293.2 mg, 0.9 mmol, 1.5 equiv), bis(pinacolato)diboron (228 mg, 0.9 mmol, 1.5 equiv), 4-iodoanisole (140.4 mg, 0.6 mmol, 1.0 equiv) and CH_3CN (2 mL) was stirred at room temperature for 24 h. The crude product was purified by column chromatography on silica gel (10% ethyl acetate/hexanes) to afford the title compound as a colorless oil (128.9 mg, 92% yield). The NMR spectra of **8b** agree with the literature data.[69, 72, 88]

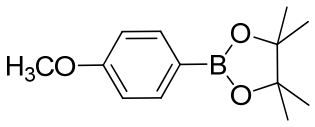

8b

^{1}H NMR (400 MHz, $CDCl_3$): δ 7.78 (d, *J* = 8.6 Hz, 2H, Ar*H*), 6.91 (d, *J* = 8.7 Hz, 2H, Ar*H*), 3.83 (s, 3H, OC*H*$_3$), 1.35 [s, 12H, (C*H*$_3$)$_4$].

^{13}C NMR (100 MHz, $CDCl_3$): δ 162.2 (C), 136.5 (2 × CH), 113.3 (2 × CH, C), 83.6 (2 × C), 55.1 (CH_3), 24.9 (4 × CH_3).

^{11}B NMR (128 MHz, $CDCl_3$): δ 30.7 (s).

EI-MS (*m*/*z*, relative intensity): 234 (M^+, 62), 219 (38), 148 (45), 135 (89), 134 (100), 133 (22).

12.3.3 4,4,5,5-Tetramethyl-2-(4-nitrophenyl)-1,3,2-dioxaborolane (8c)

Following the General procedure for reaction condition optimization of Pd/Cu-catalyzed Miyaura borylation reaction, a mixture of $Pd(OAc)_2$ (2.7 mg, 0.012 mmol, 0.02 equiv), CuI (22.8 mg, 0.12 mmol, 0.2 equiv), PPh_3 (3.1 mg, 0.012 mmol, 0.02 equiv), Cs_2CO_3 (293.2 mg, 0.9 mmol, 1.5 equiv), bis(pinacolato)diboron (228 mg, 0.9 mmol, 1.5 equiv), 1-iodo-4-nitrobenzene (149.4 mg, 0.6 mmol, 1.0 equiv) and CH_3CN (2 mL) was stirred at room temperature for 24 h. The crude product was purified by column chromatography on silica gel (CH_2Cl_2) to afford the title compound as a yellow solid (138.7 mg, 93% yield). The NMR spectra of **8c** agree with the literature data.[62, 72]

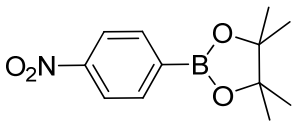

8c

^{1}H NMR (400 MHz, $CDCl_3$): δ 8.18 (d, *J* = 8.5 Hz, 2H, Ar*H*), 7.96 (d, *J* = 8.5 Hz, 2H, Ar*H*), 1.36 [s, 12H, (C*H*$_3$)$_4$].

^{13}C NMR (100 MHz, $CDCl_3$): δ 149.8 (C), 135.6 (2 × CH), 122.4 (2 × CH, C), 84.6 (2 × C), 24.8 (4 × CH_3).

^{11}B NMR (128 MHz, $CDCl_3$): δ 30.2 (s).

EI-MS (*m*/*z*, relative intensity): 249 (M^+, 5), 234 (100), 163 (64), 150 (31), 149 (8), 104 (11), 85 (9), 58 (11).

12.3.4 4-(4,4,5,5-Tetramethyl-1,3,2-dioxaborolan-2-yl)phenol (8d)

Following the General procedure for reaction condition optimization of Pd/Cu-catalyzed Miyaura borylation reaction, a mixture of $Pd(OAc)_2$ (2.7 mg, 0.012 mmol, 0.02 equiv), CuI (22.8 mg, 0.12 mmol, 0.2 equiv), PPh_3 (3.1 mg, 0.012 mmol, 0.02 equiv), Cs_2CO_3 (293.2 mg, 0.9 mmol, 1.5 equiv), bis(pinacolato)diboron (228 mg, 0.9 mmol, 1.5 equiv), 4-iodophenol (132 mg, 0.6 mmol, 1.0 equiv) and CH_3CN (2 mL) was stirred at room temperature for 24 h. The crude product was purified by preparative TLC (10% ethyl acetate/hexanes) to afford the title compound as a white solid (100.4 mg, 76% yield). The NMR spectra of **8d** agree with the literature data.[69, 89]

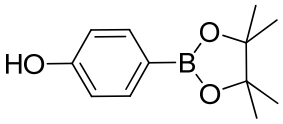

8d

^{1}H NMR (400 MHz, $CDCl_3$): δ 7.70 (d, *J* = 8.5 Hz, 2H, Ar*H*), 6.82 (d, *J* = 8.5 Hz, 2H, Ar*H*), 6.21 (br s, 1H, O*H*), 1.34 [s, 12H, (C*H*$_3$)$_4$].

^{13}C NMR (100 MHz, $CDCl_3$): δ 158.6 (C), 136.9 (2 × CH), 114.9 (2 × CH, C), 83.8 (2 × C), 24.7 (4 × CH_3).

^{11}B NMR (128 MHz, $CDCl_3$): δ 30.8 (s).

EI-MS (*m*/*z*, relative intensity): 220 (M^+, 43), 205 (50), 134 (45), 121 (100), 120 (99), 119 (19).

12.3.5 4,4,5,5-Tetramethyl-2-(4-(trifluoromethyl)-phenyl)-1,3,2-dioxaborolane (8e)

Following the General procedure for reaction condition optimization of Pd/Cu-catalyzed Miyaura borylation reaction, a mixture of $Pd(OAc)_2$ (2.7 mg, 0.012 mmol, 0.02 equiv), CuI (22.8 mg, 0.12 mmol, 0.2 equiv), PPh_3 (3.1 mg, 0.012 mmol, 0.02 equiv), Cs_2CO_3 (293.2 mg, 0.9 mmol, 1.5 equiv), bis(pinacolato)diboron (228 mg, 0.9 mmol,1.5 equiv), 4-iodobenzotrifluoride (163.2 mg, 0.6 mmol, 1.0 equiv) and CH_3CN (2 mL) was stirred at room temperature for 24 h. The crude product was purified by preparative TLC (40% dichloromethane/hexanes) to afford the title compound as a white solid (108.1 mg, 66% yield). The NMR spectra of **8e** agree with the literature data.[74, 76, 88, 99]

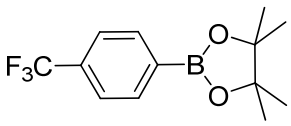

8e

^{1}H NMR (400 MHz, $CDCl_3$): δ 7.95 (d, *J* = 7.8 Hz, 2H, Ar*H*), 7.64 (d, *J* = 7.9 Hz, 2H, Ar*H*), 1.38 [s, 12H, (C*H*$_3$)$_4$].

^{13}C NMR (100 MHz, $CDCl_3$): δ 135.0 (2 × CH, C), 132.8 (q, *J* = 32.0 Hz, C), 124.3 (q, *J* = 4.0 Hz, 2 × CH), 124.2 (q, *J* = 270.0 Hz, CF_3), 84.3 (2 × C), 24.8 (4 × CH_3).

^{19}F NMR (376 MHz, $CDCl_3$): δ –63.1 (s, 3F)

^{11}B NMR (128 MHz, $CDCl_3$): δ 30.7 (s).

EI-MS (*m*/*z*, relative intensity): 272 (M^+, 9), 257 (100), 256 (24), 186 (81), 173 (84), 172 (22), 85 (12), 58 (12).

12.3.6 1-(4-(4,4,5,5-Tetramethyl-1,3,2-dioxaborolan-2-yl)phenyl)ethanone (8f)

Following the General procedure for reaction condition optimization of Pd/Cu-catalyzed Miyaura borylation reaction, a mixture of $Pd(OAc)_2$ (2.7 mg, 0.012 mmol, 0.02 equiv), CuI (22.8 mg, 0.12 mmol, 0.2 equiv), PPh_3 (3.1 mg, 0.012 mmol, 0.02 equiv), Cs_2CO_3 (293.2 mg, 0.9 mmol, 1.5 equiv), bis(pinacolato)diboron (228

mg, 0.9 mmol, 1.5 equiv), 4'-iodoacetophenone (147.6 mg, 0.6 mmol, 1.0 equiv) and CH_3CN (2 mL) was stirred at room temperature for 24 h. The crude product was purified by preparative TLC (30% acetone/hexanes) to afford the title compound as a white solid (138.4 mg, 91% yield). The NMR spectra of **8f** agree with the literature data.[62, 88]

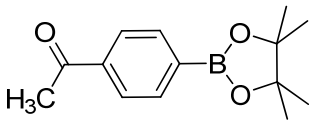

8f

^{1}H NMR (400 MHz, $CDCl_3$): δ 7.91 (d, *J* = 8.0 Hz, 2H, Ar*H*), 7.87 (d, *J* = 8.2 Hz, 2H, Ar*H*), 2.58 (s, 3H, COC*H*$_3$), 1.33 [s, 12H, (C*H*$_3$)$_4$].

^{13}C NMR (100 MHz, $CDCl_3$): δ 198.3 (C), 138.9 (2 × C), 134.8 (2 × CH), 127.2 (2 × CH), 84.1 (2 × C), 26.6 (CH_3), 24.9 (4 × CH_3).

^{11}B NMR (128 MHz, $CDCl_3$): δ 30.8 (s).

EI-MS (*m*/*z*, relative intensity): 246 (M^+, 18), 231 (100), 231 (100), 160 (27), 147 (61), 131 (15), 103 (11), 85 (7).

12.3.7 4-(4,4,5,5-Tetramethyl-1,3,2-dioxaborolan-2-yl)benzamide (8g)

Following the General procedure for reaction condition optimization of Pd/Cu-catalyzed Miyaura borylation reaction, a mixture of $Pd(OAc)_2$ (2.7 mg, 0.012 mmol, 0.02 equiv), CuI (22.8 mg, 0.12 mmol, 0.2 equiv), PPh_3 (3.1 mg, 0.012 mmol, 0.02 equiv), Cs_2CO_3 (293.2 mg, 0.9 mmol, 1.5 equiv), bis(pinacolato)diboron (228 mg, 0.9 mmol, 1.5 equiv) 4-iodobenzamide (147.6 mg, 0.6 mmol, 1.0 equiv) and CH_3CN (2 mL) was stirred at room temperature for 24 h. The crude product was purified by recrystallization (CH_2Cl_2/hexanes) to afford the title compound as a white solid (132.5 mg, 89% yield). The NMR spectra of **8g** agree with the literature data.[72]

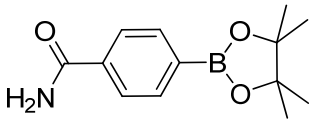

8g

^{1}H NMR (400 MHz, $CDCl_3$): δ 7.87 (d, *J* = 8.0 Hz, 2H, Ar*H*), 7.79 (d, *J* = 8.1 Hz, 2H, Ar*H*), 6.31 (br s, 2H, CONH_2) 1.34 [s, 12H, (CH_3)$_4$].

^{13}C NMR (100 MHz, $CDCl_3$): δ 169.5 (C), 135.5 (2 × C), 135.0 (2 × CH), 126.5 (2 × CH), 84.2 (2 × C), 24.9 (4 × CH_3).

^{11}B NMR (128 MHz, $CDCl_3$): δ 30.8 (s).

EI-MS (*m*/*z*, relative intensity): 247 (M^+, 23), 232 (60), 231 (21), 214 (75), 213 (21), 204 (11), 190 (9), 186 (12), 162 (12), 161 (72), 148 (100), 147 (28), 143 (62) 131 (22), 130 (48), 129 (17), 103 (22), 58 (18).

12.3.8 Methyl 4-(4,4,5,5-tetramethyl-1,3,2-dioxaborolan-2-yl)benzoate (8h)

Following the General procedure for reaction condition optimization of Pd/Cu-catalyzed Miyaura borylation reaction, a mixture of $Pd(OAc)_2$ (2.7 mg, 0.012 mmol, 0.02 equiv), CuI (22.8 mg, 0.12 mmol, 0.2 equiv), PPh_3 (3.1 mg, 0.012 mmol, 0.02 equiv), Cs_2CO_3 (293.2 mg, 0.9 mmol, 1.5 equiv), bis(pinacolato)diboron (228 mg, 0.9 mmol, 1.5 equiv), methyl 4-iodobenzoate (157.2 mg, 0.6 mmol, 1.0 equiv) and CH_3CN (2 mL) was stirred at room temperature for 24 h. The crude product was purified by preparative TLC (1:5 ether/hexanes) to afford the title compound as a white solid (132.5 mg, 81% yield). The NMR spectra of **8h** agree with the literature data.[72, 100]

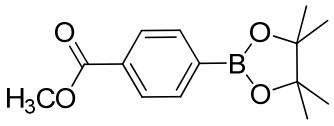

8h

^{1}H NMR (400 MHz, $CDCl_3$): δ 8.03 (d, *J* = 8.2 Hz, 2H, Ar*H*), 7.88 (d, *J* = 8.2 Hz, 2H, Ar*H*), 3.92 (s, 3H, CO_2CH_3), 1.36 [s, 12H, (CH_3)$_4$].

^{13}C NMR (100 MHz, $CDCl_3$): δ 167.0 (C), 134.6 (2 × CH), 132.2 (2 × C), 128.5 (2 × CH), 84.1 (2 × C), 52.0 (CH_3), 24.8 (4 × CH_3).

^{11}B NMR (128 MHz, $CDCl_3$): δ 30.8 (s).

EI-MS (*m*/*z*, relative intensity): 262 (M^+, 17), 247 (72), 246 (18), 176 (87), 163 (100), 162 (26), 131 (18), 103 (17).

12.3.9 2-(4-Chlorophenyl)-4,4,5,5-tetramethyl-1,3,2-dioxaborolane (8i)

Following the General procedure for reaction condition optimization of Pd/Cu-catalyzed Miyaura borylation reaction, a mixture of $Pd(OAc)_2$ (2.7 mg, 0.012 mmol, 0.02 equiv), CuI (22.8 mg, 0.12 mmol, 0.2 equiv), PPh_3 (3.1 mg, 0.012 mmol, 0.02 equiv), Cs_2CO_3 (293.2 mg, 0.9 mmol, 1.5 equiv), bis(pinacolato)diboron (228 mg, 0.9 mmol, 1.5 equiv), 1-chloro-4-iodobenzene (143.1 mg, 0.6 mmol, 1.0 equiv) and CH_3CN (2 mL) was stirred at room temperature for 24 h. The crude product was purified by column chromatography on silica gel (hexanes) to afford the title compound as a colorless oil (136.6 mg, 96% yield). The NMR spectra of **8i** agree with the literature data.[87, 88]

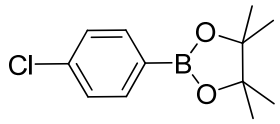

8i

^{1}H NMR (400 MHz, $CDCl_3$): δ 7.74 (d, *J* = 8.3 Hz, 2H, Ar*H*), 7.35 (d, *J* = 8.3 Hz, 2H, Ar*H*), 1.34 [s, 12H, (CH_3)$_4$].

^{13}C NMR (100 MHz, $CDCl_3$): δ 137.5 (C), 136.1 (2 × CH), 128.0 (2 × CH, C), 84.0 (2 × C), 24.8 (4 × CH_3).

^{11}B NMR (128 MHz, $CDCl_3$): δ 31.1 (s).

EI-MS (*m*/*z*, relative intensity): 238 (M^+, 30), 225 (28), 224 (16), 223 (84), 222 (19), 152 (58), 141 (32), 140 (20), 139 (100), 138 (42), 85 (15), 59 (10).

12.3.10 2-(4-Bromophenyl)-4,4,5,5-tetramethyl-1,3,2-dioxaborolane (8j)

Following the General procedure for reaction condition optimization of Pd/Cu-catalyzed Miyaura borylation reaction, a mixture of $Pd(OAc)_2$ (2.7 mg, 0.012 mmol, 0.02 equiv), CuI (22.8 mg, 0.12 mmol, 0.2 equiv), PPh_3 (3.1 mg, 0.012 mmol,

0.02 equiv), Cs_2CO_3 (293.2 mg, 0.9 mmol, 1.5 equiv), bis(pinacolato)diboron (228 mg, 0.9 mmol, 1.5 equiv), 1-bromo-4-iodobenzene (169.7 mg, 0.6 mmol, 1.0 equiv) and CH_3CN (2 mL) was stirred at room temperature for 24 h. The crude product was purified by column chromatography on silica gel (hexanes) to afford the title compound as a light yellow liquid (119.4 mg, 70% yield). The NMR spectra of **8j** agree with the literature data.[87, 88]

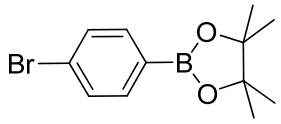

8j

^{1}H NMR (400 MHz, $CDCl_3$): δ 7.67 (d, *J* = 8.0 Hz, 2H, Ar*H*), 7.51 (d, *J* = 8.4 Hz, 2H, Ar*H*), 1.35 [s, 12H, (C*H*$_3$)$_4$].

^{13}C NMR (100 MHz, $CDCl_3$): δ 136.3 (2 × CH), 130.9 (2 × CH, C), 126.2 (C), 84.0 (2 × C), 24.8 (4 × CH_3).

^{11}B NMR (128 MHz, $CDCl_3$): δ 31.4 (s).

EI-MS (*m*/*z*, relative intensity): 284 (M^+, 38), 283 (19), 282 (40), 269 (92), 268 (34), 267 (94), 266 (23), 198 (68), 196 (70), 185 (91), 184 (55), 183 (100), 182 (50), 104, (24), 103 (33), 77 (19), 59 (15).

12.3.11 4,4,5,5-Tetramethyl-2-*o*-tolyl-1,3,2-dioxaborolane (8k)

Following the General procedure for reaction condition optimization of Pd/Cu-catalyzed Miyaura borylation reaction, a mixture of $Pd(OAc)_2$ (2.7 mg, 0.012 mmol, 0.02 equiv), CuI (22.8 mg, 0.12 mmol, 0.2 equiv), PPh_3 (3.1 mg, 0.012 mmol, 0.02 equiv), Cs_2CO_3 (293.2 mg, 0.9 mmol, 1.5 equiv), bis(pinacolato)diboron (228 mg, 0.9 mmol,1.5 equiv), 2-iodotoluene (76.4 μL, 0.6 mmol, 1.0 equiv) and CH_3CN (2 mL) was stirred at room temperature for 24 h. The crude product was purified by preparative TLC (5% ethyl acetate/hexanes) to afford the title compound as a white solid (68 mg, 52% yield). The NMR spectra of product **8k** agree with the literature data.[87, 88]

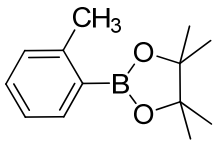

8k

^{1}H NMR (400 MHz, $CDCl_3$): δ 7.85–7.83(m, 1H, Ar*H*), 7.40–7.36 (m, 1H, Ar*H*), 7.24–7.21 (m, 2H, Ar*H*), 2.61 (s, 3H, C*H*$_3$), 1.41 [s, 12H, (C*H*$_3$)$_4$].

^{13}C NMR (100 MHz, $CDCl_3$): δ 144.8 (C), 135.8 (CH, C), 130.8 (CH), 129.7 (CH), 124.7 (CH), 83.4 (2 × C), 24.9 (4 × CH_3), 22.2 (CH_3).

^{11}B NMR (128 MHz, $CDCl_3$): δ 30.8 (s).

EI-MS (*m*/*z*, relative intensity): 218 (M^+, 29), 203 (41), 161 (92), 160 (42), 119 (100), 118 (88), 117 (43), 91 (18), 85 (11).

12.3.12 2-(2,6-Dimethylphenyl)-4,4,5,5-tetramethyl-1,3,2-dioxaborolane (8l)

Following the General procedure for reaction condition optimization of Pd/Cu-catalyzed Miyaura borylation reaction, a mixture of $Pd(OAc)_2$ (2.7 mg, 0.012 mmol, 0.02 equiv), CuI (22.8 mg, 0.12 mmol, 0.2 equiv), PPh_3 (3.1 mg, 0.012 mmol, 0.02 equiv), Cs_2CO_3 (293.2 mg, 0.9 mmol, 1.5 equiv), bis(pinacolato)diboron (228 mg, 0.9 mmol,1.5 equiv), 2-iodo-1,3-dimethylbenzene (86.5 μL, 0.6 mmol, 1.0 equiv) and CH_3CN (2 mL) was stirred at room temperature for 24 h. The crude product was purified by preparative TLC (5% ethyl acetate/hexanes) to afford the title compound as a white solid (43.5 mg, 31% yield). The NMR spectra of **8l** agree with the literature data.[89]

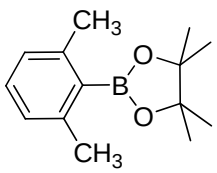

8l

^{1}H NMR (400 MHz, $CDCl_3$): δ 7.14 (t, *J* = 7.6 Hz, 1H, Ar*H*), 6.96 (d, *J* = 7.6 Hz, 2H, Ar*H*), 2.41 [s, 6H, (C*H*$_3$)$_2$], 1.40 [s, 12H, (C*H*$_3$)$_4$].

^{13}C NMR (100 MHz, $CDCl_3$): δ 141.7 (3 × C), 129.1 (CH), 126.4 (2 × CH), 83.6 (2 × C), 24.9 (4 × CH_3), 22.2 (2 × CH_3).

^{11}B NMR (128 MHz, $CDCl_3$): δ 33.6 (s).

EI-MS (*m*/*z*, relative intensity): 232 (M^+, 29), 175 (100), 174 (33), 133 (51), 132 (63), 131 (29), 105 (12), 91 (13).

12.3.13 4,4,5,5-Tetramethyl-2-(thiophen-3-yl)-1,3,2-dioxaborolane (8m)

Following the General procedure for reaction condition optimization of Pd/Cu-catalyzed Miyaura borylation reaction, a mixture of $Pd(OAc)_2$ (2.7 mg, 0.012 mmol, 0.02 equiv), CuI (22.8 mg, 0.12 mmol, 0.2 equiv), PPh_3 (3.1 mg, 0.012 mmol, 0.02 equiv), Cs_2CO_3 (293.2 mg, 0.9 mmol, 1.5 equiv), bis(pinacolato)diboron (228 mg, 0.9 mmol, 1.5 equiv), 3-iodothiophene (61 μL, 0.6 mmol, 1.0 equiv) and CH_3CN (2 mL) was stirred at room temperature for 24 h. The crude product was purified by column chromatography on silica gel (0–5% ethyl acetate/hexanes) to afford the title compound as a white solid (79.3 mg, 63% yield). The NMR spectra of **8m** agree with the literature data.[69, 101, 102]

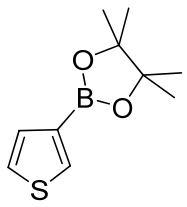

8m

^{1}H NMR (400 MHz, $CDCl_3$): δ 7.95 (dd, *J* = 2.6, 0.9 Hz, 1H, Ar*H*), 7.44 (dd, *J* = 4.8, 0.9 Hz, 2H, Ar*H*), 7.36 (dd, *J* = 4.8, 2.7 Hz, 1H, Ar*H*), 1.35 [s, 12H, (CH_3)$_4$].

^{13}C NMR (100 MHz, $CDCl_3$): δ 136.4 (C), 132.0 (CH), 125.3 (2 × CH), 83.6 (2 × C), 24.8 (4 × CH_3).

^{11}B NMR (128 MHz, $CDCl_3$): δ 29.3 (s).

EI-MS (*m*/*z*, relative intensity): 210 (M^+, 33), 195 (22), 152 (13), 124 (100), 111 (77), 110 (43), 85 (18).

12.4 Mercury poisoning test for the synergistic Pd/Cu-catalyzed Miyaura borylation reaction (Table 10.8, entry 3)

Under air, the reaction vial charged with an excess of Hg (Hg:Pd = 400:1) was added hexamethylbenzene (0.06 mmol, 9.7 mg, 0.1 equiv), $Pd(OAc)_2$ (0.012 mmol, 2.7 mg, 2.0 mol), CuI (22.8 mg, 0.12 mmol, 0.2 equiv), PPh_3 (3.1 mg, 0.012 mmol, 0.02 equiv), Cs_2CO_3 (293.2 mg, 0.9 mmol, 1.5 equiv), bis(pinacolato)diboron (228 mg, 0.9 mmol, 1.5 equiv), iodobenzene (67 μL, 0.6 mmol, 1.0 equiv) and CH_3CN (2 mL) and was stirred at room temperature for 2 h. The mixture was diluted with dichloromethane (5 mL), washed with water (2 × 15 mL), brine (1 × 15 mL), and dried over Na_2SO_4. The organic layer was concentrated *in vacuo* to afford the crude product **8a**. The yield of the product was determined by GC method. A 91% yield was obtained in the presence of excess Hg.

REFERENCES

1. Miyaura N, Suzuki A. Palladium-catalyzed cross-coupling reactions of organoboron compounds. Chem Rev. 1995;95(7):2457–83.
2. Suzuki A. Recent advances in the cross-coupling reactions of organoboron derivatives with organic electrophiles, 1995–1998. J Organomet Chem. 1999;576(1–2):147–68.
3. Kotha S, Lahiri K, Kashinath D. Recent applications of the Suzuki–Miyaura cross-coupling reaction in organic synthesis. Tetrahedron. 2002;58(48): 9633–95.
4. Bellina F, Carpita A, Rossi R. Palladium catalysts for the Suzuki cross-coupling reaction: an overview of recent advances. Synthesis. 2004(15):2419–40.
5. Kürti L, Czakó B. Strategic applications of named reactions in organic synthesis: background and detailed mechanisms: Elsevier Academic Press; 2005.
6. Smith GB, Dezeny GC, Hughes DL, King AO, Verhoeven TR. Mechanistic studies of the Suzuki cross-coupling reaction. J Org Chem. 1994;59(26): 8151–6.
7. Widegren JA, Bennett MA, Finke RG. Is it homogeneous or heterogeneous catalysis? identification of bulk ruthenium metal as the true catalyst in benzene hydrogenations starting with the monometallic precursor, Ru(II)(η^6-C_6Me_6)$(OAc)_2$, plus kinetic characterization of the heterogeneous nucleation, then autocatalytic surface-growth mechanism of metal Film formation. J Am Chem Soc. 2003;125(34): 10301–10.
8. Matos K, Soderquist JA. Alkylboranes in the Suzuki−Miyaura coupling: stereochemical and mechanistic studies. J Org Chem. 1998;63(3):461–70.
9. Amatore C, Jutand A, Le Duc G. Kinetic data for the transmetalation/reductive elimination in palladium-catalyzed Suzuki–Miyaura reactions: unexpected triple role of hydroxide ions used as base. Chem Eur J. 2011;17(8):2492–503.

10. Amatore C, Jutand A, M'Barki MA. Evidence of the formation of zerovalent palladium from $Pd(OAc)_2$ and triphenylphosphine. Organometallics. 1992;11(9):3009–13.
11. Clayden J, Greeves N, Warren S. Organic Chemistry: OUP Oxford; 2012.
12. Widegren JA, Finke RG. A review of the problem of distinguishing true homogeneous catalysis from soluble or other metal-particle heterogeneous catalysis under reducing conditions. J Mol Catal A: Chem. 2003;198(1–2):317–41.
13. van Leeuwen PWNM. Decomposition pathways of homogeneous catalysts. Applied Catalysis A: General. 2001;212(1–2):61–81.
14. Rao GK, Kumar A, Kumar B, Kumar D, Singh AK. Palladium(II)-selenated schiff base complex catalyzed Suzuki–Miyaura coupling: dependence of efficiency on alkyl chain length of ligand. Dalton Trans. 2012;41(7):1931–7.
15. Rao GK, Kumar A, Kumar S, Dupare UB, Singh AK. Palladacycles of thioethers catalyzing Suzuki–Miyaura C–C coupling: generation and catalytic activity of nanoparticles. Organometallics. 2013;32(8):2452–8.
16. Sharma KN, Joshi H, Singh VV, Singh P, Singh AK. Palladium(II) complexes of pyrazolated thio/selenoethers: syntheses, structures, single source precursors of Pd_4Se and PdSe nanoparticles and potential for catalyzing Suzuki–Miyaura coupling. Dalton Trans. 2013;42(11):3908–18.
17. Littke AF, Dai C, Fu GC. Versatile catalysts for the Suzuki cross-coupling of arylboronic acids with aryl and vinyl halides and triflates under mild conditions. J Am Chem Soc. 2000;122(17):4020–8.
18. Yin J, Rainka MP, Zhang XX, Buchwald SL. A highly active Suzuki catalyst for the synthesis of sterically hindered biaryls: Novel ligand coordination. J Am Chem Soc. 2002;124(7):1162–3.
19. Adjabeng G, Brenstrum T, Wilson J, Frampton C, Robertson A, Hillhouse J, et al. Novel class of tertiary phosphine ligands based on a phospha-adamantane framework and use in the Suzuki cross-coupling reactions of aryl halides under mild conditions. Org Lett. 2003;5(6):953–5.

20. Martin R, Buchwald SL. Palladium-catalyzed Suzuki–Miyaura cross-coupling reactions employing dialkylbiaryl phosphine ligands. Acc Chem Res. 2008;41(11):1461–73.
21. Billingsley KL, Anderson KW, Buchwald SL. A highly active catalyst for Suzuki–Miyaura cross-coupling reactions of heteroaryl compounds. Angew Chem Int Ed. 2006;45(21):3484–8.
22. Fleckenstein CA, Plenio H. Efficient Suzuki−Miyaura coupling of (hetero)aryl chlorides with thiophene- and furanboronic acids in aqueous *n*-butanol. J Org Chem. 2008;73(8):3236–44.
23. Stewart B, Harriman A, Higham LJ. Predicting the air stability of phosphines. Organometallics. 2011;30(20):5338–43.
24. Weissman H, Milstein D. Highly active Pd(II) cyclometallated imine catalyst for the Suzuki reaction. Chem Commun. 1999(18):1901–2.
25. Grasa GA, Hillier AC, Nolan SP. Convenient and efficient Suzuki–Miyaura cross-coupling catalyzed by a palladium/diazabutadiene system. Org Lett. 2001;3(7):1077–80.
26. Li S, Lin Y, Cao J, Zhang S. Guanidine/$Pd(OAc)_2$-catalyzed room temperature Suzuki cross-coupling reaction in aqueous media under aerobic conditions. J Org Chem. 2007;72(11):4067–72.
27. Herrmann WA. N-heterocyclic carbenes: a new concept in organometallic catalysis. Angew Chem Int Ed. 2002;41(8):1290–309.
28. Herrmann WA, Böhm VPW, Gstöttmayr CWK, Grosche M, Reisinger CP, Weskamp T. Synthesis, structure and catalytic application of palladium(II) complexes bearing N-heterocyclic carbenes and phosphines. J Organomet Chem. 2001;617-618:616–28.
29. Altenhoff G, Goddard R, Lehmann CW, Glorius F. Sterically demanding, bioxazoline-derived N-heterocyclic carbene ligands with restricted flexibility for catalysis. J Am Chem Soc. 2004;126(46):15195–201.
30. Kantchev EAB, O'Brien CJ, Organ MG. Palladium complexes of N-heterocyclic carbenes as catalysts for cross-coupling reactions – A synthetic chemist's perspective. Angew Chem Int Ed. 2007;46(16):2768–813.

31. Schaper LA, Hock SJ, Herrmann WA, Kühn FE. Synthesis and application of water-soluble NHC transition-metal complexes. Angew Chem Int Ed. 2013;52(1):270–89.
32. Hashmi ASK, Lothschütz C, Böhling C, Rominger F. From Isonitriles to carbenes: synthesis of new NAC– and NHC–palladium(II) compounds and their catalytic activity. Organometallics. 2011;30(8):2411–7.
33. Dube KS, Harrop TC. Structure and properties of an eight-coordinate Mn(II) complex that demonstrates a high water relaxivity. Dalton Trans. 2011;40(29):7496–8.
34. Boudier A, Breuil P-AR, Magna L, Olivier-Bourbigou H, Braunstein P. Nickel(II) complexes with imino-imidazole chelating ligands bearing pendant donor groups (SR, OR, NR_2, PR_2) as precatalysts in ethylene oligomerization. J Organomet Chem. 2012;718(0):31–7.
35 Liu J, Chen J, Zhao J, Zhao Y, Li L, Zhang H. A modified procedure for the synthesis of 1-arylimidazoles. Synthesis. 2003(17):2661–6.
36. Wiedermann J, Mereiter K, Kirchner K. Palladium imine and amine complexes derived from 2-thiophenecarboxaldehyde as catalysts for the Suzuki cross-coupling of aryl bromides. J Mol Catal A: Chem. 2006;257(1–2):67–72.
37. Zhou H, Zhang WZ, Wang YM, Qu JP, Lu XB. N-heterocyclic carbene functionalized polymer for reversible fixation-release of CO_2. Macromolecules. 2009;42(15):5419–21.
38. Laine TV, Klinga M, Leskelä M. Synthesis and X-ray structures of new mononuclear and dinuclear diimine complexes of late transition metals. Eur J Inorg Chem. 1999(6):959–64.
39. Schmid M, Eberhardt R, Klinga M, Leskelä M, Rieger B. New C_2v- and chiral C_2-symmetric olefin polymerization catalysts based on nickel(II) and palladium(II) diimine complexes bearing 2,6-diphenyl aniline moieties: Synthesis, structural characterization, and first insight into polymerization properties. Organometallics. 2001;20(11):2321–30.
40. Laine TV, Piironen U, Lappalainen K, Klinga M, Aitola E, Leskelä M. Pyridinylimine-based nickel(II) and palladium(II) complexes: preparation,

structural characterization and use as alkene polymerization catalysts. J Organomet Chem. 2000;606(2):112–24.

41. Done MC, Rüther T, Cavell KJ, Kilner M, Peacock EJ, Braussaud N, et al. Novel cationic and neutral Pd(II) complexes bearing imidazole based chelate ligands: synthesis, structural characterisation and catalytic behaviour. J Organomet Chem. 2000;607(1–2):78–92.
42. Sperling RA, Parak WJ. Surface modification, functionalization and bioconjugation of colloidal inorganic nanoparticles. Phil Trans R Soc A. 2010;368 (1915):1333–83.
43. Mino T, Shirae Y, Sakamoto M, Fujita T. Phosphine-free hydrazone-Pd complex as the catalyst precursor for a Suzuki-Miyaura reaction under mild aerobic conditions. J Org Chem. 2005;70(6):2191–4.
44. Amadio E, Scrivanti A, Chessa G, Matteoli U, Beghetto V, Bertoldini M, et al. Synthesis, characterization and low temperature self assembling of (η^3-allyl)palladium complexes with 2-pyridyl-1,2,3-triazole bidentate ligands. Study of the catalytic activity in Suzuki–Miyaura reaction. J Organomet Chem. 2012;716(0):193–200.
45. Jindabot S, Teerachanan K, Thongkam P, Kiatisevi S, Khamnaen T, Phiriyawirut P, et al. Palladium(II) complexes featuring bidentate pyridine–triazole ligands: synthesis, structures, and catalytic activities for Suzuki–Miyaura coupling reactions. J Organomet Chem. 2014;750(0):35–40.
46. John A, Shaikh MM, Ghosh P. Suzuki–Miyaura cross-coupling of aryl chlorides catalyzed by palladium precatalysts of N/O-functionalized pyrazolyl ligands. Inorg Chim Acta. 2010;363(12):3113–21.
47. Wang H-S, Wang Y-C, Pan Y-M, Zhao S-L, Chen Z-F. Simultaneous reduction of nitro- to amino-group in the palladium-catalyzed Suzuki cross-coupling reaction. Tetrahedron Lett. 2008;49(16):2634–7.
48. Bulut H, Artok L, Yilmazu S. Suzuki cross-coupling reaction of aryl halides with arylboronic acids catalysed by Pd(II)-NaY zeolite. Tetrahedron Lett. 2003; 44(2):289–91.

49. Narayanan R, El-Sayed MA. Effect of catalysis on the stability of metallic nanoparticles: Suzuki reaction catalyzed by PVP-palladium nanoparticles. J Am Chem Soc. 2003;125(27):8340–7.
50. Bilati U, Allémann E, Doelker E. Development of a nanoprecipitation method intended for the entrapment of hydrophilic drugs into nanoparticles. Eur J Pharm Sci. 2005;24(1):67–75.
51. Adrio LA, Nguyen BN, Guilera G, Livingston AG, Hii KK. Speciation of $Pd(OAc)_2$ in ligandless Suzuki–Miyaura reactions. Catal Sci Technol. 2012;2(2):316–23.
52. MUTUSLAB: pK_a values of commond bases. [Online]. [cited 2014 Jan 19]; Avaiable from: http://mutuslab.cs.uwindsor.ca/green/59-331/pka%-20bases.pdf
53. Amatore C, Jutand A, Le Duc G. Mechanistic origin of antagonist effects of usual anionic bases (OH^-, CO_3^{2-}) as modulated by their countercations (Na^+, Cs^+, K^+) in palladium-catalyzed Suzuki–Miyaura reactions. Chem Eur J. 2012; 18(21):6616–25.
54. Amatore C, Le Duc G, Jutand A. Mechanism of palladium-catalyzed Suzuki–Miyaura reactions: multiple and antagonistic roles of anionic "bases" and their countercations. Chem Eur J. 2013;19(31):10082–93
55. Barder TE, Walker SD, Martinelli JR, Buchwald SL. Catalysts for Suzuki–Miyaura coupling processes: scope and studies of the effect of ligand structure. J Am Chem Soc. 2005;127(13):4685–96.
56. Liu C, Zhang Y, Liu N, Qiu J. A simple and efficient approach for the palladium-catalyzed ligand-free Suzuki reaction in water. Green Chem. 2012;14(11): 2999–3003.
57. SMART v.5.6. Madison, WI, USA: Bruker AXS Inc; 2000.
58. SAINT v.4. Madison, WI, USA: Siemens analytical X-ray systems, Inc; 1996.
59. Mackay S, Gilmore CJ, Edwards C, Stewart N, Shankland K. maXus Computer program for the solution and refinement of crystal structures Bruker nonius. the netherlands, MacScience, Japan & The University of Glasgow.

60. Altomare A, Burla MC, Camalli M, Cascarano GL, Giacovazzo C, Guagliardi A, et al. SIR97: a new tool for crystal structure determination and refinement. J Appl Crystallogr. 1999;32(1):115–9.
61. Sheldrick GM. SHELXTL v.6.12. Madison, WI, USA: Siemens Analytical X-ray Systems, Inc; 1997.
62. Ishiyama T, Murata M, Miyaura N. Palladium(0)-catalyzed cross-coupling reaction of alkoxydiboron with haloarenes: A direct procedure for arylboronic esters. J Org Chem. 1995;60(23):7508–10.
63. Miyaura N. Organoboron compounds. In: Miyaura N, editor. Cross-coupling reactions: Springer Berlin Heidelberg; 2002.
64. Merino P, Tejero T. Expanding the limits of organoboron chemistry: synthesis of functionalized arylboronates. Angew Chem Int Ed. 2010;49(40):7164–5.
65. Hutton CA, Skaff O. A convenient preparation of dityrosine via Miyaura borylation–Suzuki coupling of iodotyrosine derivatives. Tetrahedron Lett. 2003;44(26):4895–8.
66. Partyka DV. Transmetalation of unsaturated carbon nucleophiles from boron-containing species to the mid to late d-block metals of relevance to catalytic C−X coupling reactions (X = C, F, N, O, Pb, S, Se, Te). Chem Rev. 2011;111(3):1529–95.
67. Ishiyama T, Itoh Y, Kitano T, Miyaura N. Synthesis of arylboronates via the palladium(0)-catalyzed cross-coupling reaction of tetra(alkoxo)diborons with aryl triflates. Tetrahedron Lett. 1997;38(19):3447–50.
68. Ishiyama T, Ishida K, Miyaura N. Synthesis of pinacol arylboronates via cross-coupling reaction of bis(pinacolato)diboron with chloroarenes catalyzed by palladium(0)–tricyclohexylphosphine complexes. Tetrahedron. 2001; 57(49):9813–6.
69. Billingsley KL, Barder TE, Buchwald SL. Palladium-catalyzed borylation of aryl chlorides: scope, applications, and computational studies. Angew Chem Int Ed. 2007;46(28):5359–63.
70. Tang W, Keshipeddy S, Zhang Y, Wei X, Savoie J, Patel ND, et al. Efficient monophosphorus ligands for Palladium-catalyzed Miyaura borylation. Org Lett. 2011;13(6):1366–9.

71. Kawamorita S, Ohmiya H, Iwai T, Sawamura M. Palladium-catalyzed borylation of sterically demanding aryl halides with a silica-supported compact phosphane ligand. Angew Chem Int Ed. 2011;50(36):8363–6.
72. Yamamoto T, Morita T, Takagi J, Yamakawa T. $NiCl_2(PMe_3)_2$-catalyzed borylation of aryl chlorides. Org Lett. 2011;13(21):5766–9.
73. Iverson CN, Smith MR. Stoichiometric and catalytic B−C bond formation from unactivated hydrocarbons and boranes. J Am Chem Soc. 1999;121(33): 7696–7.
74. Cho J-Y, Iverson CN, Smith MR. Steric and chelate directing effects in aromatic borylation. J Am Chem Soc. 2000;122(51):12868–9.
75. Cho J-Y, Tse MK, Holmes D, Maleczka Jr RE, Smith MR. Remarkably selective Iridium catalysts for the elaboration of aromatic C–H bonds. Science. 2002;295(5553):305–8.
76. Ishiyama T, Takagi J, Ishida K, Miyaura N, Anastasi NR, Hartwig JF. Mild Iridium-catalyzed borylation of arenes. High turnover numbers, room temperature reactions, and isolation of a potential intermediate. J Am Chem Soc. 2002;124(3):390–1.
77. Ishiyama T, Takagi J, Hartwig JF, Miyaura N. A stoichiometric aromatic C–H borylation catalyzed by iridium(I)/2,2′-bipyridine complexes at room temperature. Angew Chem Int Ed. 2002;41(16):3056–8.
78. Mertins K, Zapf A, Beller M. Catalytic borylation of *o*-xylene and heteroarenes via C–H activation. J Mol Catal A: Chem. 2004;207(1):21–5.
79. Takagi J, Sato K, Hartwig JF, Ishiyama T, Miyaura N. Iridium-catalyzed C–H coupling reaction of heteroaromatic compounds with bis(pinacolato)-diboron: regioselective synthesis of heteroarylboronates. Tetrahedron Lett. 2002;43(32):5649–51.
80. Mkhalid IAI, Coventry DN, Albesa-Jove D, Batsanov AS, Howard JAK, Perutz RN, et al. Ir-catalyzed borylation of C–H bonds in N-containing heterocycles: regioselectivity in the synthesis of heteroaryl boronate esters. Angew Chem Int Ed. 2006;45(3):489–91.
81. Ishiyama T, Nobuta Y, Hartwig JF, Miyaura N. Room temperature borylation of arenes and heteroarenes using stoichiometric amounts of pinacolborane

catalyzed by iridium complexes in an inert solvent. Chem Commun. 2003(23):2924–5.

82. Chotana GA, Kallepalli VA, Maleczka Jr RE, Smith III MR. Iridium-catalyzed borylation of thiophenes: versatile, synthetic elaboration founded on selective C–H functionalization. Tetrahedron. 2008;64(26):6103–14.
83. Datta A, Kollhofer A, Plenio H. Ir-catalyzed C-H activation in the synthesis of borylated ferrocenes and half sandwich compounds. Chem Commun. 2004(13):1508–9.
84. Coventry DN, Batsanov AS, Goeta AE, Howard JAK, Marder TB, Perutz RN. Selective Ir-catalyzed borylation of polycyclic aromatic hydrocarbons: structures of naphthalene-2,6-bis(boronate), pyrene-2,7-bis(boronate) and perylene-2,5,8,11-tetra(boronate) esters. Chem Commun. 2005(16):2172–4.
85. Mkhalid IAI, Barnard JH, Marder TB, Murphy JM, Hartwig JF. C−H activation for the construction of C−B bonds. Chem Rev. 2010;110(2):890–931.
86. Zhu W, Ma D. Formation of arylboronates by a CuI-catalyzed coupling reaction of pinacolborane with aryl iodides at room temperature. Org Lett. 2006;8(2):261–3.
87. Kleeberg C, Dang L, Lin Z, Marder TB. A facile route to aryl boronates: room-temperature, copper-catalyzed borylation of aryl halides with alkoxy diboron reagents. Angew Chem Int Ed. 2009;48(29):5350–4.
88. Mo F, Jiang Y, Qiu D, Zhang Y, Wang J. Direct conversion of arylamines to pinacol boronates: a metal-free borylation process. Angew Chem Int Ed. 2010;49(10):1846–9.
89. Qiu D, Jin L, Zheng Z, Meng H, Mo F, Wang X, et al. Synthesis of pinacol arylboronates from aromatic amines: a metal-free transformation. J Org Chem. 2012;78(5):1923–33.
90. Zhang J, Wu H-H, Zhang J. Cesium carbonate mediated borylation of aryl iodides with diboron in methanol. Eur J Org Chem. 2013;2013(28):6263–6.
91. Safron SA, King GA, Horvat RC. Molecular beam chemistry. Formation of phenyl cations from C_6H_5X molecules. J Am Chem Soc. 1981;103(21): 6333–7.64.

92. Savarin C, Liebeskind LS. Nonbasic, Room temperature, palladium-catalyzed coupling of aryl and alkenyl iodides with boronic acids mediated by copper(I) thiophene-2-carboxylate (CuTC). Org Lett. 2001;3(14):2149–52.

93. Kim YW, Niphakis MJ, Georg GI. Copper-assisted palladium(II)-catalyzed direct arylation of cyclic enaminones with arylboronic acids. J Org Chem. 2012; 77(21):9496–503.

94. Wayland BB, Schramm RF. Cationic and neutral chloride complexes of palladium(II) with the nonaqueous solvent donors acetonitrile, dimethyl sulfoxide, and a series of amides. Mixed sulfur and oxygen coordination sites in a dimethyl sulfoxide complex. Inorg Chem. 1969;8(4):971–6.

95. Ene AB, Archipov T, Roduner E. Competitive adsorption and interaction of benzene and oxygen on Cu/HZSM5 zeolites. J Phys Chem C. 2011;115(9): 3688–94.

96. Ene AB, Bauer M, Archipov T, Roduner E. Adsorption of oxygen on copper in Cu/HZSM5 zeolites. Phys Chem Chem Phys. 2010;12(24):6520–31.

97. Clary JW, Rettenmaier TJ, Snelling R, Bryks W, Banwell J, Wipke WT, et al. Hydride as a leaving group in the reaction of pinacolborane with halides under ambient grignard and barbier conditions. One-pot synthesis of alkyl, aryl, heteroaryl, vinyl, and allyl pinacolboronic esters. J Org Chem. 2011; 76(23):9602–10.

98. Morandi S, Caselli E, Forni A, Bucciarelli M, Torre G, Prati F. Enantiomeric excess of 1,2-diols by formation of cyclic boronates: an improved method. Tetrahedron: Asymmetry. 2005;16(17):2918–26.

99. Murata M, Sambommatsu T, Watanabe S, Masuda Y. An efficient catalyst system for palladium-catalyzed borylation of aryl halides with pinacol-borane. Synlett. 2006(12):1867–70.

100. Jiang Q, Ryan M, Zhichkin P. Use of in situ isopropoxide protection in the metal–halogen exchange of arylboronates. J Org Chem. 2007;72(17): 6618–20.

101. Claudel S, Gosmini C, Paris JM, Périchon J. A novel transmetallation of arylzinc species into arylboronates from aryl halides in a barbier procedure. Chem Commun. 2007(35):3667–9.

102. Koolmeister T, Södergren M, Scobie M. Pinacolyl boronic esters as components in the Petasis reaction. Tetrahedron Lett. 2002;43(34):5965–8.

APPENDICES

APPENDIX A
CALIBRATION CURVES

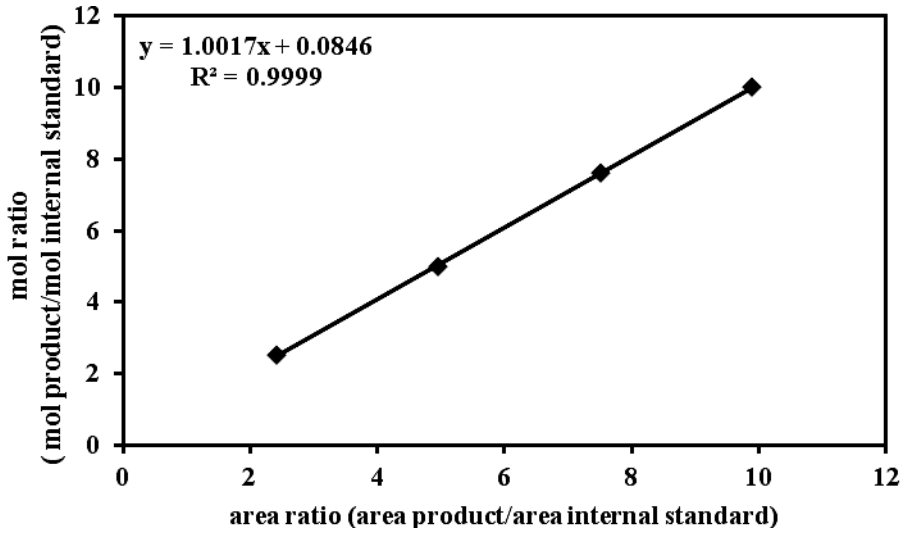

Figure 13.1. Calibration curve for the Suzuki-Miyaura cross-coupling reaction.

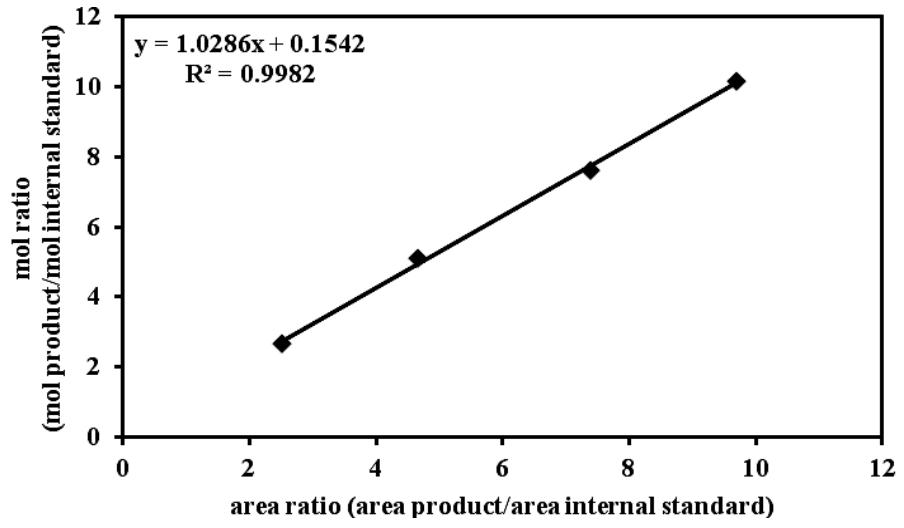

Figure 13.2. Calibration curve for the Pd/Cu-catalyzed Miyaura borylation reaction.

APPENDIX B
NMR SPETRA OF LIGANDS

1. NMR spectra of compound (1)

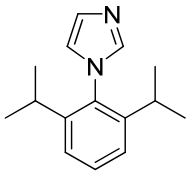

1

^{1}H NMR in $CDCl_3$

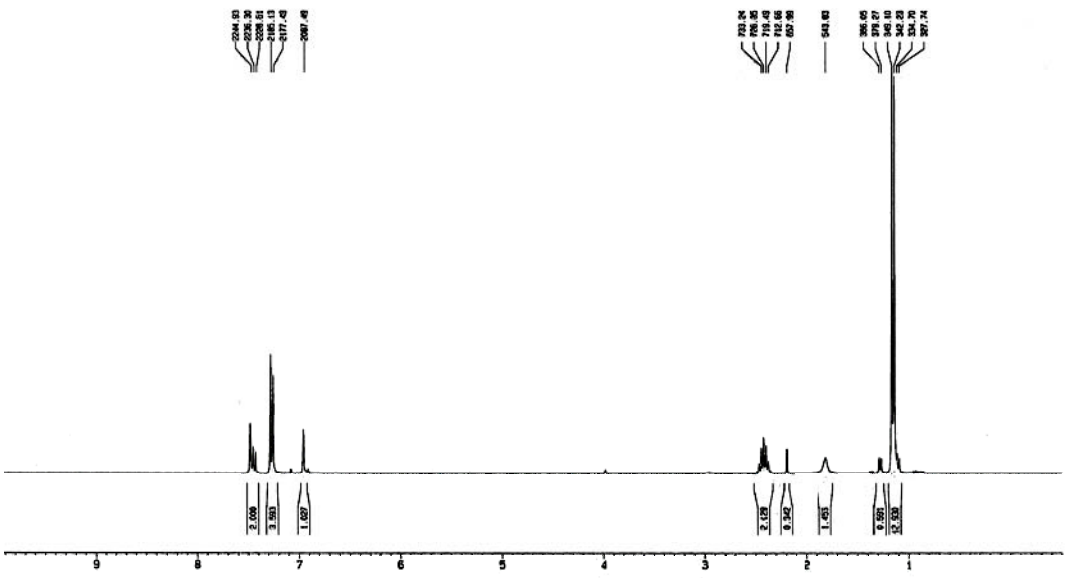

Figure 13.3. NMR spectra of compound **1**.

^{13}C NMR in $CDCl_3$

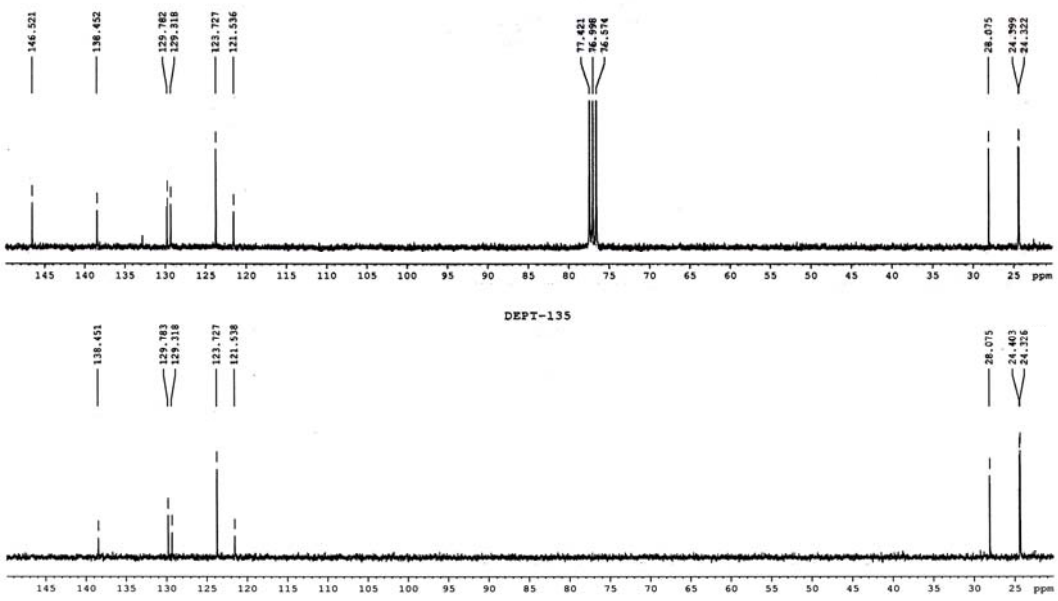

Figure 13.3 (cont.). NMR spectra of **1**.

2 NMR spectra of compound (2)

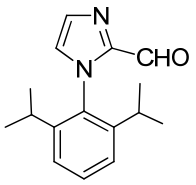

2

^{1}H NMR in $CDCl_3$

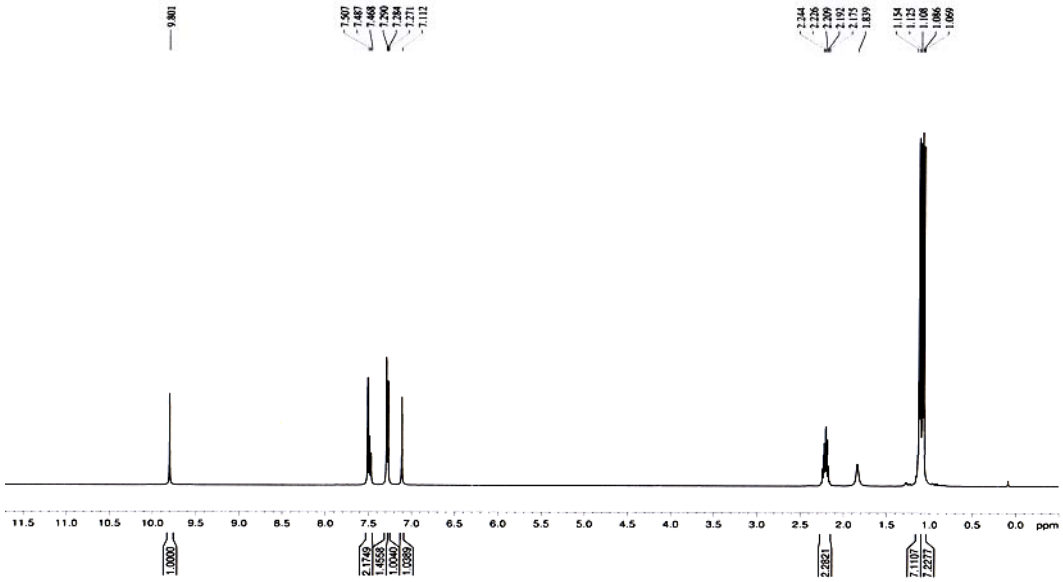

^{13}C NMR in $CDCl_3$

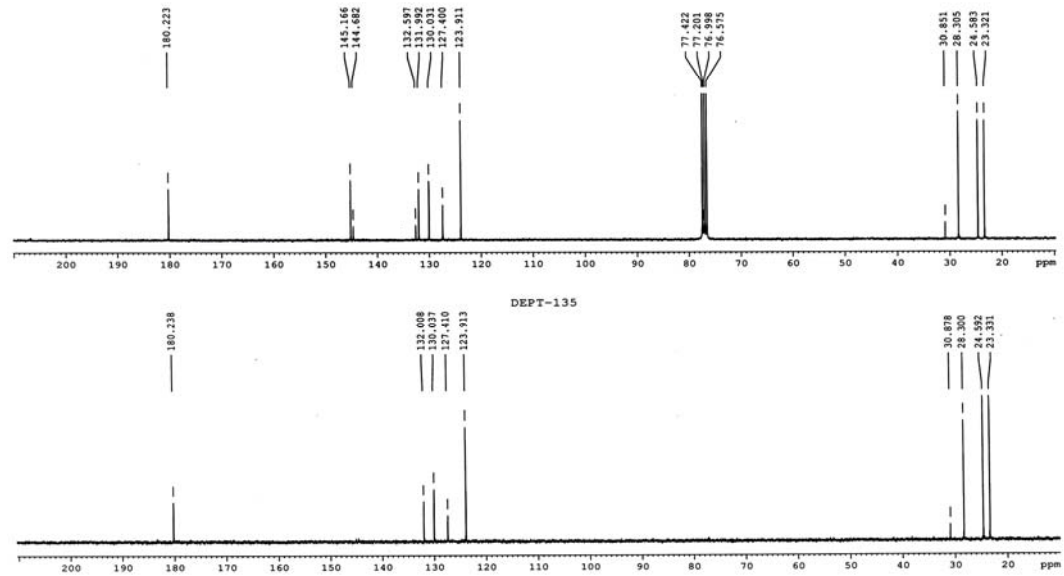

Figure 13.4. NMR spectra of compound **2**.

APPENDIX C

NMR SPECTRA OF PALLADIUM COMPLEXES

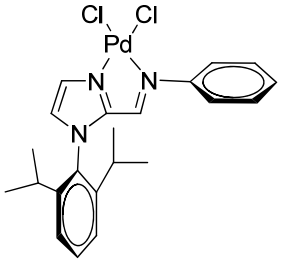

4a

^{1}H NMR in $CDCl_3$

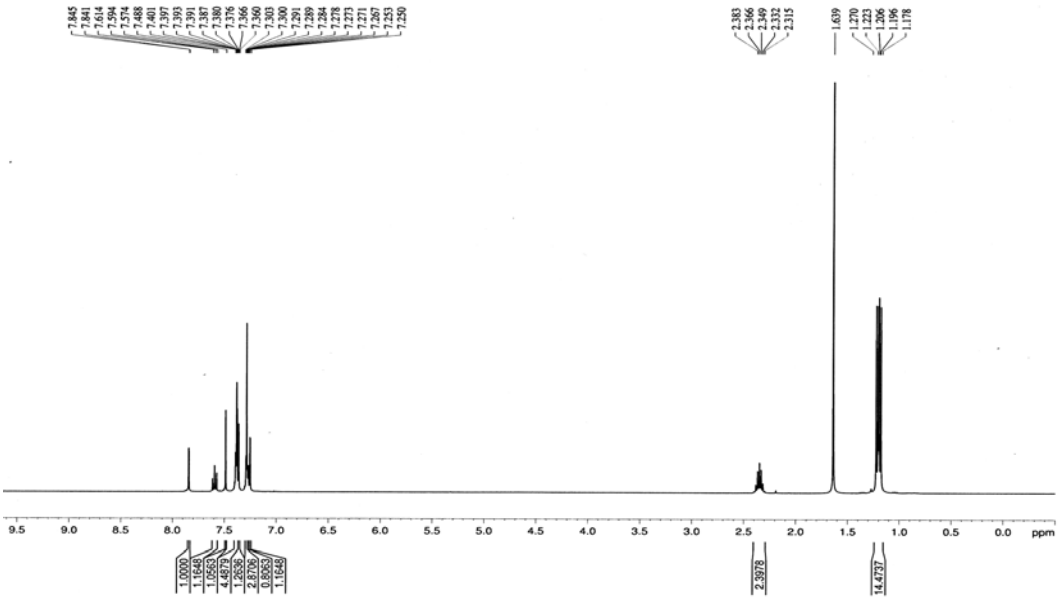

Figure 13.5. NMR spectra of complex **4a**.

^{13}C NMR in $CDCl_3$

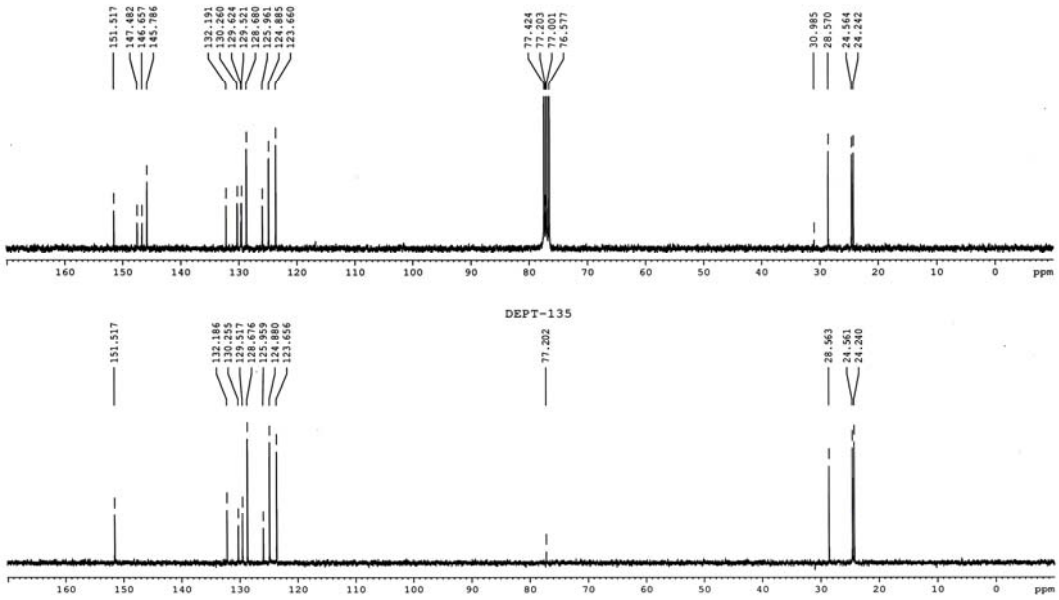

Figure 13.5 (cont.). NMR spectra of complex **4a**.

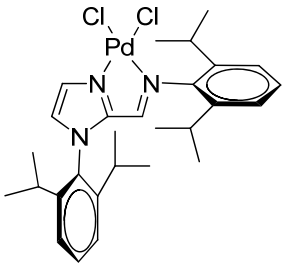

4b

^{1}H NMR in $CDCl_3$

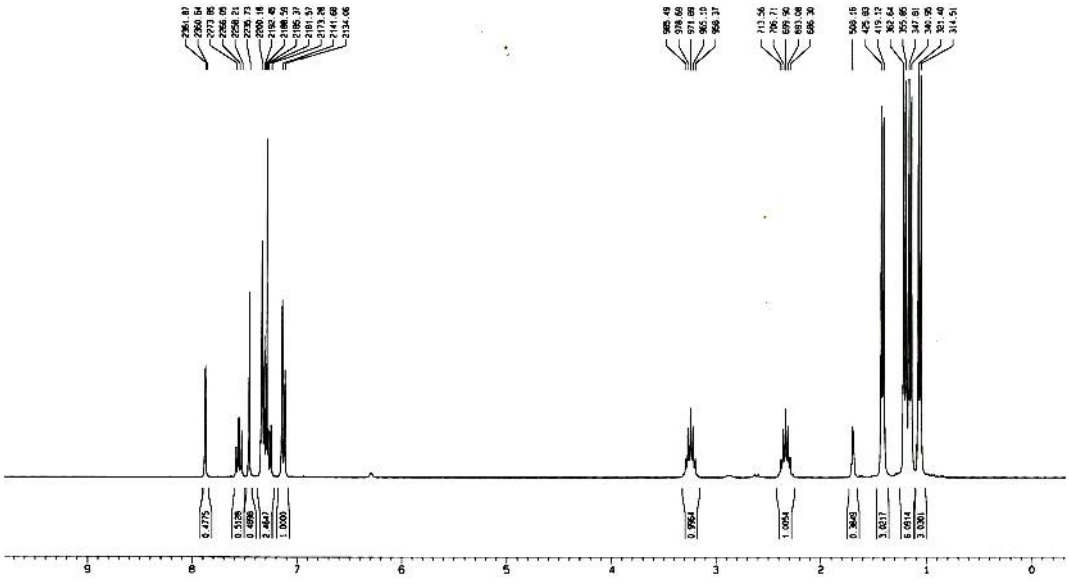

^{13}C NMR in $CDCl_3$

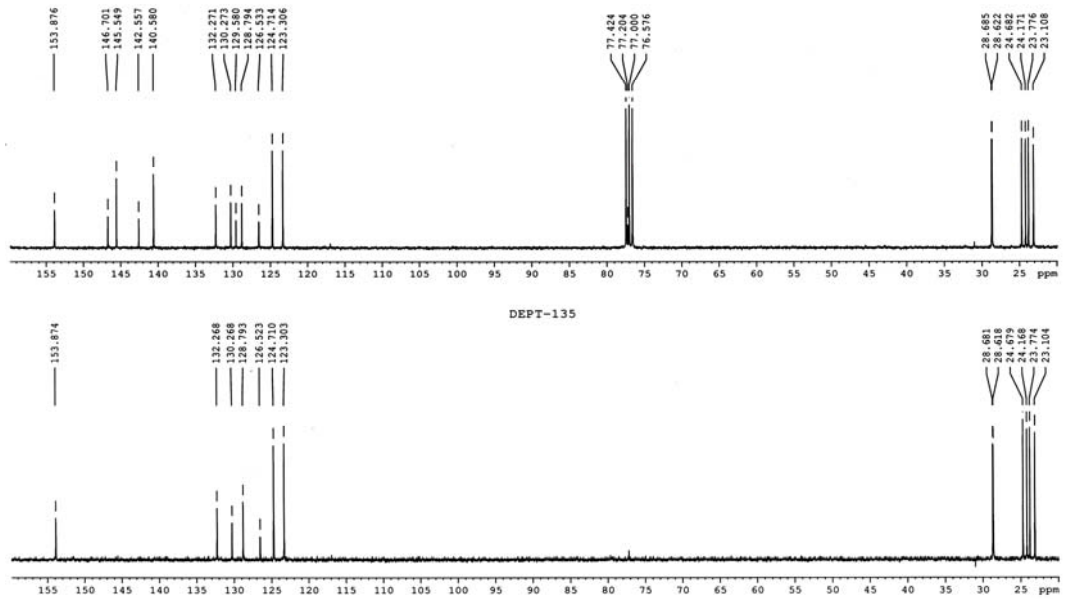

Figure 13.6. NMR spectra of complex **4b**.

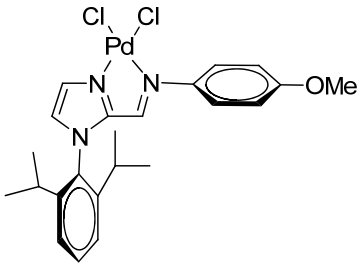

4c

^{1}H NMR in $CDCl_3$

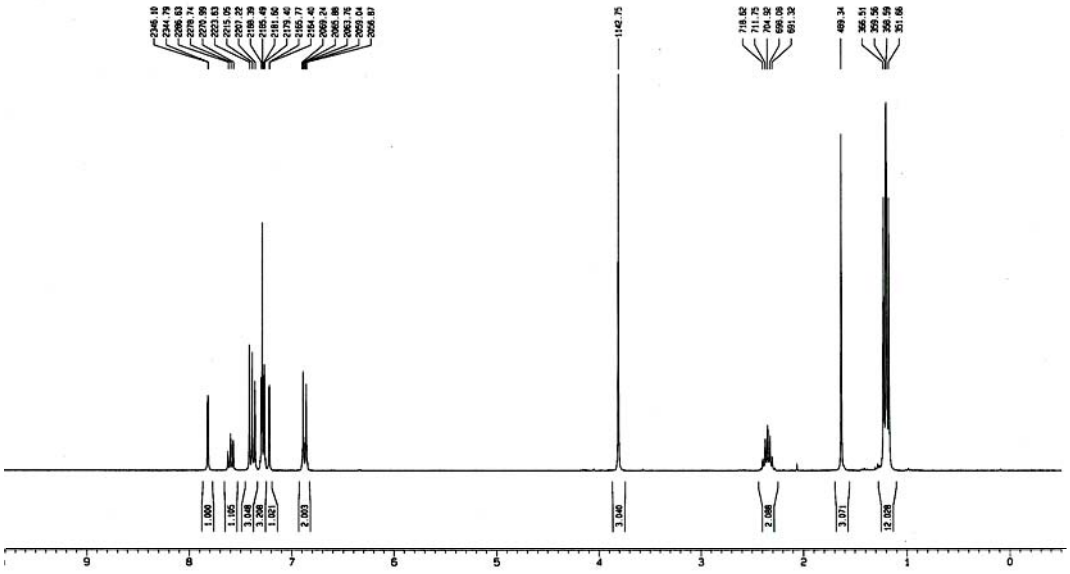

^{13}C NMR in $CDCl_3$

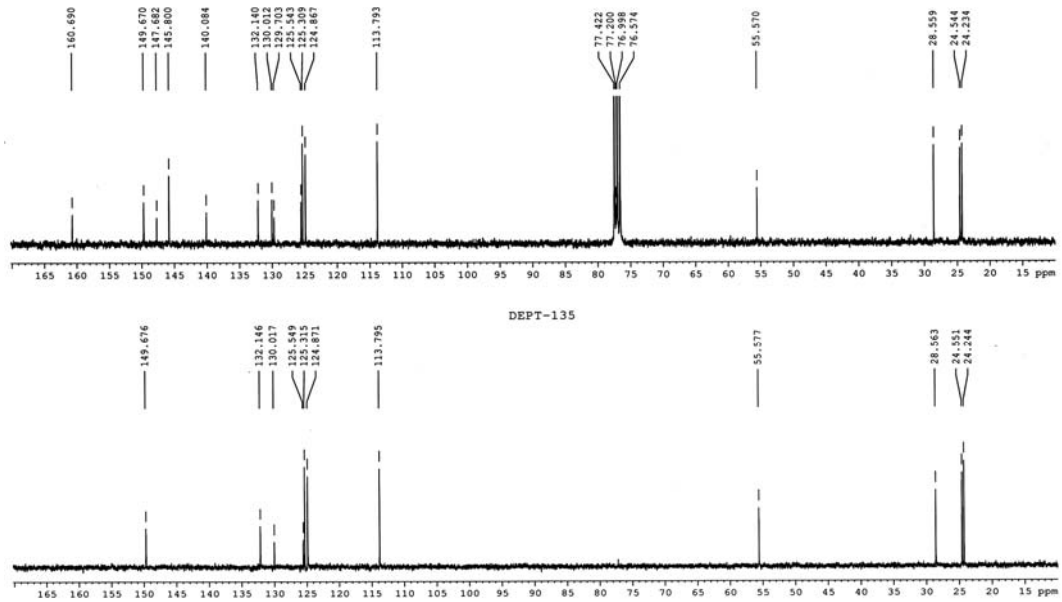

Figure 13.7. NMR spectra of complex **4c**.

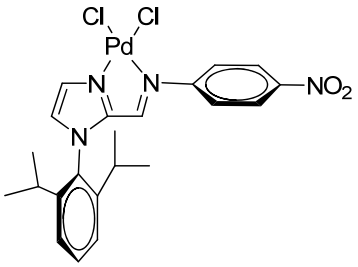

4d

^{1}H NMR in $CDCl_3$

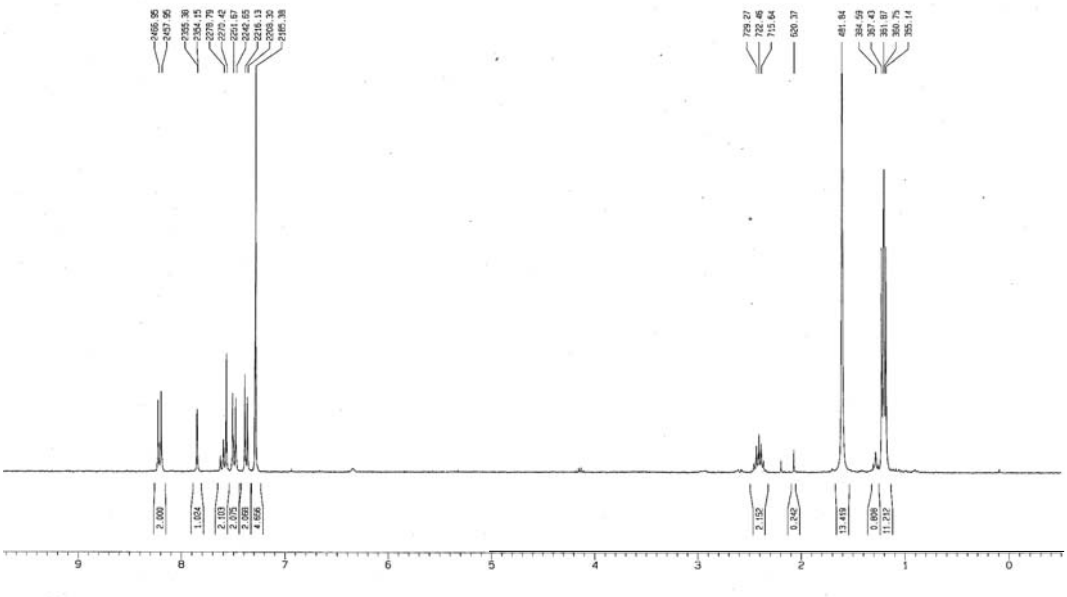

^{13}C NMR in $CDCl_3$

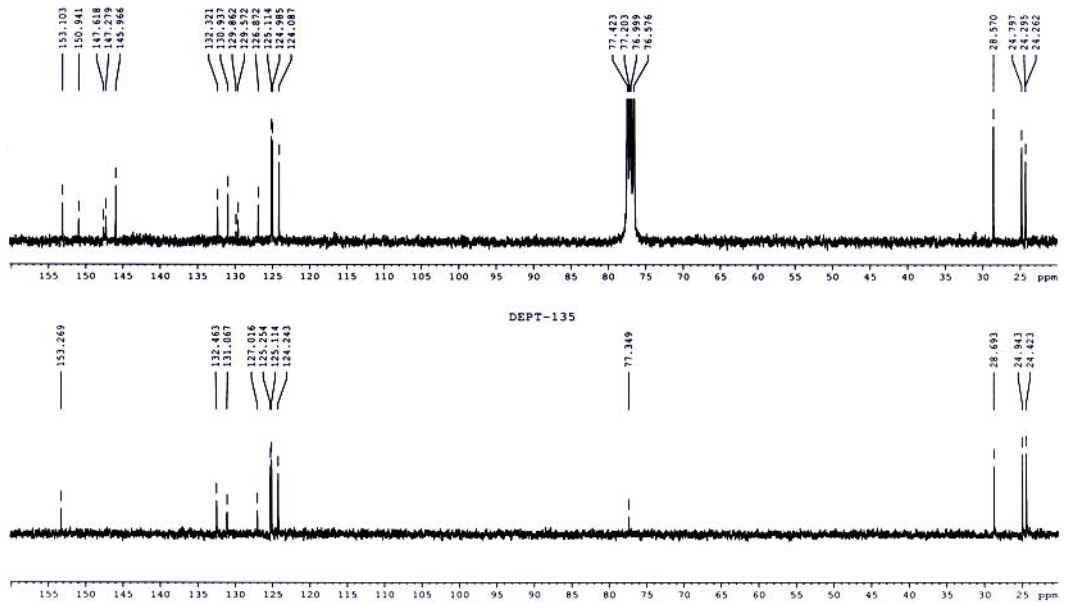

Figure 13.8. NMR spectra of complex **4d**

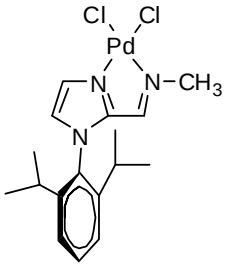

4e

^{1}H NMR in $CDCl_3$

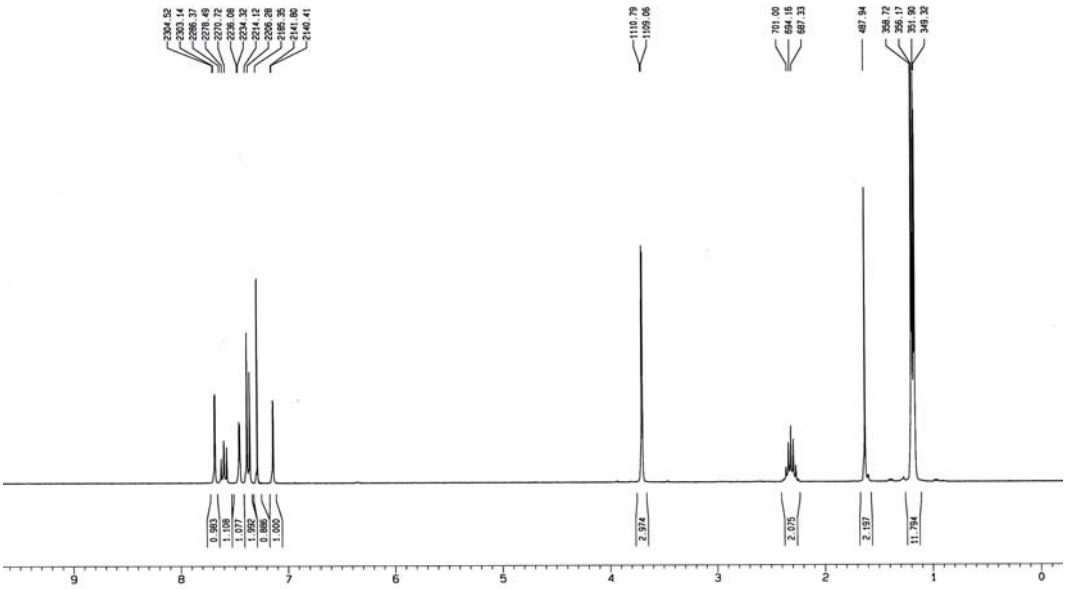

^{13}C NMR in $CDCl_3$

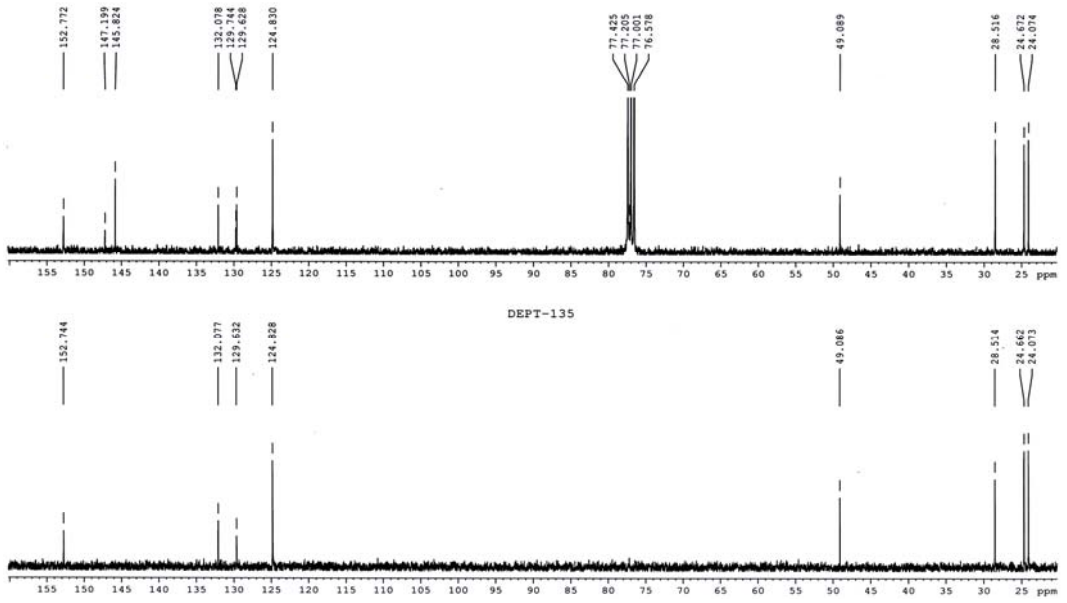

Figure 13.9. NMR spectra of complex **4e**.

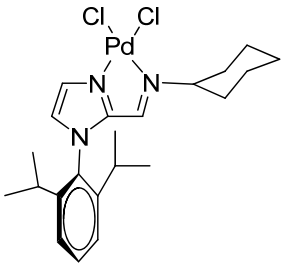

4f

^{1}H NMR in $CDCl_3$

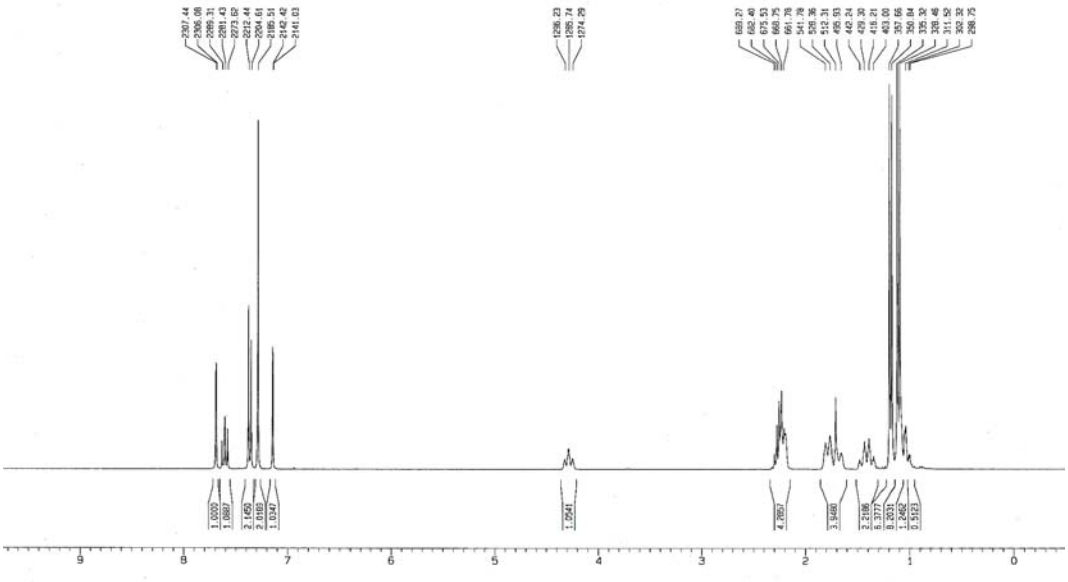

^{13}C NMR in $CDCl_3$

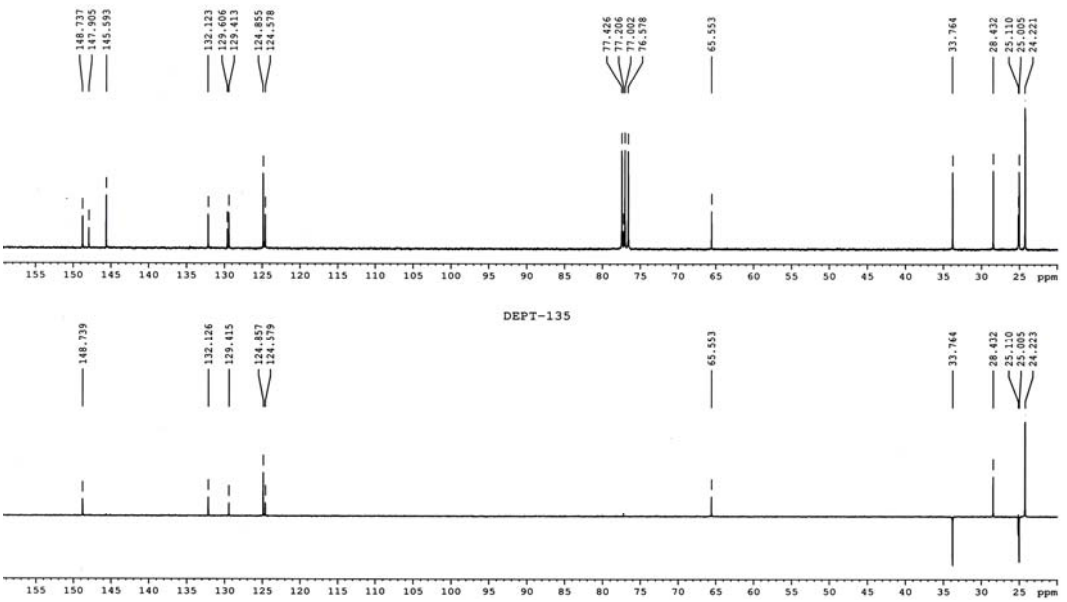

DEPT-135

Figure 13.10. NMR spectra of complex **4f**.

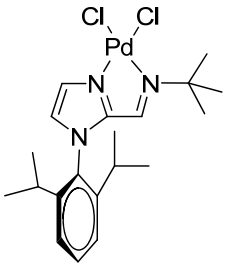

4g

^{1}H NMR in $CDCl_3$

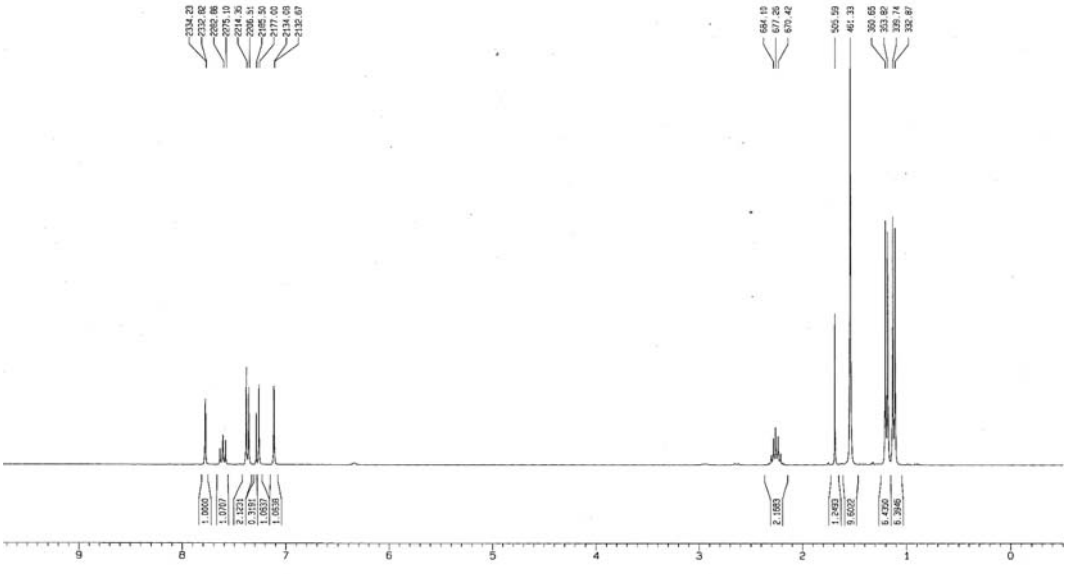

^{13}C NMR in $CDCl_3$

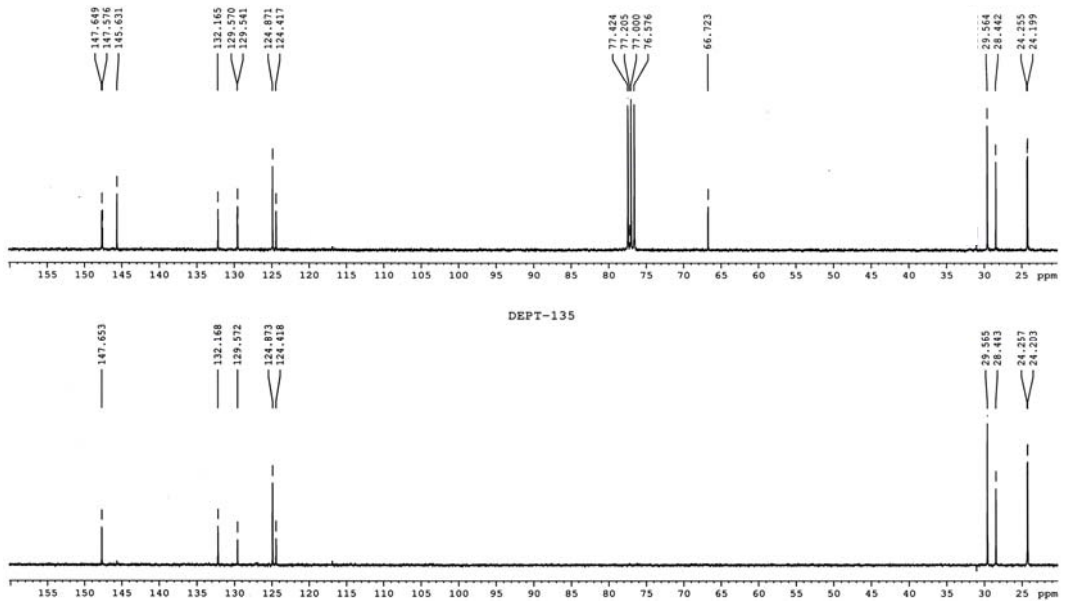

Figure 13.11. NMR spectra of complex **4g**.

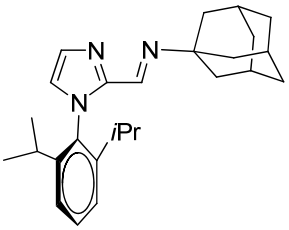

3h

^{1}H NMR in $CDCl_3$

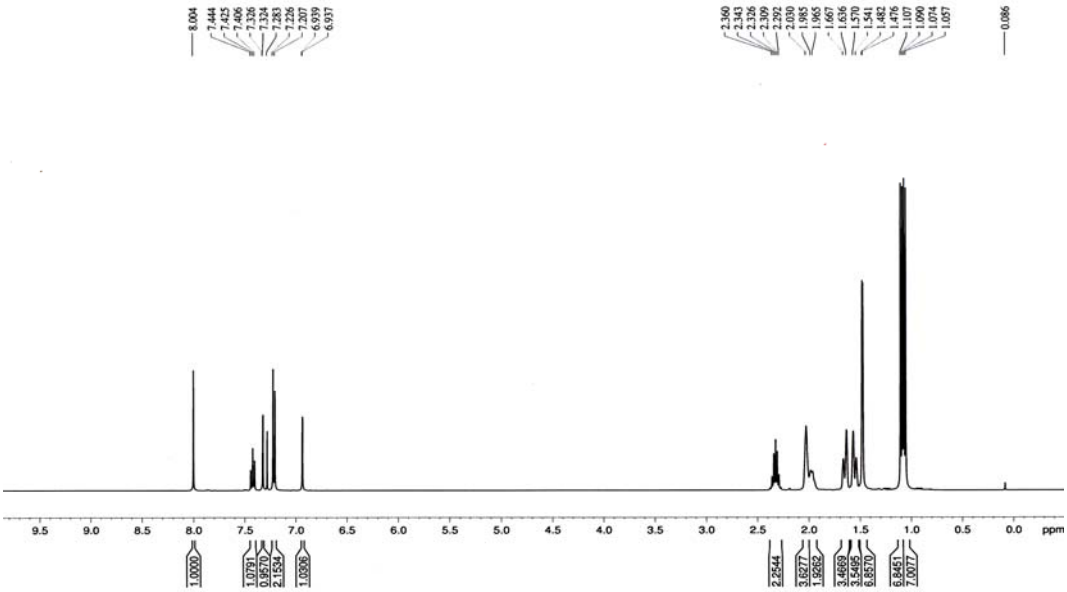

^{13}C NMR in $CDCl_3$

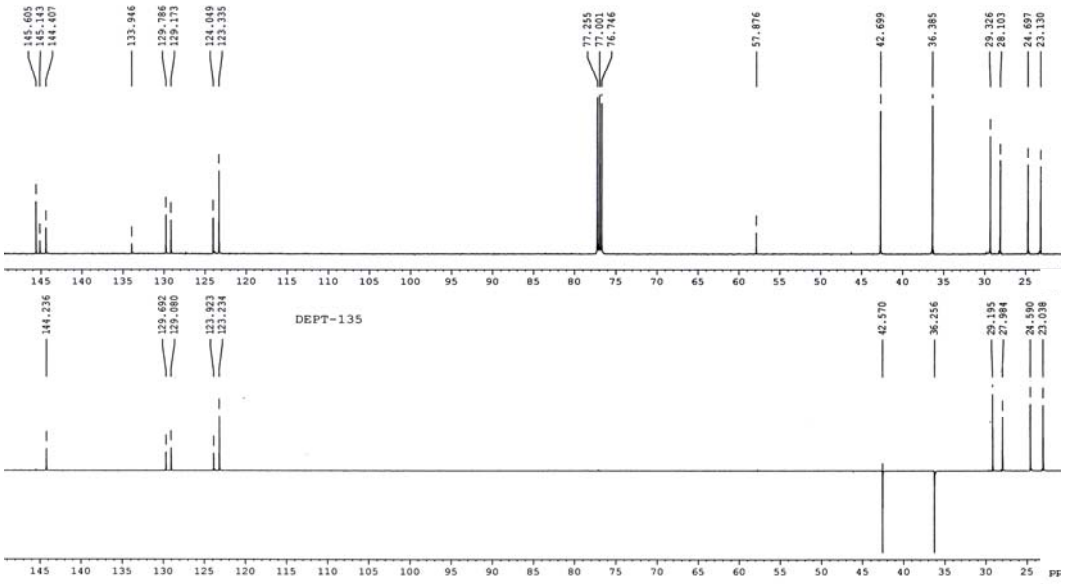

Figure 13.12. NMR spectra of compound **3h**.

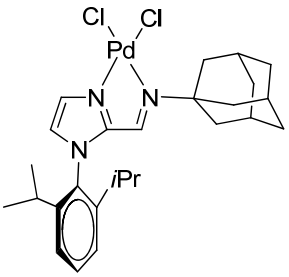

4h

^{1}H NMR in $CDCl_3$

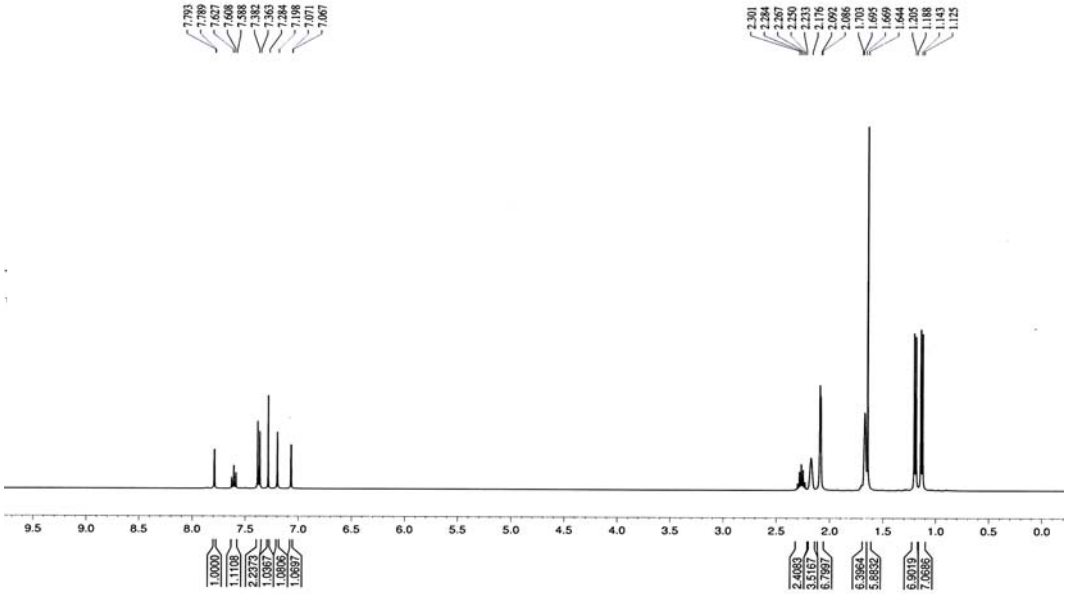

^{13}C NMR in $CDCl_3$

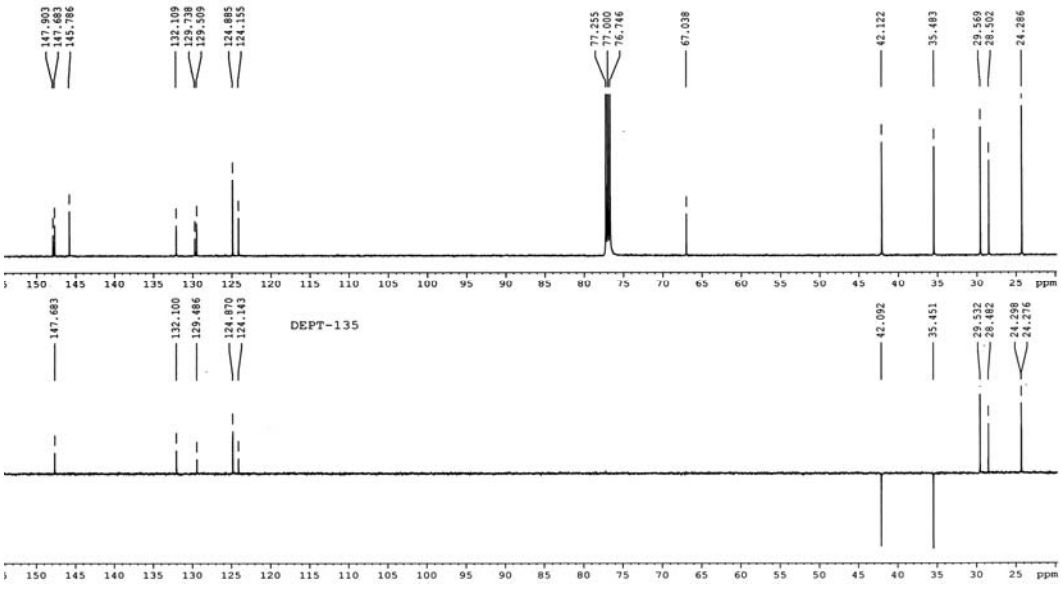

Figure 13.13. NMR spectra of **4h**.

APPENDIX D

NMR SPECTRA OF BIPHENYL COMPOUNDS (5a–p)

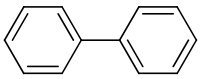

5a

^{1}H NMR in $CDCl_3$

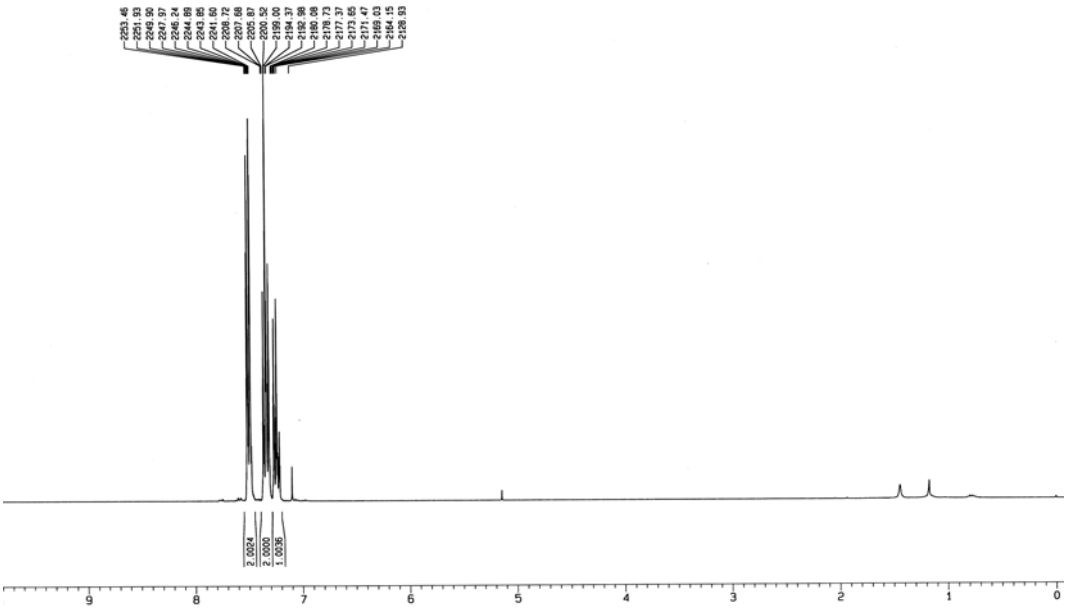

Figure 13.14. NMR spectra of compound **5a**.

^{13}C NMR in $CDCl_3$

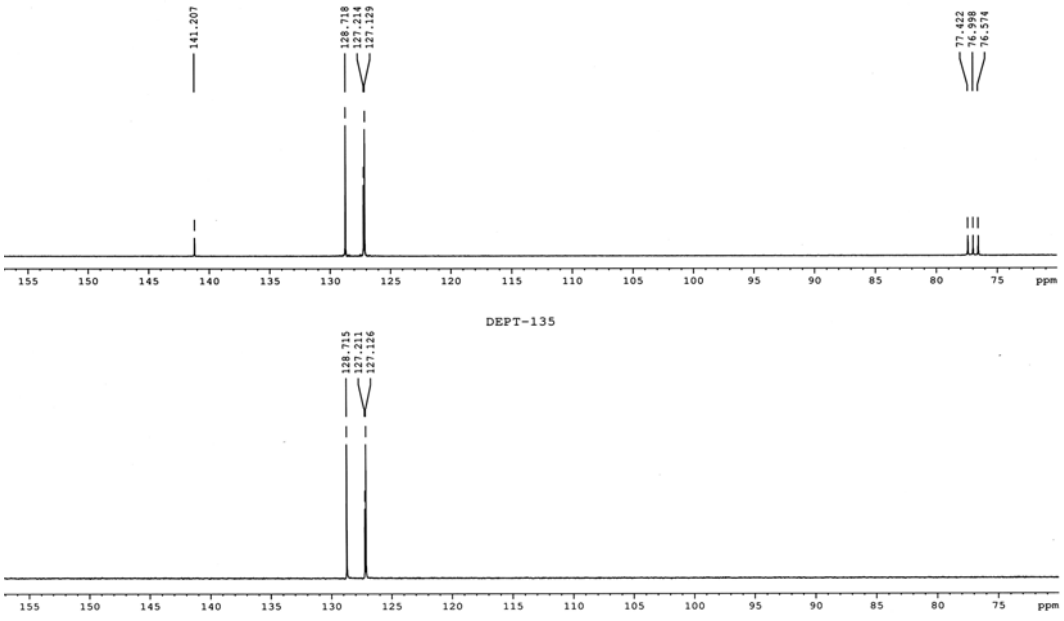

Figure 13.14 (cont.). NMR spectra of compound **5a**.

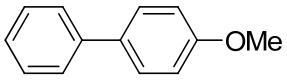

5b

^{1}H NMR in $CDCl_3$

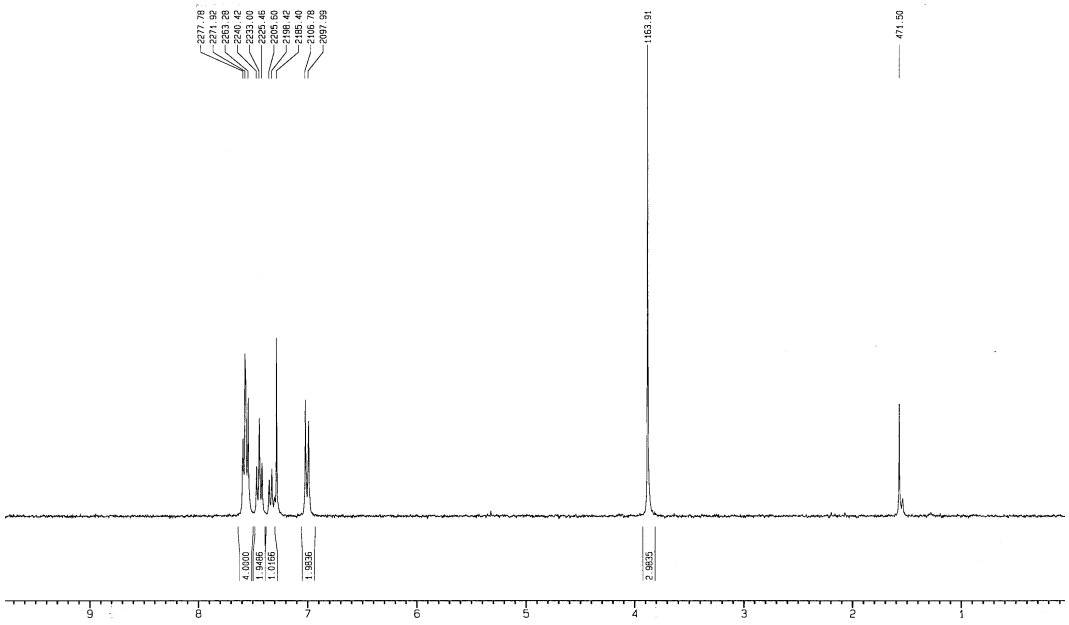

^{13}C NMR in $CDCl_3$

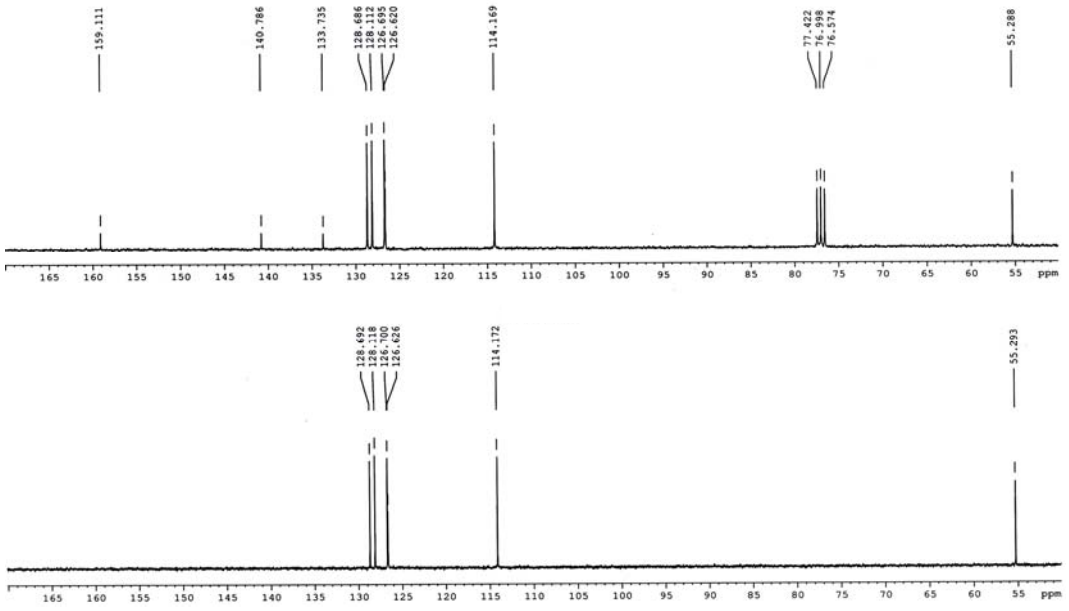

Figure 13.15. NMR spectra of compound **5b**.

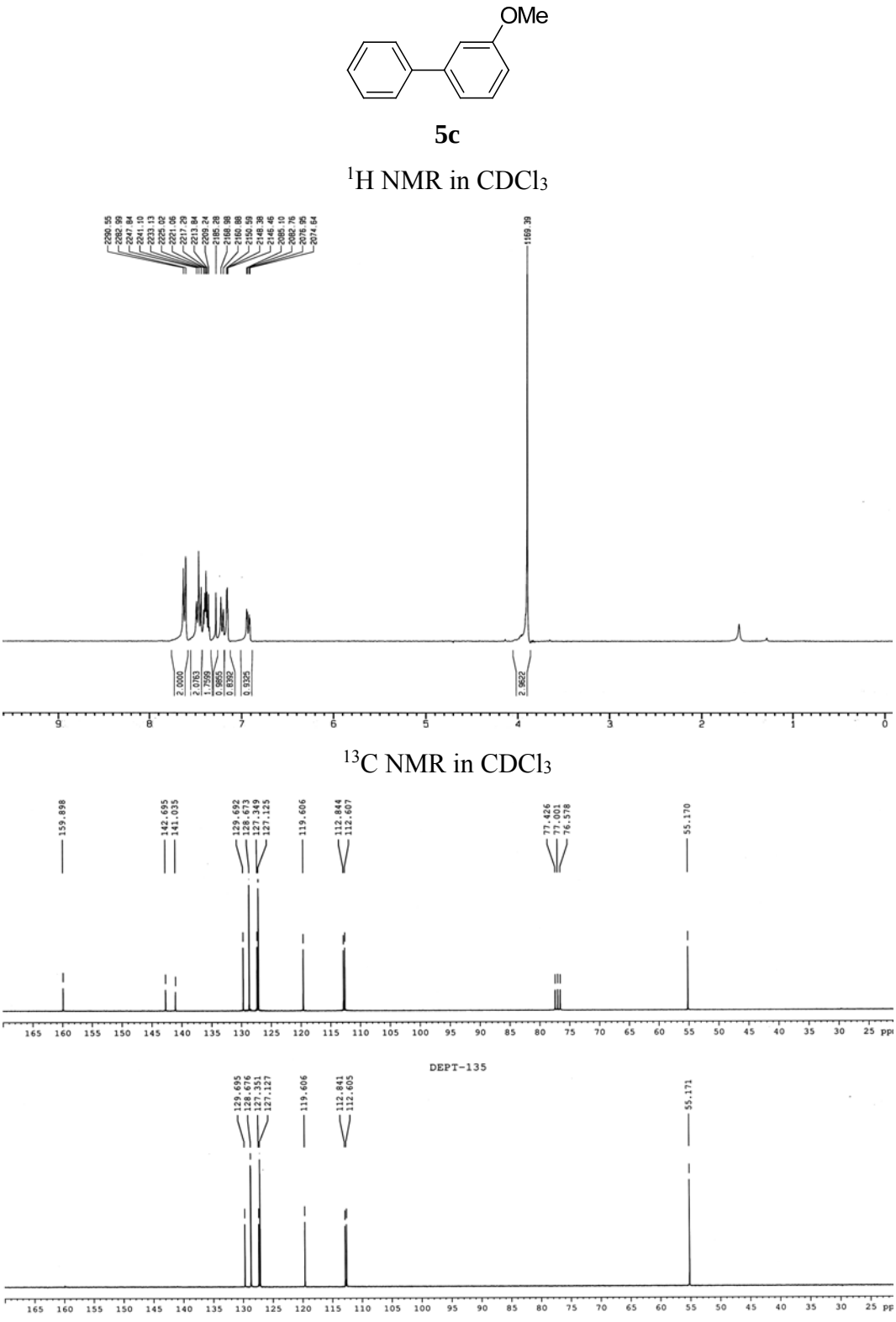

Figure 13.16. NMR spectra of compound **5c**.

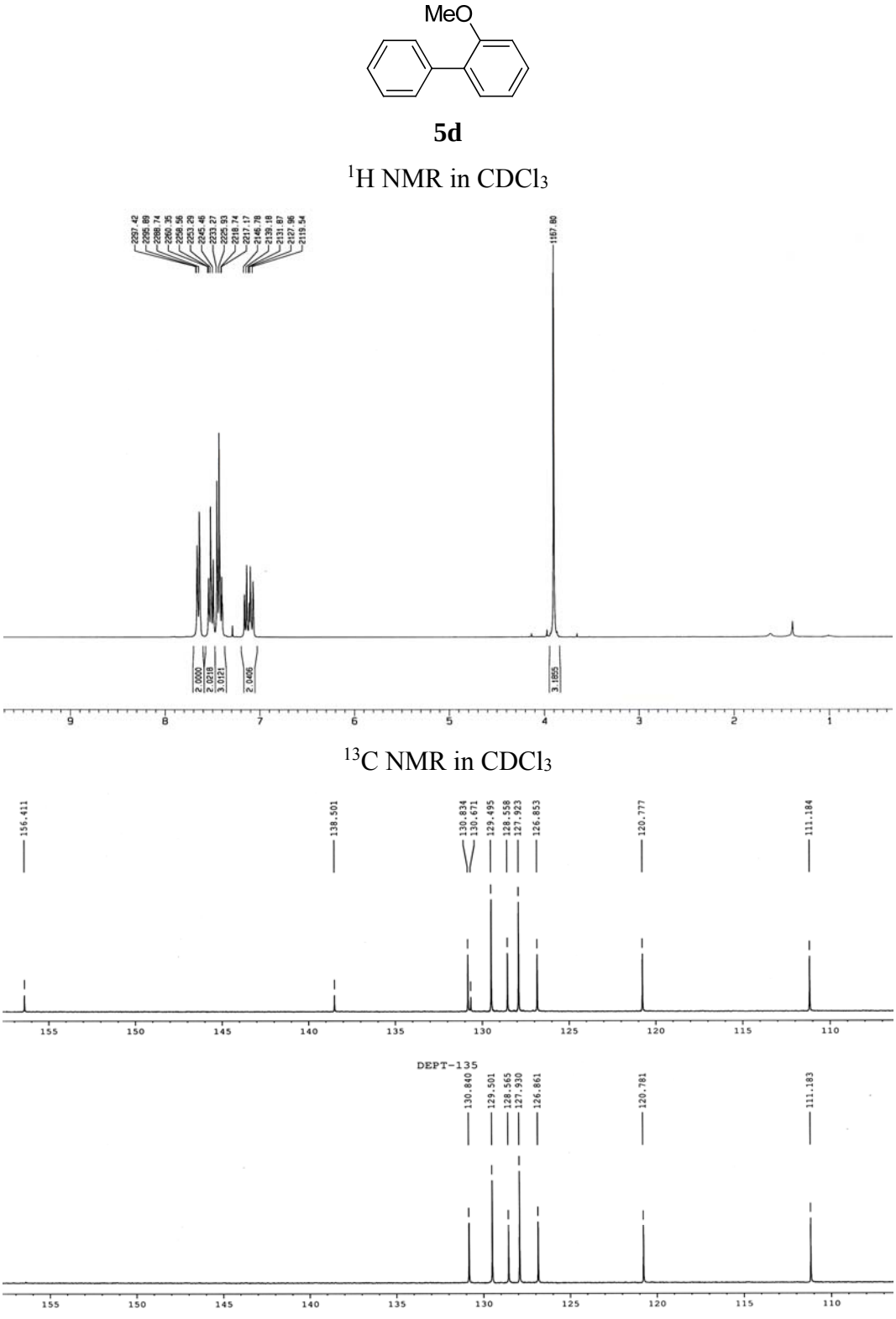

Figure 13.17. NMR spectra of compound **5d**.

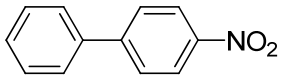

5e

^{1}H NMR in $CDCl_3$

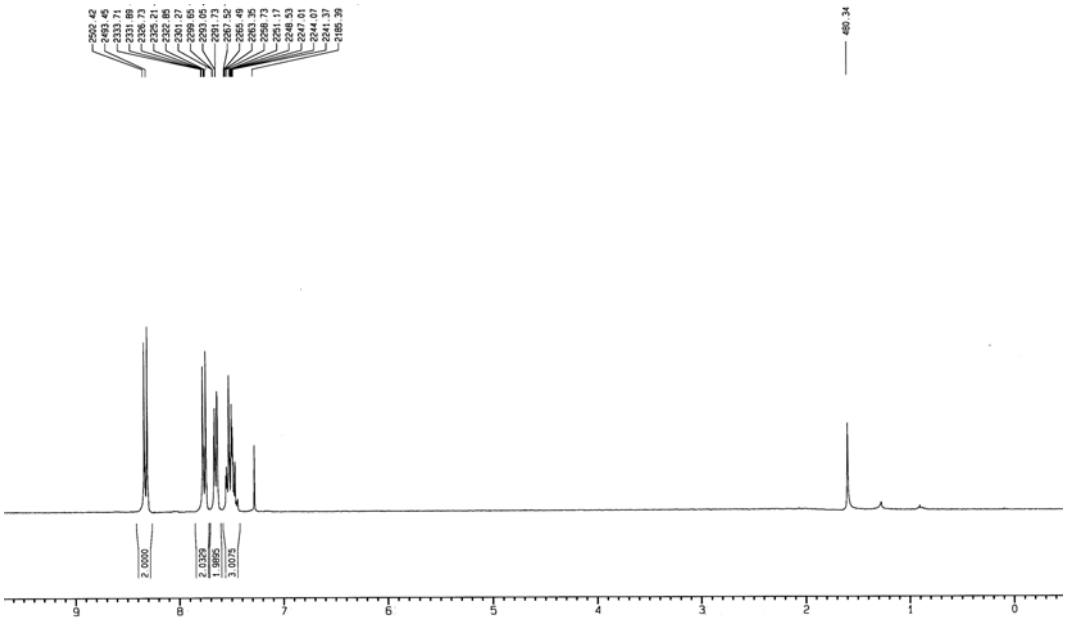

^{13}C NMR in $CDCl_3$

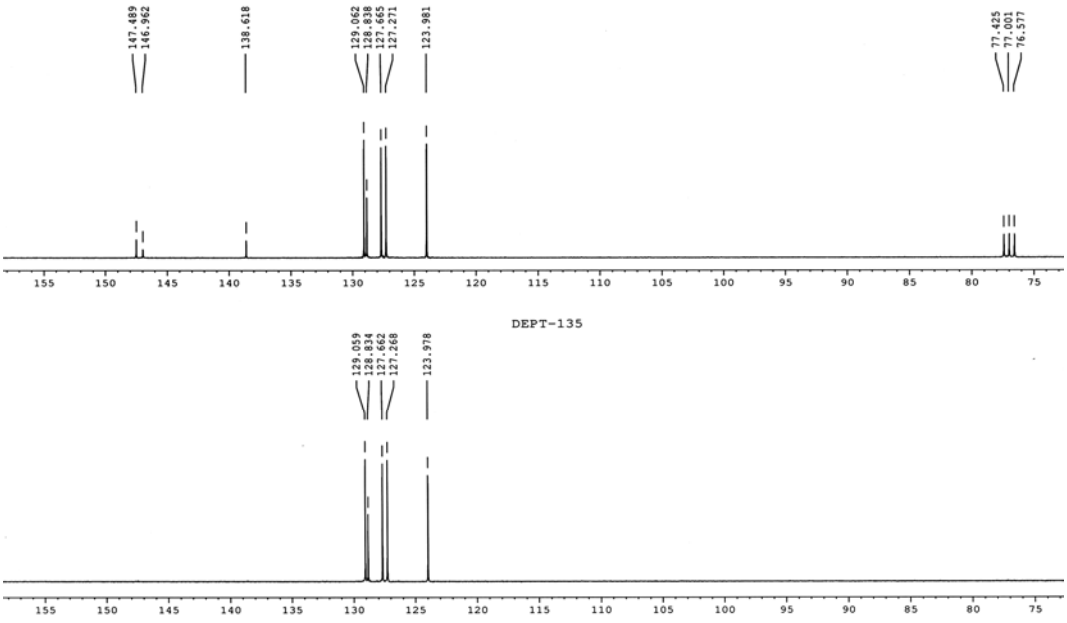

DEPT-135

Figure 13.18. NMR spectra of compound **5e**.

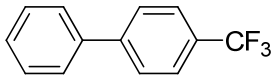

5f

^{1}H NMR in $CDCl_3$

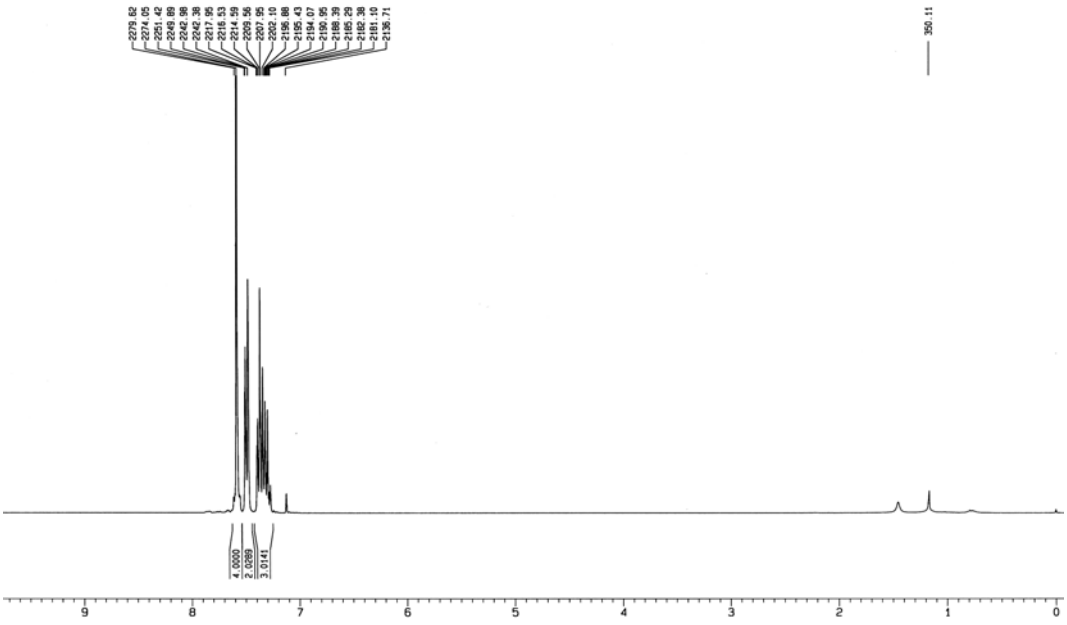

^{13}C NMR in $CDCl_3$

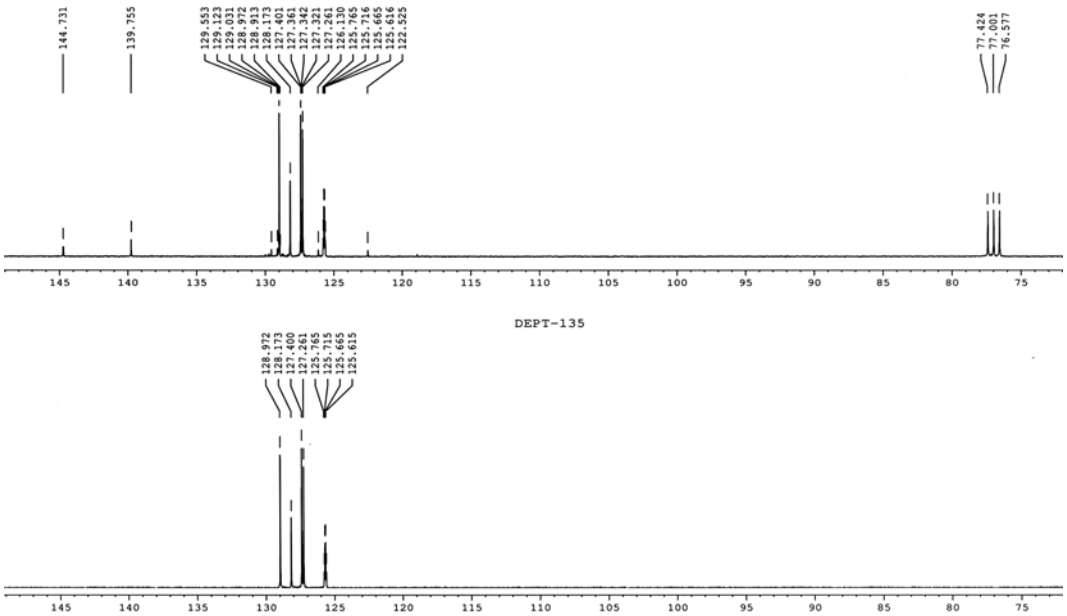

Figure 13.19. NMR spectra of compound **5f**.

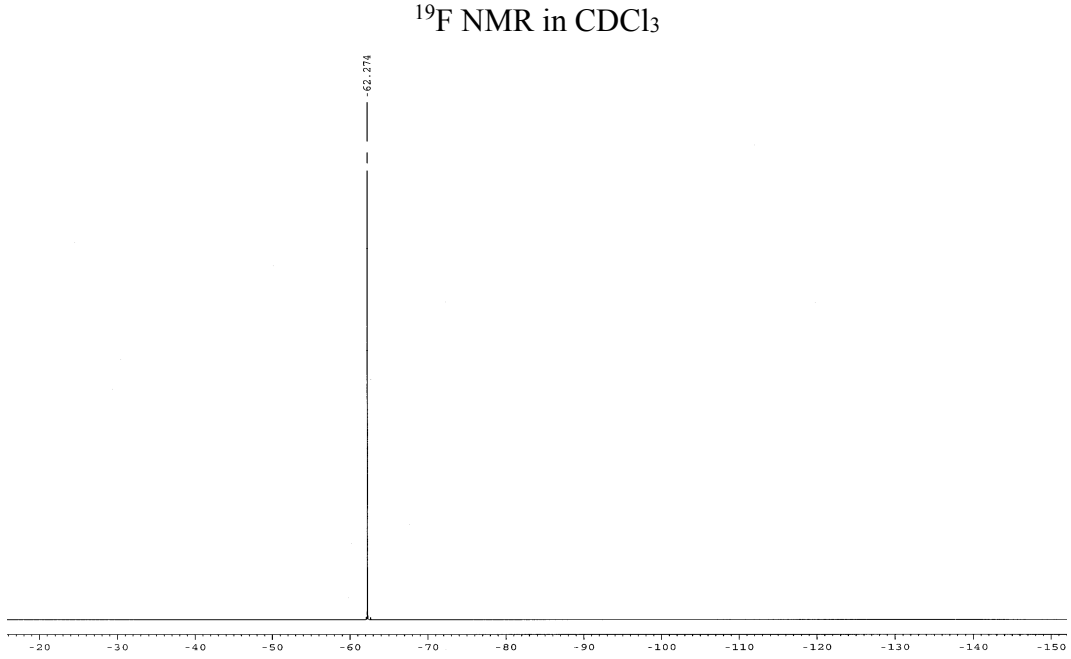

Figure 13.19 (cont.). NMR spectra of compound **5f**.

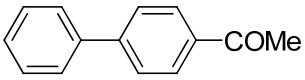

5g

^{1}H NMR in $CDCl_3$

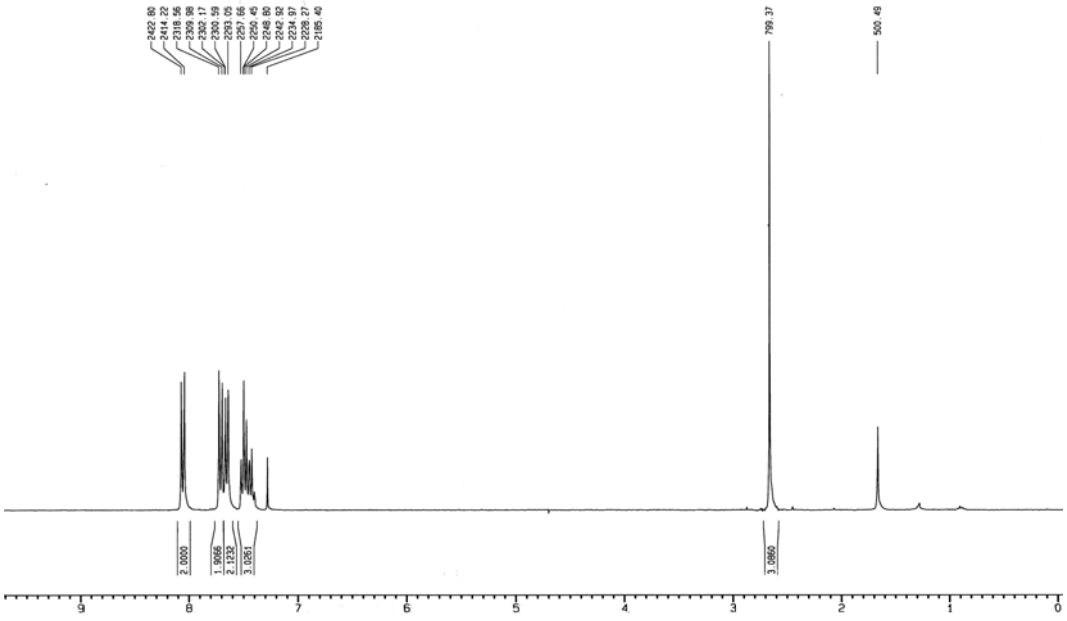

^{13}C NMR in $CDCl_3$

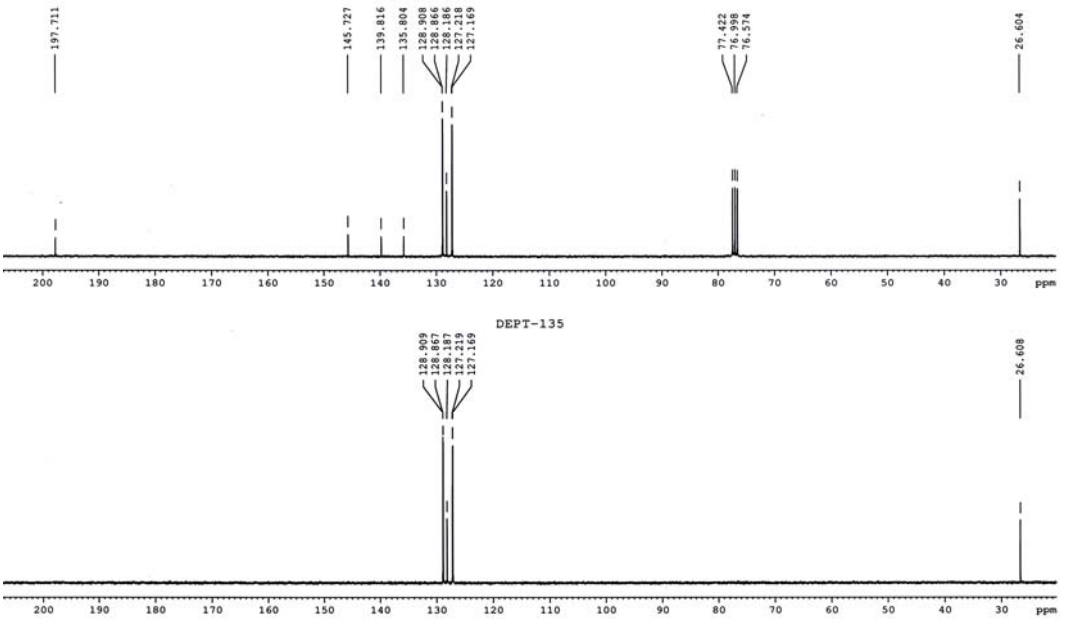

Figure 13.20. NMR spectra of compound **5g**.

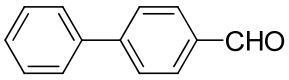

5h

^{1}H NMR in $CDCl_3$

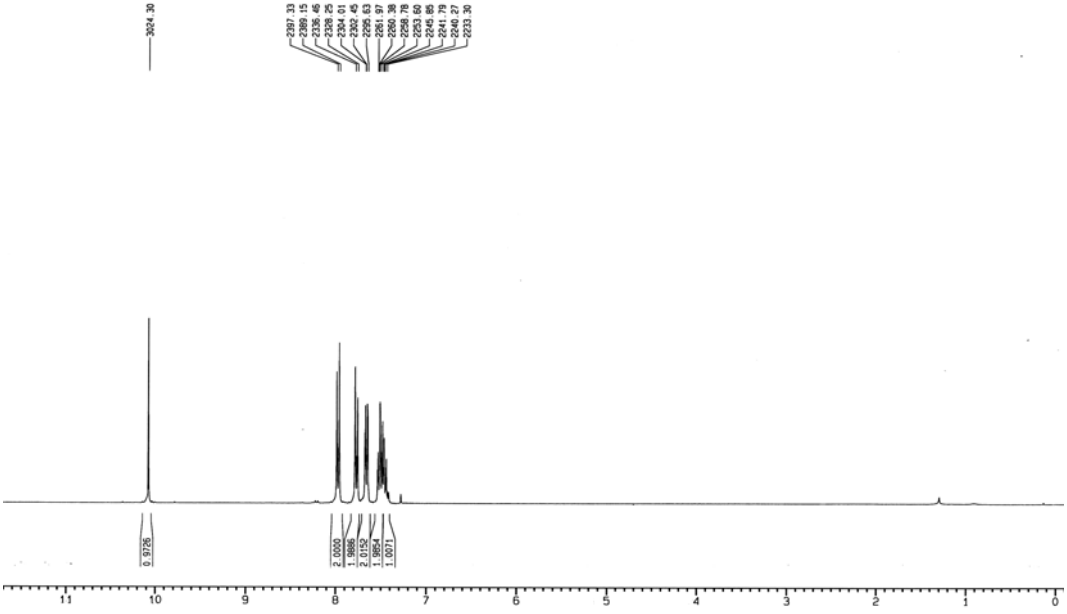

^{13}C NMR in $CDCl_3$

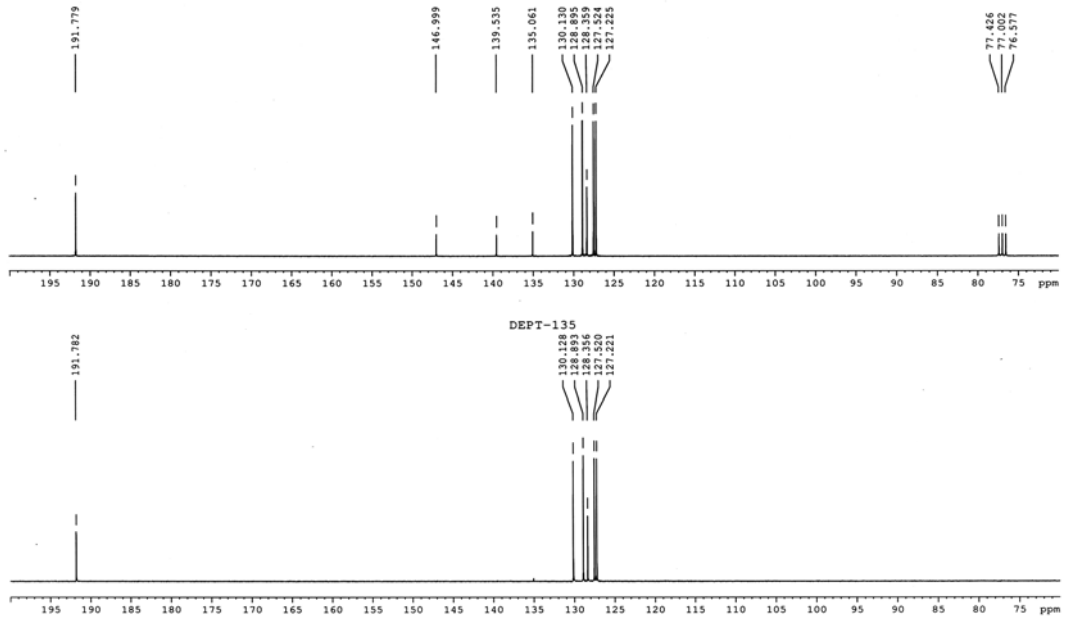

Figure 13.21. NMR spectra of compound **5h**.

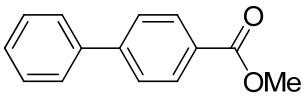

5i

^{1}H NMR in $CDCl_3$

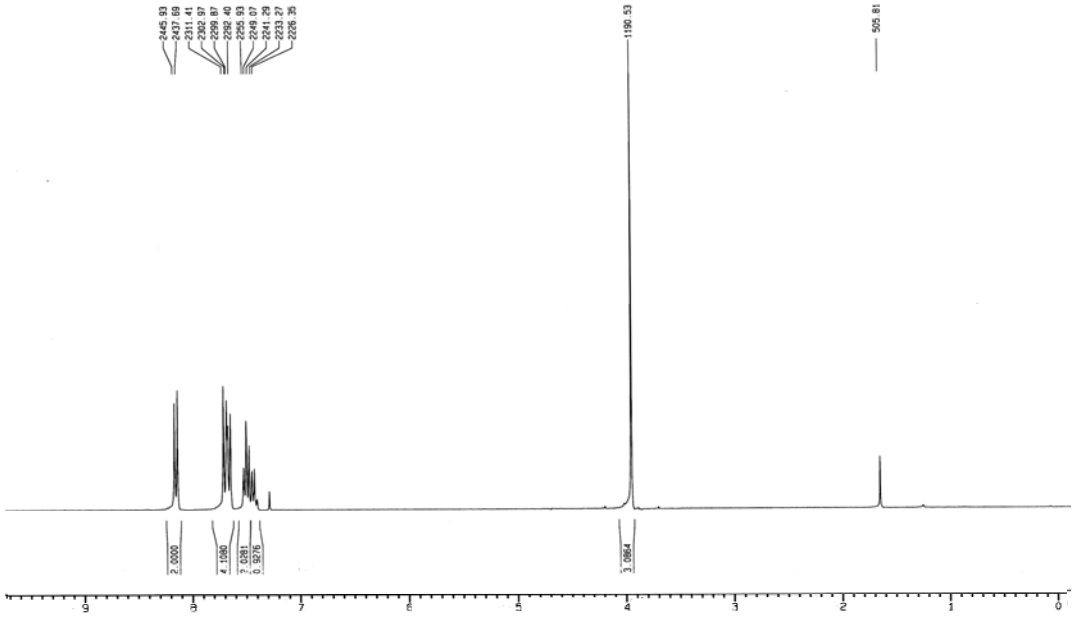

^{13}C NMR in $CDCl_3$

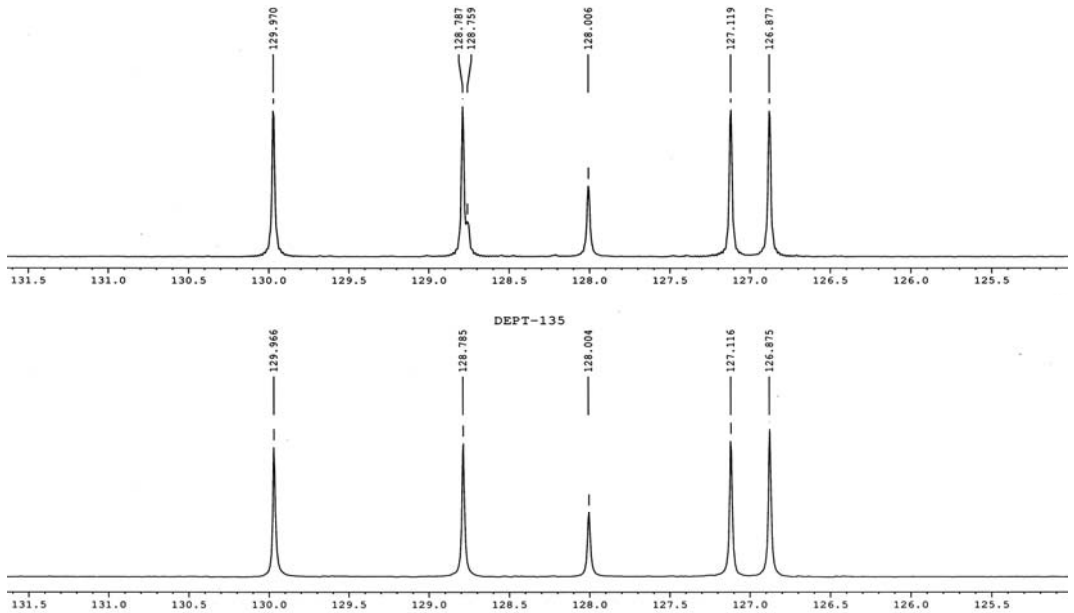

Figure 13.22. NMR spectra of compound **5i**.

^{13}C NMR in $CDCl_3$

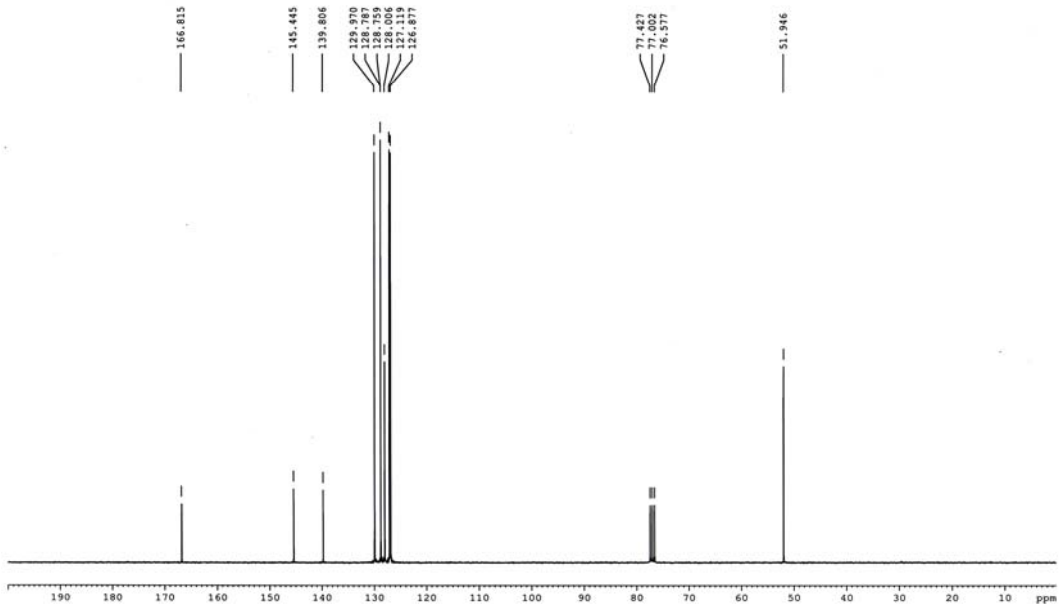

Figure 13.22 (cont.). NMR spectra of compound **5i**.

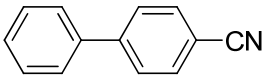

5j

^{1}H NMR in $CDCl_3$

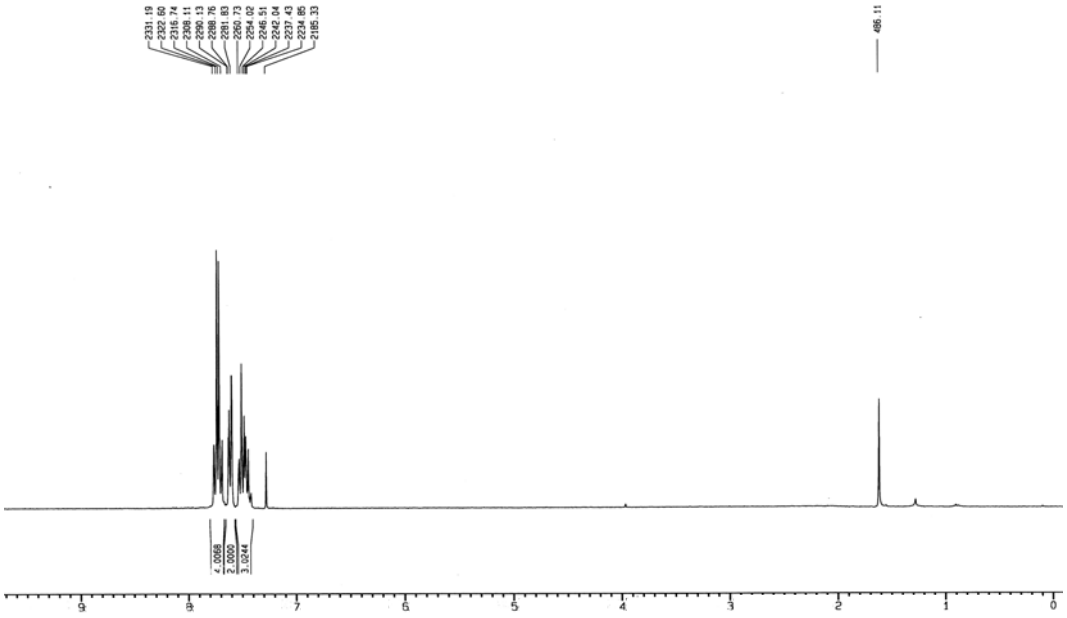

^{13}C NMR in $CDCl_3$

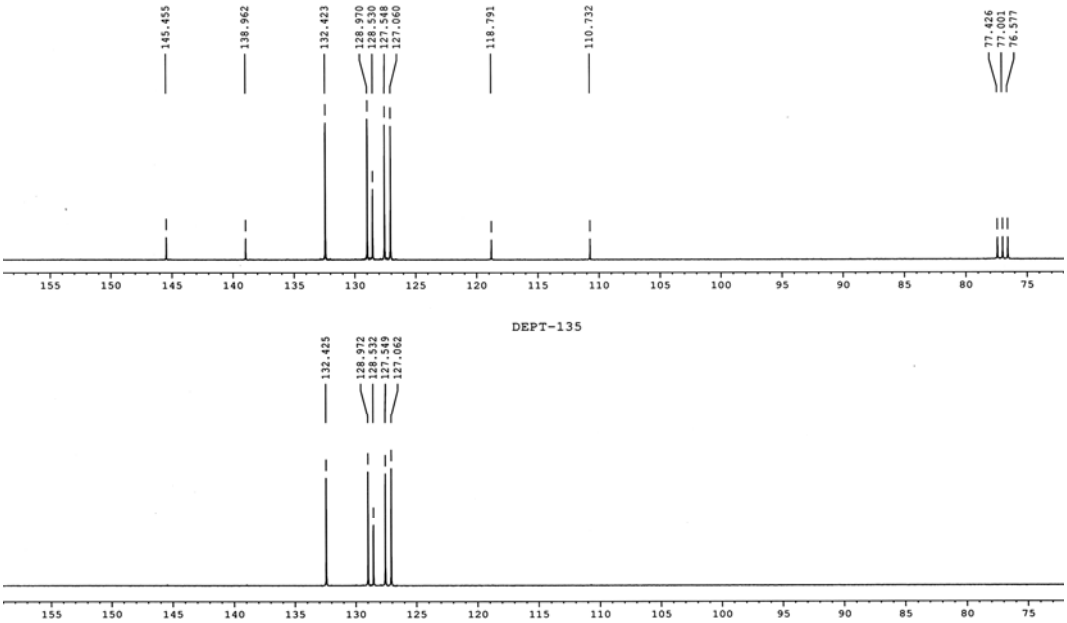

Figure 13.23. NMR spectra of compound **5j**.

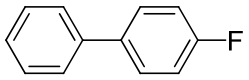

5k

^{1}H NMR in $CDCl_3$

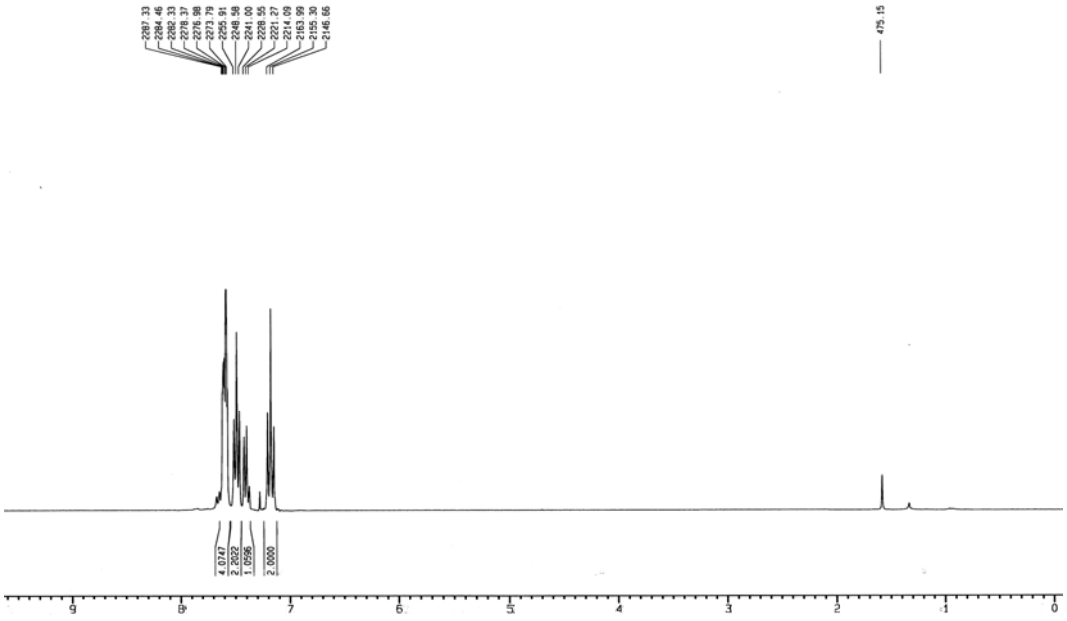

^{13}C NMR in $CDCl_3$

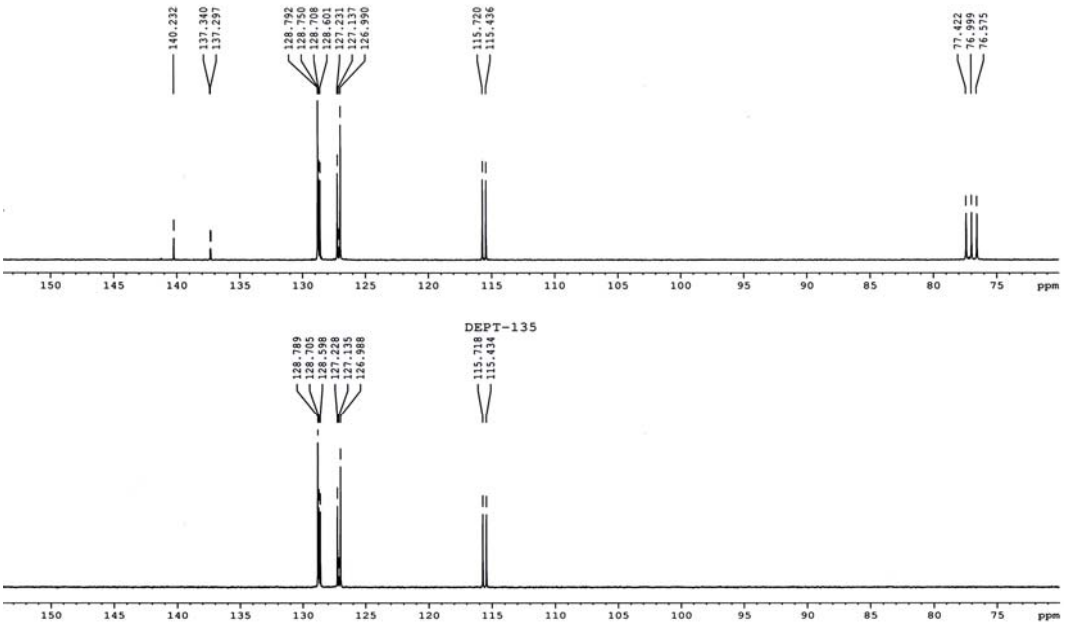

Figure 13.24. NMR spectra of compound **5k**.

^{19}F NMR in $CDCl_3$

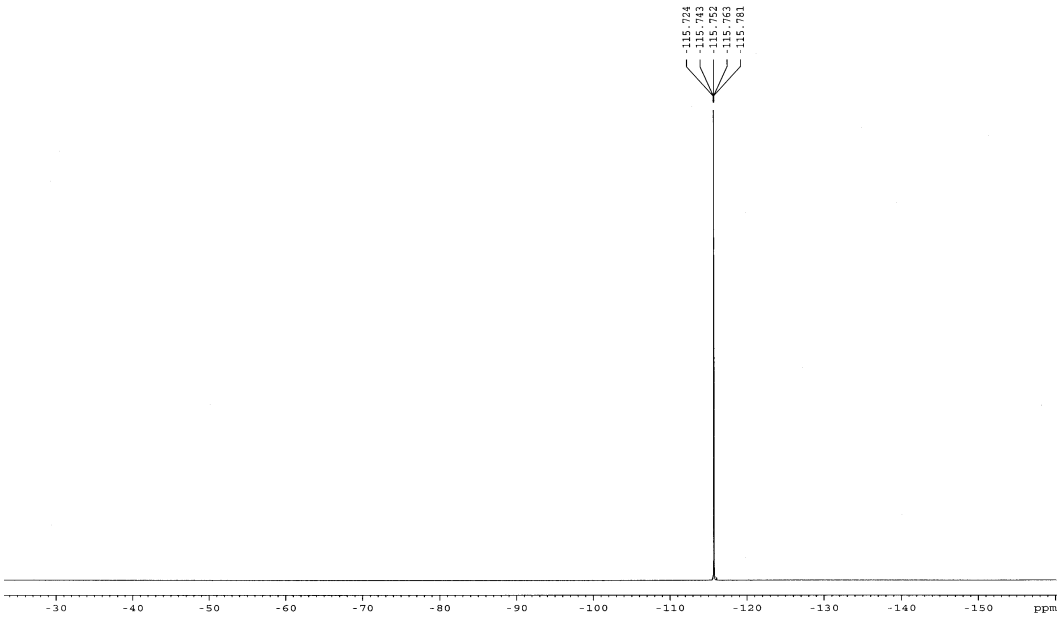

Figure 13.24 (cont.). NMR spectra of compound **5k**.

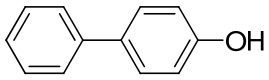

5l

^{1}H NMR in $CDCl_3$

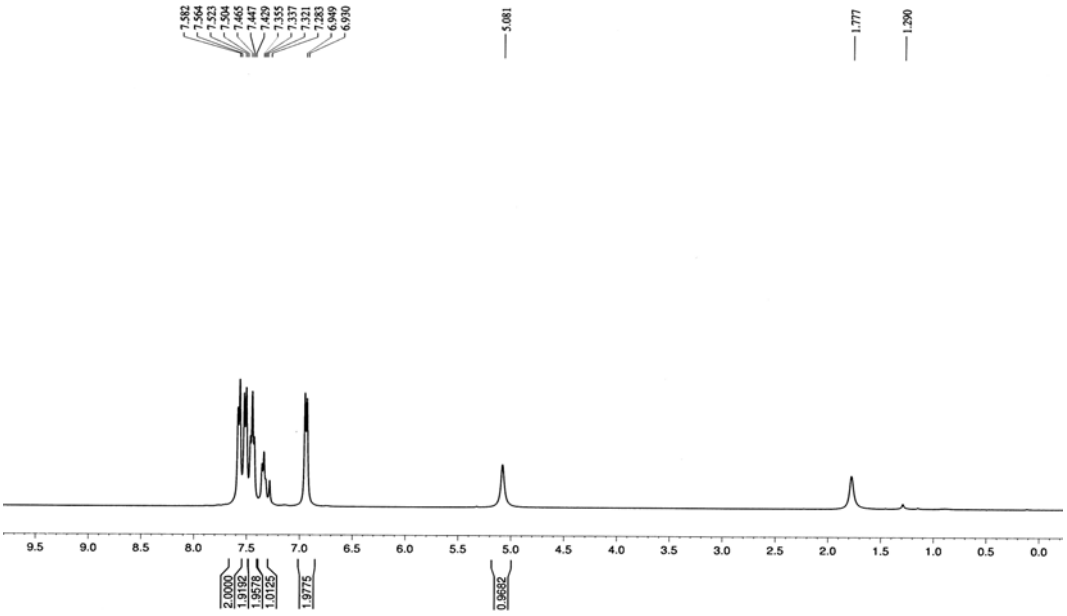

^{13}C NMR in $CDCl_3$

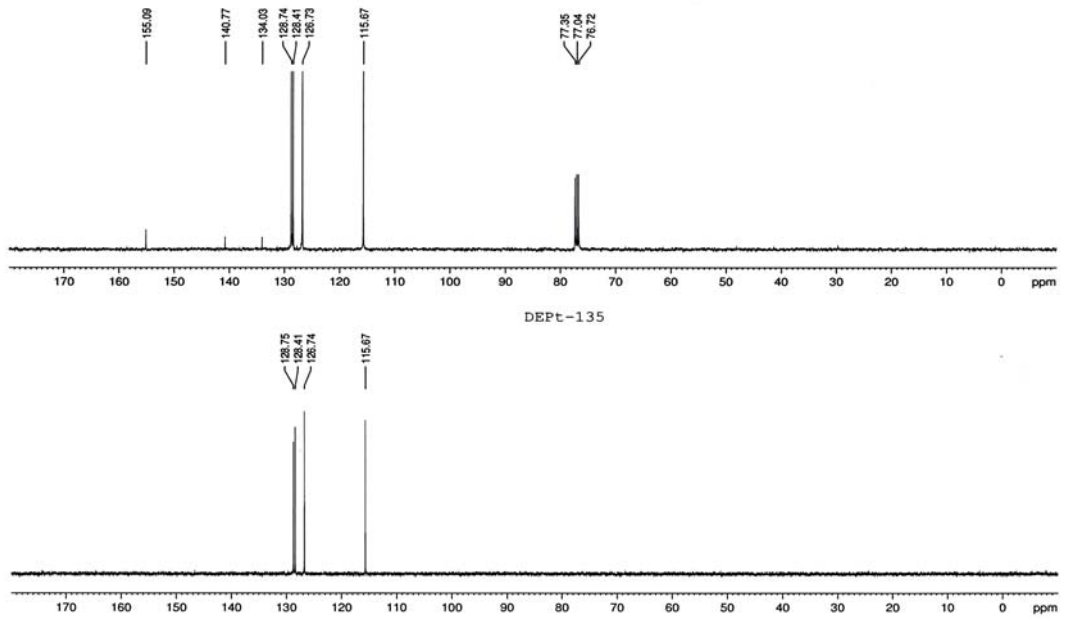

Figure 13.25. NMR spectra of compound **5l**

.

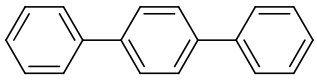

5m

^{1}H NMR in $CDCl_3$

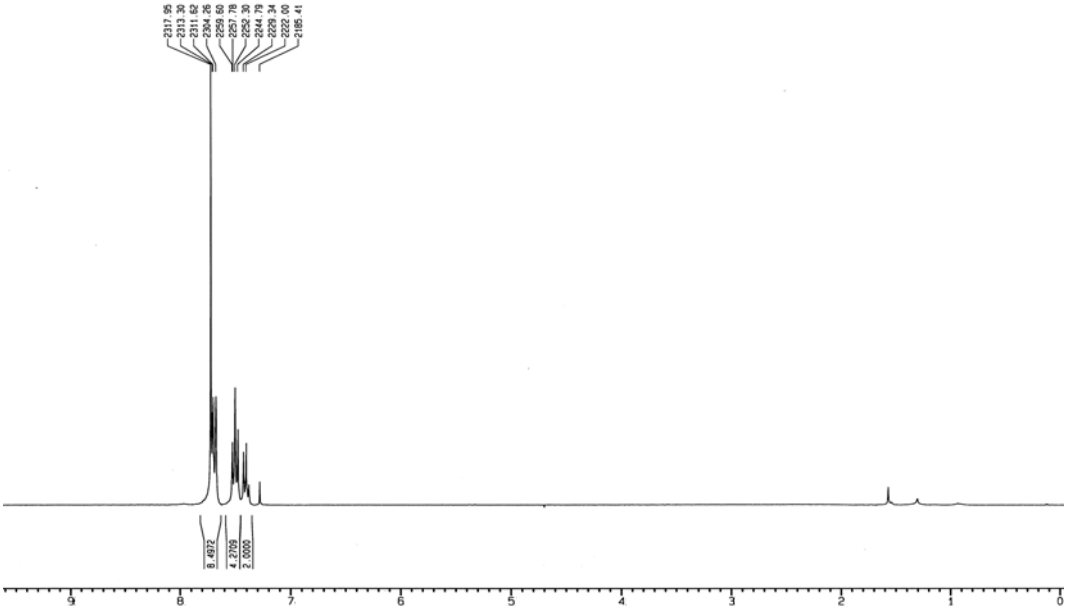

^{13}C NMR in $CDCl_3$

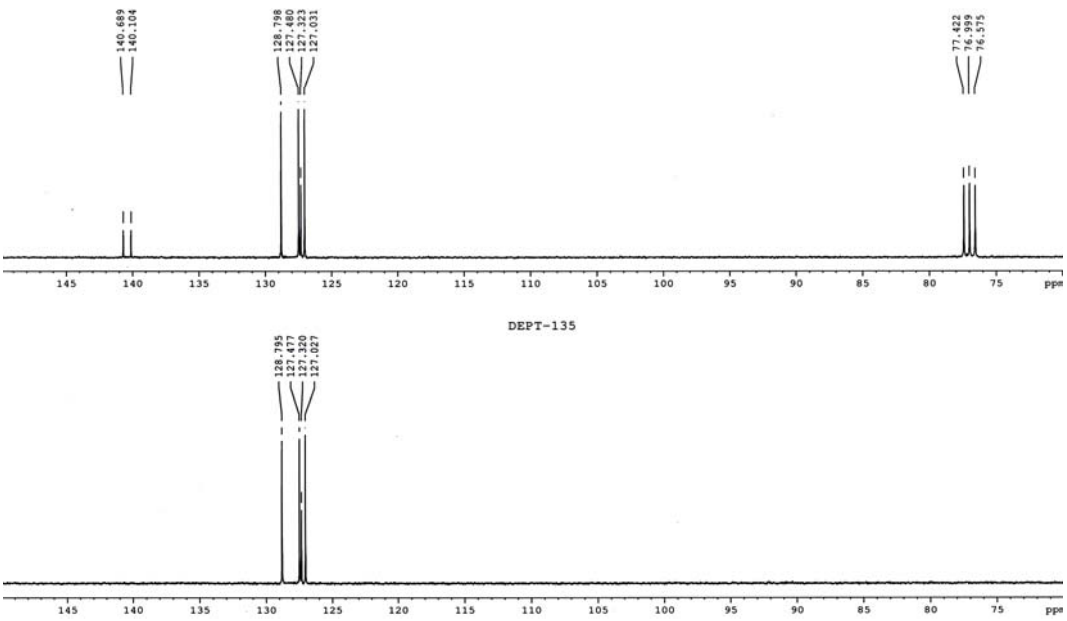

Figure 13.26. NMR spectra of compound **5m**.

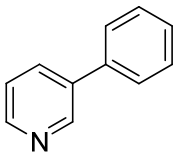

5n

^{1}H NMR in $CDCl_3$

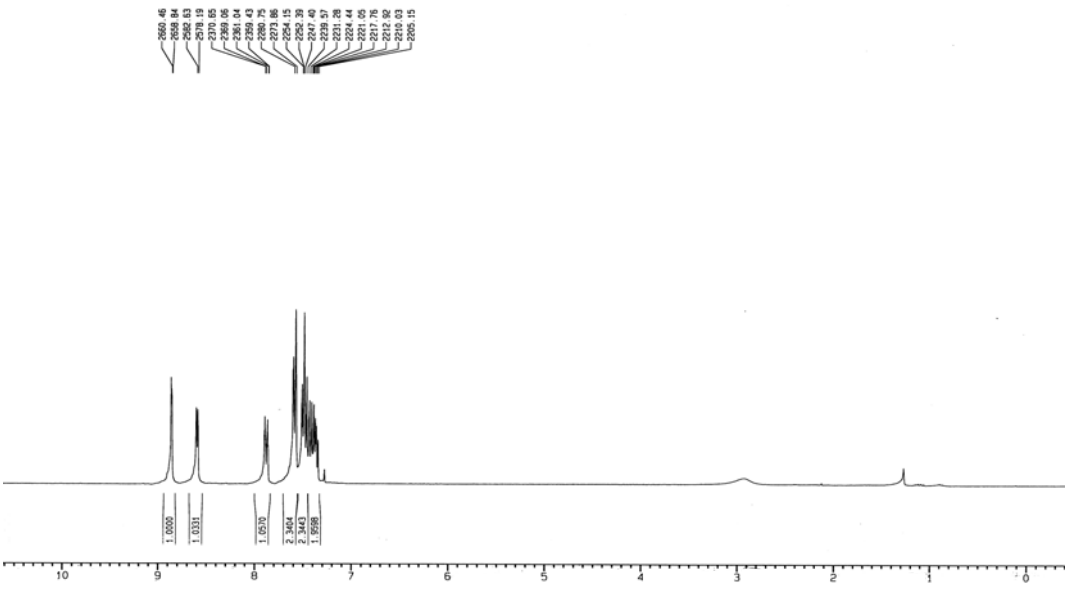

^{13}C NMR in $CDCl_3$

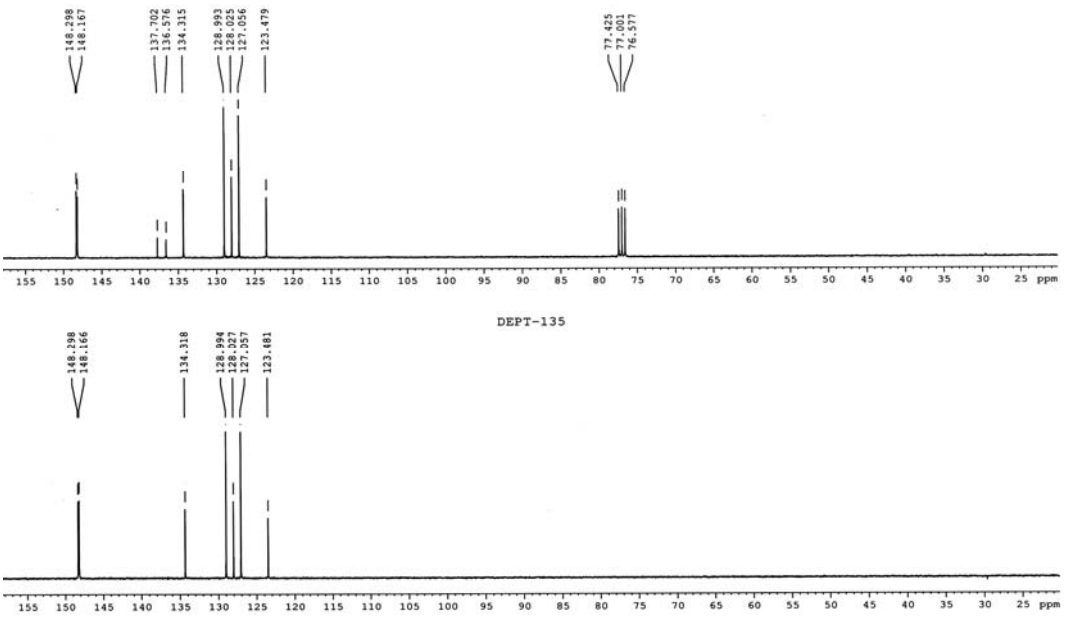

Figure 13.27. NMR spectra of compound **5n**.

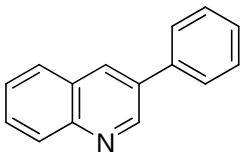

5o

^{1}H NMR in $CDCl_3$

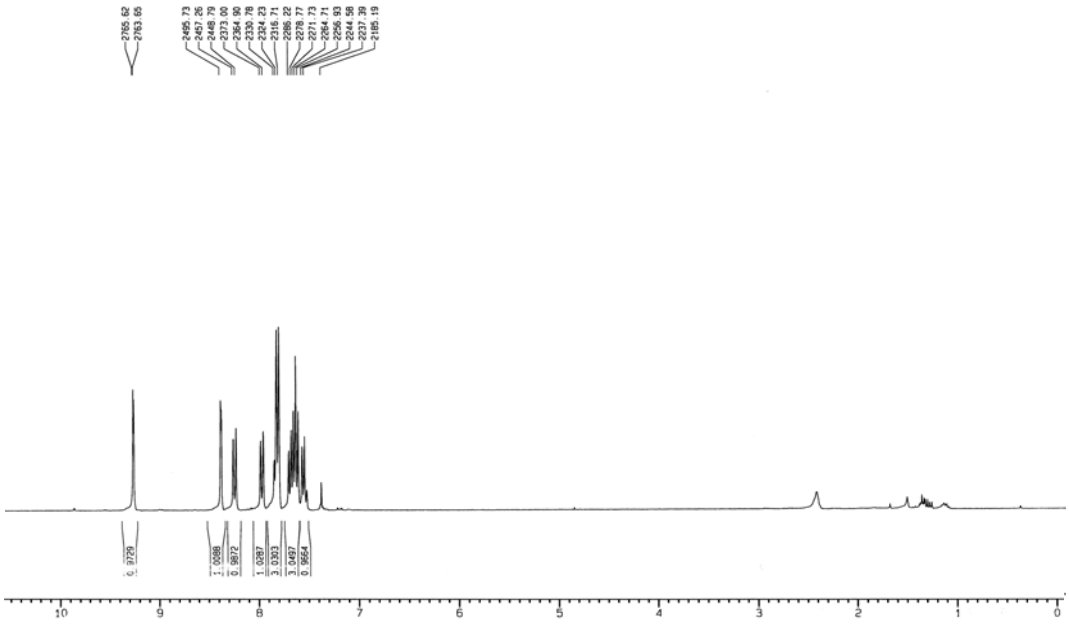

^{13}C NMR in $CDCl_3$

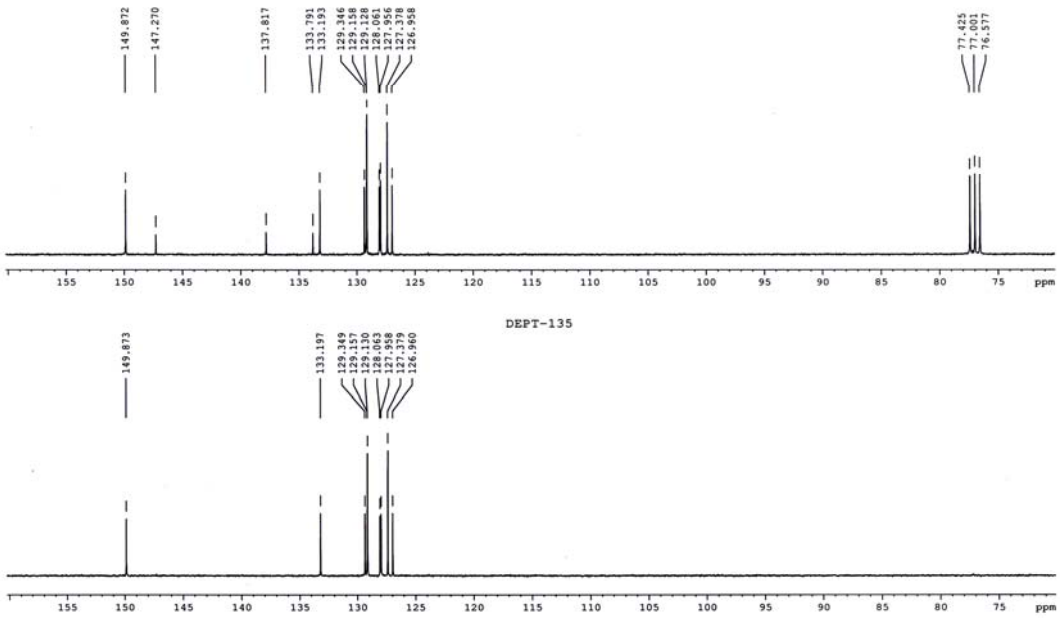

Figure 13.28. NMR spectra of compound **5o**.

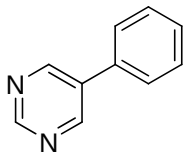

5p

^{1}H NMR in $CDCl_3$

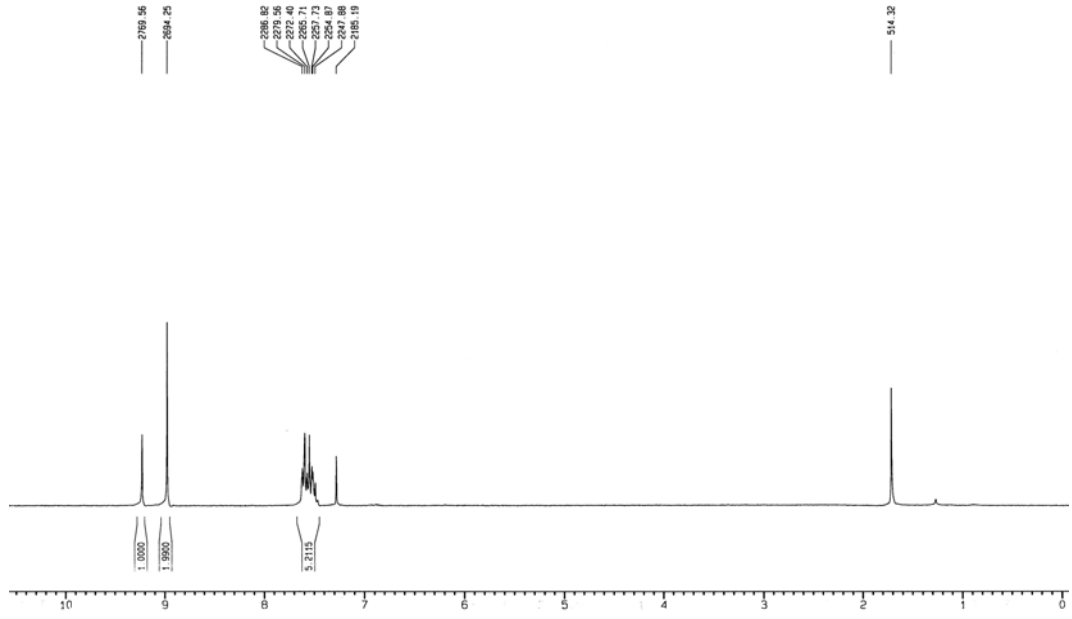

^{13}C NMR in $CDCl_3$

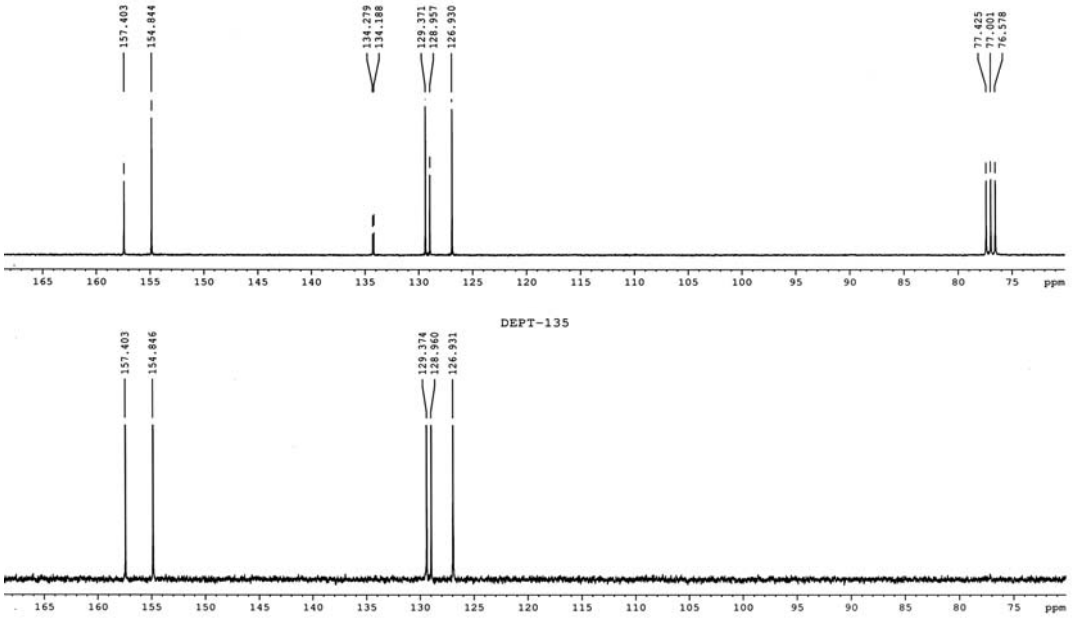

Figure 13.29. NMR spectra of compound **5p**.

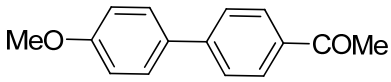

5q

^{1}H NMR in $CDCl_3$

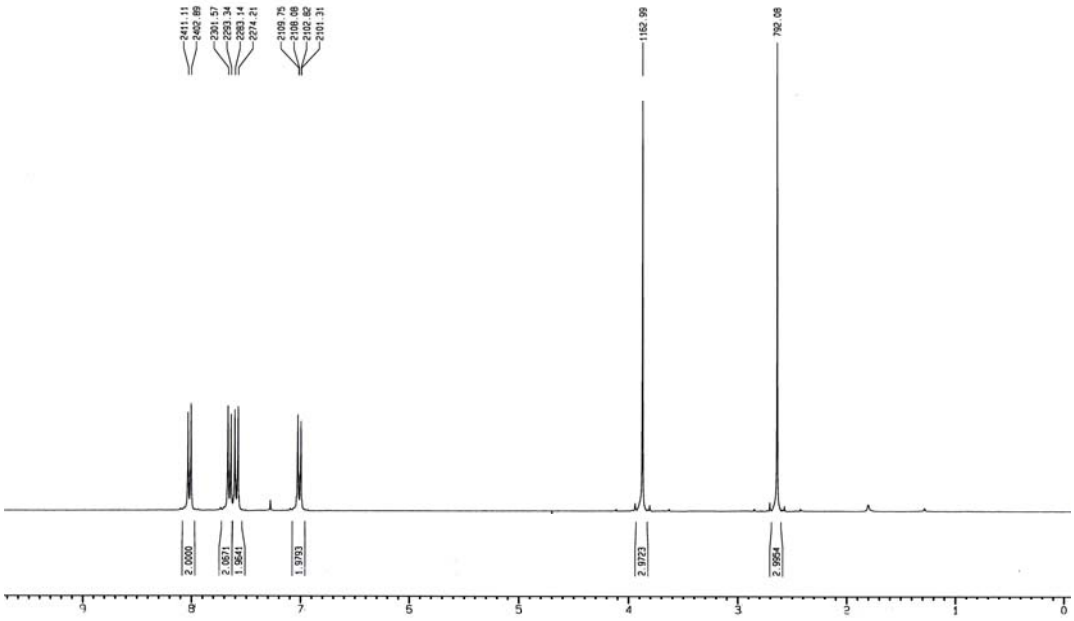

^{13}C NMR in $CDCl_3$

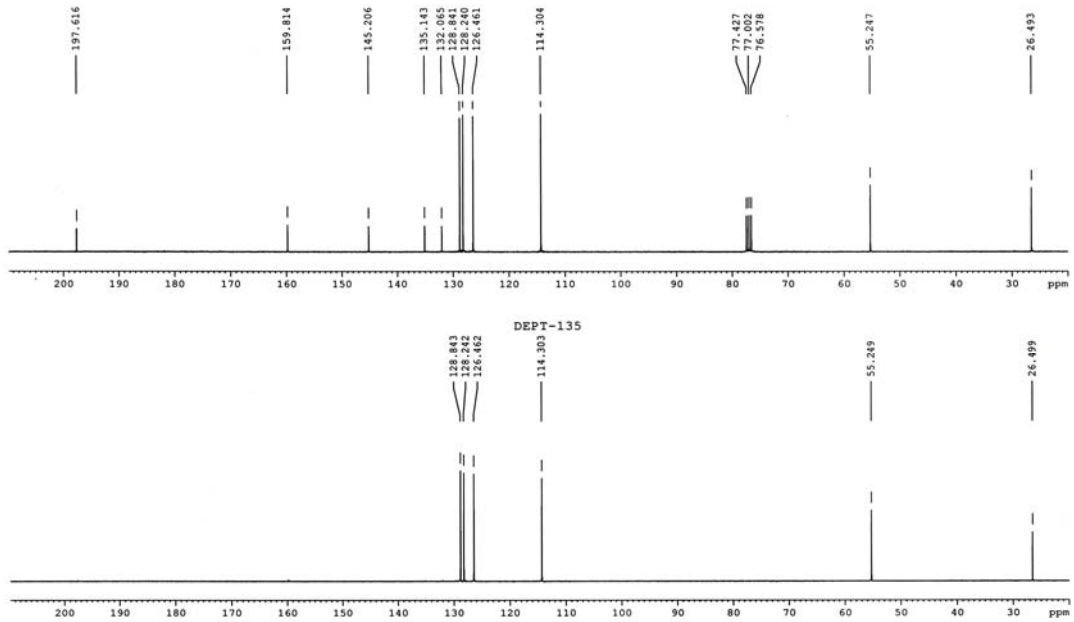

Figure 13.30. NMR spectra of compound **5q**.

APPENDIX E

NMR SPECTRA OF BORYLATION COMPOUNDS (8a–m)

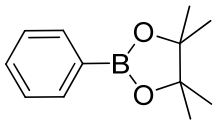

8a

^{1}H NMR in $CDCl_3$

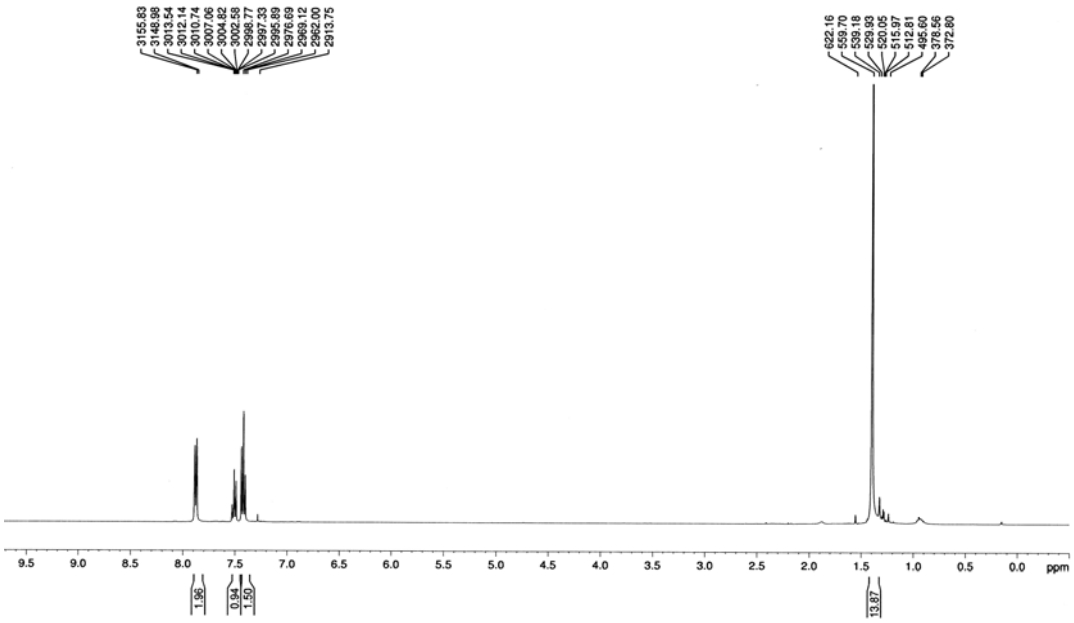

Figure 13.31. NMR spectra of compound **8a**.

^{13}C NMR in $CDCl_3$

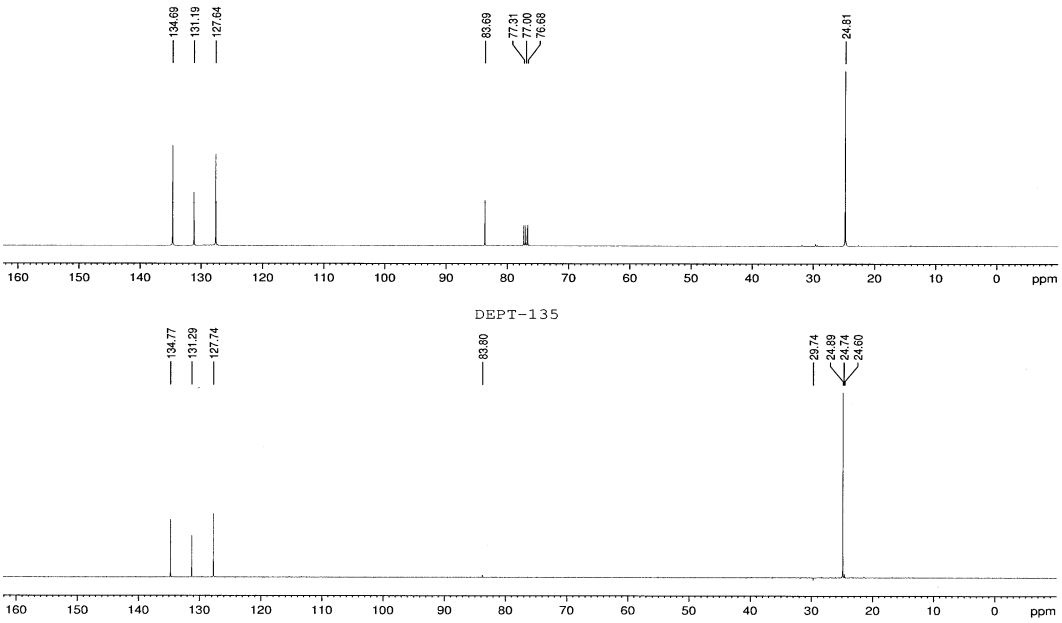

^{11}B NMR in $CDCl_3$

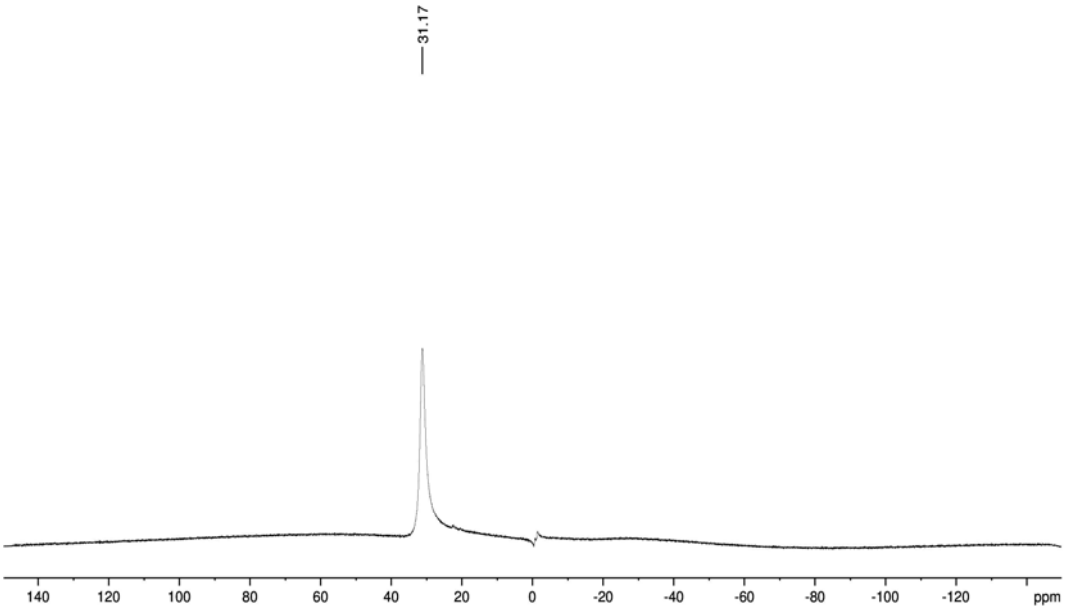

Figure 13.31 (cont.). NMR spectra of compound **8a**.

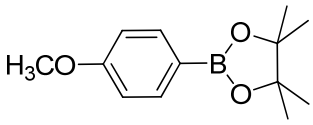

8b

^{1}H NMR in $CDCl_3$

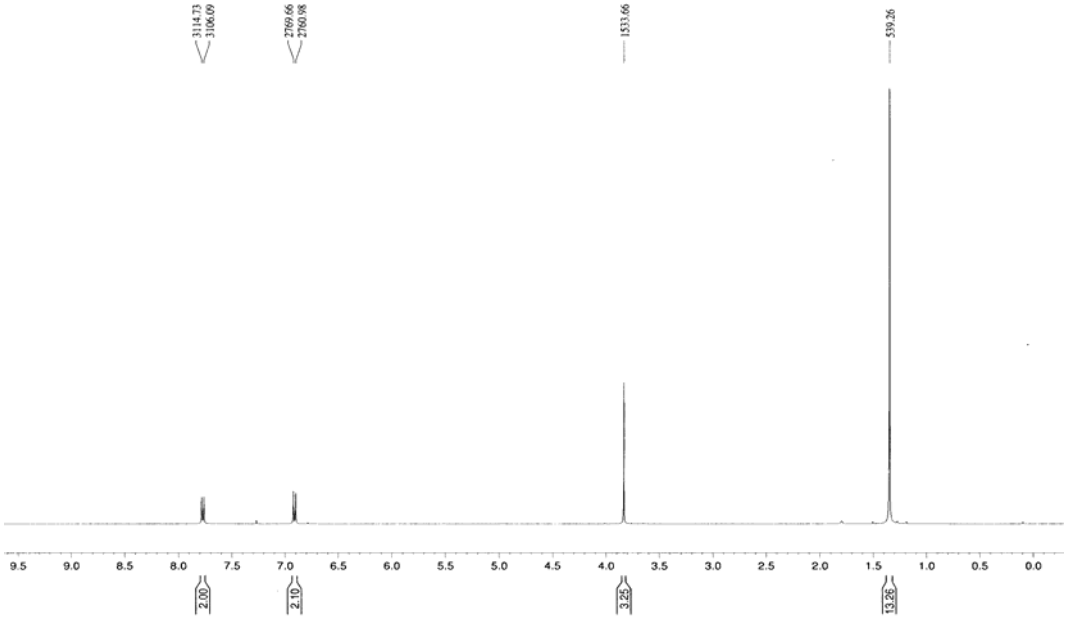

^{13}C NMR in $CDCl_3$

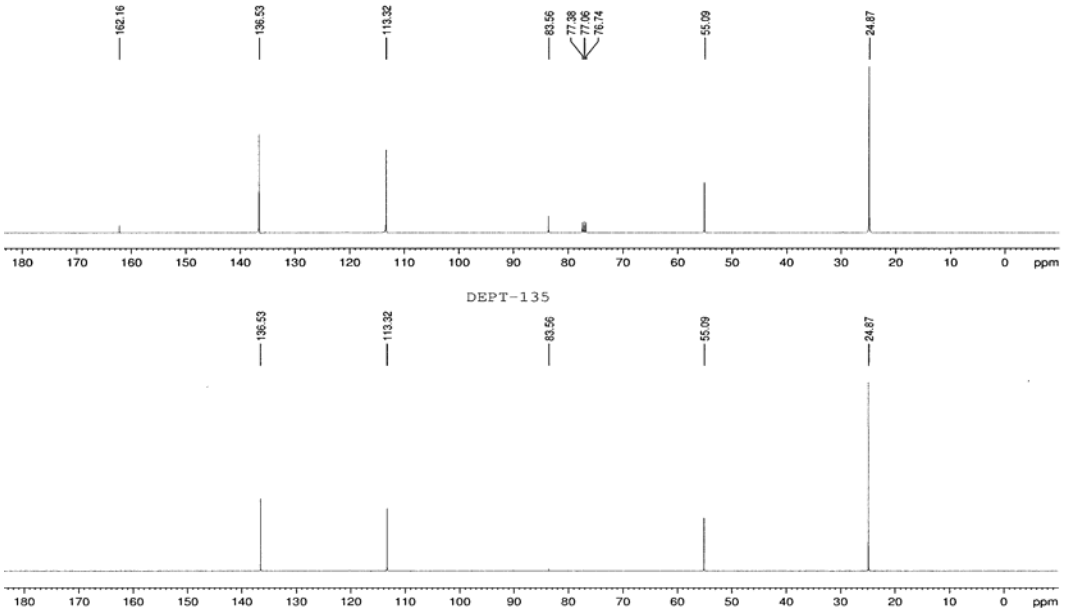

Figure 13.32. NMR spectra of compound **8b**.

^{11}B NMR in $CDCl_3$

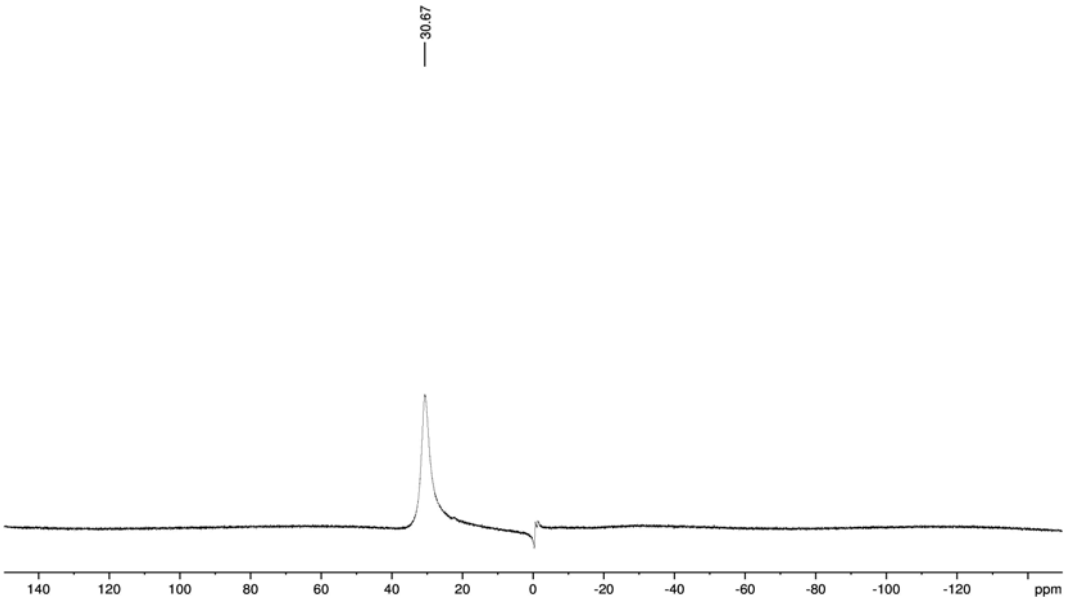

Figure 13.32 (cont.). NMR spectra of compound **8b**.

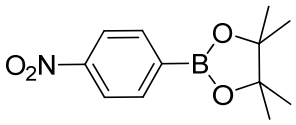

8c

^{1}H NMR in $CDCl_3$

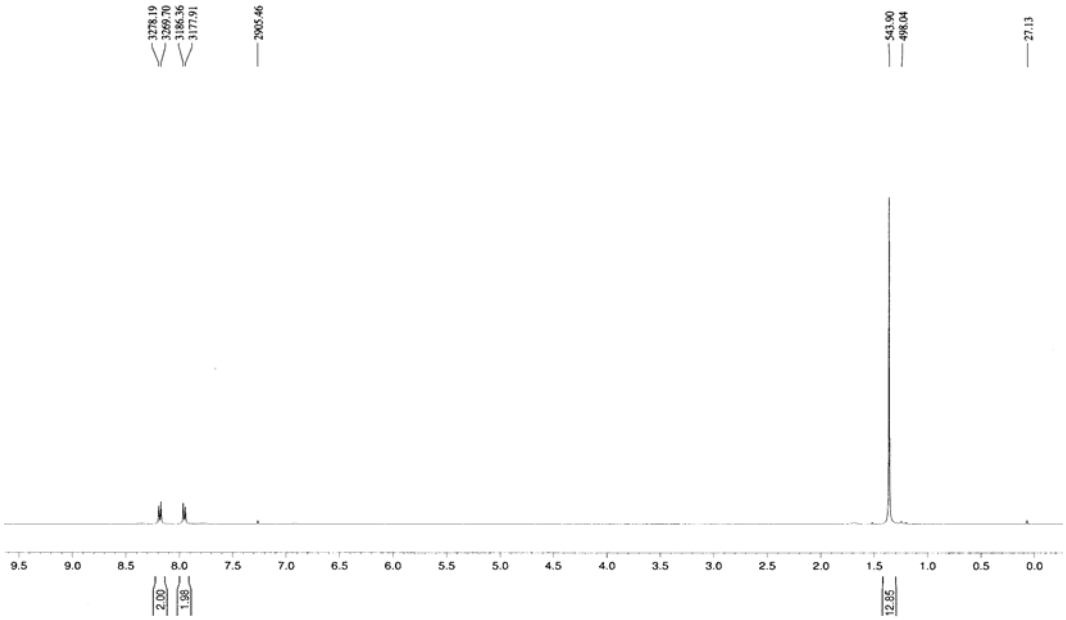

^{13}C NMR in $CDCl_3$

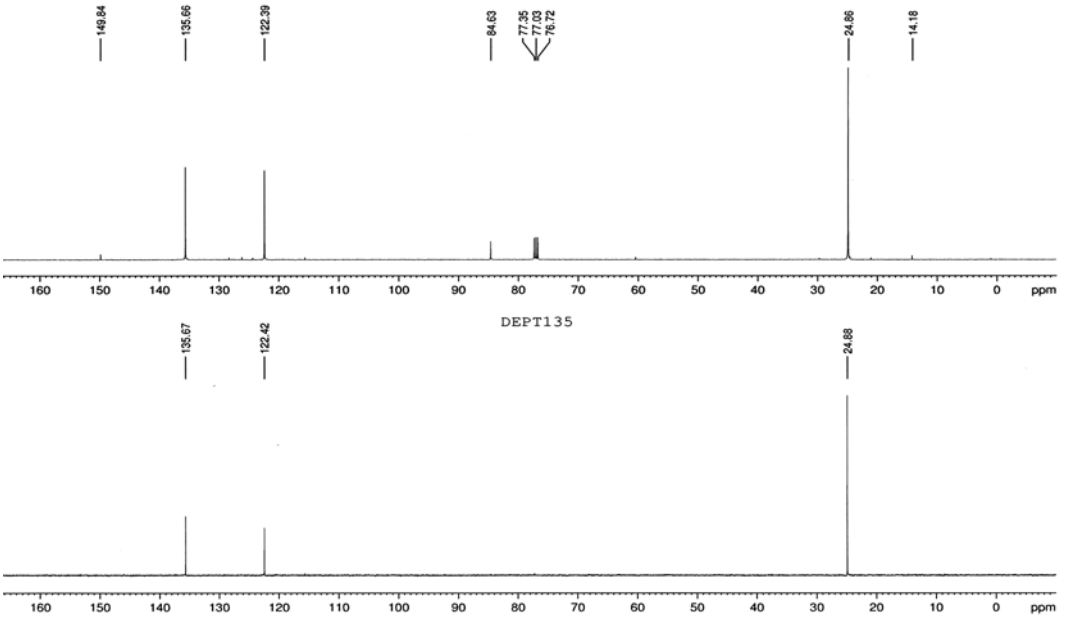

Figure 13.33. NMR spectra of compound **8c**.

^{11}B NMR in $CDCl_3$

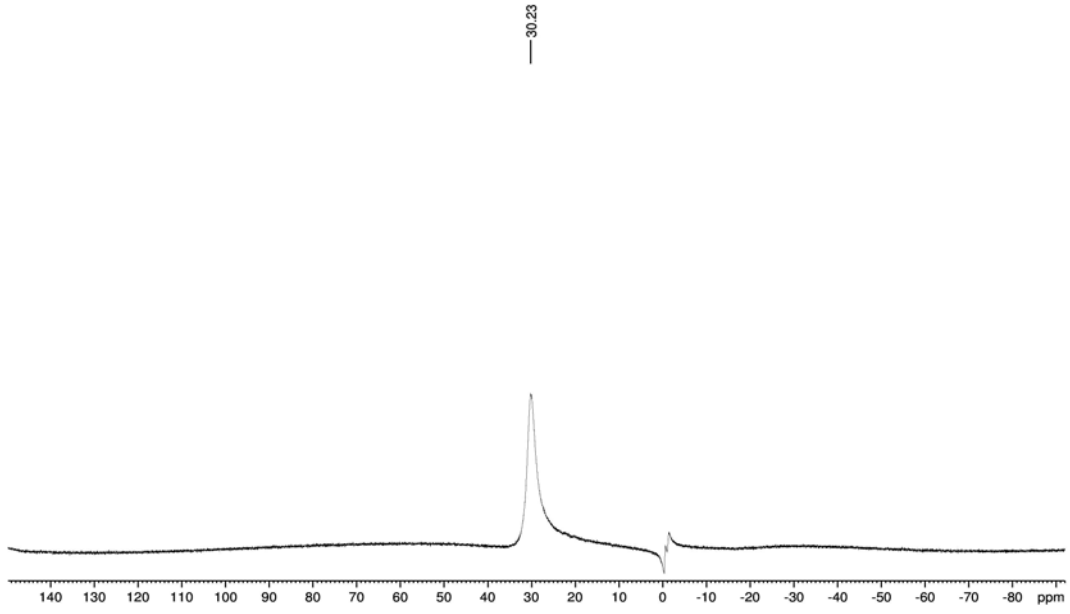

Figure 13.33 (cont.). NMR spectra of compound **8c**.

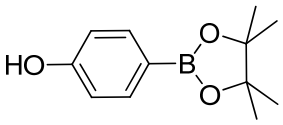

8d

^{1}H NMR in $CDCl_3$

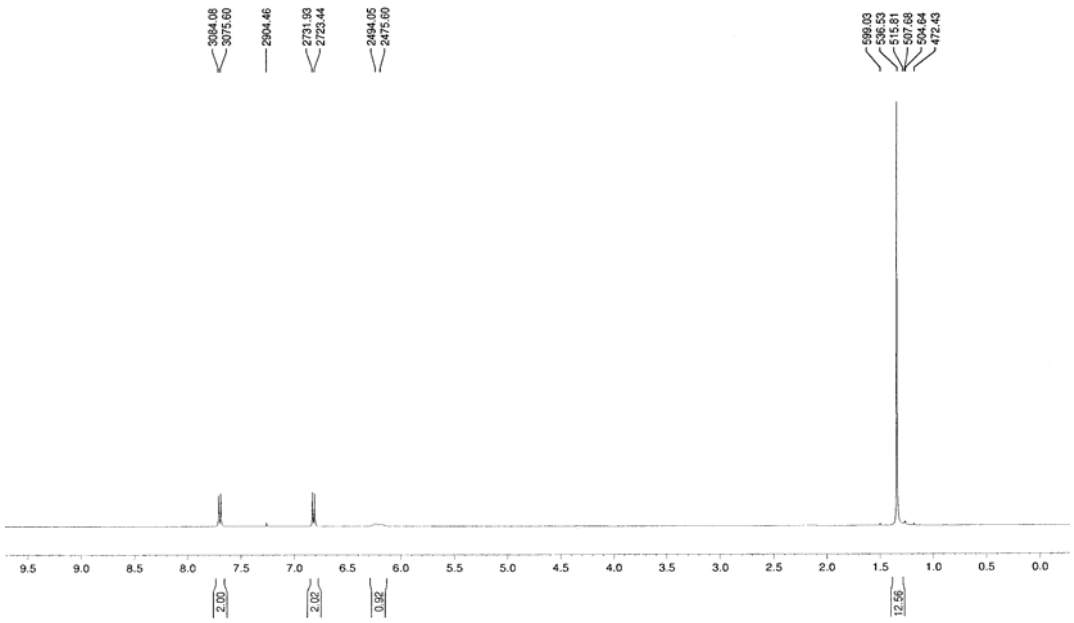

^{13}C NMR in $CDCl_3$

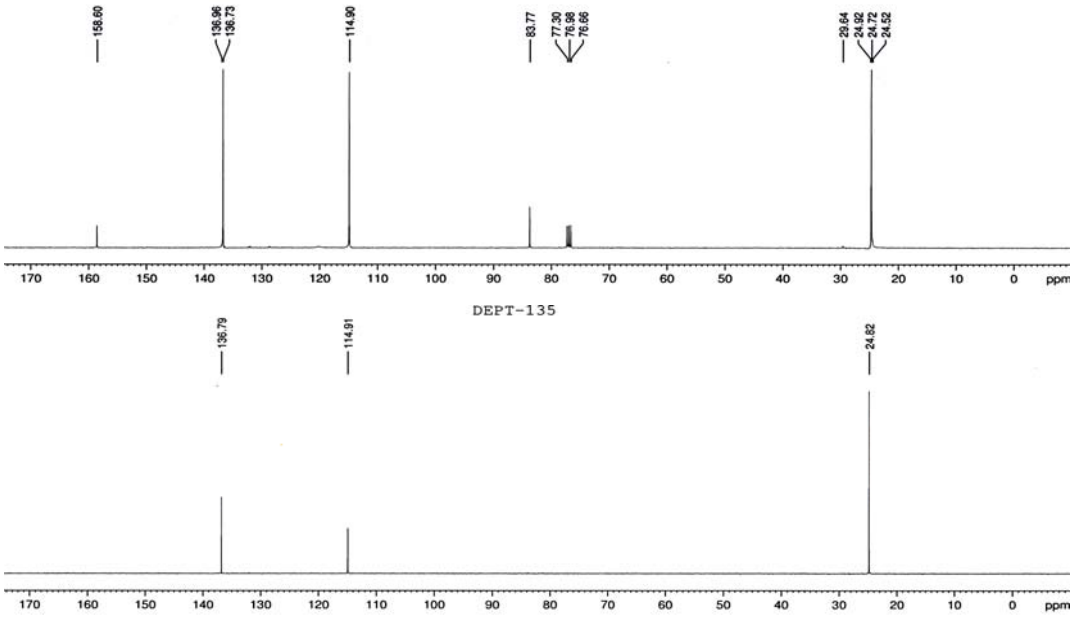

Figure 13.34. NMR spectra of compound **8d**.

^{11}B NMR in $CDCl_3$

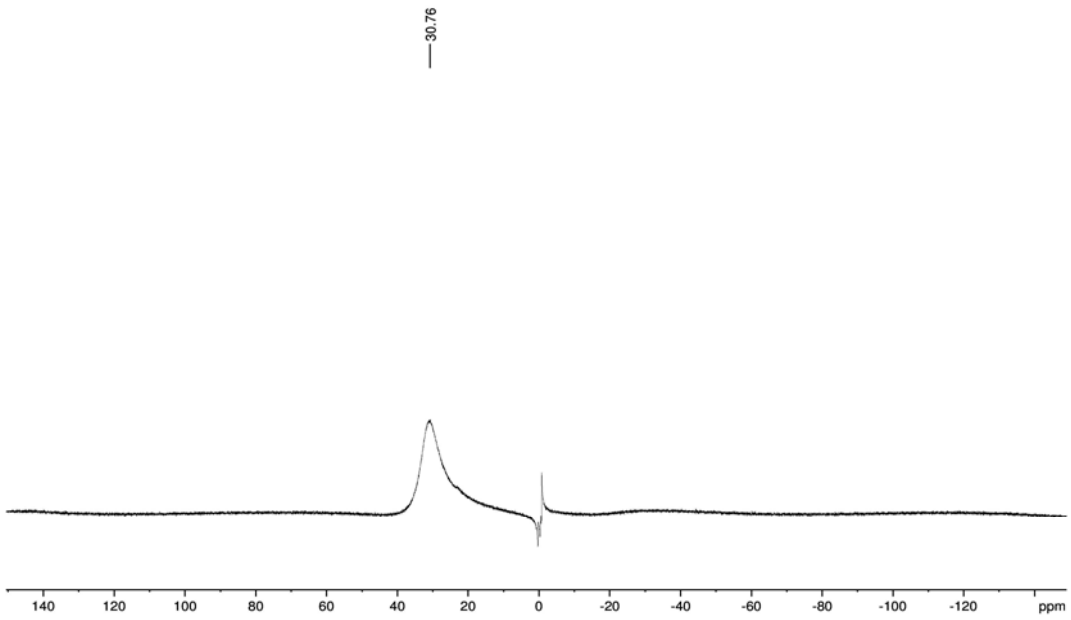

Figure 13.34 (cont.). NMR spectra of compound **8d**.

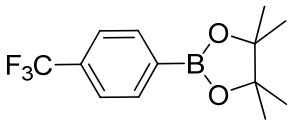

8e

^{1}H NMR in $CDCl_3$

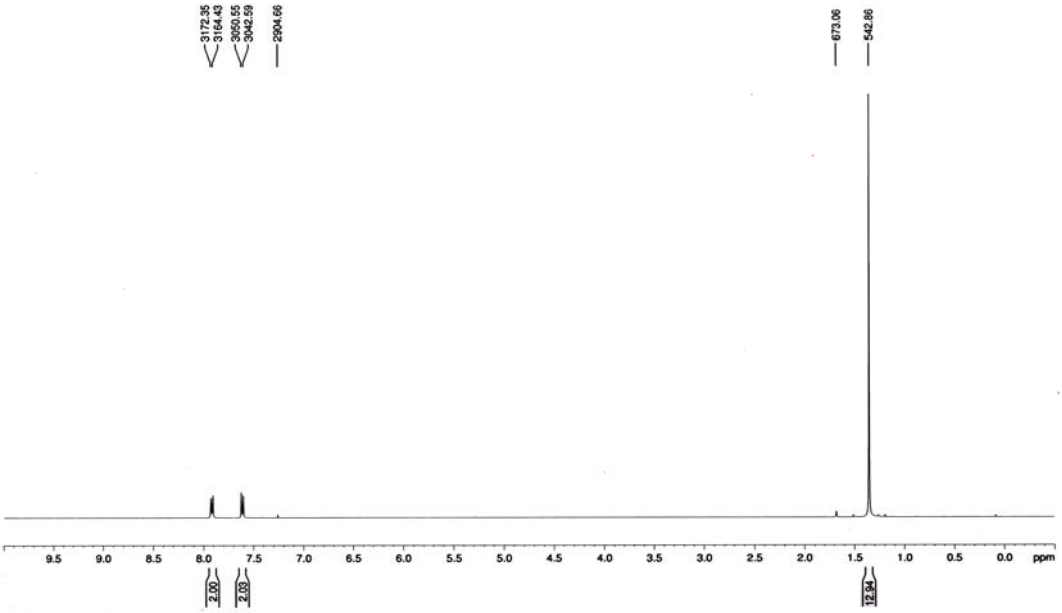

^{13}C NMR in $CDCl_3$

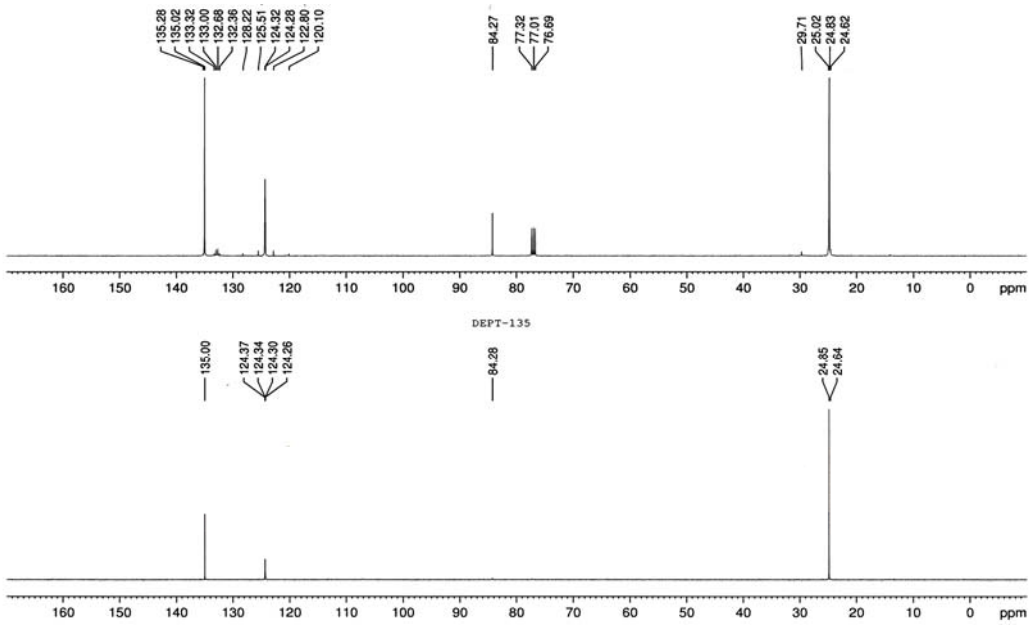

Figure 13.35. NMR spectra of compound **8e**.

^{19}F NMR in $CDCl_3$

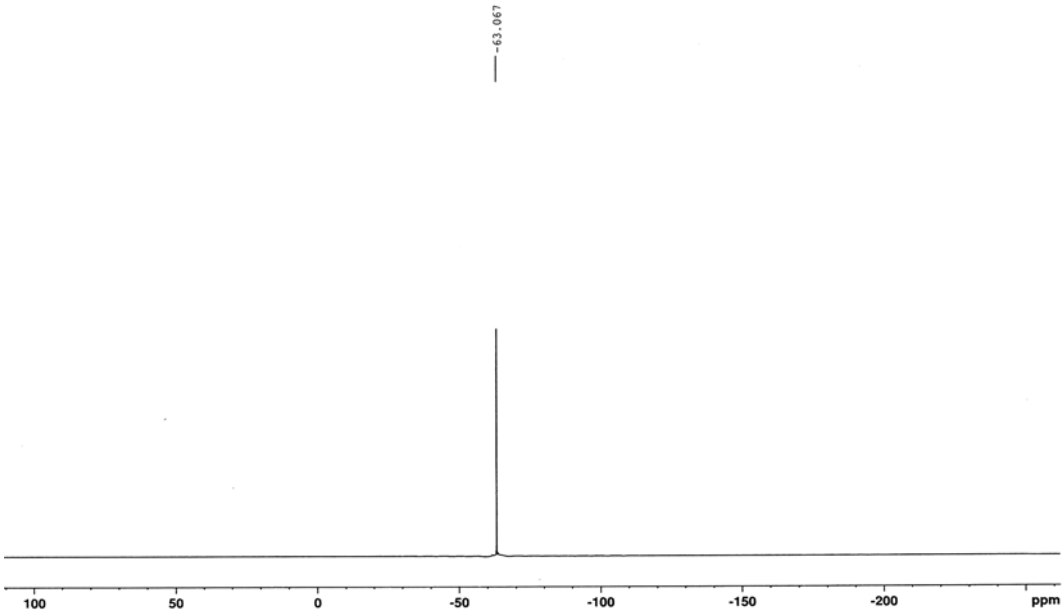

^{11}B NMR in $CDCl_3$

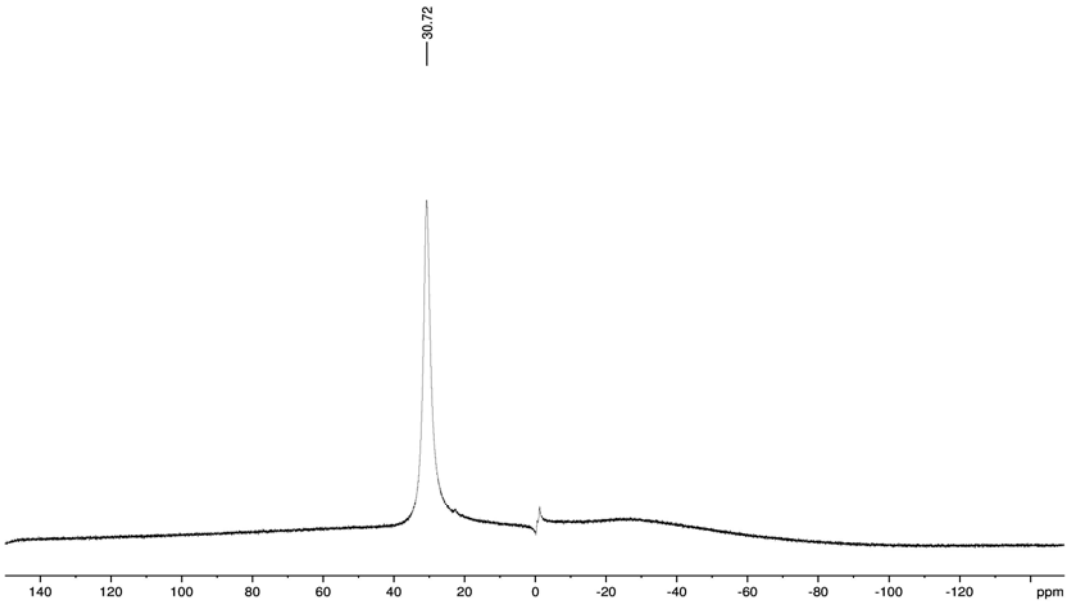

Figure 13.35 (cont.). NMR spectra of compound **8e**.

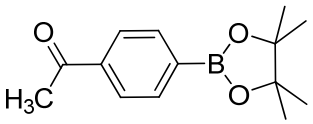

8f

^{1}H NMR in $CDCl_3$

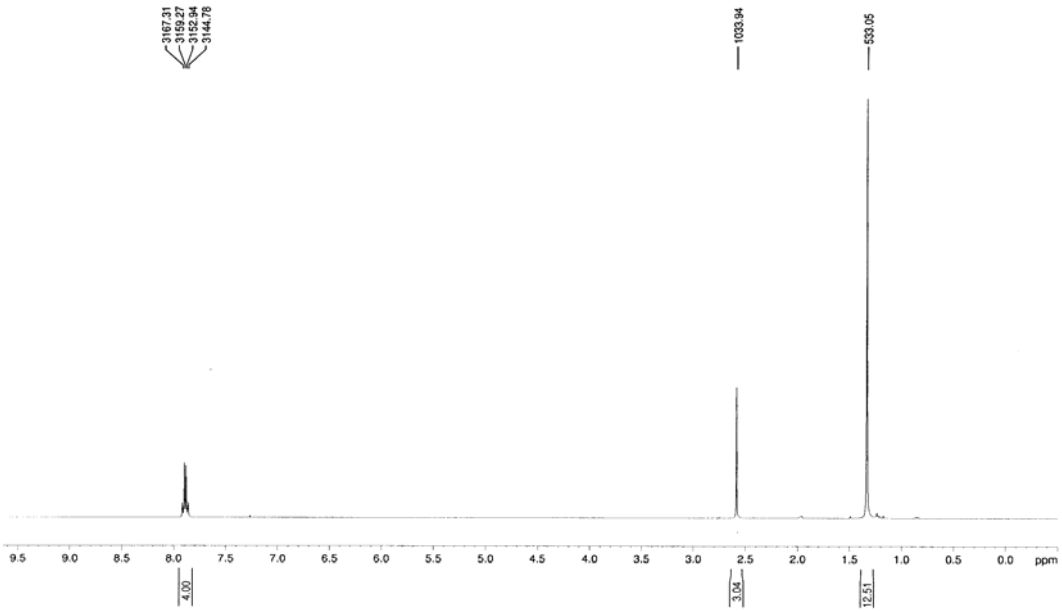

^{13}C NMR in $CDCl_3$

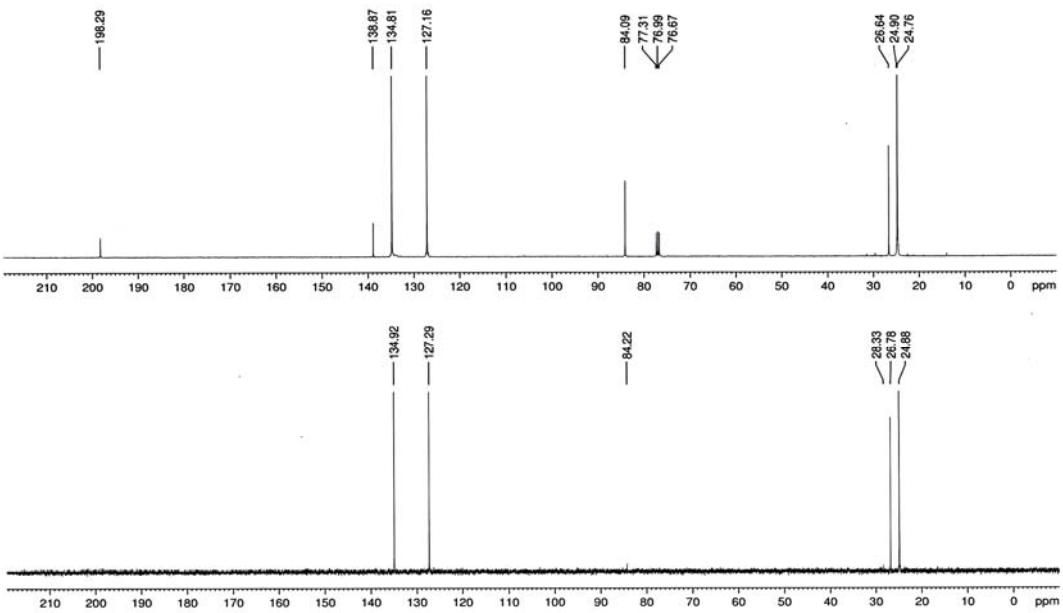

Figure 13.36. NMR spectra of compound **8f**.

^{11}B NMR in $CDCl_3$

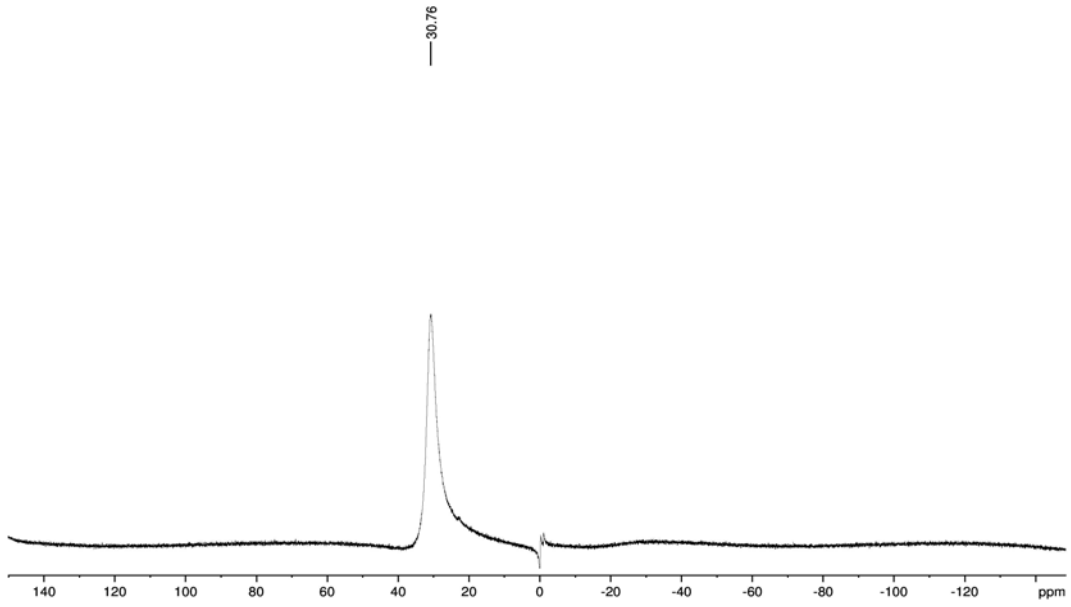

Figure 13.36 (cont.). NMR spectra of compound **8f**.

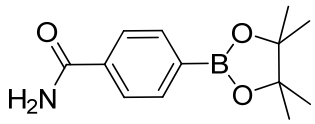

8g

^{1}H NMR in $CDCl_3$

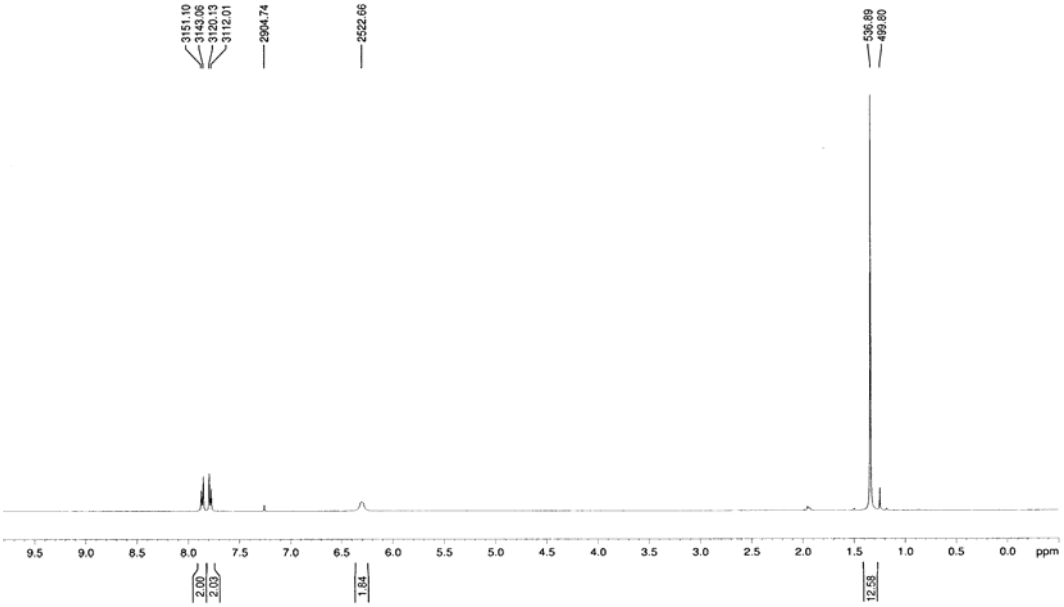

^{13}C NMR in $CDCl_3$

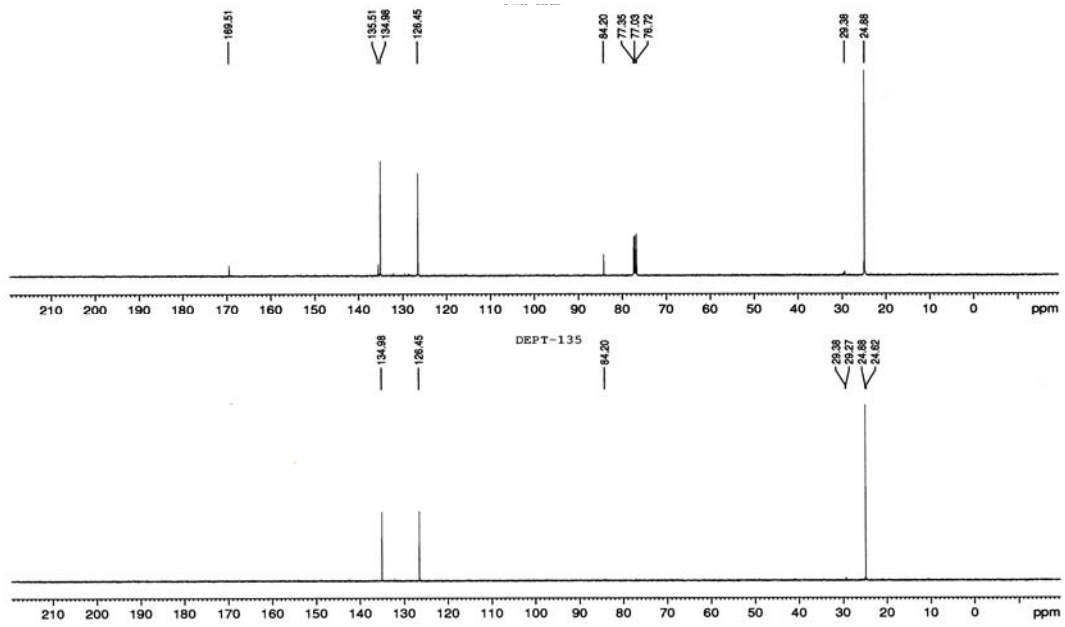

Figure 13.37. NMR spectra of compound **8g**.

^{11}B NMR in $CDCl_3$

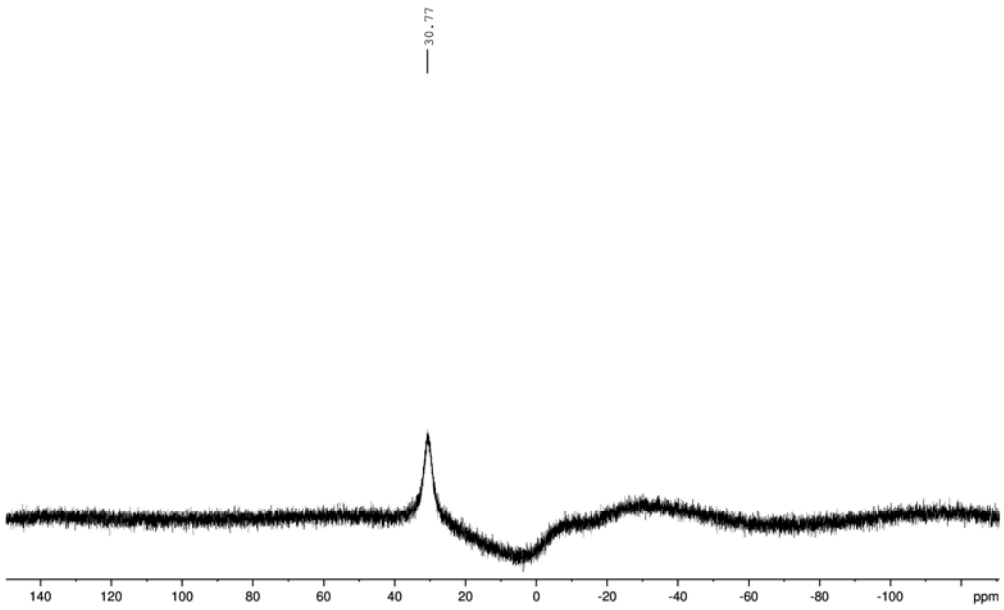

Figure 13.37 (cont.). NMR spectra of compound **8g**.

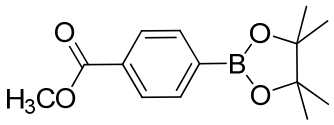

8h

^{1}H NMR in $CDCl_3$

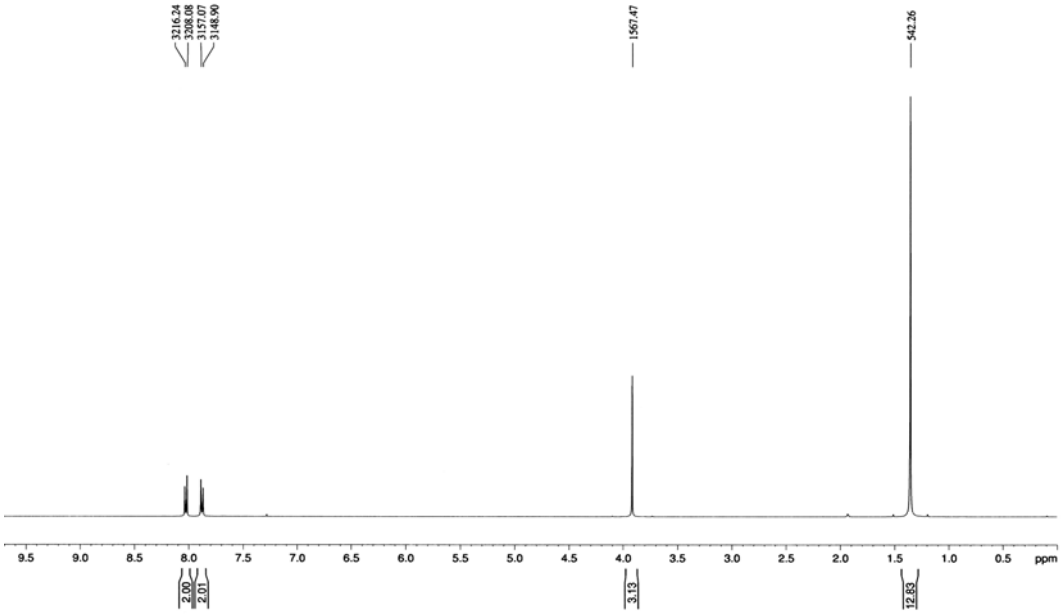

^{13}C NMR in $CDCl_3$

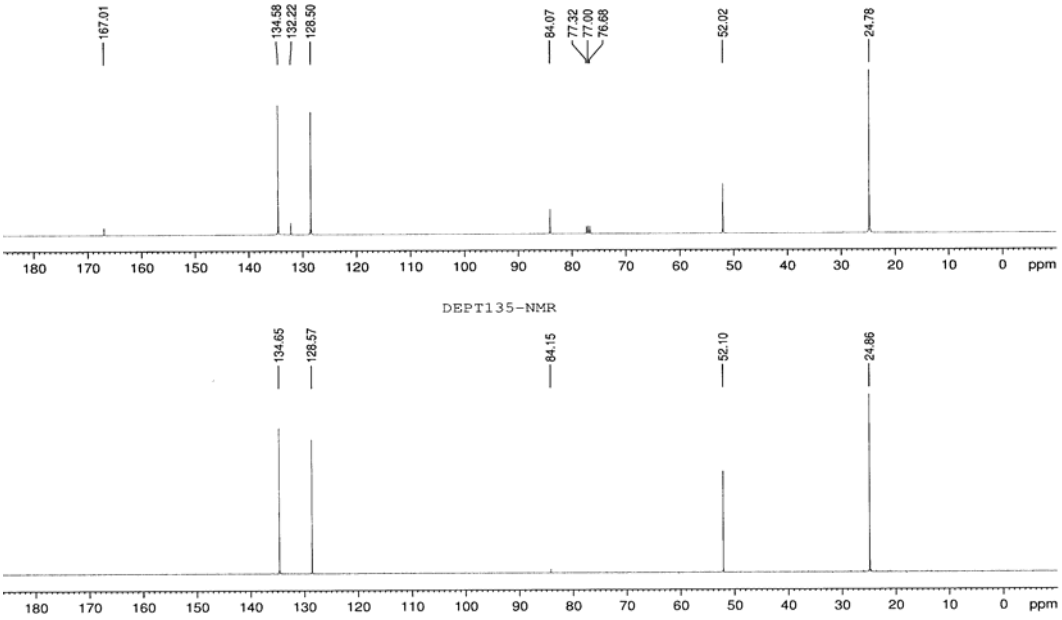

Figure 13.38. NMR spectra of compound **8h**.

^{11}B NMR in $CDCl_3$

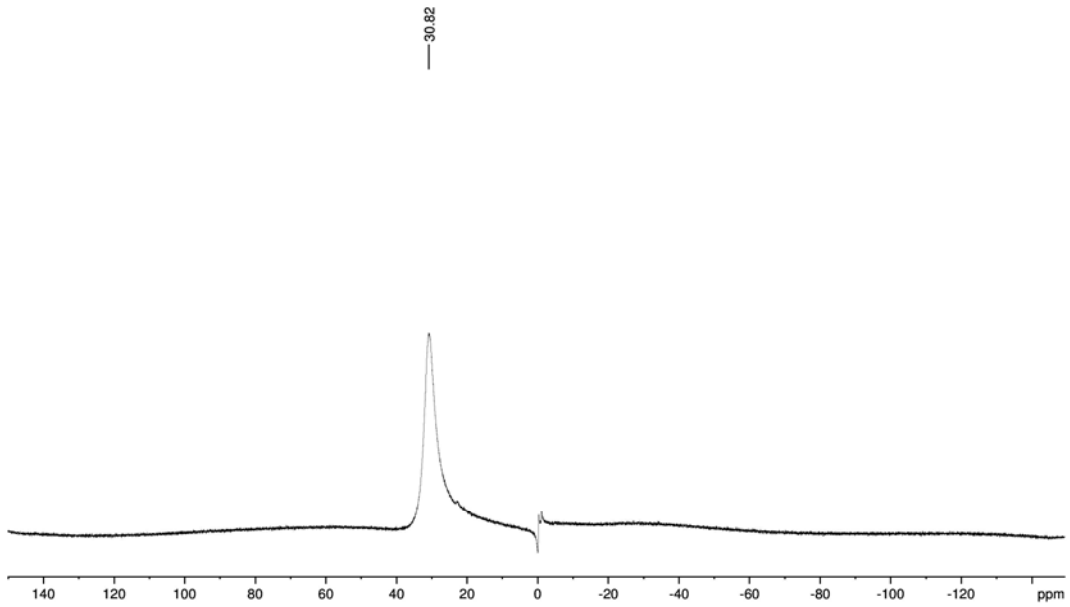

Figure 13.38 (cont.). NMR spectra of compound **8h**.

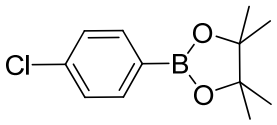

8i

^{1}H NMR in $CDCl_3$

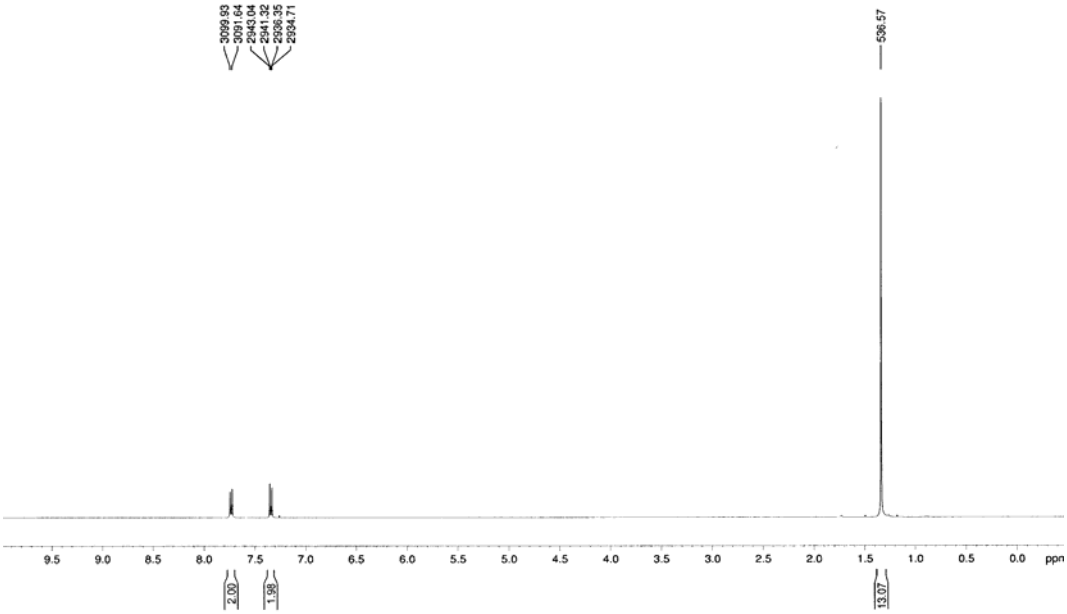

^{13}C NMR in $CDCl_3$

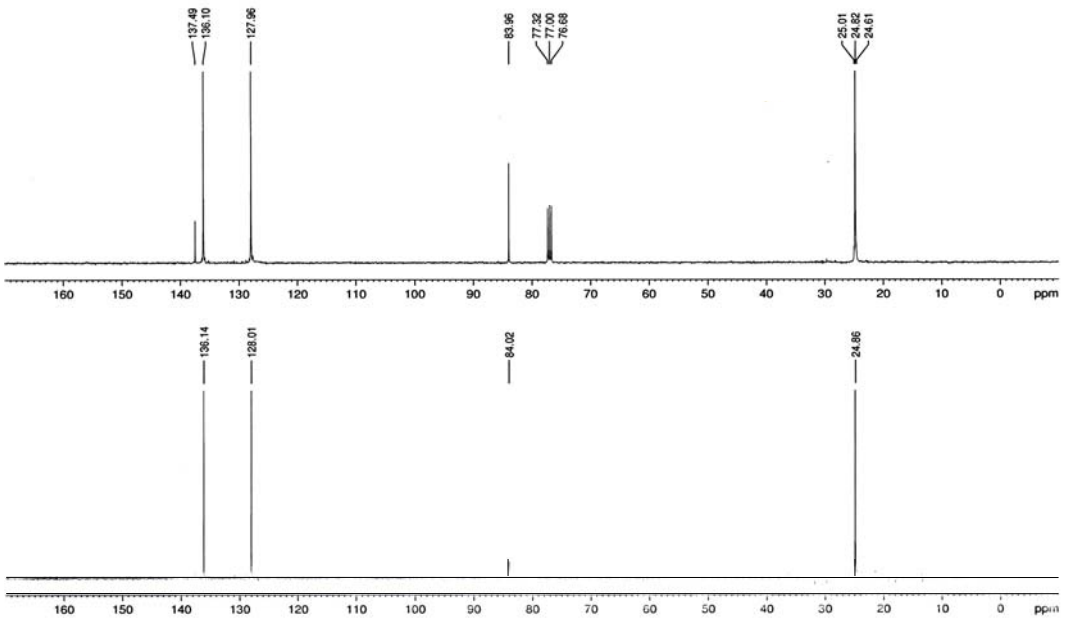

Figure 13.39. NMR spectra of compound **8i**.

^{11}B NMR in $CDCl_3$

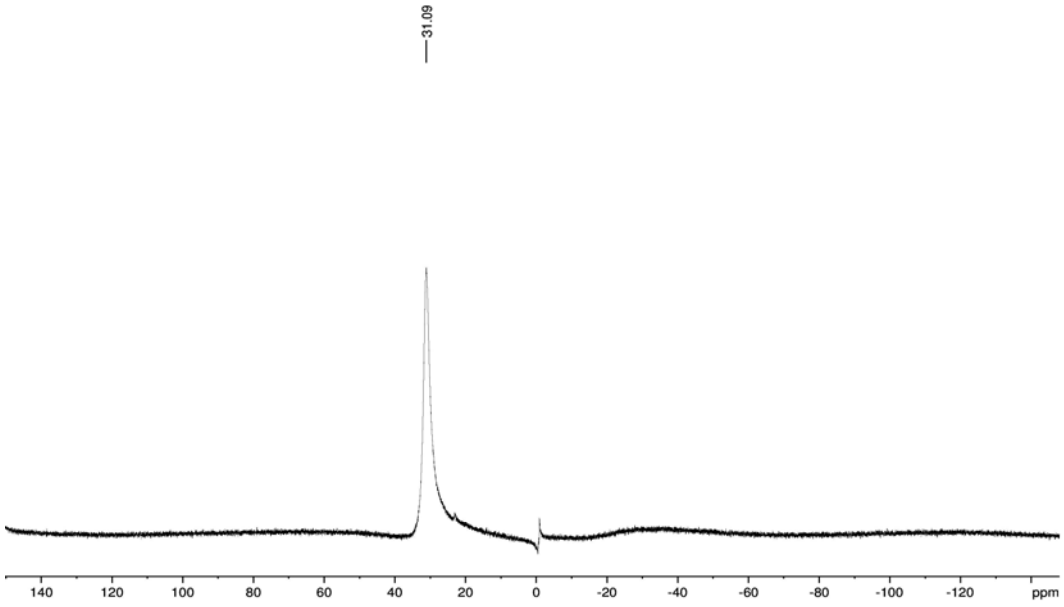

Figure 13.39 (cont.). NMR spectra of compound **8i**.

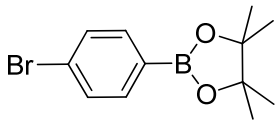

8j

^{1}H NMR in $CDCl_3$

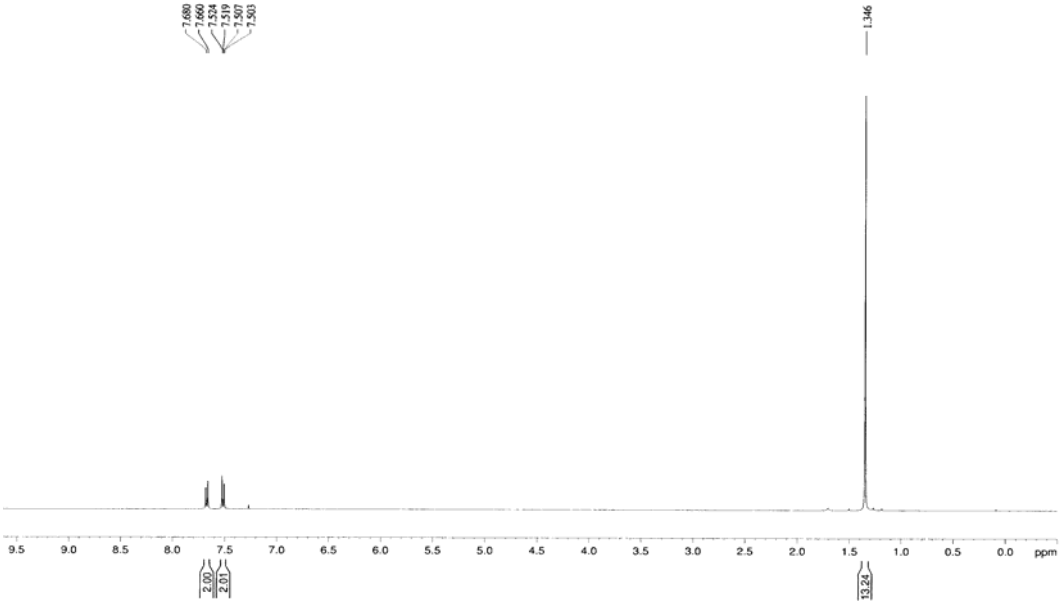

^{13}C NMR in $CDCl_3$

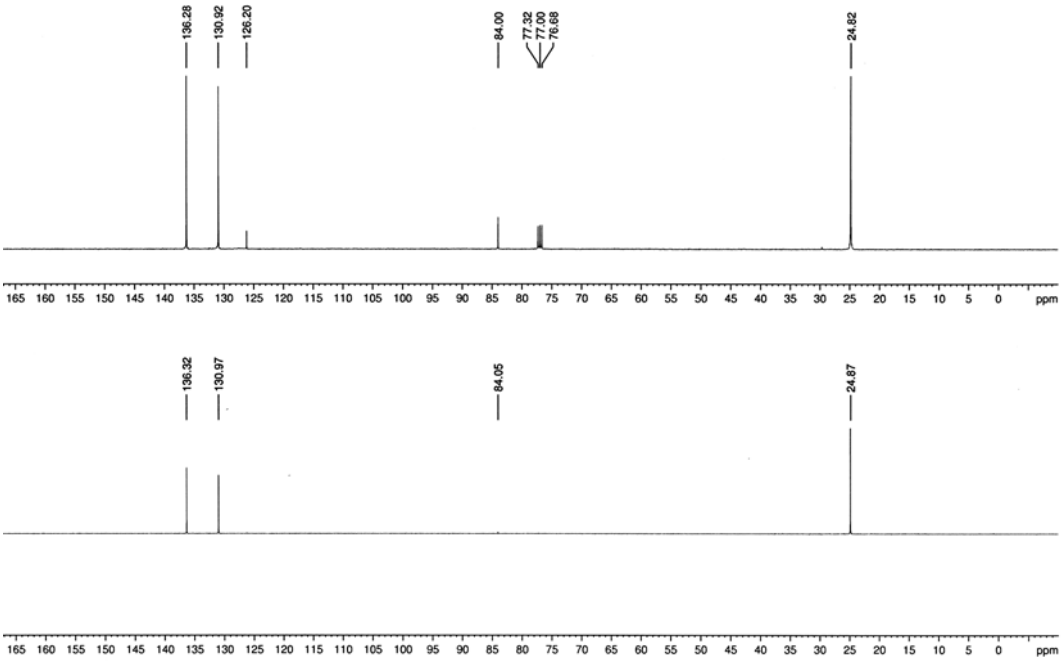

Figure 13.40. NMR spectra of compound **8j**.

^{11}B NMR in $CDCl_3$

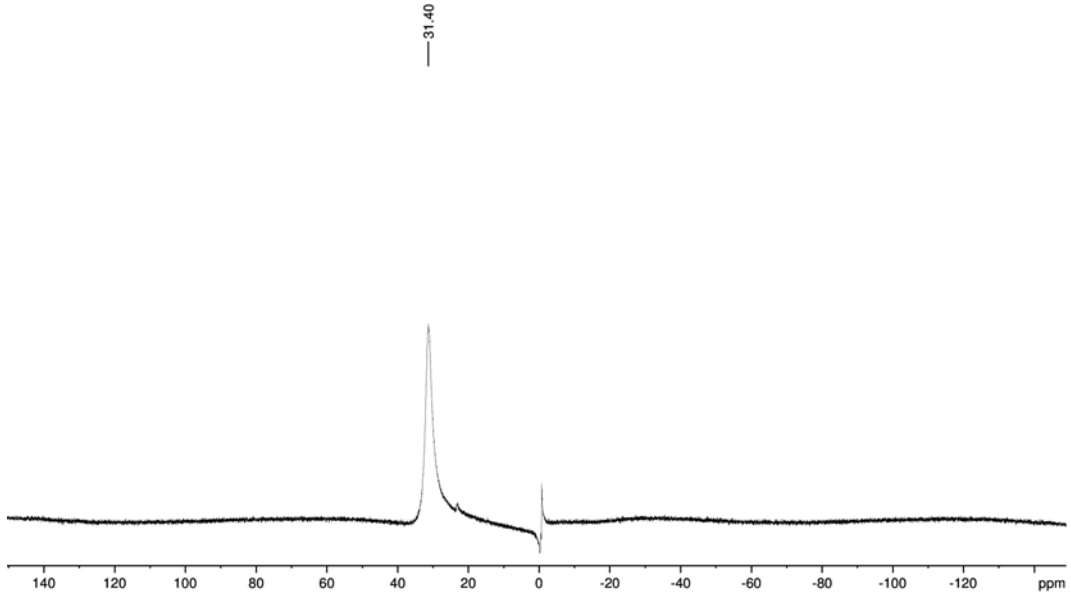

Figure 13.40 (cont.). NMR spectra of compound **8j**.

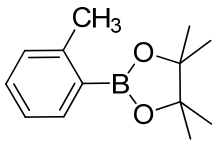

8k

^{1}H NMR in $CDCl_3$

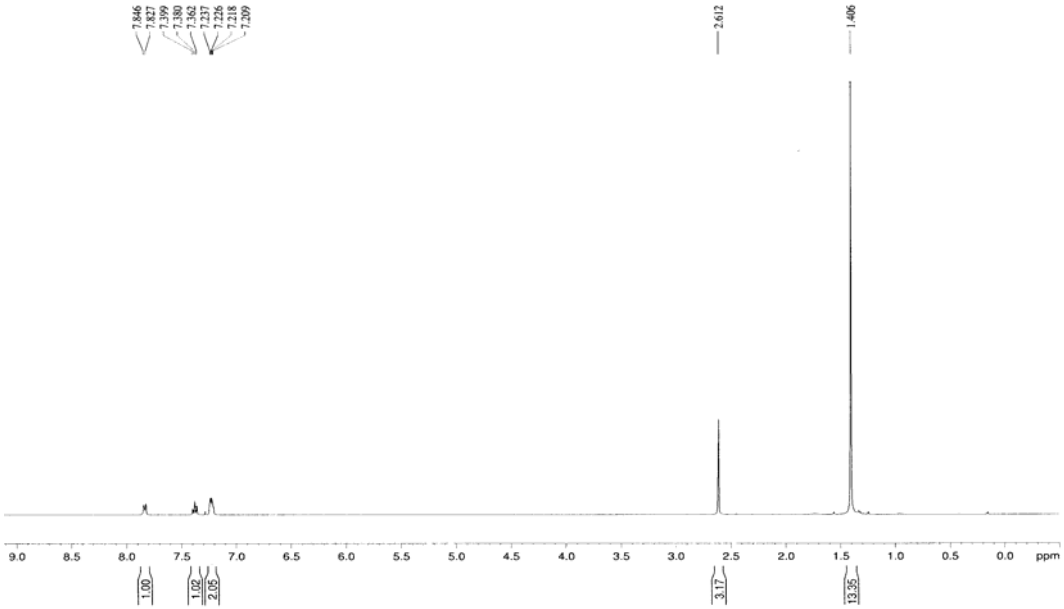

^{13}C NMR in $CDCl_3$

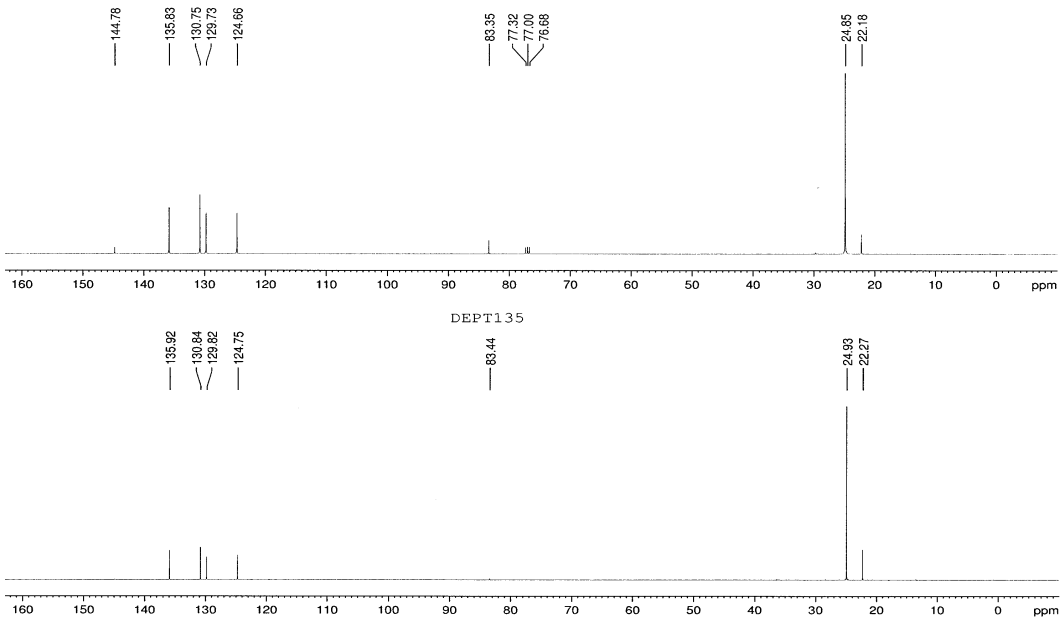

Figure 13.41. NMR spectra of compound **8k**.

^{11}B NMR in $CDCl_3$

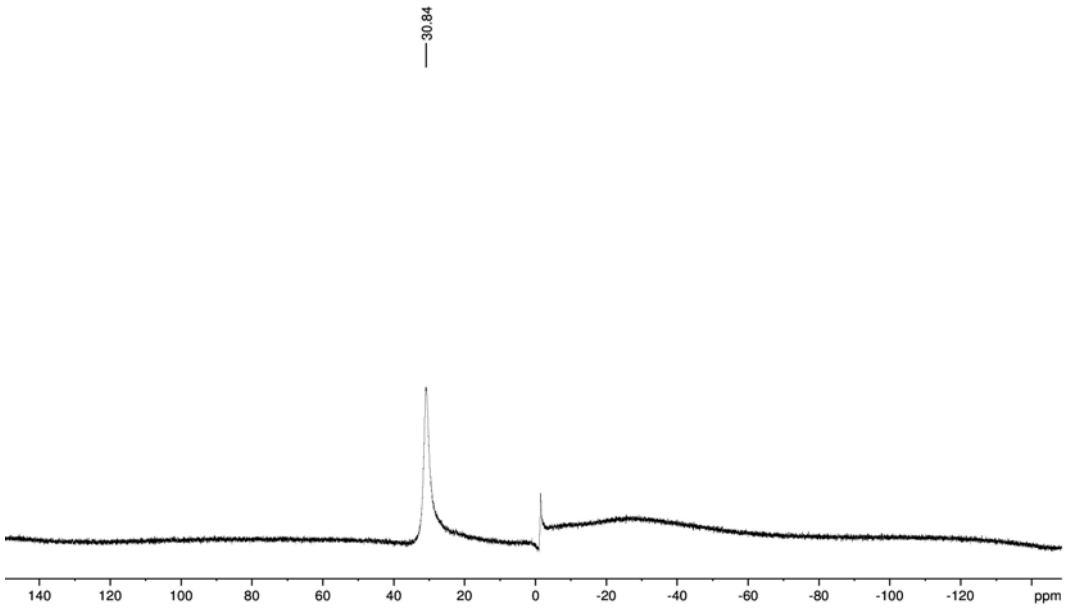

Figure 13.41 (cont.). NMR spectra of compound **8k**.

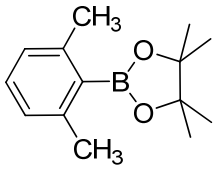

8l

^{1}H NMR in $CDCl_3$

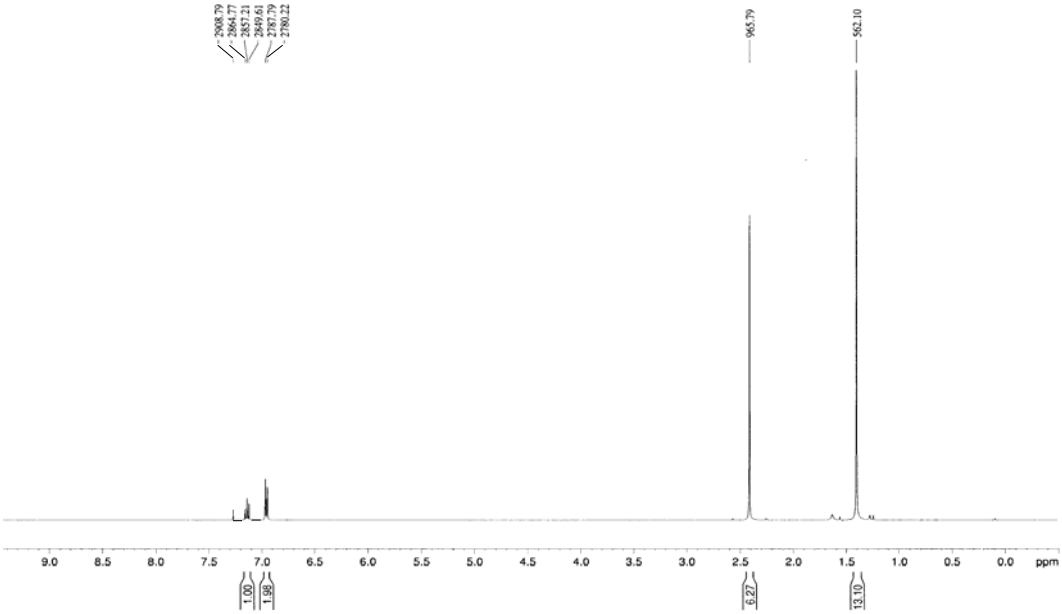

^{13}C NMR in $CDCl_3$

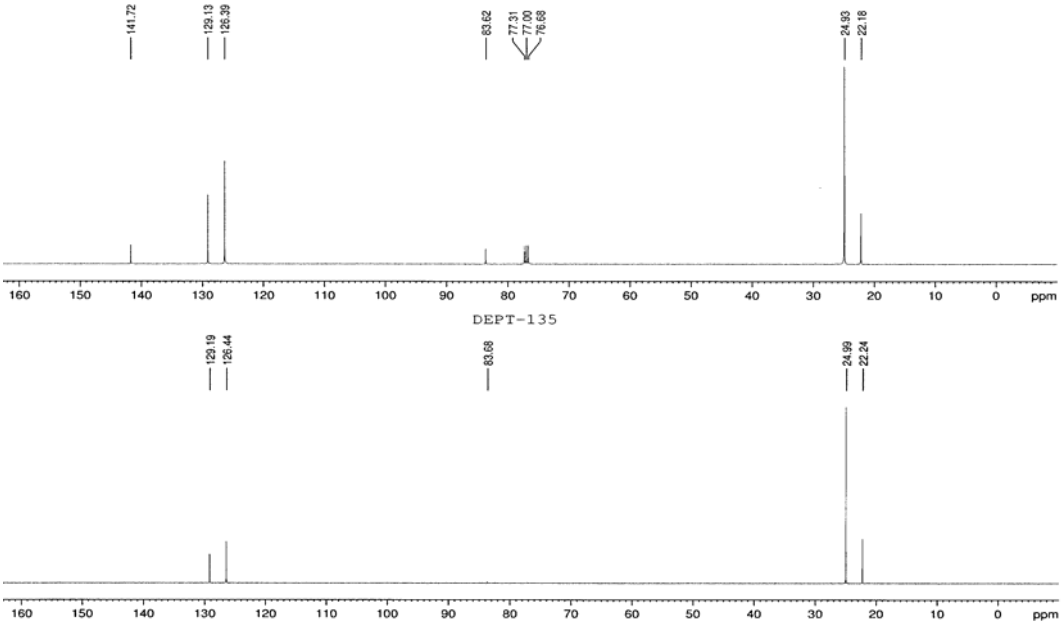

Figure 13.42. NMR spectra of compound **8l**.

^{11}B NMR in $CDCl_3$

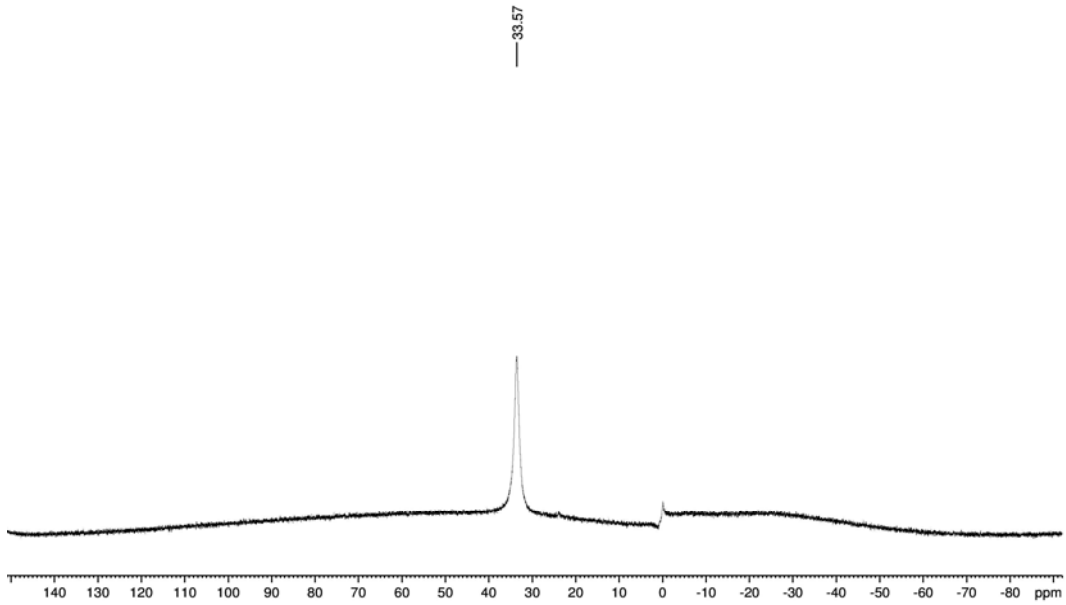

Figure 13.42 (cont.). NMR spectra of compound **8l**.

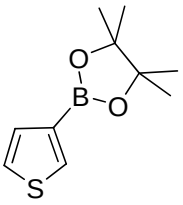

8m

^{1}H NMR in $CDCl_3$

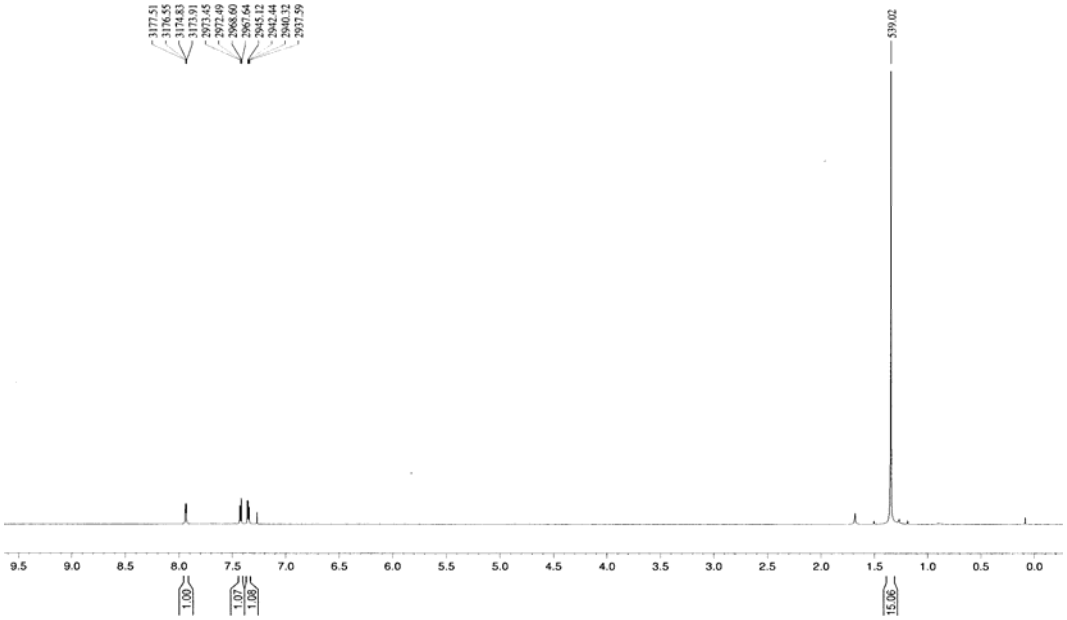

^{13}C NMR in $CDCl_3$

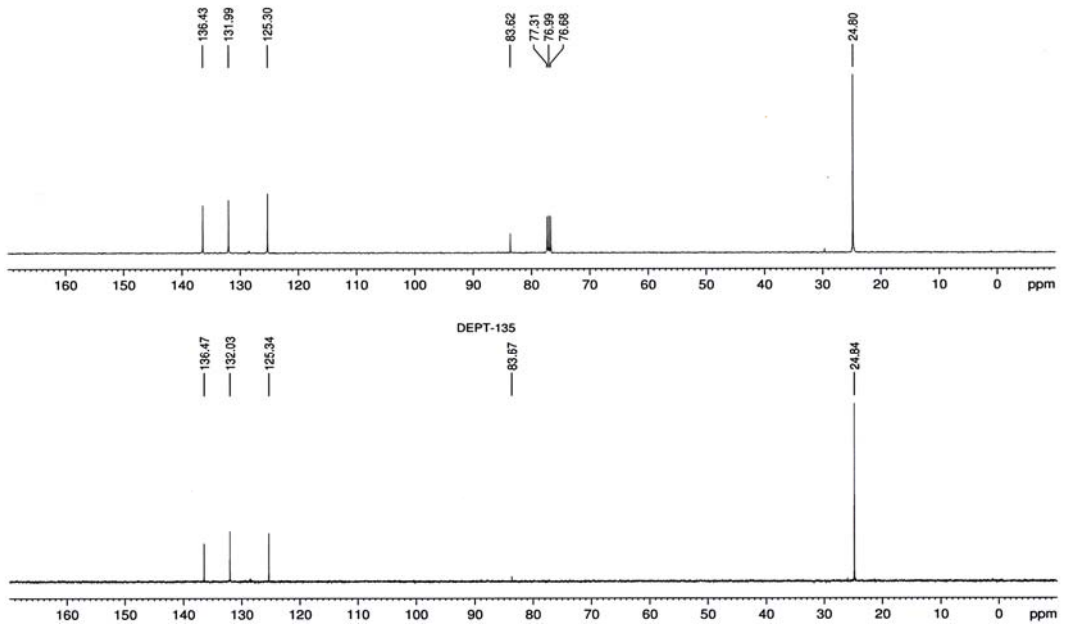

Figure 13.43. NMR spectra of compound **8m**.

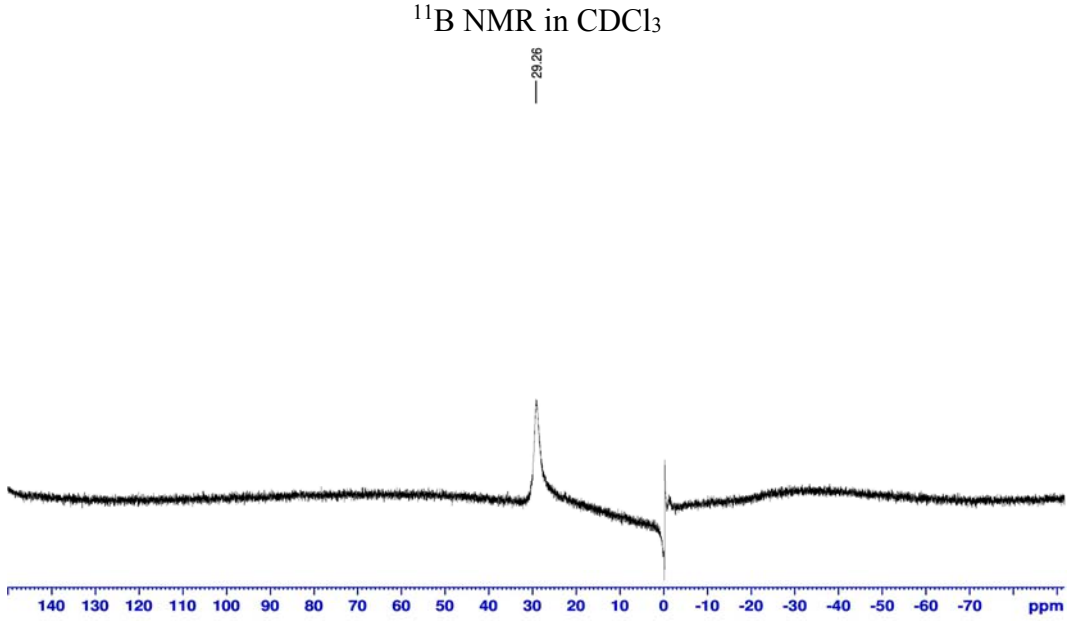

Figure 13.43 (cont.). NMR spectra of compound **8m**.

APPENDIX F
X-RAY DATA OF PALLADIUM COMPLEXES

1. X-ray data of complex (4b)

Table 13.1. Fractional atomic coordinates ($\times 10^4$) and equivalent isotropic displacement parameters ($Å^2 \times 10^3$). U_{eq} is defined as 1/3 of the trace of the orthogonalised U_{IJ} tensor.

Atom	x	y	z	$U_{(eq)}$
Pd1	260.3(2)	1001.58(15)	4900.43(15)	42.51(19)
C17	2260(3)	1504.9(19)	4379.2(17)	45.2(10)
C18	2298(3)	2171(2)	4298(2)	59.0(12)
C26	2998(3)	440(3)	4628(2)	69.3(15)
C11	-780(4)	1425(3)	2523(2)	71.9(14)
C22	3074(3)	1147(2)	4520(2)	54.3(11)
C23	1410(3)	2552(2)	4174(3)	69.7(14)
C21	3980(3)	1456(3)	4562(2)	69.8(15)
C19	3228(4)	2446(3)	4352(3)	71.8(15)
C20	4052(4)	2094(3)	4469(3)	74.0(15)
C27	3477(4)	232(4)	5175(3)	109(3)
C24	1335(5)	3134(3)	4540(4)	119(3)
C12	-424(6)	2082(3)	2339(4)	112(2)
C28	3371(5)	52(3)	4131(4)	115(2)
C14	888(7)	-658(3)	2960(3)	120(3)
C13	-1801(4)	1304(4)	2263(3)	102(2)
C25	1369(6)	2738(5)	3546(4)	135(3)
C16	144(9)	-1186(4)	2836(5)	176(5)
C15	1909(9)	-906(5)	2927(5)	200(6)
N1	1335(2)	1189.9(16)	4299.6(14)	42.2(8)
N2	-367(2)	623.5(16)	4206.1(15)	43.5(8)
N3	-263(2)	413.8(18)	3291.8(16)	50.7(9)
C1	1112(3)	997.0(18)	3801.0(19)	42.3(9)
C2	184(2)	684(2)	3744.3(18)	40.5(9)
C5	133(3)	395(2)	2717.5(19)	53.6(11)
C3	-1188(3)	294(2)	4050(2)	58.5(12)
C10	715(4)	-114(3)	2563(2)	68.2(13)
C4	-1125(3)	173(2)	3488(2)	66.2(13)

Table 13.1 (cont.). Fractional atomic coordinates ($\times 10^4$) and equivalent isotropic displacement parameters ($Å^2 \times 10^3$). U_{eq} is defined as 1/3 of the trace of the orthogonalised U_{IJ} tensor.

Atom	**x**	**y**	**z**	**$U_{(eq)}$**
C9	1088(4)	-102(3)	2016(3)	89.5(19)
C6	-88(4)	902(3)	2355(2)	60.9(13)
C7	329(5)	891(3)	1819(3)	86.0(19)
C8	915(4)	385(4)	1650(3)	93(2)
Cl2	1084.4(10)	1439.7(8)	5635.4(6)	84.9(5)
Cl1	-1041.4(8)	757.1(6)	5462.9(5)	61.1(3)
Cl3	3568(2)	2002.8(16)	846.5(14)	189.7(14)
Cl4	3601(3)	3169(2)	1305(2)	248(2)
C29	2744(5)	2570(3)	1074(3)	105(2)
Cl5	2020(10)	2170(12)	1483(10)	480(20)
Cl6	2170(7)	2585(6)	1680(5)	235(7)

Table 13.2. Anisotropic displacement parameters ($Å^2 \times 10^3$). The anisotropic displacement factor exponent takes the form: $-2\pi^2[h^2a^{*2}U_{11}+2hka^*b^*U_{12}+\ldots]$.

Atom	U_{11}	U_{22}	U_{33}	U_{23}	U_{13}	U_{12}
Pd1	44.7(3)	40.6(3)	42.2(3)	0.56(13)	2.21(13)	-7.08(12)
C17	46(2)	50(2)	40(2)	-0.6(18)	3.6(18)	-16.4(19)
C18	57(3)	56(3)	64(3)	-5(2)	7(2)	-10(2)
C26	47(2)	68(3)	93(4)	30(3)	-10(2)	-2(2)
C11	93(4)	70(3)	53(3)	-5(3)	-7(3)	14(3)
C22	45(2)	64(3)	54(3)	10(2)	-3(2)	-14(2)
C23	58(3)	54(3)	97(4)	13(3)	12(3)	-6(2)
C21	47(2)	85(4)	78(4)	4(3)	-9(2)	-13(2)
C19	67(3)	58(3)	90(4)	-4(3)	15(3)	-23(3)
C20	53(3)	82(4)	87(4)	-4(3)	4(3)	-24(3)
C27	83(4)	133(6)	112(5)	64(5)	-25(4)	-9(4)
C24	98(4)	72(4)	189(9)	-33(5)	17(5)	12(4)
C12	145(6)	79(5)	113(6)	-3(4)	3(5)	6(4)
C28	159(6)	68(4)	117(6)	15(4)	31(5)	2(4)
C14	202(8)	80(5)	77(5)	-10(4)	-6(5)	63(6)
C13	79(4)	125(6)	103(5)	-20(5)	-10(4)	30(4)
C25	110(5)	164(8)	133(7)	50(6)	3(5)	36(6)
C16	323(16)	64(5)	142(10)	13(6)	48(9)	7(8)
C15	252(12)	201(11)	146(9)	-32(8)	-74(10)	147(10)
N1	39.1(16)	44.4(19)	43(2)	5.3(16)	1.8(15)	-5.2(14)
N2	39.9(16)	43.3(19)	47(2)	-0.2(16)	1.9(14)	-4.2(14)
N3	52(2)	50(2)	50(2)	-6.4(18)	-0.7(16)	-9.9(16)
C1	39.7(19)	39(2)	49(3)	2.1(18)	1.0(19)	-0.8(16)
C2	36.9(19)	44(2)	40(2)	-5.6(19)	-4.0(17)	1.2(16)
C5	52(2)	65(3)	45(3)	-13(2)	-8.1(19)	-4(2)
C3	52(2)	63(3)	61(3)	-3(2)	0(2)	-19(2)
C10	76(3)	72(3)	57(3)	-21(3)	-7(3)	12(3)
C4	60(3)	69(3)	69(3)	-15(3)	-3(2)	-24(2)
C9	93(4)	105(5)	70(4)	-30(4)	-5(3)	33(4)
C6	64(3)	72(3)	47(3)	-10(2)	-5(2)	-1(2)
C7	114(5)	95(5)	48(3)	3(3)	8(3)	10(4)
C8	103(4)	128(6)	47(3)	-13(4)	10(3)	13(4)
Cl2	93.4(9)	109.5(12)	51.8(8)	-12.2(7)	-1.9(6)	-48.4(8)
Cl1	58.0(6)	64.5(7)	60.9(7)	1.6(6)	17.6(5)	-8.3(5)
Cl3	228(3)	179(3)	162(2)	13(2)	-4(2)	116(2)
Cl4	245(4)	233(4)	265(5)	-33(3)	-124(4)	18(3)
C29	106(5)	103(5)	104(5)	-2(4)	-23(4)	44(4)
Cl5	142(7)	810(40)	490(30)	520(30)	22(10)	-34(14)
Cl6	163(8)	344(13)	198(7)	171(8)	83(6)	165(10)

Table 13.3. Bond lengths.

Atom	Atom	Length (Å)	Atom	Atom	Length (Å)
Pd1	N2	2.007(3)	C14	C16	1.538(13)
Pd1	N1	2.073(3)	N1	C1	1.276(5)
Pd1	Cl2	2.2583(13)	N2	C2	1.325(5)
Pd1	Cl1	2.2731(11)	N2	C3	1.371(5)
C17	C22	1.385(6)	N3	C2	1.351(5)
C17	C18	1.424(6)	N3	C4	1.363(6)
C17	N1	1.440(5)	N3	C5	1.453(6)
C18	C19	1.402(6)	C1	C2	1.436(5)
C18	C23	1.485(7)	C5	C10	1.388(7)
C26	C27	1.507(8)	C5	C6	1.401(7)
C26	C28	1.516(9)	C3	C4	1.345(7)
C26	C22	1.522(7)	C10	C9	1.381(8)
C11	C6	1.509(7)	C9	C8	1.362(9)
C11	C12	1.534(9)	C6	C7	1.381(9)
C11	C13	1.543(8)	C7	C8	1.394(9)
C22	C21	1.401(6)	Cl3	C29	1.730(7)
C23	C24	1.504(8)	Cl4	C29	1.808(8)
C23	C25	1.526(10)	Cl4	Cl6	2.474(12)
C21	C20	1.371(8)	C29	Cl5	1.616(14)
C19	C20	1.377(7)	C29	Cl6	1.622(12)
C14	C15	1.491(13)	Cl5	Cl6	1.01(4)
C14	C10	1.501(9)			

Table 13.4. Bond angles.

Atom	Atom	Atom	Angle (˚)	Atom	Atom	Atom	Angle (˚)
N2	Pd1	N1	80.00(13)	C2	N2	Pd1	112.6(2)
N2	Pd1	Cl2	175.00(9)	C3	N2	Pd1	140.3(3)
N1	Pd1	Cl2	95.04(10)	C2	N3	C4	106.4(4)
N2	Pd1	Cl1	92.71(9)	C2	N3	C5	124.9(3)
N1	Pd1	Cl1	172.61(10)	C4	N3	C5	128.7(4)
Cl2	Pd1	Cl1	92.26(5)	N1	C1	C2	116.3(4)
C22	C17	C18	122.9(4)	N2	C2	N3	110.2(3)
C22	C17	N1	118.8(4)	N2	C2	C1	118.0(4)
C18	C17	N1	118.3(4)	N3	C2	C1	131.8(4)
C19	C18	C17	115.6(4)	C10	C5	C6	124.0(5)
C19	C18	C23	122.1(4)	C10	C5	N3	118.5(5)
C17	C18	C23	122.3(4)	C6	C5	N3	117.5(4)
C27	C26	C28	110.6(5)	C4	C3	N2	107.9(4)
C27	C26	C22	113.6(5)	C9	C10	C5	116.1(5)
C28	C26	C22	112.5(5)	C9	C10	C14	122.2(5)
C6	C11	C12	113.2(5)	C5	C10	C14	121.6(5)
C6	C11	C13	109.9(5)	C3	C4	N3	108.3(4)
C12	C11	C13	109.0(5)	C8	C9	C10	122.4(5)
C17	C22	C21	118.0(4)	C7	C6	C5	116.9(5)
C17	C22	C26	121.5(4)	C7	C6	C11	120.5(6)
C21	C22	C26	120.5(4)	C5	C6	C11	122.6(5)
C18	C23	C24	112.9(5)	C6	C7	C8	120.5(6)
C18	C23	C25	111.0(5)	C9	C8	C7	120.1(6)
C24	C23	C25	109.7(6)	C29	Cl4	Cl6	40.9(4)
C20	C21	C22	120.8(5)	Cl5	C29	Cl6	36.5(13)
C20	C19	C18	122.2(5)	Cl5	C29	Cl3	102.6(9)
C21	C20	C19	120.3(4)	Cl6	C29	Cl3	126.8(5)
C15	C14	C10	112.6(9)	Cl5	C29	Cl4	125.8(12)
C15	C14	C16	110.6(8)	Cl6	C29	Cl4	92.1(7)
C10	C14	C16	109.7(7)	Cl3	C29	Cl4	99.1(4)
C1	N1	C17	118.5(3)	Cl6	Cl5	C29	72.1(12)
C1	N1	Pd1	113.2(3)	Cl5	Cl6	C29	71.4(12)
C17	N1	Pd1	128.4(3)	Cl5	Cl6	Cl4	115.5(12)
C2	N2	C3	107.1(4)	C29	Cl6	Cl4	46.9(4)

Table 13.5. Hydrogen atom coordinates (Å×10^4) and isotropic displacement parameters (Å^2×10^3).

Atom	x	y	z	$U_{(eq)}$
H26	2306	368	4659	83
H11	-834	1416	2931	86
H23	860	2277	4232	84
H21	4551	1220	4670	84
H19	3293	2894	4300	86
H20	4683	2294	4477	89
H27A	3391	-215	5221	131
H27B	3195	449	5495	131
H27C	4164	327	5153	131
H24A	755	3373	4455	143
H24B	1901	3399	4495	143
H24C	1303	2983	4925	143
H12A	208	2162	2504	135
H12B	-877	2401	2463	135
H12C	-373	2092	1932	135
H28A	3295	-388	4219	138
H28B	4050	141	4059	138
H28C	2993	153	3798	138
H14	784	-515	3344	144
H13A	-2043	898	2378	123
H13B	-1744	1318	1856	123
H13C	-2248	1627	2388	123
H25A	782	2977	3479	162
H25B	1365	2367	3311	162
H25C	1930	2992	3455	162
H16A	-499	-1005	2862	211
H16B	196	-1534	3097	211
H16C	255	-1334	2455	211
H15A	2377	-585	3023	240
H15B	2029	-1053	2546	240
H15C	1971	-1253	3188	240
H1	1560	1064	3492	51
H3	-1669	201	4337	70
H4	-1551	-42	3226	79
H9	1499	-443	1891	107
H7	214	1237	1564	103
H8	1198	372	1276	111

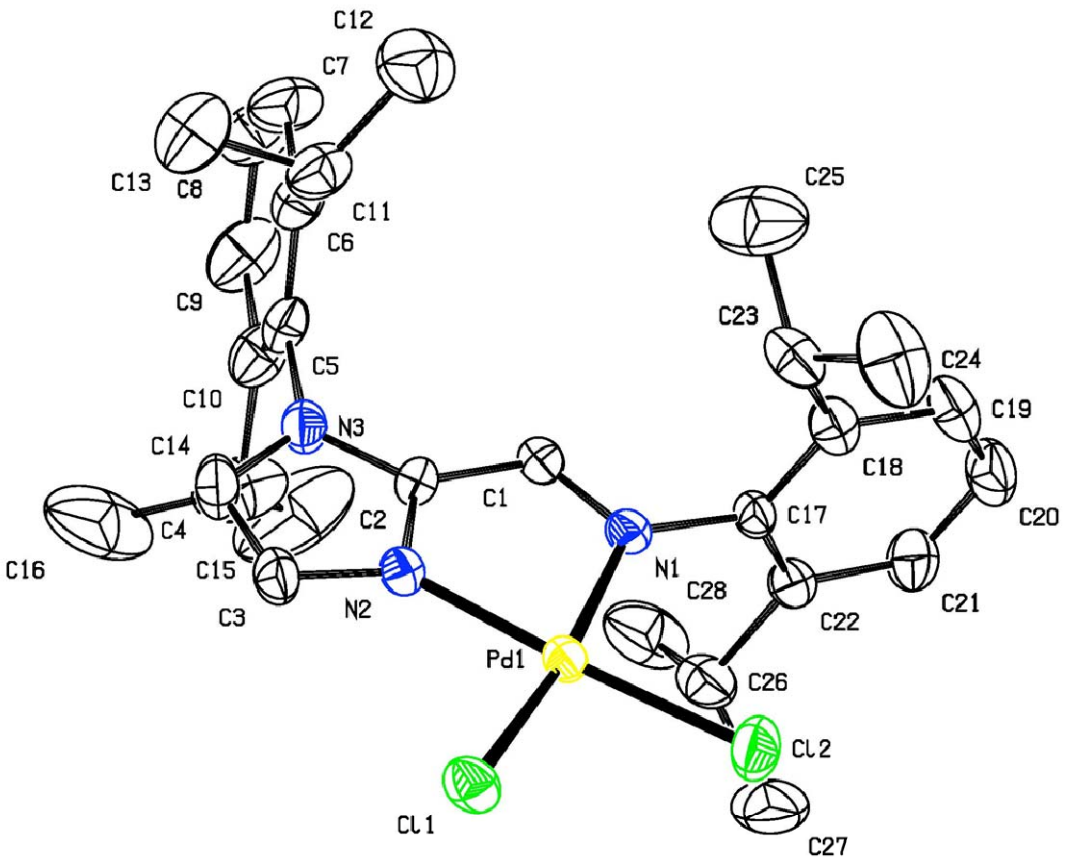

Figure 13.44. X-ray structure of **4b**

2. X-ray data of complex (4h)

Table 13.6. Fractional atomic coordinates ($\times 10^4$) and equivalent isotropic displacement parameters ($Å^2 \times 10^3$). U_{eq} is defined as 1/3 of the trace of the orthogonalised U_{IJ} tensor.

Atom	x	y	z	$U_{(eq)}$
Pd1	7161.8(2)	1294.17(15)	5554.58(15)	19.97(8)
Cl1	8068.5(7)	2417.9(6)	6744.1(5)	30.41(19)
Cl2	6322.4(9)	2835.3(6)	4715.2(6)	43.6(3)
N1	6394(2)	12.3(17)	4604.5(16)	18.5(5)
N2	8064(2)	-19.3(17)	6294.9(16)	21.0(5)
N3	8586(2)	-1757.5(18)	6337.0(17)	19.9(5)
C17	5390(3)	107(2)	3684.2(19)	19.1(6)
C4	9312(3)	-1319(2)	7153(2)	25.5(7)
C2	7826(3)	-946(2)	5821(2)	20.3(6)
C23	3925(3)	-825(2)	2262(2)	24.9(7)
C5	8695(3)	-2845(2)	6044(2)	20.8(6)
C18	4402(3)	659(2)	3665(2)	22.2(7)
C9	8274(3)	-4790(2)	5834(2)	24.4(7)
C25	5751(3)	827(2)	3198(2)	23.2(7)
C24	2948(3)	-268(2)	2245(2)	26.0(7)
C11	9894(3)	-1896(2)	5588(2)	31.3(8)
C26	4959(3)	-1024(2)	3214(2)	23.3(7)
C20	3761(3)	1602(2)	2265(2)	26.3(7)
C19	3385(3)	856(2)	2724(2)	25.1(7)
C21	4722(3)	1022(2)	2261(2)	26.3(7)
C6	9334(3)	-2906(2)	5696(2)	25.2(7)
C3	8982(3)	-238(2)	7118(2)	24.1(7)
C1	6892(3)	-935(2)	4927(2)	21.2(6)
C10	8140(3)	-3757(2)	6109(2)	20.6(6)
C14	7427(3)	-3676(2)	6471(3)	35.0(9)
C7	9434(3)	-3950(2)	5429(3)	34.9(9)
C22	4283(3)	-99(2)	1788(2)	31.2(8)
C8	8907(3)	-4880(2)	5494(2)	32.0(8)
C16	8041(5)	-4172(5)	7360(3)	85.6(18)
C12	9259(4)	-1577(3)	4636(3)	45.7(10)
C13	11171(3)	-2077(3)	5992(3)	40.5(9)
C15	6260(4)	-4229(5)	5853(4)	85.1(18)

Table 13.7. Anisotropic displacement parameters ($Å^2 \times 10^3$). The anisotropic displacement factor exponent takes the form: $-2\pi^2[h^2a^{*2}U_{11}+2hka^*b^*U_{12}+\ldots]$.

Atom	U_{11}	U_{22}	U_{33}	U_{23}	U_{13}	U_{12}
Pd1	21.94(14)	10.44(11)	21.65(14)	-1.75(8)	9.10(11)	-1.46(8)
Cl1	35.9(5)	17.7(3)	25.7(4)	-6.8(3)	10.8(4)	-7.6(3)
Cl2	57.8(6)	11.4(3)	29.4(5)	1.0(3)	6.4(5)	1.1(3)
N1	18.4(13)	12.9(10)	22.2(14)	-3.1(9)	10.5(12)	-1.5(9)
N2	21.2(14)	14.4(11)	24.7(15)	-3.8(10)	11.6(13)	-2(1)
N3	18.9(14)	14.8(11)	23.1(14)	-0.1(10)	10.4(12)	1.6(9)
C17	20.6(16)	13.4(12)	18.8(15)	-1.2(11)	8.8(14)	-0.5(11)
C4	22.1(17)	23.4(15)	23.8(17)	2.7(12)	9.1(15)	5.1(12)
C2	21.6(17)	11.9(11)	28.0(18)	-1.8(11)	14.6(15)	-0.1(11)
C23	26.5(18)	18.7(14)	22.4(18)	-7.4(12)	9.9(15)	-0.7(12)
C5	20.9(17)	15.8(13)	22.7(17)	0.8(11)	10.9(15)	6.0(11)
C18	27.2(18)	14.2(13)	25.4(18)	-0.4(11)	15.2(15)	1.8(11)
C9	25.9(18)	19.1(14)	24.9(17)	0.6(12)	12.7(15)	0.7(12)
C25	25.2(18)	19.2(13)	26.8(18)	-0.5(12)	15.9(16)	-1.2(12)
C24	22.3(18)	22.9(14)	24.0(18)	-0.3(12)	8.1(15)	-2.7(12)
C11	39(2)	23.7(15)	43(2)	-0.9(14)	30(2)	-0.4(14)
C26	23.2(17)	15.0(13)	25.7(18)	-4.9(12)	10.6(15)	0.3(11)
C20	29.7(19)	21.8(14)	22.1(17)	2.6(12)	11.7(15)	3.3(13)
C19	21.5(17)	19.4(13)	33(2)	-0.6(13)	15.0(16)	2.1(12)
C21	28.3(19)	24.9(14)	25.3(18)	1.3(13)	15.2(16)	-3.3(13)
C6	23.7(18)	20.3(14)	30.6(19)	-2.5(12)	15.1(16)	-0.6(12)
C3	20.6(17)	22.0(14)	24.0(17)	-4.3(12)	9.6(15)	-0.5(12)
C1	22.3(17)	14.9(12)	23.6(17)	-3.7(11)	11.6(15)	-2.0(12)
C10	18.1(16)	18.1(13)	20.4(16)	-0.2(11)	8.1(13)	1.7(11)
C14	45(2)	22.3(15)	57(3)	-4.3(15)	41(2)	-0.5(14)
C7	47(2)	28.8(16)	46(2)	-7.5(15)	37(2)	-2.0(15)
C22	35(2)	30.9(16)	24.6(19)	-4.9(14)	15.0(17)	0.1(14)
C8	43(2)	18.8(14)	42(2)	-8.1(14)	29(2)	0.6(14)
C16	108(5)	125(4)	65(4)	23(3)	73(4)	31(4)
C12	43(3)	41.0(19)	47(3)	13.6(18)	22(2)	-3.3(18)
C13	32(2)	45(2)	40(2)	6.5(17)	18(2)	-4.0(16)
C15	52(3)	118(4)	110(5)	-42(4)	61(4)	-28(3)

Table 13.8. Bond lengths.

Atom	Atom	Length (Å)	Atom	Atom	Length (Å)
Pd1	Cl1	2.2695(8)	C5	C6	1.391(4)
Pd1	Cl2	2.2721(8)	C5	C10	1.396(4)
Pd1	N1	2.120(2)	C18	C19	1.525(4)
Pd1	N2	2.002(2)	C9	C10	1.397(4)
N1	C17	1.482(4)	C9	C8	1.373(4)
N1	C1	1.291(3)	C25	C21	1.526(4)
N2	C2	1.340(3)	C24	C19	1.539(4)
N2	C3	1.356(4)	C11	C6	1.527(4)
N3	C4	1.367(4)	C11	C12	1.515(5)
N3	C2	1.360(4)	C11	C13	1.528(5)
N3	C5	1.458(3)	C20	C19	1.535(4)
C17	C18	1.535(4)	C20	C21	1.537(4)
C17	C25	1.542(4)	C21	C22	1.532(4)
C17	C26	1.541(4)	C6	C7	1.386(4)
C4	C3	1.367(4)	C10	C14	1.514(4)
C2	C1	1.421(4)	C14	C16	1.490(6)
C23	C24	1.525(4)	C14	C15	1.525(6)
C23	C26	1.545(4)	C7	C8	1.389(4)
C23	C22	1.525(4)			

Table 13.9. Bond angles.

Atom	Atom	Atom	Angle (˚)	Atom	Atom	Atom	Angle (˚)
Cl1	Pd1	Cl2	88.45(3)	C10	C5	N3	118.7(3)
N1	Pd1	Cl1	169.79(6)	C19	C18	C17	109.9(2)
N1	Pd1	Cl2	101.33(7)	C8	C9	C10	120.4(3)
N2	Pd1	Cl1	90.60(7)	C21	C25	C17	110.0(3)
N2	Pd1	Cl2	173.25(7)	C23	C24	C19	108.3(2)
N2	Pd1	N1	80.04(9)	C6	C11	C13	112.5(3)
C17	N1	Pd1	127.52(16)	C12	C11	C6	110.8(3)
C1	N1	Pd1	111.5(2)	C12	C11	C13	110.7(3)
C1	N1	C17	121.0(2)	C17	C26	C23	109.1(2)
C2	N2	Pd1	112.1(2)	C19	C20	C21	109.6(2)
C2	N2	C3	107.7(2)	C18	C19	C24	109.6(2)
C3	N2	Pd1	139.08(19)	C18	C19	C20	109.5(3)
C4	N3	C5	126.2(2)	C20	C19	C24	109.7(3)
C2	N3	C4	107.5(2)	C25	C21	C20	109.3(3)
C2	N3	C5	125.8(3)	C25	C21	C22	109.5(2)
N1	C17	C18	108.5(2)	C22	C21	C20	109.4(3)
N1	C17	C25	107.8(2)	C5	C6	C11	123.4(3)
N1	C17	C26	113.5(2)	C7	C6	C5	116.6(3)
C18	C17	C25	110.8(2)	C7	C6	C11	119.9(3)
C18	C17	C26	108.0(2)	N2	C3	C4	108.6(3)
C26	C17	C25	108.3(2)	N1	C1	C2	116.8(2)
C3	C4	N3	107.1(3)	C5	C10	C9	117.3(3)
N2	C2	N3	109.2(3)	C5	C10	C14	123.2(2)
N2	C2	C1	118.9(2)	C9	C10	C14	119.5(2)
N3	C2	C1	131.9(3)	C10	C14	C15	110.3(3)
C24	C23	C26	110.0(3)	C16	C14	C10	111.2(3)
C24	C23	C22	110.0(2)	C16	C14	C15	111.0(4)
C22	C23	C26	110.3(3)	C6	C7	C8	121.4(3)
C6	C5	N3	117.7(2)	C23	C22	C21	109.0(2)
C6	C5	C10	123.6(2)	C9	C8	C7	120.5(3)

Table 13.10. Hydrogen atom coordinates ($Å \times 10^4$) and isotropic displacement parameters ($Å^2 \times 10^3$).

Atom	x	y	z	$U_{(eq)}$
H45	7298(4)	344(3)	333(3)	83.0(18)
H30	4145(5)	1425(3)	2060(2)	85.1(18)
H38	5833(4)	2288(3)	755(3)	84.9(18)
H43	9535(4)	1228(3)	346(3)	85.0(19)
H41	8292(4)	2883(3)	692(3)	86.1(19)
H42	9657(4)	2290(3)	521(3)	89.4(19)
H47a	8220(30)	490(20)	-487(5)	154(4)
H47b	9167(7)	300(30)	-153(10)	154(4)
H47c	8330(40)	-198(8)	-249(14)	154(4)
H40a	6890(30)	3403(17)	520(20)	178(5)
H40b	6350(50)	3005(4)	60(4)	178(5)
H40c	5750(30)	3357(19)	530(20)	178(5)
H31a	4110(20)	2395(5)	2550(30)	174(4)
H31b	4660(50)	2084(11)	3070(5)	174(4)
H31c	5200(20)	2165(14)	2480(20)	174(4)
H46a	9040(17)	180(20)	951(17)	165(4)
H46b	7970(30)	140(20)	1197(8)	165(4)
H46c	8360(40)	-383(4)	775(10)	165(4)
H33	5766(8)	-510(4)	1651(3)	149(4)
H32a	3259(8)	1260(30)	3145(4)	154(4)
H32b	2767(15)	1647(15)	2650(20)	154(4)
H32c	2930(20)	918(17)	2580(20)	154(4)
H39a	6350(60)	2368(5)	1688(4)	198(5)
H39b	6950(30)	2980(30)	1547(9)	198(5)
H39c	5810(30)	2990(30)	1525(8)	198(5)
H34a	5210(60)	-1530(20)	1910(30)	252(8)
H34b	5210(60)	-1330(40)	2553(17)	252(8)
H34c	4472(10)	-1019(16)	2120(50)	252(8)
H35a	7070(30)	-1070(60)	2442(18)	300(10)
H35b	7040(30)	-1220(40)	1790(40)	300(10)
H35c	7386(11)	-558(14)	2000(50)	300(10)
H54	6531(3)	1055.8(19)	1509(2)	51.5(12)
H52	3307(3)	172(2)	710(2)	70.2(15)
H53	3413(4)	-44(3)	1729(2)	78.3(17)
H58	6487(5)	-435(4)	3105(3)	106(2)
H60	5232(5)	1226(4)	3430(3)	103(2)
H59	6170(5)	381(4)	3716(3)	110(2)
H65	2364(5)	2721(3)	758(3)	118(3)

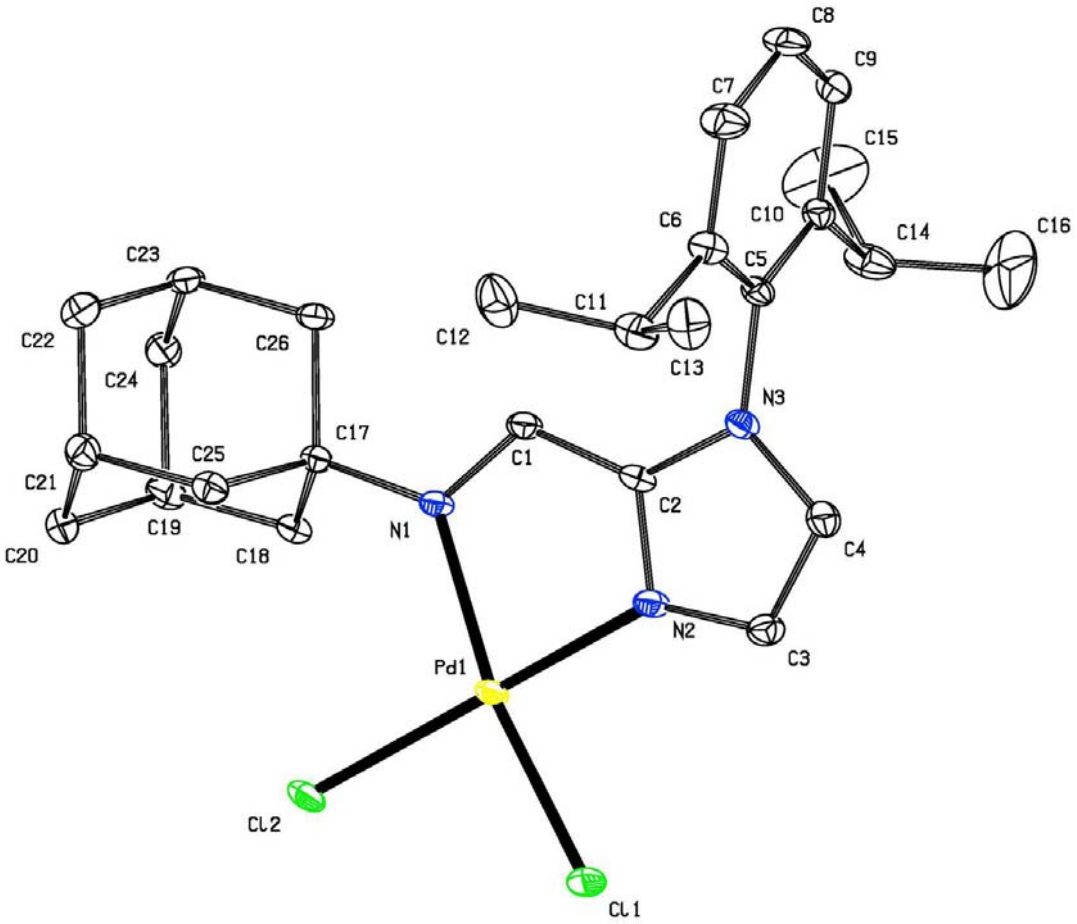

Figure 13.45. X-ray structure of **4h**.

APPENDIX G

RESEARCH OUTPUT, PUBLICATION PART I

Journal of Organometallic Chemistry 752 (2014) 161–170

Contents lists available at ScienceDirect

Journal of Organometallic Chemistry

journal homepage: www.elsevier.com/locate/jorganchem

Air-stable imidazole-imine palladium complexes for Suzuki–Miyaura coupling: Toward an efficient, green synthesis of biaryl compounds

Jadsada Ratniyom, Thanawat Chaiprasert, Songyos Pramjit, Sirilata Yotphan, Preeyanuch Sangtrirutnugul, Pailin Srisuratsiri, Palangpon Kongsaeree, Supavadee Kiatisevi*

Center for Alternative Energy, Department of Chemistry and Center of Excellence for Innovation in Chemistry (PERCH-CIC), Faculty of Science, Mahidol University, 272 Rama 6 Road, Ratchthewee, Bangkok, Thailand

ARTICLE INFO

Article history:
Received 18 October 2013
Received in revised form
29 November 2013
Accepted 5 December 2013

Keywords:
Imidazole-imine ligand
Air-stable palladium complex
Suzuki–Miyaura cross-coupling reaction

ABSTRACT

New imidazole-imine ligands have been developed for the air and moisture stable Pd-catalyzed Suzuki–Miyaura cross-coupling reaction. Under optimized reaction conditions, coupling products from a wide range of aryl halides and aryl boronic acids were obtained in excellent yields.

1. Introduction

Many important reactions for carbon–carbon bond formation have been continuously developed over the past four decades. Among these, Suzuki–Miyaura cross-coupling reaction is one of the most effective methods for constructing biaryl structures which are wide-spread in many naturally occurring bioactive products [1–4]. This reaction has two significant advantages over other cross-coupling processes. Aryl boronic acid reactants are readily available and react under mild conditions. In addition, the inorganic by-products are usually easy to remove. However, several existing Suzuki–Miyaura cross-coupling methods generally employ palladium complexes supported by phosphine ligands [5–7], which are often sensitive to air oxidation and require air-sensitive handling. This oxygen sensitivity of catalyst is one of the crucial limitations that hamper the development of practical biaryl synthesis. Therefore, air- and moisture-stable ligands, which are easily prepared from inexpensive, commercially available starting materials, are needed for the improvement of Pd-catalyzed cross coupling reaction.

Our effort to develop an improved Suzuki reaction protocol has centered on the search for a catalytic system consisting of rigid phosphine-free ligands. The ligands with nitrogen-based frameworks such as, N-heterocyclic carbenes [8–12], nitrogen-acyclic carbenes [13], cyclometalated imine [14], diazabutadiene [15], and guanidines [16] have been reported. Despite the achievements of modest to high yields of products, the systems require high reaction temperatures under an inert atmosphere. In our studies, we selected the new imidazole-imine backbone due to its structural rigidity, strong σ-donating property and low-cost. In addition, compared to phosphine ligands, the imidazole-imine ligands are easier to prepare and more resistant to air. Substituents on the nitrogen atom of the imine moiety also play important roles in tuning steric and electronic properties of the molecule. Furthermore, no catalytic study of transition metal complexes supported by the bidentate, imidazole-imine based ligands has previously been investigated. Only structural, spectroscopic and water relaxivity properties of manganese(II) complexed with tetradentate imidazole-imine ligands have been reported [17].

Herein, we wish to report the synthesis of a series of new, air- and moisture-stable palladium complexes with imine ligands based on *N*-arylated imidazoles (Scheme 1) and their application in Suzuki–Miyaura cross-coupling reactions.

* Corresponding author. Tel.: +66 2 201 5131; fax: +66 2 354 7151.
E-mail address: supavadee.mon@mahidol.ac.th (S. Kiatisevi).

0022-328X/$ – see front matter © 2013 Elsevier B.V. All rights reserved.
http://dx.doi.org/10.1016/j.jorganchem.2013.12.015

2. Results and discussion

2.1. Synthesis and X-ray crystal structure

As an access to imidazole-imine Pd complexes **3**, compound **1** was first prepared from a four-component condensation of the corresponding amine with formaldehyde, ammonium chloride, and glyoxal [18]. The 1-(2,6-diisopropylphenyl)-1*H*-imidazole compound was deprotonated by *n*-butyl lithium at −30 °C, and reacted with *N*,*N*-dimethylformamide to afford **1** in a quantitative yield. Compound **2** was obtained via the condensation of **1** with corresponding primary amines and used, without further purifications, to react with (COD)$PdCl_2$ to afford complexes **3a**–**3h** in good yields (Scheme 1).

The structural characterization of the ligands and complexes was carried out by ^1H, ^{13}C NMR spectroscopy, elemental analysis and HRMS. The ^1H NMR spectrum of the starting material **1** showed a signal of the aldehyde proton at 9.80 ppm and two singlet signals of imidazole protons at 7.51 ppm and 7.11 ppm which can be ascribed to H-4 and H-5, respectively. The NMR data are consistent with those of similar compounds described in the literature [18,19]. These imidazole protons also gave ^3J cross peaks with C-2 on the basis of HMBC correlation. In addition, only H-5 exhibited HMBC cross peaks with C-7, leaving the position of this proton at C-5. This result was confirmed by the signal enhancement of H-5 that was observed upon irradiation of methyl protons (H-12 and H-13) in an NOEDIFF experiment. According to the ^1H-COSY NMR spectral data, H-4 and H-5 appeared as distinct singlet signals and no cross-peak signal was found, suggesting no correlation between these two protons. However, the NOE enhancement of H-4 was detected upon irradiation of H-5 as shown in Fig. 1. Based on the HMBC and NOEDIFF results, H-4 and H-5 were attached on the neighboring carbon atoms and could thus be assigned as vicinal protons.

The structures of the imidazole-imine palladium complexes **3a**–**h** which were readily prepared from the reaction of ligands with (COD)$PdCl_2$ in chloroform also exhibited some characteristic ^1H NMR data and multiplicity of the two protons on the imidazole ring. Interestingly, their equivalent resonances were observed as doublet signals with low coupling constants ranging from 1.2 Hz to 1.6 Hz. For instance, the protons, H-4 and H-5, of complex **3h** appeared at 7.79 ppm and 7.07 ppm (J = 1.6 Hz), respectively, as shown in Fig. 2. Similarly, in case of the free imine ligand **2h**, the protons also resonated as the doublet signals at 7.33 ppm and 6.94 ppm (J = 0.8 Hz) (see Supporting information for the NMR data of the isolated ligand **2h**). The appearance of a cross-peak signal of complex **3h** in a ^1H-COSY spectrum indicated the correlation between these imidazole protons. The outcome of this study was also supported by the NOEDIFF results. Inspection of the NOEDIFF spectrum revealed the presence of NOE contacts which allow us to define the spatial relationship between the ligand protons, H-4 and H-5, as well as between the imine and H-16 methylene protons (Fig. 1). Moreover, the ^1H NMR data was also used to confirm the coordination of complex **3h**. The upfield shift of the characteristic singlet signal of the imine proton, H-6, with respect to the free ligand ($\delta_{coord} - \delta_{free} = -0.8$ ppm) was observed.

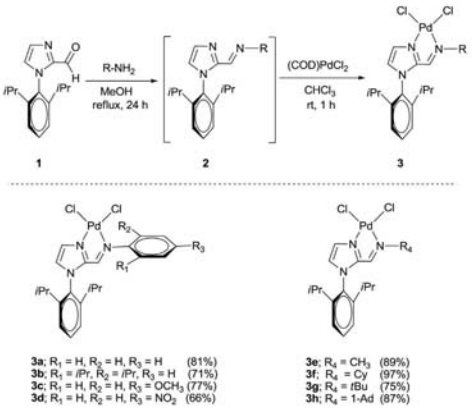

Scheme 1. Synthesis of imidazole-imine Pd complexes.

To further confirm the structure of the Pd complexes, crystals suitable for X-ray diffraction studies of **3b** and **3h** were obtained by slow diffusion of hexane into a chloroform solution. As shown in Figs. 3 and 4, the solid state of both palladium complexes revealed a distorted square planar geometry around Pd(II) center with the angle sum of approximately 360°. The imidazole-imine ligand coordinates to Pd(II) in a bidentate binding mode through imidazole and imine nitrogen atoms as expected. The closest C···C distances between isopropyl aryl substituents on imidazole and imine substituents (2,6-^{i}PrC_6H_3 and 1-adamantyl) are 3.993(13) Å (for **3b**) and 5.117(8) Å (for **3h**). The Pd–N1(imine) bond distances are slightly more than the expected range [20–22] and about 0.1 Å longer than those of Pd–N2(imidazole) [23]. All Pd–Cl bond lengths are similar and in the range of 2.26–2.27 Å, indicating comparable *trans* influence of imidazole and imine ligands. The N1–Pd–N2 bite angles of **3b** and **3h** are 80.00(13)° and 80.04(9)°, respectively (Table 1). Based on crystal data, 1-adamantyl substituent appears to be more sterically hindered than 2,6-^{i}PrC_6H_3, as evidenced by the unusually long Pd–N1 bond, larger N1–Pd–Cl2 angle of 101.33(7)° for **3h** [*cf.* 95.04(10)° for **3b**], and smaller Cl1–Pd–Cl2 angle of 88.45(3)° [*cf.* to 92.26(5)° for **3b**].

2.2. Suzuki–Miyaura cross-coupling catalyzed by imidazole-imine Pd complexes

To evaluate the catalytic activity of **3a**–**3h** for the palladium-catalyzed Suzuki–Miyaura cross-coupling, a reaction between phenyl boronic acid and *p*-bromoanisole was used as the model reaction at room temperature under aerobic conditions (Table 2). Interestingly, quantitative yields of the coupling product were obtained when catalysts **3b** and **3d** were used. However, compared to **3b**, palladium complexes of the more sterically hindered imine ligands **3g** and **3h** afforded only moderate product yields (entries 7 and 8). We also found that ligands **3e**–**h** which were prepared with the alkyl substituents tend to result in lower yields than those with the aromatic ones. Moreover, appropriated steric bulks at the imine moiety are crucial to achieve good catalytic activities, as very large substituents such as *tert*-butyl and 1-adamantyl only showed low activities. In comparison, the catalytic activity of palladium complexes containing our imidazole-imine ligands are superior to those with commercially available ligands including pyridine, phenanthroline, BINAP, and in the absence of ligand (Supporting information; Table S1).

Despite the fact that both catalysts **3b** and **3d** exhibited similar catalytic properties, we chose **3b** as the control catalyst for determining optimal conditions for palladium-catalyzed cross-coupling reaction of *p*-bromoanisole with phenyl boronic acid due to the more complicated preparation of **3d**. We then began to optimize reaction conditions by examining the catalyst loading and found that highly efficient catalysis could still be maintained even at

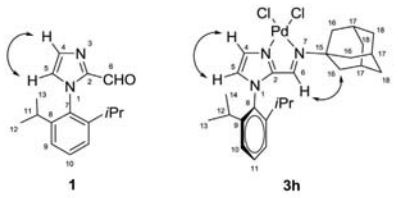

1 3h

Complex 3h	δ (ppm)
H-4	7.79
H-5	7.07
H-6	7.20
H-16	2.09

Fig. 1. Double arrows show the NOE contacts in aldehyde **1** and complex **3h**.

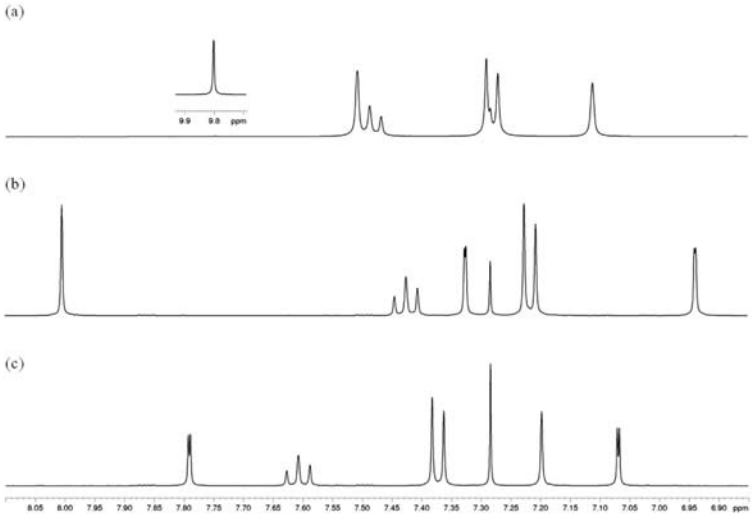

Fig. 2. ^{1}H NMR spectra of (a) aldehyde **1**; (b) ligand **2h** and; (c) complex **3h**.

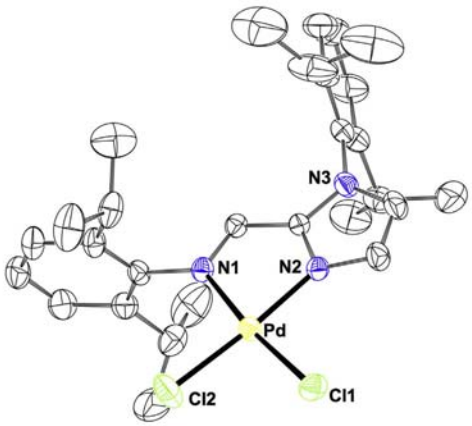

Fig. 3. ORTEP diagram of **3b** with 30% probability ellipsoids and partial labeling scheme. Hydrogen atoms and a molecule of $CHCl_3$ are omitted for clarity.

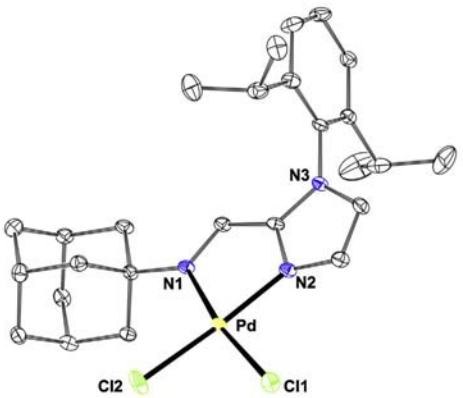

Fig. 4. ORTEP diagram of **3h** with 30% probability ellipsoids and partial labeling scheme. Hydrogen atoms are omitted for clarity.

Table 1
Selected bond lengths (Å) and bond angles (°) for **3b** and **3h**.

	Bond length (Å)			Bond angle (°)	
	3b	**3h**		**3b**	**3h**
Pd–N1	2.073(3)	2.120(2)	N1–Pd–N2	80.00(13)	80.04(9)
Pd–N2	2.007(3)	2.002(2)	Cl1–Pd–Cl2	92.26(5)	88.45(3)
Pd–Cl1	2.273(1)	2.270(1)	N1–Pd–Cl2	95.04(10)	101.33(7)
Pd–Cl2	2.258(1)	2.272(1)	N2–Pd–Cl1	92.71(9)	90.60(7)

catalyst loading as low as 0.15 mol% with a TON up to 666 (highest TON up to 12,000 with 0.001 mol % catalyst loading) (Table 3). Complex **3b** also exhibited higher efficiencies in terms of yields/TONs than the majority of those reported for the similar *N,N*-bidentate palladium catalysts with 4-$MeOC_6H_4Br$ as substrate. For example, the catalytic systems consisting of $Pd(OAc)_2$/hydrazone [24] and $Pd(OAc)_2$/guadinine [16] were reported to have TONs up to 44.5 and 180, respectively. Also, the procedure using pyridyltriazole ligands resulted in a TON up to 180 [25]. Another pyridyltriazole based catalytic system recently reported by some of us exhibited a comparable activity (yields up to 85% with 0.1 mol % catalyst loading and a TON up to 850) [26]. An additional experiment under ambient conditions was carried out by varying the reaction time. The quantitative yield of 4-methoxybiphenyl could be achieved with the shortest reaction time of 4 h (Supporting information; Table S2).

We also probed the effect of solvent and observed that aprotic solvents such as THF, DMF, acetonitrile, toluene, chloroform, acetone, and DMSO afforded low product yields in the range of 2–27%. On contrary, higher coupling product yields were obtained in methanol. Interestingly, although the coupling reaction in H_2O resulted in a low product yield, a small percentage of water in methanol has a beneficial effect on the reaction rate as found with other catalytic systems [27–29] (Supporting information; Tables S3 and S4). It was found that a 4:1 mixture of CH_3OH:H_2O at the *p*-bromoanisole concentration of 0.2 M provided the biaryl product in a quantitative yield. Next, we sought to determine which base offered the best result of the coupling reaction under the optimized conditions: 0.15 mol% of **3b** in the 4:1 CH_3OH:H_2O solvent. As a result, *p*-bromoanisole was successfully coupled with phenyl boronic acid in the highest product yield when K_2CO_3 was used as a base (Supporting information; Table S5).

Under the optimized reaction conditions, a wide variety of aryl halide substrates were highly reactive, generally giving the desired coupling products in good to quantitative yields (Table 4). The substrate scope was found to be remarkably broad, as the reaction tolerated both electron-donating and electron-withdrawing substituents. For example, with the exception of *ortho*-methoxy substituent, the electron-donating methoxy groups at *meta* and *para* positions gave the corresponding coupling products in quantitative yields (entries 2–5). Most aryl halides with an electron-withdrawing substituent resulted in excellent product yields *i.e.*,

Table 2
Ligand screening for Suzuki–Miyaura cross-coupling reaction between *p*-bromoanisole and phenyl boronic acid.[a]

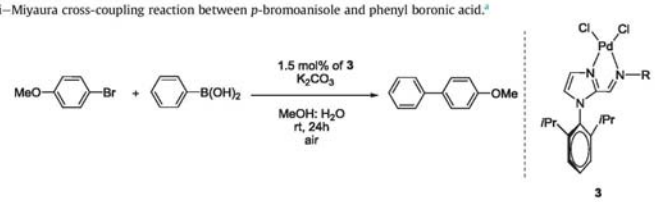

3

Entry	Complexes	R	Yield (%)[b]
1	**3a**		91
2	**3b**		>99
3	**3c**		82
4	**3d**		>99
5	**3e**		88
6	**3f**		83
7	**3g**		73
8	**3h**		69

[a] Reaction condition: 1.5 mol% of Pd catalyst, 0.5 mmol of *p*-bromoanisole, 0.6 mmol of phenyl boronic acid, 1.1 mmol of K_2CO_3, 2 mL of MeOH, 0.5 mL of H_2O, rt, 24 h. All reactions were carried out in air.
[b] The yield was determined by GC analysis using hexamethylbenzene as a calibrated internal standard.

Table 3
Catalytic activity of complex **3b** on the Suzuki–Miyaura cross-coupling reaction of *p*-bromoanisole with phenyl boronic acid.[a]

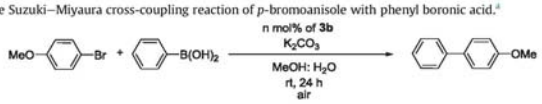

Entry	*n* mol%	Yield (%)[b]	TON
1	0.0001	0	0
2	0.001	12	12,000
3	0.01	85	8500
4	0.1	99	990
5	0.15	>99	666
6	0.2	>99	500
7	0.3	>99	333
8	0.4	>99	250
9	0.75	>99	133
10	1.5	>99	66
11	3	>99	33

[a] Reaction condition: 0.5 mmol of *p*-bromoanisole 0.6 mmol of phenyl boronic acid, 1.1 mmol of K_2CO_3, 2 mL of MeOH, 0.5 mL of H_2O, rt, 24 h.
[b] The yield was determined by GC analysis using hexamethylbenzene as a calibrated internal standard.

more than 90% (entries 6–11), except for *para*-fluoro (65%), hydroxyl (84%), and phenyl (86%) groups (entries 12–14). When heterocyclic halides were used as substrates, moderate yields of the coupling products were obtained (entries 15–17), presumably due to nitrogen coordination and subsequent inactivation of the palladium catalyst. Based on the results thus far, no significant effect on product yields was observed from varying aryl bromide substrates, suggesting relatively fast oxidative addition. Moreover, no reaction was observed when *p*-chloroanisole was used as a substrate (Data not shown).

In Table 5, C–C coupling between the electron-rich 4-methoxyphenyl boronic acid and bromobenzene gave products in high yields (entries 1–3). However, the yields decreased with the electron-withdrawing 4-acetylphenyl boronic acid substrate (entries 4 and 5). Furthermore, an electron-deficient acetyl substituent on aryl bromide afforded an increase in product yields, from 80% to 90% (entries 1 and 6). It seems that although electronic properties of aryl halides do not significantly affect the reaction rates, the presence of electron-withdrawing substituent on phenyl boronic acid apparently decreases product yields.

It should be noted that, formation of palladium black was not observed with catalyst **3b** during the course of the reactions. In order to elucidate whether Pd(0) nanoparticles are involved in the reaction, we have also carried out a mercury poisoning test with **3b**. A coupling reaction between *p*-bromoanisole and $PhB(OH)_2$ in the presence of excess Hg (Hg:Pd = 400:1) under the reaction conditions described for entry 2 (Table 4) showed a decrease of product yield (down to 33%). The drop in the coupling product yield implies that the cross-coupling reactions were catalyzed, to some extent, by heterogeneous Pd(0) nanoparticles [30,31]. Furthermore, a previous study on the catalytic activity of Pd(0) species in the Suzuki–Miyaura cross-coupling reaction has shown that O_2 can prevent Pd(0) nanoparticle aggregation [32], probably by inhibiting the formation of Pd–Pd bonds through the adsorption of O_2 [33,34]. This could be a reason why our catalytic system can operate in air.

3. Conclusion

In summary, an efficient, air-stable protocol for the palladium-catalyzed Suzuki–Miyaura cross-coupling reaction has been developed. The use of imidazole-imine supporting ligands offers substantial catalyst improvements with regard to air-stability and catalytic efficiency. The catalytic studies have also shown that our catalyst system is wide in substrate scope, uses low catalyst loading, and generates water-soluble by-products. These are consistent with characteristics of green chemistry.

4. Experimental

4.1. General information

All reagents were purchased from commercial sources and used without further purification. *n*-BuLi was titrated with diphenylacetic acid to confirm the correct concentration. The $(COD)PdCl_2$ was prepared following the literature procedure [35]. DMF was distilled from CaH_2, stored over 4 Å molecular sieves, and handled under argon atmosphere. Thin layer chromatography (TLC) was purchased on Merck silica gel 60 F_{254} aluminum sheets. Column chromatography was performed using Merck silica gel 60 (70–230 mesh.). NMR spectra were recorded on Bruker DPX-300 (300 MHz) and Bruker Ascend™ 400 (400 MHz) spectrometers. The chemical shifts (δ) for ^1H are given in ppm and referenced to the residual proton signal of the deuterated solvent. The chemical shifts (δ) for ^{13}C are referenced relative to the signal from the carbon of the deuterated solvent. The high resolution mass spectra were recorded on HR-TOF-MS Micromass model VQ-TOF2 spectrometer. The elemental analyses were performed by Perkin Elmer Elemental Analyzer 2400 CHN. Gas chromatography analysis was performed on Agilent Technologies 6890N with FID detector and HP-1 capillary column (polymethylsiloxane, 25 m, 0.32 mm, 0.17 μm film thickness). Gas chromatography-mass analysis was performed on Agilent Technologies 7890A with 5975C inert XL MSD with Triple-Axis detector and HP-5 capillary column (polydimethylsiloxane with 5% phenyl group, 20 m, 0.25 mm, 0.25 μm film thickness) using helium as a carrier gas.

4.2. X-ray crystallography

Crystallographic analyses of complexes **3b** and **3h** were carried out at the Mahidol crystallographic facility. Diffraction measurements were made on a 4 K Bruker SMART [36] CCD area detector diffractometer using graphite-monochromated Mo $K\alpha$ radiation ($\lambda = 0.71073$ Å). Crystals were mounted in paratone oil and held at room temperature during data collection. Cell constants and an orientation matrix for data collection were obtained from a least-square refinement using the measured positions of reflections in

Table 4
Study of substrate scopes for Suzuki–Miyaura cross-coupling reaction between aryl halides and phenyl boronic acid.[a]

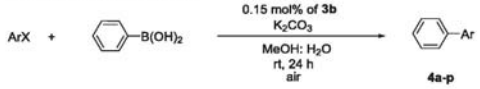

4a-p

Entry	ArX	Product	Yield[b] (%)
1		**4a**	95
2	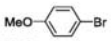	**4b**	>99[c]
3		**4c**	>99
4		**4d**	68
5	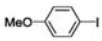	**4b**	95[c]
6	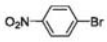	**4e**	92
7	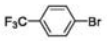	**4f**	>99
8	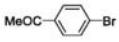	**4g**	>99
9	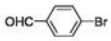	**4h**	91
10	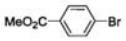	**4i**	97
11		**4j**	98
12	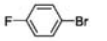	**4k**	65
13	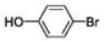	**4l**	84
14	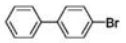	**4m**	86
15		**4n**	60[d]
16		**4o**	41[d]
17		**4p**	45[d]

[a] Reaction condition: 0.15 mol% of Pd catalysts, 0.5 mmol of aryl halide, 0.6 mmol of phenyl boronic acid, 1.1 mmol of K_2CO_3, 2 mL of MeOH, 0.5 mL of H_2O, rt, 24 h. All reactions were carried out in air.
[b] Isolated yield.
[c] GC yield.
[d] 1.5 mol% catalyst loading.

Table 5
Study of substrate scopes for Suzuki–Miyaura cross-coupling reaction between aryl halides and aryl boronic acids.[a]

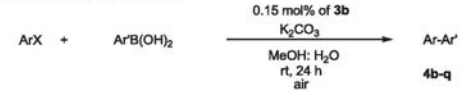

4b-q

Entry	ArX	Ar'B(OH)$_2$	Product	Yield[b] (%)
1		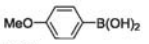	**4b**	80
2		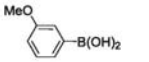	**4c**	75
3		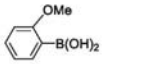	**4d**	85[c]
4		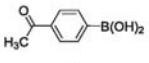	**4g**	64[c]
5	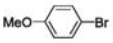	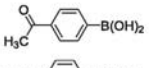	**4q**	68[c]
6	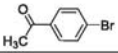	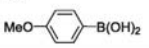	**4q**	90[c]

[a] Reaction condition: 0.15 mol% of Pd catalysts, 0.5 mmol of aryl halide, 0.6 mmol of phenyl boronic acid, 1.1 mmol of K_2CO_3, 2 mL of MeOH, 0.5 mL of H_2O, rt, 24 h. All reactions were carried out in air.
[b] Isolated yield.
[c] 1.5 mol% catalyst loading.

the range $0.998° < \theta < 28.4°$ (for **3b**) and $0.998° < \theta < 29.1°$ (for **3h**). The frame data were integrated by the program SAINT [37] and corrected for Lorentz and polarization effects. The structure was solved by the maXus crystallographic software package [38], using

Table 6
Crystal data for **3b** and **3h**.

	3b•$CHCl_3$	**3h**
Empirical formula	$C_{29}H_{37}Cl_5N_3Pd$	$C_{26}H_{35}Cl_2N_3Pd$
FW	711.27	566.87
Cryst color, habit	Orange, cube	Orange, cube
Cryst size (mm)	0.35 × 0.25 × 0.20	0.30 × 0.25 × 0.20
Cryst system	Orthorhombic	Monoclinic
Space group	*Pbca* (#61)	$P2_1/c$ (#14)
a (Å)	13.6508(2)	14.2165(6)
b (Å)	21.1682(4)	11.9991(3)
c (Å)	23.4645(4)	18.7543(7)
α (deg)	90.00	90.00
β (deg)	90.00	125.0801(14)
γ (deg)	90.00	90.00
Volume (Å^3)	6780.50(2)	2618.09(16)
θ range (deg)	0.998–26.4	0.998–29.1
Z	8	4
T/K	298	298
D_{calc} (g/cm^3)	1.392	1.438
μ (mm^{-1})	0.963	0.931
No. of reflns	6914	7035
No. of params refined	353	289
Refln/param ratio	19.6	24.3
Final residuals R_1[a]; wR_2[b]	0.0557; 0.1852	0.0478; 0.1126
Goodness of fit indicator[c]	1.331	0.987
Max. shift/error in final LS cycle	0.001	0.001

[a] $R = \Sigma||F_o| - |F_c||/\Sigma|F_o|$.
[b] $wR_2 = [\sum[w(F_o^2 - F_c^2)^2]/\sum[w(F_o^2)^2]]^{1/2}$, where $w = [\sigma^2(F_o^2) + (aP)^2 + bP]^{-1}$.
[c] GOF $= [\Sigma w(|F_o| - |F_c|)^2/(N_{obs} - N_{param})]^{1/2}$.

direct methods (SIR97) [39] and refined by full-matrix least-squares method on $(F_{obs})^2$ using the SHELXTL-PC V 6.12 software package [40] (Table 6).

X-ray quality crystals of **3b** and **3h** were grown by layer diffusion of hexane onto the $CHCl_3$ solution of the palladium complexes at room temperature.

Complex **3b** crystallizes in the orthorhombic *Pbca* space group with each asymmetric unit cell containing one molecules of **3b** and one distorted $CHCl_3$ molecule. The $CHCl_3$ molecule was modeled with Cl5 and Cl6 atoms each occupying a half-occupancy with no hydrogen. Large thermal ellipsoids were observed for isopropyl groups. All non-hydrogen atoms were refined anisotropically while the hydrogen atoms were placed in calculated positions and not refined.

Complex **3h** crystallized in the monoclinic $P2_1/c$ space group with each asymmetric unit containing one molecule of **3h**. Large thermal ellipsoids were observed for isopropyl groups. All non-hydrogen atoms were refined anisotropically while the hydrogen atoms were placed in calculated positions and not refined.

4.3. Synthesis of 1-(2,6-diisopropylphenyl)-1H-imidazole

The 1-(2,6-diisopropylphenyl)-1*H*-imidazole was prepared according to the literature procedure [18]. The crude product was purified by column chromatography (SiO_2, EtOAc). The NMR spectra agree with published data [18]. ^{1}H NMR (300 MHz, $CDCl_3$): δ 7.48 (s, 1H), 7.46 (t, J = 7.9 Hz, 1H), 7.28 (s, 1H), 7.27 (d, J = 7.4 Hz, 2H), 6.96 (s, 1H), 2.41 (sept, J = 6.9 Hz, 2H), 1.15 (d, J = 6.9 Hz, 12H). ^{13}C NMR (75 MHz, $CDCl_3$): δ = 146.5, 138.5, 132.8, 129.8, 129.3, 123.7, 121.5, 28.1, 24.4, 24.3. HRMS (ESI): calcd. for $C_{15}H_{20}N_2$ $[M + H]^+$ 229.1705; Found: 229.1727.

4.4. Synthesis of 1-(2,6-diisopropylphenyl)-1H-imidazole-2-carboxaldehyde (1)

In a 100 mL round-bottomed flask equipped with a magnetic stir bar was charged with 1-(2,6-diisopropylphenyl)-1*H*-imidazole (855 mg, 3.74 mmol, 1.0 equiv), closed with three-way, evacuated and backfilled with argon (this procedure was repeated three times). The dried THF (20 mL) was added by syringe then *n*-BuLi (1.17 M in hexane, 3.9 mL, 4.48 mmol, 1.2 equiv) was slowly added at −30 °C. The reaction mixture was allowed to warm to room temperature and stirred for 3 h. Dried DMF (0.45 mL, 5.61 mmol, 1.5 equiv) was added under argon atmosphere and continually stirred for 16 h. The saturated NH_4Cl solution was added to reaction flask and poured into the separatory funnel. The aqueous phase was extracted with CH_2Cl_2 (3 × 10 mL), washed with brine (1 × 10 mL) and dried with Na_2SO_4. The combined organic phase was concentrated under vacuum. The crude product was purified by column chromatography (SiO_2, CH_2Cl_2) to afford the pure product **1** (955 mg, 99%) as a white solid. ^{1}H NMR (400 MHz, $CDCl_3$): δ = 9.80 (s, 1H), 7.51 (s, 1H), 7.49 (t, J = 7.7 Hz, 1H), 7.28 (d, J = 7.7 Hz, 2H), 7.11 (br s, 1H), 2.21 (sept, J = 6.8 Hz, 2H), 1.12 (d, J = 6.8 Hz, 6H), 1.08 (d, J = 6.8 Hz, 6H). ^{13}C NMR (75 MHz, $CDCl_3$): δ = 180.2, 145.1, 144.6, 132.5, 132.0, 130.0, 127.4, 123.9, 28.3, 24.6, 23.3. HRMS (ESI): calcd. for $C_{16}H_{20}N_2O$ $[M + H]^+$ 257.1654, Found: 257.1631.

4.5. General procedure for the preparation of palladium complexes (3a–h)

In a 50 mL round-bottomed flask equipped with a magnetic stir bar and a reflux condenser was charged with 1-(2,6-diisopropylphenyl)-1*H*-imidazole-2-carboxaldehyde (1.0 equiv) and the corresponding primary amine (1.0 equiv). Then, MeOH (6 mL) was added into the reaction vial. The reaction mixture was refluxed for 16 h and concentrated under reduced pressure to afford the target imine ligand (the imine ligand was used in the next step without further purification) (**Note**: If the starting material is *p*-nitroaniline, a Dean–Stark trap will be used and the reaction mixture will be refluxed for 48 h). In a 10 mL vial equipped with magnetic stir bar was charged with (COD)$PdCl_2$ (1.0 equiv) and the corresponding imine ligand (1.0 equiv) under air condition. Chloroform (0.05 M) was added as solvent into the reaction vial. The reaction mixture was stirred at room temperature for 1 h. The solvent was evaporated. The crude product was recrystallized three times by using chloroform and hexane to give pure palladium complexes.

4.5.1. Synthesis of palladium complex (3a)

((1-(2,6-Diisopropylphenyl)-1*H*-imidazol-2-yl)methylene)aniline ligand was prepared from **1** (76.9 mg, 0.3 mmol, 1.0 equiv) and aniline (27.4 μL, 0.3 mmol, 1.0 equiv) in MeOH (6 mL, 0.05 M). The crude imine ligand was reacted with (COD)$PdCl_2$ (86.2 mg, 0.3 mmol, 1.0 equiv) in chloroform (6 mL, 0.05 M) following the general procedure for the preparation of palladium complexes to afford complex **3a** as a red crystalline (124 mg, 81%). ^{1}H NMR (400 MHz, $CDCl_3$): δ 7.84 (d, J = 1.4 Hz, 1H), 7.59 (t, J = 8.0 Hz, 1H), 7.49 (s, 1H), 7.40–7.36 (m, 5H), 7.30–7.27 (m, 2H), 7.25 (d, J = 1.4 Hz, 1H), 2.35 (sept, J = 6.9 Hz, 2H), 1.21 (d, J = 6.9 Hz, 6H), 1.19 (d, J = 6.9 Hz, 6H). ^{13}C NMR (75 MHz, $CDCl_3$): δ 151.5, 147.5, 146.7, 145.8, 132.2, 130.3, 129.6, 129.5, 128.7, 126.0, 124.9, 123.7, 28.6, 24.6, 24.2. HRMS (ESI): calcd. for $C_{22}H_{25}Cl_2N_3Pd$ $[M + Na]^+$ 532.0351, Found: 532.0352.

4.5.2. Synthesis of palladium complex (3b)

((1-(2,6-Diisopropylphenyl)-1*H*-imidazol-2-yl)methylene)-2,6-diisopropylaniline ligand was prepared from **1** (76.9 mg, 0.3 mmol, 1.0 equiv) and 2,6-diisopropylamine (56.6 μL, 0.3 mmol, 1.0 equiv) in MeOH (6 mL, 0.05 M). The crude imine ligand was reacted with (COD)$PdCl_2$ (86.2 mg, 0.3 mmol, 1.0 equiv) in chloroform (6 mL, 0.05 M) following the general procedure for the preparation of palladium complexes to afford complex **3b** as a red crystalline (127 mg, 71%). ^{1}H NMR (300 MHz, $CDCl_3$): δ 7.88 (d, J = 1.2 Hz, 1H), 7.57 (t, J = 7.9 Hz, 1H), 7.47 (s, 1H), 7.35–7.26 (m, 3H), 7.14 (d, J = 7.9 Hz, 2H), 3.27 (sept, J = 6.9 Hz, 2H), 2.34 (sept, J = 6.7 Hz, 2H), 1.42 (d, J = 6.9 Hz, 6H), 1.21 (d, J = 6.7 Hz, 6H), 1.18 (d, J = 6.7 Hz, 6H), 1.06 (d, J = 6.9 Hz, 6H). ^{13}C NMR (75 MHz, $CDCl_3$): δ = 207.0, 153.8, 146.8, 145.7, 142.6, 140.6, 132.3, 130.3, 129.6, 128.9, 126.3, 124.8, 123.3, 28.7, 24.7, 24.2, 23.8, 23.2. HRMS (ESI): calcd. for $C_{28}H_{37}Cl_2N_3Pd$ $[M + Na]^+$ 616.1291; Found: 616.1291. Anal. Calcd. for $C_{28}H_{37}Cl_2N_3Pd$: C, 56.72; H, 6.29; N, 7.09. Found: C, 56.85; H, 6.74; N, 7.15.

4.5.3. Synthesis of palladium complex (3c)

((1-(2,6-Diisopropylphenyl)-1*H*-imidazol-2-yl)methylene)-4-methoxyaniline ligand was prepared from **1** (76.9 mg, 0.3 mmol, 1.0 equiv) and *p*-anisidine (36.9 mg, 0.3 mmol, 1.0 equiv) in MeOH (6 mL, 0.05 M). The crude imine ligand was reacted with (COD)$PdCl_2$ (86.2 mg, 0.3 mmol, 1.0 equiv) in chloroform (6 mL, 0.05 M) following the general procedure for the preparation of palladium complexes to afford complex **3c** as a red crystalline (124 mg, 77%). ^{1}H NMR (300 MHz, $CDCl_3$): δ = 7.82 (d, J = 1.3 Hz, 1H), 7.60 (t, J = 7.8 Hz, 1H), 7.41 (s, 1H), 7.37 (d, J = 7.8 Hz, 2H), 7.29–7.26 (m, 2H), 7.22 (d, J = 1.3 Hz, 1H), 6.87 (d, J = 9.0 Hz, 2H), 3.81 (s, 3H), 2.35 (sept, J = 6.9 Hz, 2H), 1.21 (d, J = 6.9 Hz, 6H), 1.18 (d, J = 6.9 Hz, 6H). ^{13}C NMR (75 MHz, $CDCl_3$): δ = 160.7, 149.7, 147.7, 145.8, 140.0, 132.1, 130.0, 129.7, 125.5, 125.3, 124.9, 113.8, 55.6, 28.6, 24.5, 24.2. HRMS (ESI): calcd. for $C_{23}H_{27}Cl_2N_3OPd$ $[M + Na]^+$ 562.0457; Found: 562.0457.

*4.5.4. Synthesis of palladium complex (**3d**)*

((1-(2,6-Diisopropylphenyl)-1*H*-imidazol-2-yl)methylene)-4-nitroaniline ligand was prepared from **1** (76.9 mg, 0.3 mmol, 1.0 equiv) and *p*-nitroaniline (41.4 mg, 0.3 mmol, 1.0 equiv) in MeOH (6 mL, 0.05 M). The crude imine ligand was reacted with $(COD)PdCl_2$ (86.2 mg, 0.3 mmol, 1.0 equiv) in chloroform (6 mL, 0.05 M) following the general procedure for the preparation of palladium complexes to afford complex **3d** as an orange solid (110 mg, 66%). ^{1}H NMR (300 MHz, $CDCl_3$): δ = 8.21 (d, J = 9.0 Hz, 2H), 7.85 (d, J = 1.2 Hz, 1H), 7.62–7.57 (m, 2H), 7.49 (d, J = 9.0 Hz, 2H), 7.37 (d, J = 7.8 Hz, 2H), 2.41 (sept, J = 6.8 Hz, 2H), 1.22–1.18 (m, 12H). ^{13}C NMR (75 MHz, $CDCl_3$): δ = 153.1, 150.9, 147.6, 147.3, 146.0, 132.3, 130.9, 129.9, 129.6, 126.9, 125.1, 125.0, 124.1, 28.6, 24.8, 24.3. HRMS (ESI): calcd. for $C_{22}H_{24}Cl_2N_4O_2Pd$ $[M + Na]^+$ 577.0202, Found: 577.0202.

*4.5.5. Synthesis of palladium complex (**3e**)*

((1-(2,6-Diisopropylphenyl)-1*H*-imidazol-2-yl)methylene) methylamine ligand was prepared from **1** (64 mg, 0.25 mmol, 1.0 equiv) and 40 %w/w methylamine solution (22 μL, 0.25 mmol, 1.0 equiv) in MeOH (4 mL, 0.05 M). The crude imine ligand was reacted with $(COD)PdCl_2$ (71.8 mg, 0.25 mmol, 1.0 equiv) in chloroform (5 mL, 0.05 M) following the general procedure for the preparation of palladium complexes to afford complex **3e** as a yellow solid (99.3 mg, 89%). ^{1}H NMR (300 MHz, $CDCl_3$): δ = 7.68 (d, J = 1.4 Hz, 1H), 7.59 (t, J = 7.8 Hz, 1H), 7.45 (m, 1H), 7.37 (d, J = 7.8 Hz, 2H), 7.14 (d, J = 1.4 Hz, 1H), 3.70 (s, 3H), 2.31 (sept, J = 6.8 Hz, 2H), 1.20–1.16 (m, 12H). ^{13}C NMR (75 MHz, $CDCl_3$): δ = 152.8, 147.2, 145.8, 132.1, 129.7, 129.6, 124.8, 49.1, 28.5, 24.7, 24.1. Anal. Calcd. for $C_{17}H_{23}Cl_2N_3Pd$: C, 45.71; H, 5.19; N, 9.41. Found: C, 45.77; H, 5.21; N, 9.22.

*4.5.6. Synthesis of palladium complex (**3f**)*

((1-(2,6-Diisopropylphenyl)-1*H*-imidazol-2-yl)methylene) cyclohexylamine ligand was prepared from **1** (128 mg, 0.3 mmol, 1.0 equiv) and cyclohexylamine (34.4 μL, 0.3 mmol, 1.0 equiv) in MeOH (6 mL, 0.05 M). The crude imine ligand was reacted with $(COD)PdCl_2$ (86.2 mg, 0.3 mmol, 1.0 equiv) in chloroform (5 mL, 0.05 M) following the general procedure for the preparation of palladium complexes to afford complex **3f** as a red crystalline (149.9 mg, 97%). ^{1}H NMR (300 MHz, $CDCl_3$): δ = 7.69 (d, J = 1.4 Hz, 1H), 7.60 (t, J = 7.8 Hz, 1H), 7.36 (d, J = 7.8 Hz, 2H), 7.28 (m, 1H), 7.14 (d, J = 1.4 Hz, 1H), 4.29 (m, 1H), 2.30–2.20 (m, 4H), 1.81–1.65 (m, 4H), 1.41 (m, 2H), 1.19–1.10 (m, 12H), 1.04–0.99 (m, 2H). ^{13}C NMR (75 MHz, $CDCl_3$): δ = 148.7, 147.9, 145.6, 132.1, 129.6, 129.4, 124.9, 124.6, 65.5, 33.8, 28.4, 25.1, 25.0, 24.2. HRMS (ESI): calcd. for $C_{22}H_{31}Cl_2N_3Pd$ $[M + Na]^+$ 538.0820, Found: 538.0820.

*4.5.7. Synthesis of palladium complex (**3g**)*

((1-(2,6-Diisopropylphenyl)-1*H*-imidazol-2-yl)methylene)-*tert*-butylamine ligand was prepared from **1** (64 mg, 0.25 mmol, 1.0 equiv) and *tert*-butylamine (26.4 μL, 0.25 mmol, 1.0 equiv) in MeOH (4 mL, 0.05 M). The crude imine ligand was reacted with $(COD)PdCl_2$ (71.8 mg, 0.25 mmol, 1.0 equiv) in chloroform (5 mL, 0.05 M) following the general procedure for the preparation of palladium complexes to afford complex **3g** as a red crystalline (93.9 mg, 75%). ^{1}H NMR (300 MHz, $CDCl_3$): δ = 7.78 (d, J = 1.4 Hz, 1H), 7.61 (t, J = 7.8 Hz, 1H), 7.37 (d, J = 7.8 Hz, 2H), 7.26 (m, 1H), 7.11 (d, J = 1.4 Hz, 1H), 2.26 (sept, J = 6.7 Hz, 2H), 1.54 (s, 9H), 1.19 (d, J = 6.7 Hz, 6H), 1.12 (d, J = 6.7 Hz, 6H). ^{13}C NMR (75 MHz, $CDCl_3$): δ = 147.7, 147.6, 145.6, 132.2, 129.6, 129.5, 124.9, 124.4, 66.7, 29.6, 28.4, 24.3, 24.2. Anal. Calcd. for $C_{20}H_{29}Cl_2N_3Pd$: C, 49.14; H, 5.98; N, 8.60. Found: C, 49.28; H, 6.03; N, 8.48.

*4.5.8. Synthesis of palladium complex (**3h**)*

((1-(2,6-Diisopropylphenyl)-1*H*-imidazol-2-yl)methylene) adamantylamine ligand was prepared from **1** (89.7 mg, 0.35 mmol, 1.0 equiv) and 1-adamantylamine (52.9 mg, 0.35 mmol, 1.0 equiv) in MeOH (7 mL, 0.05 M). The crude imine ligand was reacted with $(COD)PdCl_2$ (100 mg, 0.35 mmol, 1.0 equiv) in chloroform (7 mL, 0.05 M) following the general procedure for the preparation of palladium complexes to afford complex **3h** as a red microcrystalline (86.7 mg, 87%). ^{1}H NMR (400 MHz, $CDCl_3$): δ = 7.79 (d, J = 1.6 Hz, 1H), 7.61 (t, J = 7.7 Hz, 1H), 7.37 (d, J = 7.7 Hz, 2H), 7.20 (s, 1H), 7.07 (d, J = 1.6 Hz, 1H), 2.27 (sept, J = 7.0 Hz, 2H), 2.18 (m, 3H), 2.09 (m, 6H), 1.70 (m, 6H), 1.20 (d, J = 7.0 Hz, 6H), 1.14 (d, J = 7.0 Hz, 6H). ^{13}C NMR (75 MHz, $CDCl_3$): δ = 147.9, 147.7, 145.8, 132.1, 129.7, 129.5, 124.9, 124.1, 67.0, 42.1, 35.5, 29.5, 28.5, 24.31, 24.30. Anal. Calcd. for $C_{26}H_{35}Cl_2N_3Pd$; C, 55.09; H, 6.22; N, 7.41. Found: C, 55.16; H, 6.59; N, 7.31.

4.6. General procedure for screening of palladium complexes for Suzuki–Miyaura cross coupling reaction (Table 1)

In the air condition, a 10 mL vial equipped with a magnetic stir bar was charged with Pd complexes (1.5 mol%), hexamethylbenzene (0.05 mmol, 0.0081 g, 0.1 equiv) phenyl boronic acid (0.6 mmol, 0.073 g, 1.2 equiv), K_2CO_3 (1.1 mmol, 0.153 g, 2.2 equiv) and *p*-bromoanisole (0.5 mmol, 0.062 mL, 1.0 equiv). MeOH (2 mL) and water (0.5 mL) were mixed and added to the reaction mixture. The reaction vial was capped and vigorously stirred at room temperature for 24 h. The reaction mixture was extracted with CH_2Cl_2 (3 × 10 mL), washed with water (2 × 10 mL), brine (1 × 10 mL) and dried over Na_2SO_4. Solvent was then evaporated. The reaction was monitored by GC-FID to determine the yield of the product based on integration relative to hexamethylbenzene as an internal standard.

4.7. General procedure for the investigation of the effect of catalyst loading, base, solvent, time and substrate scopes on Suzuki–Miyaura cross coupling reaction (Tables S1–S5, Tables 4 and 5)

In the air condition, hexamethylbenzene (0.05 mmol, 0.0081 g, 0.1 equiv), aryl halide (0.5 mmol, 1 equiv), aryl boronic acid (0.6 mmol, 1.2 equiv), base (1.1 mmol, 2.2 equiv) and solvent was subsequently added into a 10 mL vial equipped with a magnetic stir bar. The 5 mM Pd catalyst solution in MeOH was added as indicated in the table. The reaction vial was capped and vigorously stirred at room temperature for desired time as indicated. The reaction mixture was extracted with CH_2Cl_2 (3 × 10 mL), washed with water (2 × 10 mL), brine (1 × 10 mL) and dried over Na_2SO_4. The combined organic phase was then concentrated to afford the crude coupling product. The reaction was monitored by GC-FID based on integration relative to hexamethylbenzene as an internal standard. The crude product was finally isolated by column chromatography (0–10%: EtOAc/hexane) to afford the desired product.

*4.8. Analytical data of coupling products (**4a–q**)*

*4.8.1. Biphenyl (**4a**, Table 4, entry 1)*

^{1}H NMR (300 MHz, $CDCl_3$): δ = 7.65 (d, J = 7.7 Hz, 4H), 7.49 (t, J = 7.7 Hz, 4H), 7.37 (m, 2H). EI-MS (*m*/*z*, relative intensity): 155 (14), 154 (M^+, 100), 153 (42), 152 (29). CAS Number: 92-52-4.

*4.8.2. 4-Methoxybiphenyl (**4b**, Table 4, entries 2 and 5; Table 5, entry 1)*

^{1}H NMR (300 MHz, $CDCl_3$): δ = 7.57 (t, J = 8.7 Hz, 4H), 7.44 (t, J = 7.5 Hz, 2H), 7.35–7.28 (m, 1H), 7.00 (d, J = 8.7 Hz, 2H), 3.88 (s,

3H). EI-MS (*m*/*z*, relative intensity): 185 (14), 184 (M^+, 100), 169 (46), 141 (45), 115 (33). CAS Number: 613-37-6.

*4.8.3. 3-Methoxybiphenyl (**4c**, Table 4, entry 3; Table 5, entry 2)*

^{1}H NMR (300 MHz, $CDCl_3$): δ = 7.62 (d, J = 7.5 Hz, 2H), 7.47 (t, J = 7.5 Hz, 2H), 7.42–7.36 (m, 2H), 7.22 (d, J = 8.1 Hz, 1H), 7.16 (m, 1H), 6.94 (d, J = 8.1 Hz, 1H), 3.90 (s, 3H). EI-MS (*m*/*z*, relative intensity): 185 (15), 184 (M^+, 100), 154 (23), 153 (20), 141 (32), 115 (30). CAS Number: 2113-56-6.

*4.8.4. 2-Methoxybiphenyl (**4d**, Table 4, entry 4; Table 5, entry 3)*

^{1}H NMR (300 MHz, $CDCl_3$): δ = 7.64 (d, J = 7.2 Hz, 2H), 7.51 (t, J = 7.4 Hz, 2H), 7.42 (t, J = 7.3 Hz, 3H), 7.15–7.06 (m, 2H), 3.89 (s, 3H). EI-MS (*m*/*z*, relative intensity): 185 (14), 184 (M^+, 100), 183 (21), 169 (54), 168 (15), 141 (37), 139 (17), 115 (37). CAS Number: 86-26-0.

*4.8.5. 4-Nitrobiphenyl (**4e**, Table 4, entry 6): ^{1}H NMR (300 MHz, $CDCl_3$)*

δ = 8.33 (d, J = 9.0 Hz, 2H), 7.76 (d, J = 9.0 Hz, 2H), 7.67–7.64 (m, 2H), 7.56–7.47 (m, 3H). EI-MS (*m*/*z*, relative intensity): 200 (13), 199 (M^+, 97), 169 (35), 153 (28), 152 (100), 151 (30), 141 (28). CAS Number: 92-93-3.

*4.8.6. 4-(Trifluoromethyl)biphenyl (**4f**, Table 4, entry 7)*

^{1}H NMR (300 MHz, $CDCl_3$): δ = 7.61–7.55 (m, 4H), 7.49 (m, 2H), 7.39–7.27 (m, 3H). EI-MS (*m*/*z*, relative intensity): 223 (13), 222 (M^+, 100), 201 (10), 151 (20). CAS Number: 398-36-7.

*4.8.7. 4-Acetylbiphenyl (**4g**, Table 4, entry 8; Table 5, entry 4)*

^{1}H NMR (300 MHz, $CDCl_3$): δ = 8.06 (d, J = 8.6 Hz, 2H.), 7.71 (d, J = 8.6 Hz, 2H), 7.66 (d, J = 8.1 Hz, 2H), 7.50 (t, J = 7.2 Hz, 2H), 7.43 (t, J = 7.2 Hz, 1H), 2.66 (s, 3H). EI-MS (*m*/*z*, relative intensity): 196 (M^+, 50), 181 (100), 153 (35), 152 (58), 151 (16). CAS Number: 92-91-1.

*4.8.8. 4-Biphenylcarboxaldehyde (**4h**, Table 4, entry 9)*

^{1}H NMR (300 MHz, $CDCl_3$): δ = 10.09 (s, 1H), 7.98 (d, J = 8.2 Hz, 2H), 7.77 (d, J = 8.2 Hz, 2H), 7.66 (d, J = 6.8 Hz, 2H), 7.54–7.44 (m, 3H). EI-MS (*m*/*z*, relative intensity): 183 (13), 182 (M^+, 96), 181 (100), 153 (38), 152 (63), 151 (18). CAS Number: 3218-36-8.

*4.8.9. Methyl biphenyl-4-carboxylate (**4i**, Table 4, entry 10)*

^{1}H NMR (300 MHz, $CDCl_3$): δ = 8.14 (d, J = 8.2 Hz, 2H), 7.69 (d, J = 8.4 Hz, 2H), 7.65 (d, J = 7.5 Hz, 2H), 7.50 (t, J = 7.3 Hz, 2H), 7.42 (t, J = 7.1 Hz, 1H), 3.97 (s, 3H). EI-MS (*m*/*z*, relative intensity): 212 (M^+, 65), 182 (13), 181 (100), 153 (28), 152 (60), 151 (17). CAS Number: 720-75-2.

*4.8.10. 4-Cyanobiphenyl (**4j**, Table 4, entry 11)*

^{1}H NMR (300 MHz, $CDCl_3$): δ = 7.76 (d, J = 8.6 Hz, 2H), 7.71 (d, J = 8.6 Hz, 2H), 7.62 (d, J = 6.9 Hz, 2H), 7.54–7.45 (m, 3H). EI-MS (*m*/*z*, relative intensity): 179 (M^+, 100), 178 (24), 151 (12). CAS Number: 2920-38-9.

*4.8.11. 4-Fluorobiphenyl (**4k**, Table 4, entry 12)*

^{1}H NMR (300 MHz, $CDCl_3$): δ = 7.62–7.58 (m, 4H), 7.50 (t, J = 7.4 Hz, 2H), 7.40 (t, J = 7.4 Hz, 1H), 7.18 (t, J = 8.7 Hz, 2H). EI-MS (*m*/*z*, relative intensity): 173 (13), 172 (M^+, 100), 171 (36), 170 (25). CAS Number: 324-74-3.

*4.8.12. 4-Hydroxybiphenyl (**4l**, Table 4, entry 13)*

^{1}H NMR (300 MHz, $CDCl_3$): δ = 7.58 (d, J = 8.5 Hz, 2H), 7.52 (d, J = 8.5 Hz, 2H), 7.45 (t, J = 7.5 Hz, 2H), 7.34 (t, J = 7.5 Hz, 1H), 6.94 (d, J = 8.5 Hz, 2H), 5.08 (br s, 1H). EI-MS (*m*/*z*, relative intensity): 171 (13), 170 (M^+, 100), 141 (22), 115 (28). CAS Number: 92-69-3.

*4.8.13. p-Terphenyl (**4m**, Table 4, entry 14)*

^{1}H NMR (300 MHz, $CDCl_3$): δ = 7.73–7.71 (m, 4H), 7.69 (d, J = 7.4 Hz, 4H), 7.51 (t, J = 7.4 Hz, 4H), 7.41 (t, J = 7.4 Hz, 2H). EI-MS (*m*/*z*, relative intensity): 231 (19), 230 (M^+, 100), 228 (13). CAS Number: 92-94-4.

*4.8.14. 3-Phenylpyridine (**4n**, Table 4, entry 15)*

^{1}H NMR (300 MHz, $CDCl_3$): δ = 8.88 (s, 1H), 8.62 (d, J = 4.4 Hz, 1H), 7.91 (d, J = 8.0 Hz, 1H), 7.61 (d, J = 7.4 Hz, 2H), 7.51 (t, J = 7.4 Hz, 2H), 7.46–7.37 (m, 2H). EI-MS (*m*/*z*, relative intensity): 155 (M^+, 100), 154 (50), 127 (14), 102 (11). CAS Number: 1008-88-4.

*4.8.15. 3-Phenylquinoline (**4o**, Table 4, entry 16)*

^{1}H NMR (300 MHz, $CDCl_3$): δ = 9.21 (s, 1H), 8.32 (s, 1H), 8.18 (d, J = 8.3 Hz, 1H), 7.90 (d, J = 8.3 Hz, 1H), 7.77–7.22 (m, 3H), 7.62–7.52 (m, 3H), 7.46 (t, J = 7.2 Hz, 1H). EI-MS (*m*/*z*, relative intensity): 206 (16), 205 (M^+, 100), 204 (53), 176 (14). CAS Number: 1666-96-2.

*4.8.16. 5-Phenylpyrimidine (**4p**, Table 4, entry 17)*

^{1}H NMR (300 MHz, $CDCl_3$): δ = 9.23 (s, 1H), 8.98 (s, 2H), 7.62–7.49 (m, 5H). EI-MS (*m*/*z*, relative intensity): 157 (12), 156 (M^+, 100), 155 (17), 102 (64). CAS Number: 34771-45-4.

*4.8.17. 1-(4′-Methoxybiphenyl-4-yl)ethanone (**4q**, Table 5, entries 5 and 6)*

^{1}H NMR (300 MHz, $CDCl_3$): δ = 8.02 (d, J = 8.2 Hz, 2H), 7.66 (d, J = 8.2 Hz, 2H), 7.60 (d, J = 8.9 Hz, 2H), 7.02 (d, J = 8.4 Hz, 2H), 3.87 (s, 3H), 2.64 (s, 3H). EI-MS (*m*/*z*, relative intensity): 226 (M^+, 66), 212 (18), 211 (100), 183 (11), 168 (19), 139 (25). CAS Number: 13021-18-6.

4.9. Hg poisoning test

The reaction vial charged with an excess of Hg (Hg:Pd = 400:1) was added hexamethylbenzene (0.05 mmol, 0.0081 g, 0.1 equiv), phenyl boronic acid (0.6 mmol, 0.073 g, 1.2 equiv), K_2CO_3 (1.1 mmol, 0.153 g, 2.2 equiv), *p*-bromoanisole (0.5 mmol, 0.062 μL, 1.0 equiv), MeOH (2 mL) and water (0.5 mL), followed by 0.00075 mmol of Pd catalyst **3b** (0.15 mol%). After 24 h, the mixture was extracted by CH_2Cl_2 (3 × 10 mL), washed with water (2 × 10 mL), brine (1 × 10 mL), dried over Na_2SO_4, and solvent was concentrated to afford the crude 4-methoxybiphenyl product. The yield was determined by GC method. A 33% yield was obtained in the presence of excess of Hg.

Acknowledgments

This work was supported by the Department of Chemistry, Faculty of Science, Mahidol University and the Center of Excellence for Innovation in Chemistry (PERCH-CIC). The authors would like to thank Mrs. Suttiporn Pikulthong and Mr. Samran Prabpai for their experimental help. We also would like to thank Department of Chemistry and Center of Instrumental Facility (CIF) at Faculty of Science, Mahidol University for facilities.

Appendix A. Supplementary data

Supplementary data related to this article can be found at http://dx.doi.org/10.1016/j.jorganchem.2013.12.015.

References

[1] N. Miyaura, A. Suzuki, Chem. Rev. 95 (1995) 2457–2483.
[2] A. Suzuki, J. Organomet. Chem. 576 (1999) 147–168.
[3] S. Kotha, K. Lahiri, D. Kashinath, Tetrahedron 58 (2002) 9633–9695.

[4] F. Bellina, A. Carpita, R. Rossi, Synthesis (2004) 2419–2440.
[5] A.F. Littke, C. Dai, G.C. Fu, J. Am. Chem. Soc. 122 (2000) 4020–4028.
[6] J. Yin, M.P. Rainka, X.X. Zhang, S.L. Buchwald, J. Am. Chem. Soc. 124 (2002) 1162–1163.
[7] G. Adjabeng, T. Brenstrum, J. Wilson, C. Frampton, A. Robertson, J. Hillhouse, J. McNulty, A. Capretta, Org. Lett. 5 (2003) 953–955.
[8] W.A. Herrmann, Angew. Chem. Int. Ed. 41 (2002) 1290–1309.
[9] W.A. Herrmann, V.P.W. Böhm, C.W.K. Gstöttmayr, M. Grosche, C.P. Reisinger, T. Weskamp, J. Organomet. Chem. 617–618 (2001) 616–628.
[10] G. Altenhoff, R. Goddard, C.W. Lehmann, F. Glorius, J. Am. Chem. Soc. 126 (2004) 15195–15201.
[11] E.A.B. Kantchev, C.J. O'Brien, M.G. Organ, Angew. Chem. Int. Ed. 46 (2007) 2768–2813.
[12] L.A. Schaper, S.J. Hock, W.A. Herrmann, F.E. Kühn, Angew. Chem. Int. Ed. 52 (2013) 270–289.
[13] A.S.K. Hashmi, C. Lothschütz, Organometallics 30 (2011) 2411–2417.
[14] H. Weissman, D. Milstein, Chem. Commun. (1999) 1901–1902.
[15] G.A. Grasa, A.C. Hillier, S.P. Nolan, Org. Lett. 3 (2001) 1077–1080.
[16] S. Li, Y. Lin, J. Cao, S. Zhang, J. Org. Chem. 72 (2007) 4067–4072.
[17] K.S. Dube, T.C. Harrop, Dalton Trans. 40 (2011) 7496–7498.
[18] J. Liu, J. Chen, J. Zhao, Y. Zhao, L. Li, H. Zhang, Synthesis (2003) 2661–2666.
[19] H. Zhou, W.Z. Zhang, Y.M. Wang, J.P. Qu, Z.B. Lu, Macromolecules 42 (2009) 5419–5421.
[20] T.V. Laine, M. Klinga, M. Leskelä, Eur. J. Inorg. Chem. (1999) 959–964.
[21] M. Schmid, R. Eberhardt, M. Klinga, M. Leskelä, B. Rieger, Organometallics 20 (2001) 2321–2330.
[22] T.V. Laine, U. Piironen, K. Lappalainen, M. Klinga, E. Aitola, M. Leskelä, J. Organomet. Chem. 606 (2002) 112–124.
[23] M.C. Done, T. Rüther, K.J. Cavell, M. Kilner, E.J. Peacock, N. Braussaud, B.W. Skelton, A. White, J. Organomet. Chem. 607 (2000) 78–92.
[24] T. Mino, Y. Shirae, M. Sakamoto, T. Fujita, J. Org. Chem. 70 (2005) 2191–2194.
[25] E. Amadio, A. Scrivanti, G. Chessa, U. Matteoli, V. Beghetto, M. Bertoldini, M. Rancan, A. Dolmella, A. Venzo, R. Bertani, J. Organomet. Chem. 716 (2012) 193–200.
[26] S. Jindabot, K. Teerachanan, P. Thongkam, S. Kiatisevi, T. Khamnaen, P. Phiriyawirut, S. Charoenchaidet, T. Sooksimuang, P. Kongsaeree, P. Sangtrirutnugul, J. Organomet. Chem. 750 (2014) 35–40.
[27] A. John, M.M. Shaikh, P. Ghosh, Inorg. Chim. Acta 363 (2010) 3113–3121.
[28] H.-S. Wang, Y.-C. Wang, Y.-M. Pan, S.-L. Zhao, Z.-F. Chen, Tetrahedron Lett. 49 (2008) 2634–2637.
[29] H. Bulut, L. Artok, S. Yilmazu, Tetrahedron Lett. 44 (2003) 289–291.
[30] G.K. Rao, A. Kumar, B. Kumar, D. Kumar, A.K. Singh, Dalton Trans. 41 (2012) 1931–1937.
[31] G.K. Rao, A. Kumar, S. Kumar, U.B. Dupare, A.K. Singh, Organometallics 32 (2013) 2452–2458.
[32] L.A. Adrio, B.N. Nguyen, G. Guilera, A.G. Livingston, K.K. Hii, Catal. Sci. Technol. 2 (2012) 316–323.
[33] A.N. Salanov, A.I. Titkov, V.N. Bibin, Kinet. Catal. 47 (2006) 430–436.
[34] A.N. Salanov, E.A. Suprun, Kinet. Catal. 50 (2009) 31–39.
[35] J. Wiedermann, K. Mereiter, K. Kirchner, J. Mol. Catal. A Chem. 257 (2006) 67–72.
[36] SMART v.5.6, Bruker AXS Inc., Madison, WI, USA, 2000.
[37] SAINT v.4, Siemens Analytical X-ray Systems, Inc., Madison, WI, USA, 1996.
[38] S. Mackay, C.J. Gilmore, C. Edwards, N. Stewart, K. Shankland, maXus Computer Program for the Solution and Refinement of Crystal Structures Bruker Nonius, The Netherlands, MacScience, Japan & The University of Glasgow.
[39] A. Altomare, M.C. Burla, M. Camalli, G. Cascarano, C. Giacovazzo, A. Guagliardi, A.G.G. Moliterni, G. Polidori, R.J. Spagna, Appl. Crystallogr. 32 (1999) 115.
[40] G.M. Sheldrick, SHELXTL v.6.12, Siemens Analytical X-ray Systems, Inc., Madison, WI, USA, 1997.

APPENDIX H
RESEARCH OUTPUT, PUBLICATION PART II

EurJOC European Journal of Organic Chemistry

SHORT COMMUNICATION

DOI: 10.1002/ejoc.201301634

Convenient Synthesis of Arylboronates through a Synergistic Pd/Cu-Catalyzed Miyaura Borylation Reaction under Atmospheric Conditions

Jadsada Ratniyom,[a] Nattanee Dechnarong,[a] Sirilata Yotphan,[a] and Supavadee Kiatisevi*[a]

Keywords: Boron / Palladium / Copper / Cross-coupling / Atmospheric conditions

A highly efficient and practical borylation reaction of aryl iodides with bis(pinacolato)diboron has been established. By using $Pd(OAc)_2$, CuI, and PPh_3 as a ligand at room temperature under air in the presence of Cs_2CO_3, the protocol proved to be general. Various functionalized arylboronates were obtained in moderate to excellent yields. In addition, a possible reaction mechanism was proposed.

Introduction

Arylboronic acids and their esters are important and useful reagents that are widely used in organic synthesis for functional-group transformations.[1] They play a key role as coupling partners in Suzuki–Miyaura cross-coupling reactions. The advantages of these organoboron compounds in cross-coupling processes include their high stability and low toxicity. Arylboronic acids and esters are typically produced by the reaction of trialkyl borates with either organolithium or Grignard reagents. However, these methods are incompatible with sensitive functional groups and require rigorous anhydrous reaction conditions.

Owing to these disadvantages, several alternative routes to synthesize borylation products have been developed. Many of them use transition-metal-catalyzed borylation reactions. Pd- and Ni-catalyzed borylation reactions of aryl halides have been used in the preparation of arylboronates.[1a,2] C–H borylations of aromatic substrates catalyzed by iridium have been reported.[3] Cu-catalyzed borylation for the synthesis of arylboronates was found to be efficient and economical.[4] Also, transition-metal-free borylations have been studied.[5] However, they require an inert gas and have either long reaction times or high reaction temperatures.

In this work, we discovered a new transition-metal catalytic system for the Miyaura borylation for which an air-sensitive technique is not required. This simple and efficient system consisting of Pd and Cu can catalyze the borylation of aryl iodides with bis(pinacolato)diboron at room temperature under atmospheric conditions to achieve arylboronates and their derivatives. Moderate to excellent yields were obtained under this synergistic catalysis.

[a] Center for Catalysis and Center of Excellence for Innovation in Chemistry (PERCH-CIC), Department of Chemistry, Faculty of Science, Mahidol University,
Rama VI Road, Bangkok 10400, Thailand
E-mail: supavadee.mon@mahidol.ac.th
http://www.sc.mahidol.ac.th/academics/staff/AC_s/Supavadee_M.htm

Supporting information for this article is available on the WWW under http://dx.doi.org/10.1002/ejoc.201301634.

Results and Discussion

We initially used phenyl iodide and bis(pinacolato)diboron as substrates in a catalytic combination between $Pd(OAc)_2$ and CuI. For the present borylation reaction under ambient conditions, a moderate yield was obtained (Table 1, Entry 1). The yield of product **3a** declined to 13% in the absence of PPh_3 and to 30% with only $Pd(OAc)_2$ (Table 1, Entries 2 and 3). A catalytic system consisting of only CuI/PPh_3 or CuI was found ineffective for this borylation reaction (Table 1, Entries 4 and 5). Moreover, no reaction was observed in the absence of both $Pd(OAc)_2$ and CuI (Table 1, Entries 6 and 7). We subsequently investigated the effect of the amount of air-stable PPh_3 ligand on the reaction and interestingly found that decreasing the amount of PPh_3 positively affected the yield of **3a** (Table 1, Entries 8–13). A 60% yield of the borylation product was afforded even with the use of 2 mol-% of PPh_3 in the presence of 0.5 mL of water (Table 1, Entry 13). The amount of CuI was next examined (Table 1, Entries 13–18). We observed an improved product yield (65%) upon using 20 mol-% of CuI (Table 1, Entry 16). In addition, we screened various Pd sources to examine their effects on the reaction (Table 1, Entries 19–22). Notably, $Pd(PPh_3)_4$ delivered a higher product yield (79%). However, this reagent requires an inert gas for storing and handling, whereas $Pd(OAc)_2$ is air- and moisture-stable and hence does not require any air-sensitive technique, which is the main interest of this research. We thus chose $Pd(OAc)_2$ (2 mol-%), CuI (20 mol-%), and PPh_3 (2 mol-%) for further evaluation of the other effects.

Table 1. Screening of reaction conditions for the Pd/Cu-catalyzed borylation of iodobenzene and bis(pinacolato)diboron.[a]

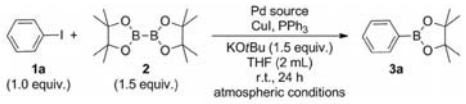

Entry	Pd source	CuI [mol-%]	PPh_3 [mol-%]	Yield[b] [%]
1	$Pd(OAc)_2$	10	13	51
2	$Pd(OAc)_2$	10	–	13
3	$Pd(OAc)_2$	–	–	30
4	–	10	13	28
5	–	10	–	4
6	–	–	–	0[d]
7	–	–	13	0[d]
8[c]	$Pd(OAc)_2$	10	30	57
9[c]	$Pd(OAc)_2$	10	18	58
10[c]	$Pd(OAc)_2$	10	13	62
11[c]	$Pd(OAc)_2$	10	10	60
12[c]	$Pd(OAc)_2$	10	5	60
13[c]	$Pd(OAc)_2$	10	2	60
14[c]	$Pd(OAc)_2$	2.5	2	47
15[c]	$Pd(OAc)_2$	5	2	56
16[c]	$Pd(OAc)_2$	20	2	65
17[c]	$Pd(OAc)_2$	30	2	65
18[c]	$Pd(OAc)_2$	50	2	63
19[c]	$PdCl_2$	20	2	53
20[c]	$Pd(PPh_3)_2Cl_2$	20	2	55
21[c]	Pd_2dba_3	20	2	56
22[c]	$Pd(PPh_3)_4$	20	2	79

[a] Reaction conditions, unless otherwise stated: Pd source (0.012 mmol), CuI, PPh_3, aryl iodide (0.6 mmol), bis(pinacolato)-diboron (0.9 mmol), KO*t*Bu (0.9 mmol), THF (2 mL), air, room temperature, 24 h. [b] Yield was determined by GC integration relative to hexamethylbenzene as an internal standard. [c] Water (0.5 mL) was added. [d] No reaction was detected by TLC/GC–MS.

We next screened a variety of co-catalysts. Various copper salts and other metal sources were investigated. The results are summarized in Table 2. CuCl and $Cu(OTf)_2$ (Tf = trifluoromethylsulfonyl) gave a product yield similar to that obtained with CuI (65%). In contrast, other metal co-catalysts, such as $NiCl_2$, $Ni(OAc)_2$, $ZnCl_2$, AgOAc, and Ag_2CO_3, and the absence of a co-catalyst gave poor results. We chose CuI as a co-catalyst to avoid the interference of other anionic species in the reaction.

Then, we studied the effect of inorganic bases and equivalency (Table 3, Entries 1–13). The highest product yield was obtained with the use of 1.5 equiv. of Cs_2CO_3. In contrast, the absence of base resulted in a drastically lower yield of **3a** (Table 3, Entry 14).

The optimized reaction conditions furnished **3a** with various types of solvents (Table 4). A quantitative yield was afforded upon using acetonitrile as the solvent (Table 4, Entry 8). In addition, we performed the reaction by using a mixture of water (0.5 mL) and acetonitrile (2 mL). As a result, the yield slightly declined to 91% (Table 4, Entry 10). We also examined the effect of reaction time and found that a quantitative yield could be obtained after 2 h (Table 5, Entry 6).

Table 2. Screening of co-catalysts for the borylation reaction.[a]

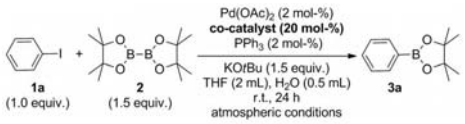

Entry	Co-catalyst	Yield[b] [%]
1	CuCl	65
2	CuBr	58
3	CuI	65
4	CuCN	3
5	$CuBr_2$	62
6	$Cu(OAc)_2$	51
7	CuO	47
8	$Cu(OTf)_2$	65
9	$Ni(OAc)_2{\cdot}4H_2O$	14
10	$NiCl_2{\cdot}6H_2O$	19
11	$ZnCl_2$	15
12	AgOAc	13
13	Ag_2CO_3	15
14	–	27

[a] Reaction conditions: $Pd(OAc)_2$ (0.012 mmol), co-catalyst (0.12 mmol), PPh_3 (0.012 mmol), aryl iodide (0.6 mmol), bis-(pinacolato)diboron (0.9 mmol), KO*t*Bu (0.9 mmol), THF (2 mL), H_2O (0.5 mL), air, room temperature, 24 h. [b] Yield was determined by GC integration relative to hexamethylbenzene as an internal standard.

Table 3. Screening of bases for the Pd/Cu-catalyzed borylation reaction.[a]

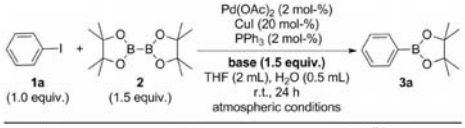

Entry	Base	Yield[b] [%]
1	LiO*t*Bu	57
2	NaO*t*Bu	59
3	KO*t*Bu	65
4	K_3PO_4	74
5	K_2CO_3	75
6	Cs_2CO_3	82
7	Ag_2CO_3	26
8	NaOH	58
9	KOH	57
10	$CsOH{\cdot}H_2O$	53
11	KOAc	69
12	KOMe	67
13	NEt_3	65
14	–	5

[a] Reaction conditions: $Pd(OAc)_2$ (0.012 mmol), CuI (0.12 mmol), PPh_3 (0.012 mmol), aryl iodide (0.6 mmol), bis(pinacolato)diboron (0.9 mmol), base (0.9 mmol), THF (2 mL), H_2O (0.5 mL), air, room temperature, 24 h. [b] Yield was determined by GC integration relative to hexamethylbenzene as an internal standard.

We proceeded to apply this borylation reaction to various ratios of acetonitrile/water so that this protocol could meet the character of green chemistry (Table 6). Poor yields were obtained if the volume of water was increased, and the

Table 4. Screening of solvents for the Pd/Cu-catalyzed borylation reaction.[a]

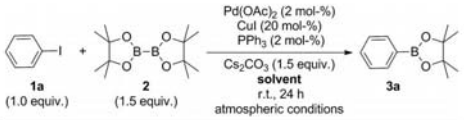

Entry	Solvent (mL)	Yield[b] [%]
1	dioxane (2)	68
2	DMF (2)	73
3	MeOH (2)	72
4	THF (2)	67
5	THF/H_2O (2:0.5)	82
6	EtOH (2)	70
7	DMSO (2)	75
8	CH_3CN (2)	97
9	H_2O (2)	16
10	CH_3CN/H_2O (2:0.5)	91

[a] Reaction conditions: $Pd(OAc)_2$ (0.012 mmol), CuI (0.12 mmol), PPh_3 (0.012 mmol), aryl iodide (0.6 mmol), bis(pinacolato)diboron (0.9 mmol), Cs_2CO_3 (0.9 mmol), solvent (2 mL), air, room temperature, 24 h. [b] Yield was determined by GC integration relative to hexamethylbenzene as an internal standard.

Table 5. Effect of reaction time on the Pd/Cu-catalyzed borylation reaction.[a]

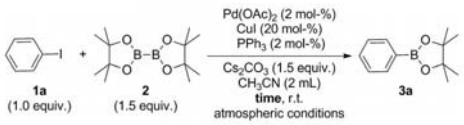

Entry	Time [h]	Yield[b] [%]
1	48	93
2	24	97
3	16	96
4	8	96
5	4	95
6	2	97
7	1	67
8	0.5	65

[a] Reactions were performed in air at room temperature for the time indicated with $Pd(OAc)_2$ (0.012 mmol), CuI (0.12 mmol), PPh_3 (0.012 mmol), aryl iodide (0.6 mmol), bis(pinacolato)diboron (0.9 mmol), Cs_2CO_3 (0.9 mmol), and CH_3CN (2 mL). [b] Yield was determined by GC integration relative to hexamethylbenzene as an internal standard.

use of only water afforded a very low yield. Moreover, the product yield was found to be independent of the amount of solvent (Table 7).

On the basis of the above optimization results, we chose the following reaction conditions: a mixture of $Pd(OAc)_2$ (2 mol-%), CuI (20 mol-%), PPh_3 (2 mol-%), and Cs_2CO_3 (1.5 equiv.) in acetonitrile (2 mL) stirred at room temperature for 2 h, which provided **3a** in 97% yield.

Under the optimal reaction conditions, the scope of the substrates was next examined. Only aryl iodides were effective substrates, whereas aryl chlorides and bromides gave

Table 6. Effect of water concentrations in CH_3CN on the Pd/Cu-catalyzed borylation reaction.[a]

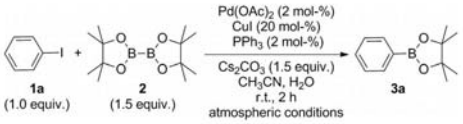

Entry	CH_3CN [mL]	H_2O [mL]	Yield[b] [%]
1	2.5	0	72
2	2.0	0.5	91
3	1.5	1	81
4	1.0	1.5	47
5	0.5	2	17
6	0	2.5	18

[a] Reaction conditions: $Pd(OAc)_2$ (0.012 mmol), CuI (0.12 mmol), PPh_3 (0.012 mmol), aryl iodide (0.6 mmol), bis(pinacolato)diboron (0.9 mmol), Cs_2CO_3 (0.9 mmol), air, room temperature, 2 h. [b] Yield was determined by GC integration relative to hexamethylbenzene as an internal standard.

Table 7. Effect of solvent concentrations on the Pd/Cu-catalyzed borylation reaction.[a]

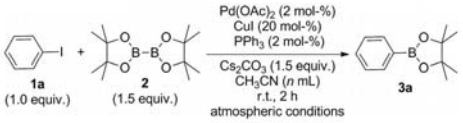

Entry	*n* [mL]	Yield[b] [%]
1	8	97
2	6	96
3	4	97
4	2	97
5	1	94

[a] Reaction conditions: $Pd(OAc)_2$ (0.012 mmol), CuI (0.12 mmol), PPh_3 (0.012 mmol), aryl iodide (0.6 mmol), bis(pinacolato)diboron (0.9 mmol), Cs_2CO_3 (0.9 mmol), CH_3CN (*n* mL), air, room temperature, 2 h. [b] Yield was determined by GC integration relative to hexamethylbenzene as an internal standard.

Table 8. Investigation of the substrate scope of the Pd/Cu-catalyzed borylation reaction.[a]

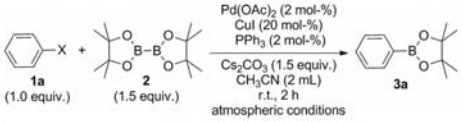

Entry	X	Yield[b] [%]
1	Cl	2
2	Br	5
3	I	97

[a] Reaction conditions: $Pd(OAc)_2$ (0.012 mmol), CuI (0.12 mmol), PPh_3 (0.012 mmol), aryl iodide (0.6 mmol), bis(pinacolato)diboron (0.9 mmol), Cs_2CO_3 (0.9 mmol), CH_3CN (2 mL), air, room temperature, 2 h. [b] Yield was determined by GC integration relative to hexamethylbenzene as an internal standard.

the corresponding products in very low yields (Table 8, Entries 1 and 2). This result suggests that this protocol can be useful for chemoselective borylation at the C–I bond if other halogen substituents are present.

Table 9. Screening of aryl iodides for the Pd/Cu-catalyzed borylation reaction.[a]

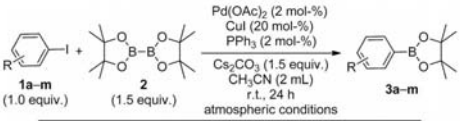

Entry	Aryl iodide	Product	Yield[b] [%]
1	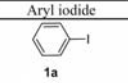 1a	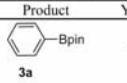 3a	76 (97)[c]
2	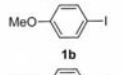 1b	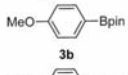 3b	92
3	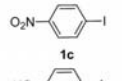 1c	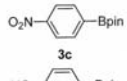 3c	93
4	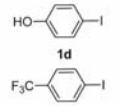 1d	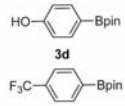 3d	76
5	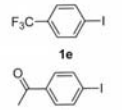 1e	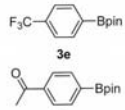 3e	66
6	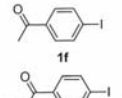 1f	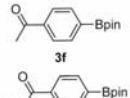 3f	91
7	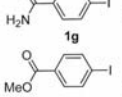 1g	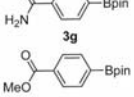 3g	89
8	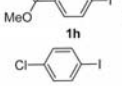 1h	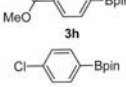 3h	81
9	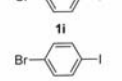 1i	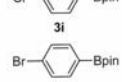 3i	96
10	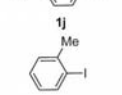 1j	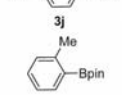 3j	70
11	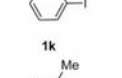 1k	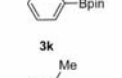 3k	50
12	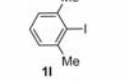 1l	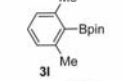 3l	31
13	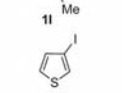 1m	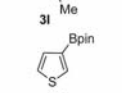 3m	63

[a] Reaction conditions: $Pd(OAc)_2$ (0.012 mmol), CuI (0.12 mmol), PPh_3 (0.012 mmol), aryl iodide (0.6 mmol), bis(pinacolato)diboron (0.9 mmol), Cs_2CO_3 (0.9 mmol), CH_3CN (2 mL), air, room temperature, 24 h. pin = $1,2\text{-}O_2C_2Me_4$. [b] Yield of isolated product. [c] Yield calculated by GC.

The present method could be applied successfully to a variety of aryl iodides bearing various types of functionalities. The results are summarized in Table 9. The scope of the aryl iodide derivatives was found to be remarkably broad. Excellent yields were obtained for substrates with both electron-donating and electron-withdrawing substituents (Table 9, Entries 2 and 3). The borylation reaction performed in air showed good tolerance for various functional groups, including hydroxide (**3d**), trifluoromethyl (**3e**), ketone (**3f**), amide (**3g**), and ester (**3h**) groups (Table 9, Entries 4–8).

Interestingly, excellent chemoselectivity was observed upon using 1-chloro-4-iodobenzene (**1i**) and 1-bromo-4-iodobenzene (**1j**), as only monoborylated products **3i** and **3j** were obtained (Table 9, Entries 9 and 10). The remaining halogen and substituent groups are ready for further transformations. This advantage could find general usage in organic synthesis and polymerization. Introducing alkyl or dialkyl groups at the *ortho* positions of the aryl iodides (i.e., as in **1k** and **1l**) resulted in moderate yields (Table 9, Entries 11 and 12), presumably because the steric hindrance of the *ortho* substituents can hamper the oxidative addition step of the catalytic cycle. Additionally, heteroaromatic iodide **1m** also gave the corresponding product **3m** in a high yield (Table 9, Entry 13).

The mechanism of this transformation is assumed to involve oxidative addition of the aryl iodide and Pd^0 to form Pd^{II} complex **5**, as presented in Scheme 1. Complex **5** reacts with an alkoxide base to form $ArPd^{II}$–OR species **6**, which is more reactive than the $ArPd^{II}$–X adduct.[1a] Copper iodide acting as a transmetalating agent reacts with the base and ligand to form L–Cu–OR intermediate **7**.[4b] Ligand exchange has been reported to occur between **7** and bis(pinacolato)diboron to afford intermediate **8**.[4b] Subsequently, **6** and **8** undergo transmetalation to form complex **9**, which induces regeneration of copper intermediate **7**. Finally, reductive elimination of **9** produces a new C–B bond of the corresponding borylation product. Further studies on the mechanism of this Pd/Cu-catalyzed borylation reaction are in progress in our laboratory.

Conclusions

An efficient Pd/Cu-catalyzed protocol for the borylation of aryl and heteroaryl iodides was developed. The synergistic catalysis can be performed in air at room temperature. This method serves as an inexpensive and convenient synthetic route to afford arylboronates. Chemoselectivity was observed in this catalytic combination. Furthermore, the reaction conditions are compatible with various sensitive functional groups, and high product yields are obtained.

Supporting Information (see footnote on the first page of this article): Experimental Section and copies of the ^1H, ^{13}C, and ^{11}B NMR spectra.

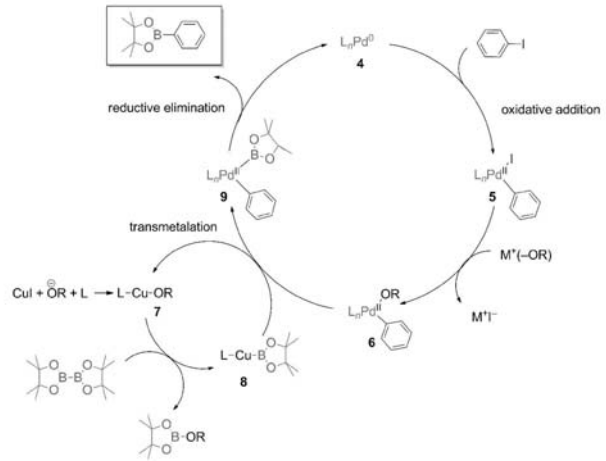

Scheme 1. Proposed plausible mechanism for the Pd/Cu-catalyzed Miyaura borylation reaction.

Acknowledgments

We thank Dr. Preeyanuch Sangtrirutnugul, Dr. Jonggol Tantirungrotechai, and Mrs. Suttiporn Pikulthong for their valuable suggestions and support. We are grateful to the Faculty of Science, Mahidol University and the Center of Excellence for Innovation in Chemistry (PERCH-CIC) for financial support. We also thank the Department of Chemistry and Center of Instrumental Facility (CIF) at the Faculty of Science, Mahidol University for facilities.

[1] a) T. Ishiyama, M. Murata, N. Miyaura, *J. Org. Chem.* **1995**, *60*, 7508–7510; b) N. Miyaura, *Cross-Coupling Reactions*, vol. 219 (Ed.: N. Miyaura), Springer, Berlin, **2002**, pp. 11–59; c) S. Kotha, K. Lahiri, D. Kashinath, *Tetrahedron* **2002**, *58*, 9633–9695; d) P. Merino, T. Tejero, *Angew. Chem.* **2010**, *122*, 7320–7322; *Angew. Chem. Int. Ed.* **2010**, *49*, 7164–7165; e) C. A. Hutton, O. Skaff, *Tetrahedron Lett.* **2003**, *44*, 4895–4898.

[2] a) M. Murata, S. Watanabe, Y. Masuda, *J. Org. Chem.* **1997**, *62*, 6458–6459; b) K. L. Billingsley, T. E. Barder, S. L. Buchwald, *Angew. Chem.* **2007**, *119*, 5455–5459; *Angew. Chem. Int. Ed.* **2007**, *46*, 5359–5363; c) T. Yamamoto, T. Morita, J. Takagi, T. Yamakawa, *Org. Lett.* **2011**, *13*, 5766–5769; d) W. Tang, S. Keshipeddy, Y. Zhang, X. Wei, J. Savoie, N. D. Patel, N. K. Yee, C. H. Senanayake, *Org. Lett.* **2011**, *13*, 1366–1369; e) W. K. Chow, O. Y. Yuen, P. Y. Choy, C. M. So, C. P. Lau, W. T. Wong, F. Y. Kwong, *RSC Adv.* **2013**, *3*, 12518–12539.

[3] a) P. Nguyen, H. P. Blom, S. A. Westcott, N. J. Taylor, T. B. Marder, *J. Am. Chem. Soc.* **1993**, *115*, 9329–9330; b) J. Y. Cho, M. K. Tse, D. Holmes, R. E. Maleczka Jr., M. R. Smith Iii, *Science* **2002**, *295*, 305–308; c) T. Ishiyama, J. Takagi, J. F. Hartwig, N. Miyaura, *Angew. Chem.* **2002**, *114*, 3182–3184; *Angew. Chem. Int. Ed.* **2002**, *41*, 3056–3058; d) I. A. I. Mkhalid, J. H. Barnard, T. B. Marder, J. M. Murphy, J. F. Hartwig, *Chem. Rev.* **2010**, *110*, 890–931.

[4] a) W. Zhu, D. Ma, *Org. Lett.* **2006**, *8*, 261–263; b) C. Kleeberg, L. Dang, Z. Lin, T. B. Marder, *Angew. Chem.* **2009**, *121*, 5454–5458; *Angew. Chem. Int. Ed.* **2009**, *48*, 5350–5354; c) R. D. Grigg, R. Van Hoveln, J. M. Schomaker, *J. Am. Chem. Soc.* **2012**, *134*, 16131–16134.

[5] a) J. Zhang, H. H. Wu, *Eur. J. Org. Chem.* **2013**, 6263–6266; b) C. Pubill-Ulldemolins, A. Bonet, C. Bo, H. Gulyás, E. Fernández, *Chem. Eur. J.* **2012**, *18*, 1121–1126; c) H. Wu, S. Radomkit, J. M. O'Brien, A. H. Hoveyda, *J. Am. Chem. Soc.* **2012**, *134*, 8277–8285; d) K. Oshima, T. Ohmura, M. Suginome, *Chem. Commun.* **2012**, *48*, 8571–8573; e) C. Sole, H. Gulyas, E. Fernandez, *Chem. Commun.* **2012**, *48*, 3769–3771; f) F. Mo, Y. Jiang, D. Qiu, Y. Zhang, J. Wang, *Angew. Chem.* **2010**, *122*, 1890–1893; *Angew. Chem. Int. Ed.* **2010**, *49*, 1846–1849; g) D. Qiu, L. Jin, Z. Zheng, H. Meng, F. Mo, X. Wang, Y. Zhang, J. Wang, *J. Org. Chem.* **2013**, *78*, 1923–1933.

Received: October 31, 2013
Published Online: January 28, 2014

BIOGRAPHY

NAME	Mr. Jadsada Ratniyom
DATE OF BIRTH	19 MAY 1988
PLACE OF BIRTH	Uttaradit, Thailand
INSTITUTIONS ATTENDED	Mahidol University, 2006–2009 Bachelor of Science (Chemistry) Mahidol University, 2010–2014 Doctor of Philosophy (Inorganic Chemistry)
RESEARCH GRANTS	Center for Innovation in Chemistry: Postgraduate Education and Research Program in Chemistry, (PERCH-CIC)
HOME ADDRESS	854/22, Ratchadapisek Road, Soi Ratchadapisek 18, Samsennok, Huaykwang, Bangkok, 10320, Thailand E-mail: hydronium_ion3@hotmail.com
PUBLICATION	Journal of Organometallic Chemistry 2014;752:161–70. European Journal of Organic Chemistry 2014;2014(7):1381–5.